

UNCLASSIFIED

AD NUMBER

AD476591

LIMITATION CHANGES

TO:

Approved for public release; distribution is unlimited.

FROM:

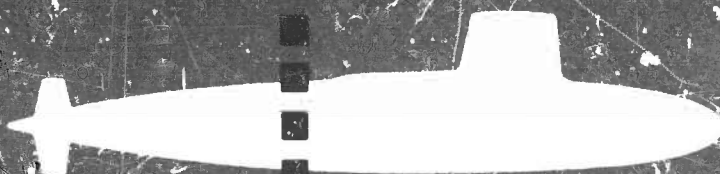
Distribution authorized to U.S. Gov't. agencies and their contractors;
Administrative/Operational Use; AUG 1965. Other requests shall be referred to Office of Naval Research, Washington, DC 20350.

AUTHORITY

onr ltr 24 aug 1968

THIS PAGE IS UNCLASSIFIED

SUBIC



Submarine Integrated Control

OFFICE OF
NAVAL
RESEARCH

GENERAL DYNAMICS CORPORATION
ELECTRIC BOAT DIVISION
GROTON, CONNECTICUT

GENERAL DYNAMICS/ELECTRIC BOAT
Research and Development Department
Groton, Connecticut

PROCESSING OF DATA FROM
SONAR SYSTEMS

VOLUME III

by

Morton Kanefsky
Allen H. Levesque
Peter M. Schultheiss
Franz B. Tuteur

Yale University

Examined: C. R. DeVoe
C. R. DeVoe
Head, Information Processing Section

Approved: Dr. A. J. van Woerkom
Dr. A. J. van Woerkom
Chief Scientist

U417-65-033
August 23, 1965



PROCESSING OF DATA FROM SONAR SYSTEMS

VOLUME III

by

Morton Kanefsky

Allen H. Levesque

Peter M. Schultheiss

Franz B. Tuteur

Report on work performed under Yale

University Contract 53-00-10-0231

from July 1, 1964, to July 1, 1965

General Dynamics/Electric Boat Research

DEPARTMENT OF ENGINEERING
AND APPLIED SCIENCE

YALE UNIVERSITY

ABSTRACT

This report is concerned with problems in passive sonar detection that arise when signal or noise properties deviate significantly from the simplest possible model (a target acting as a point source of broad band Gaussian signal in a background of isotropic Gaussian noise). The problems investigated fall under two major headings

- 1) Improvements in detectability obtainable from a knowledge of special features of signal or noise. Topics considered in this category include
 - a) Detection in a strongly anisotropic noise field due to a nearby source of interference.
 - b) Detection of targets whose radiated noise includes sinusoidal or narrow band components with appreciable power.
- 2) Degradation in detector performance resulting from a lack of adequate knowledge of signal or noise statistics or from a deliberate choice not to use all available information in order to simplify the instrumentation. Problems in the second category include
 - a) Detection in a noise field of unknown power level.
 - b) Losses due to sampling and clipping.

FOREWORD

The work described in this report was accomplished by members of the Department of Engineering and Applied Science, Dunham Laboratory, Yale University, under subcontract to the SUBIC program (contract NONr 2512(00)) during the period July 1, 1964 to July 1, 1965. The Office of Naval Research is the sponsor and General Dynamics Corporation Electric Boat Division is the prime contractor. Lcdr R.N. Crawford, USN, is Project Officer for ONR; Dr. A. J. van Woerkom is Project Coordinator for Electric Boat and Chief Scientist of the Research and Development Department.

The SUBIC program encompasses all aspects of submarine system analysis. This report is the third in a series dealing with acoustic signal processing. Progress Reports no. 17 and 18 and no. 20 through 22 are included in this volume. The information originally in Report no. 19 is included as part of Report no. 20.

TABLE OF CONTENTS

TEXT:	Processing of Data from Sonar System (Report of work performed under Yale University Contract 53-00-10-0231 with General Dynamics/ Electric Boat Company from July 1, 1964, to July 1, 1965)	1
APPENDICES:		
A.	P. M. Schultheiss, "Passive Detection of a Sonar Target in a Background of Ambient Noise and Interference from a Second Target," Progress Report No. 17, September 1964.	A-1
B.	F. B. Tuteur, "Optimal Detection of Signals in a Noise Background of Unknown Strength," Progress Report No. 18, January 1965.	B-1
C.	A. H. Levesque, "Detection of Signals of Unknown Frequency," Progress Report No. 20, June 1965.	C-1
D.	P. M. Schultheiss, "Some Suboptimal Techniques for Detecting Passive Sonar Targets in the Presence of Interference," Progress Report No. 21, June 1965.	D-1
E.	M. Kanefsky, "Passive Detection of a Weak Sonar Target from Hard-Limited Input Data," Progress Report No. 22, June 1965.	E-1

I. Introduction

The following is a summary of work performed under contract 53-00-10-0231 between Yale University and the Electric Boat Company during the period 1 July 1964 to 1 July 1965. More detailed discussions of the results as well as their derivation are contained in a series of five progress reports that are appended.

Previous reports in this series have dealt extensively with the passive detection of a directional Gaussian signal (a sonar target) in the presence of isotropic Gaussian noise. Signal and noise spectra were assumed to be known. The characteristics of the optimum (likelihood-ratio) detector were determined and it was shown that simple instrumentations in common use generally achieve a performance quite close to the optimum. It was clear from the results that significant departures from standard instrumentations could be justified only if the state of knowledge concerning signal or noise differed materially from the conditions postulated above.

The present report deals with several situations of practical importance in which the state of knowledge indeed differs substantially from the primitive assumption of directional Gaussian signal in isotropic Gaussian noise with given spectral properties. The departures take two general directions:

- 1) Cases in which the available information is stronger. Two instances of this type were considered in detail.
 - a) Much of the "noise" background is due to interference from an undesired target (e.g., a nearby ship). If the interfering signal is also Gaussian, the superposition of interference and ambient noise results in a disturbance that is still

Gaussian but no longer isotropic. With strong interference there is a high degree of anisotropy that can be used to improve detection.

- b) The target signal contains sinusoidal or very narrow-band components due to propeller motion, rotating machinery or similar causes. It is characteristic of such signals that their frequency is not known a priori, that it is likely to change over long periods of time, but that it remains essentially fixed for the length of time required in normal detection procedures. Thus one is faced with the problem of detecting sinusoidal or narrowband signals of unknown center frequency.¹

2) Cases in which the available information is weaker.

- a) One of the least realistic features of the primitive model is the assumption that the total noise power is fixed and known. In practice the total noise power is certainly not known a priori to any degree of accuracy and undoubtedly changes over prolonged periods of time. It therefore becomes

¹Depending on one's point of view one can regard the narrowband case as either a strengthening or a weakening of the initial assumption of Gaussian signal with known spectrum. If one takes as one's point of departure a narrowband signal with fixed spectrum, then recognition of the fact that the center frequency of this spectrum is unknown represents a degradation of available information. On the other hand, if one takes the point of view that over a long period of time the signal power is distributed over a wide band, then one gains considerable additional information from the knowledge that the power is in fact concentrated in a narrow band for the time intervals used in practical detection schemes. The latter point of view leads to a very natural transition to the sinusoidal case and is therefore chosen as the basis for classification here.

pertinent to inquire into the cost to the detection process of such lack of previously postulated knowledge.

- b) Regardless of the actual state of knowledge concerning signal and noise, one may deliberately choose detection procedures that fail to use all available information because of the greater simplicity of the resulting instrumentations. The relative ease of processing digital data has made it attractive to convert the hydrophone outputs into a series of binary numbers even though this clearly entails some loss of information. The effective utilization of clipped data therefore forms a subject of considerable interest.

II. Detection in the Presence of Interference

Work completed to date on the subject of passive target detection in the presence of ambient noise as well as interference is contained in Progress Reports No. 17 and 21. Progress Report No. 17 is concerned with setting absolute bounds on the detectability of targets in such an environment. Signal, interference and ambient noise are assumed to be stationary Gaussian random variables with known spectral properties. Signal and interference are taken as point sources with fixed locations while the ambient noise is endowed with no special spatial properties but is assumed to be independent from hydrophone to hydrophone. The input signal-to-noise ratio is assumed to be small.

Under these conditions the optimum (likelihood-ratio) detector is found to have the following output signal-to-noise ratio (defined as the change in average output due to signal divided by the rms output fluctuation):

$$\left(\frac{S}{N}\right)_{\text{out}} = \sqrt{\frac{T}{2\pi}} \sqrt{\int_{\omega_1}^{\omega_2} \left\{ \frac{S(\omega)}{N(\omega)} \frac{M \left[M - 1 + \frac{N(\omega)}{I(\omega)} \right] - 2 \sum_{\ell=1}^{M-1} (M - \ell) \cos \ell \omega \tau_0}{M + \frac{N(\omega)}{I(\omega)}} \right\}^2 d\omega} \quad (1)$$

T is the observation time; $S(\omega)$, $I(\omega)$ and $N(\omega)$ are the power spectra of signal, interference and ambient noise respectively. $\omega_1 \leq \omega \leq \omega_2$ is the processed frequency range (in rad/sec), M is the number of elements of a uniformly spaced linear array of hydrophones, and τ_0 is the difference between the signal delay and the interference delay from hydrophone to hydrophone.

The most important properties of the optimal instrumentation follow quickly from Eq. (1) [See Report No. 17, pp. 19-22] :

- 1) The output signal-to-noise ratio (and hence detection performance for fixed false-alarm rate) depends critically on $\frac{S(\omega)}{N(\omega)}$, but has no strong dependence on $I(\omega)$. [In the limits of large and small $\frac{N(\omega)}{I(\omega)}$ it is independent of $I(\omega)$, except for the trivial case of target and interference in angular alignment].
- 2) For $M \gg 1$ and a certain minimal angular separation of target and interference, the output signal-to-noise ratio is no smaller than that of a conventional $(M-1)$ -element linear array detecting the same signal in the same ambient noise but in the absence of interference.

These two results may be interpreted as follows: Given an array of reasonable size and a certain minimal separation of target and interference,

the presence of a localized interference, however strong, has very little influence on target detectability. The optimum detector is apparently capable of eliminating the interference without significant cost to the remainder of the detection operation. With a 40-element array, 2-ft spacing between hydrophones, $\omega_2 = 2\pi \times 5000$ rad/sec, and a broadside target, the "minimal separation" referred to above is roughly 3° . The corresponding figure for the endfire condition is about 20° .

A standard power detector--which simply aligns all hydrophone outputs with the target, adds, squares and smoothes [Report No. 17, Fig. 1]--can be distinctly inferior to the likelihood-ratio detector in an environment including interference. When interference becomes the dominant influence--which occurs when M times the interference power exceeds the ambient noise power [Report No. 17, Eq. (20)]--the output signal-to-noise ratio depends on the signal-to-interference ratio, rather than on the interference-to-ambient-noise ratio. Thus large gains in detectability can be made by the use of optimal techniques if the interference is very strong. In the strong interference regime the output signal-to-noise ratio of the conventional detector varies as \sqrt{M} , whereas that of the likelihood-ratio detector varies as M. Hence from this point of view also the likelihood-ratio detector achieves more effective utilization of the available sensor data.

The performance index of ultimate interest is probably the detection probability for a fixed false-alarm rate. Curves of this performance index as a function of input signal-to-ambient-noise ratio were computed [Report No. 17, Figs. 12 and 13]. They show advantages of the likelihood-ratio detector over the standard detector varying from moderate to large depending primarily on the interference-to-ambient-noise ratio.

The results of Report No. 17 make it clear that significant improvements in performance can be obtained in interference-dominated situations by departing from conventional detector design. There remains the question whether reasonable approximations to the theoretically possible performance can be obtained with instrumentations of acceptable complexity. Report No. 21 is addressed to some aspects of this question.

Since the likelihood-ratio detector achieves a performance largely independent of the interference at an overall cost of no more than one hydrophone, it appears reasonable to search for a simple instrumentation that eliminates interference at a sacrifice of no more than one signal channel. This is accomplished by the instrumentation shown in Report No. 21, Fig. 1. The hydrophone outputs are delayed to align the interference components (the interference direction is easily measured because the interfering signal is presumably strong). Pairwise subtraction of adjacent channels yields $M-1$ interference-free signals whose target components can now be aligned by a second set of delays. Conventional addition, squaring and smoothing follows.

An analysis of the detector just described yields an output signal-to-noise ratio quite close to that of the likelihood-ratio detector [Report No. 21, Fig. 2]. Except for targets in very close angular proximity to the interference, the degradation amounts to only about 1 db of equivalent input signal-to-ambient-noise ratio. From this point of view, therefore, the proposed instrumentation can be regarded as almost completely successful. On the other hand, if one examines the average bearing response pattern, one finds that target peaks are sharply diminished in a rather broad angular

neighborhood of the interference [Report No. 21, Figs. 4-9].¹ In qualitative terms, the zone of degraded performance extends over an angle roughly equal to the width of the beam formed by adjacent hydrophones. This observation suggests the required remedy. Instead of subtracting adjacent channels after alignment with the interference, one obtains the interference null by subtracting hydrophone pairs spaced a greater distance apart. Figure 10 of Report No. 21 gives one example of such a procedure. Analysis of a general arrangement of this type yields an average bearing response pattern clearly showing target peaks even in rather close proximity to the interference and under very unfavorable conditions of signal-to-noise ratio [Report No. 21, Figs. 11 and 12].

Taken together, Reports No. 17 and 21 indicate that significant improvements over conventional instrumentations are possible in interference-dominated situations and that the improvements can be obtained with only moderately increased complexity in instrumentation. From a practical point of view the most serious modification is the need for a second set of delay elements. While the proposed instrumentation lays no claim to optimality either in performance or in simplicity, one is tempted to speculate that the need for two sets of delay elements (or one set with storage facilities to permit sequential processing) is fairly basic, for one can hardly hope to eliminate interference without forming a beam on the interfering signal.

¹The relative significance of output signal-to-noise ratio and average bearing response is discussed in Report No. 21, Section V.

III. Detection of Sinusoidal and Narrowband Signals

Results on the detection of sinusoidal and narrowband Gaussian signals are contained in Report No. 20.¹ It should be pointed out that certain portions of this material have been reported previously. In particular, much of Chapter II was contained in Volume II of this series as Progress Report No. 15.

Report No. 20 is concerned with the effect of frequency uncertainty on the detection problem. All other assumptions are therefore chosen as simple as possible. Spectra of narrowband signals and of the noise are assumed to be flat over their respective bands and wideband signal components (undoubtedly present in practice) are ignored. The signal, sinusoidal or Gaussian with bandwidth B_S , is assumed to lie anywhere within a band $B \geq B_S$ over which the noise spectrum is flat [See Report No. 20, Fig. III.1].

The results fall into two general categories:

- 1) The physical structure of the optimum detector.
- 2) The performance of the optimum detector.

The structure of the optimum detector depends critically on the product $B_S T$ of signal bandwidth and observation time. If $B_S T \gg 1$, one has available a statistically significant sample of the Gaussian signal process. If the center frequency of the signal is known, the instrumentation problem reduces to the standard result for the detection of a Gaussian signal in Gaussian noise: a bandpass filter matched to the signal followed by conventional power detection. With unknown center frequency it is shown in Report No. 20 that the optimum detector for large output signal-to-noise ratio (good detectability) examines the output of a series of such detectors with filters having all possible signal center frequencies. If any one of the outputs exceeds an appropriate threshold, a signal is reported to be present.² In

¹Report No. 20 contains all of the information originally in No. 19 in addition to new material.

²In Report No. 20 this configuration is described as a "bandsweeping detector."

practice, of course, one cannot construct filters for each of the infinity of possible signal center frequencies. As a first approximation one can simply divide the band B into $r = B/B_S$ parts, each of width B_S . The first step of refinement might employ $2r$ overlapping filters [Report No. 20, Fig. III.4] and further approximations to the continuously variable center frequency are clearly possible. From a practical point of view, the numerical results indicate that an instrumentation with $2r$ filters already gives a fairly good approximation to the optimum, so that much more complicated detector structures should be of limited interest.

If $B_S T \ll 1$ the available sample of the narrowband Gaussian signal looks essentially like a sinusoid at the center frequency of the signal band. It is therefore not surprising to find that the optimum detector crosscorrelates the received signal with a series of sinusoids at the various possible center frequencies [See Report No. 20, Eq. (IV-22)]. Since the phase of the received signal is not known a priori the correlation is performed at each frequency against two sinusoids in quadrature with each other. Because of computational difficulties the number of crosscorrelators required for a reasonable approximation to the ideal instrumentation (using a continuously variable correlator frequency) was not investigated in as much detail as the corresponding phenomenon for $B_S T \gg 1$. It appears clear, however, that the practical spacing of correlator frequencies should be of the order of $\frac{1}{T}$ rather than B_S . Over a period of T seconds correlators using sinusoids separated by much less than $\frac{1}{T}$ cps would have essentially the same output and would therefore be highly redundant. Numerical computations were actually carried out for correlator frequencies separated by $\frac{1}{T}$ cps, and the results are felt to give a reasonable approximation to the attainable optimum [Report No. 20, Fig. IV.1].

Since a narrowband signal with $B_s T \ll 1$ is practically indistinguishable from a sinusoid, it follows that the detection of a sinusoid of unknown amplitude, frequency and phase is simply a special case of the narrowband problem. All comments concerning detector structures and performance carry over to the sinusoidal case without difficulty.

The performance of the optimum detector can be discussed from two opposite points of view, as suggested earlier. Starting with the known solution to the problem of detecting a narrowband Gaussian signal with known center frequency in broadband Gaussian noise, one can consider the degradation in performance brought about by the frequency uncertainty. If the signal can lie in any one of r disjoint frequency intervals and "signal present" is to be reported when any one of the r detectors operating on these separate intervals exceeds a fixed threshold, then the probability of false alarms increases with r for fixed threshold level. Conversely, if one wishes to maintain a fixed false-alarm rate, one must increase the threshold level with r and must therefore tolerate a somewhat lower detection probability than in the fixed-frequency case. From the other point of view one starts with a fixed signal power uniformly distributed over the entire processed band B and regards any knowledge about signal concentration in a narrower band B_s as additional information which can be used to enhance detector performance. Under a fixed power constraint the input signal-to-noise ratio R_s within the signal band varies linearly with $r = B/B_s$. For fixed center frequency and low input signal-to-noise ratio the output signal-to-noise ratio depends linearly on the input signal-to-noise ratio. Thus the output signal-to-noise ratio would vary linearly with r if it were not for the false-alarm problem produced by the need to process r separate frequency

bands. From this point of view, therefore, there are two counterbalancing effects: Improvement due to the increase of R_S with r and degradation due to the more severe false-alarm problem. The results of Report No. 20 indicate that the first effect dominates as long as $R_S \ll 1$. Under these conditions the output signal-to-noise ratio is almost as large as one would predict from the given R_S and standard theory for fixed center frequency. When R_S reaches the order of unity, however, the picture changes. Once R_S exceeds unity, the rms fluctuation of the detector output is no longer primarily due to the noise component of the input, but to the signal component. Further increases in R_S not only increase the useful output but also the output fluctuation. Computations in the region of $R_S > 1$ are tedious to perform, and not enough accurate values have been obtained to determine the exact behavior of the output signal-to-noise ratio in that region. One asymptotic value which is easily calculated is the limiting form for $B_S \rightarrow 0$ (hence $R_S \rightarrow \infty$). This is the case of a sinusoidal signal of unknown amplitude, frequency and phase. Results for this case indicate that the most favorable situation for detection is not necessarily that of greatest concentration of signal power in the narrowest possible band. [See Report No. 20, pp. 163-164, for a discussion of this problem.] Further work on the detection of signals strong in at least some portion of the frequency spectrum is planned for the future.¹ In the meantime it would appear that little or no gain in detectability is made by processing frequency bands so narrow that the expected signal-to-noise ratio within the signal band exceeds unity.²

¹Frequency uncertainty is not an essential part of this particular problem. The strong signal case has not been fully discussed in the literature even with predetermined spectral properties.

²On the other hand, the use of narrower and narrower bands can achieve values of R_S close to unity for signals of smaller and smaller intrinsic power level.

IV. Detection in an Unknown Noise Background

Report No. 18 is concerned with the degradation in detectability resulting from a lack of a priori knowledge about the noise power. It may be viewed as a first step towards a model presupposing no prior knowledge of noise statistics. In Report No. 18 the noise is still assumed to be Gaussian with known spectral shape. Only the level (and hence total power) is regarded as unknown within reasonable limits.

On a general level, the report demonstrates that a sufficient statistic for detection under the above conditions is furnished by the two-dimensional random variable (u_1, u_2) , where

$$u_1 = \bar{S} x' Q^{-1} P Q^{-1} x \quad (2)$$

$$u_2 = x' Q^{-1} x \quad (3)$$

\bar{S} is a measure of the average signal power, x is the vector of received signal samples at various hydrophones, x' is the transpose of x , Q is the normalized noise covariance matrix and P is the normalized signal covariance matrix.

If the noise power is known, Eq. (2) alone forms a sufficient statistic. The additional operation required without such knowledge is specified by Eq. (3). In the absence of signal this amounts simply to the estimation of the noise power from the available data. If a signal is present it is not possible to obtain data on the noise alone. However, the operation of Eq. (3) is matched to the noise properties (through the matrix Q^{-1}), and to the extent that signal and noise differ (in directionality, spectral properties, modulation, etc.) it can achieve a measure of discrimination.

In practice one is frequently interested in constant false-alarm rate (CFAR) performance. It is shown [Report No. 18, pp. 4-5] that a process of threshold detection on the linear combination $u_1 - a u_2$ (a a constant) yields

CFAR operation. While any other quadratic form $u_2 = x^T A x$ would also lead to CFAR operation, it is demonstrated [Report No. 18, Appendix A] that the choice $A = Q^{-1}$ has properties that are desirable although not necessarily optimum in any absolute sense.

On a more specific level, the output signal-to-noise ratio of the CFAR detector [Report No. 18, Eq. (13)] is evaluated for several particular situations of practical interest. It is shown that for large arrays ($M \gg 1$) lack of knowledge concerning the noise power has little influence on detectability because adequate estimates of the noise level can be made from Eq. (3). The cost of such estimates is roughly $\frac{1}{2}$ hydrophone; i.e., detection performance is the same as that of an array with $M - \frac{1}{2}$ hydrophones operating in a completely known noise environment. At the other extreme, when $M = 1$, detection is impossible unless signal and noise have distinguishing features other than directionality. One such feature investigated is the presence of amplitude modulation on the signal. Under these conditions it is shown that detection can be accomplished with a single hydrophone but that the advantage gained from knowledge about the modulation rapidly decreases as the number of hydrophones increases. Even with only two hydrophones, the advantage to be gained from sinusoidal modulation is equivalent to no more than about 1.5 db in input signal-to-noise ratio.

A number of computations were carried out to gain insight into the effect of differences in spectral properties of signal and noise on the above results. All such efforts led to the conclusion that the effects were minor except for extremely small arrays.

V. The Cost of Clipping

Because of the practical convenience of working with digital data, there is considerable interest in the inherent loss in detectability resulting from the required sampling and quantizing operations. Several earlier reports in this series have dealt with various aspects of this problem [Reports No. 2, 4 and 6 of Vol. I and Report No. 11 of Vol. II]. Most of these reports considered the effect of clipping on specific instrumentations. Only one [Report No. 6] attempted to assess the inherent cost of clipping, and it did so under highly idealized conditions (the initial data were assumed to be independent samples of a Gaussian random process). All the previous work dealt with Gaussian signals and noise.

Report No. 22, while working with another specific instrumentation, gives new insight into the meaning of the results obtained previously, particularly with regard to the relative importance of sampling and clipping in the degradation experienced with digital data handling techniques. It also gives some results for detection in an environment of non-Gaussian noise.

The particular instrumentation under study is the polarity coincidence array detector (PCA), a natural generalization of the polarity coincidence correlator (PCC). It observes the hard-clipped outputs of all array elements and uses as a test statistic a quantity that is in effect the maximum number of outputs having the same sign. This scheme has the following attractive properties:

- 1) If the input consists of independent samples of a Gaussian random process, it is asymptotically optimal in the Neyman-Pearson sense for small input signal-to-noise ratios.

- 2) If the input consists of independent but not necessarily Gaussian samples, the detector maintains a constant false-alarm rate independent of the input distribution.
- 3) If the input consists of dependent Gaussian samples, constant false-alarm properties are maintained in spite of possible variations in the noise power level.

Because of the asymptotic optimality in case 1) this situation is equivalent to the problem treated in Report No. 6 and one arrives at the same degradation of $\frac{2}{\pi}$ or 1.96 db in equivalent input signal-to-noise ratio.

In case 2) the degradation can be either larger or smaller than 1.96 db, depending primarily on the behavior of the noise probability density function near the origin. If the noise probability density near the origin is higher than that of a Gaussian random variable with the same power, the degradation is less than 1.96 db (impulse noise would be a case of this type). Conversely, with low values of noise probability density near the origin, there can be a substantially greater loss.

Case 3, dependent Gaussian samples, sheds light on the sampling problem because increase in dependence may be viewed as the consequence of more rapid sampling. It is shown that the loss in detectability declines as the dependence increases. One typical example yields a reduction from 1.96 db to 0.63 db degradation as the sampling rate is varied from a low value furnishing essentially independent samples to a very high value. It is important to keep in mind under what circumstances a portion of the 1.96 db loss is recoverable. If, as in Report No. 6, signal and noise are Gaussian random processes with flat power spectra over the entire processed band $(0, W)$, then a series of samples taken at intervals of $\frac{1}{2W}$ sec are independent

and completely describe the received signal. There has been no sampling loss. If these samples are now hard clipped, there is a 1.96 db loss in detectability which must apparently be charged to the clipping process. On the other hand, if the continuous signal is clipped and then sampled at a rate increasing from $2W$ samples per second to a very high value, then the degradation of detector performance declines from 1.96 db to well under 1 db.¹ From a practical point of view it is important to note that the sampling rates required in order to recover most of the 1.96 db loss are quite high compared with the nominal cutoff frequency of signal and noise spectra [See Report No. 22, Fig. 3].

Also considered in Report No. 22 are several variations of the PCA detector that may be somewhat more convenient from the point of view of practical implementation. Their figures of merit tend to be somewhat, though not drastically, inferior to that of the PCA.

Report No. 22 is part of a continuing effort to determine the cost of using digital techniques in processing sonar data for detection purposes. Additional topics in this area now under study include detection under conditions of high signal-to-noise ratio and detection in an environment dominated by strong interference.

¹From another point of view this result may be regarded as a consequence of the bandspreading produced by clipping. The clipped signal is not bandlimited to $(0, W)$ so that samples at intervals of $(1/2W)$ sec no longer completely represent it. It is clearly immaterial to this argument whether the physical operation of clipping takes place before or after the sampling operation.



PASSIVE DETECTION OF A SONAR TARGET
IN A BACKGROUND OF AMBIENT NOISE
AND INTERFERENCE FROM A SECOND TARGET

by

Peter M. Schultheiss

Progress Report No. 17

General Dynamics/Electric Boat Research

(53-00-10-0231)

September 1964

DEPARTMENT OF ENGINEERING
AND APPLIED SCIENCE

YALE UNIVERSITY

Summary

The report deals with the passive detection of a sonar target in the presence of ambient noise as well as interference from a second target, possibly very much stronger than the first. Target, interference and ambient noise are assumed to be Gaussian random processes, the ambient noise being statistically independent from hydrophone to hydrophone of the (linear) receiving array. Output signal-to-noise ratios and error probabilities are calculated for conventional and likelihood-ratio detectors.¹ The following results are obtained:

- 1) The output signal-to-noise ratio of the conventional detector varies as M for $\frac{N}{I} \gg \sqrt{M}$ and as \sqrt{M} for $\frac{N}{I} \ll \sqrt{M}$. [N = average ambient noise power, I = average interference power, M = number of hydrophones].
- 2) The output signal-to-noise ratio of the likelihood ratio detector varies as M for low as well as for high values of $\frac{N}{I}$.
- 3) The effective input noise power of the conventional detector is approximately N for $\frac{N}{I} \gg \sqrt{M}$ and I for $\frac{N}{I} \ll \sqrt{M}$.
- 4) The effective input noise power of the likelihood-ratio detector is approximately N for low as well as for high values of $\frac{N}{I}$.
- 5) Except for targets very close in bearing to the interference, the performance of the likelihood-ratio detector is no worse than that of a similar detector with one less hydrophone operating in

¹The analysis of the conventional detector assumes that the normalized autocorrelation functions of interference and ambient noise have the same exponential form. No such restriction is made in the general analysis of the likelihood-ratio detector, but many of the specific numerical results are based on the assumption that the spectra of signal, interference and ambient noise have the same form.

the same ambient noise background but in the absence of interference. Thus the cost of eliminating interference from a point source is no more than one hydrophone.

- 6) For targets angularly remote from the interference, the advantage of the likelihood-ratio detector over the conventional detector depends critically on the value of $\frac{N}{I}$. Sample calculations of miss probability for fixed false-alarm probability (for a 40-element linear array with 2-ft hydrophone spacing, processing bandwidth of 5000 cps, and false alarm rate 1%) yield an advantage equivalent to about 2 db of input signal-to-noise ratio for $\frac{N}{I} = 4$. Corresponding figures for lower values of $\frac{N}{I}$ are: 7 db for $\frac{N}{I} = 1$, 17 db for $\frac{N}{I} = 0.1$.
- 7) As the interference approaches the target in bearing, the performance of both detectors declines. For a likelihood-ratio detector with processing bandwidth of 5000 cps (using a 40-element linear array with 2-ft hydrophone spacing, target broadside, false-alarm rate 1%), this loss in performance amounts to less than $\frac{1}{2}$ db in equivalent input signal-to-noise ratio as the relative bearing of interference and target decreases from 90° to 3° . Only for relative bearings of less than 3° is the decline in performance pronounced. For a conventional detector without pre-filtering, operating under similar conditions, the decline in performance is equivalent to 5-6 db in input signal-to-noise ratio as the relative bearing varies from 90° to 3° . The corresponding figure for a conventional detector with pre-whitening is of the order of 3 db.

- 8) The ability of the likelihood-ratio and conventional detectors to detect targets in angular proximity to the interference varies in the same manner with target location relative to the array axis. It is best in the broadside condition and poorest in the endfire condition.
- 9) The effect of clipping on the average bearing response pattern of a conventional detector is no greater in the presence of interference than in its absence (interference remote in bearing from target).

I. Introduction

This report deals with the problem of passive sonar detection of a weak target signal in the presence of interference from a second target, possibly very much stronger than the first, as well as the usual ambient noise. Signal, interference and ambient noise are assumed to be independent, stationary Gaussian random processes with known spectral properties. The receiving array is assumed to be linear and to consist of M equally spaced omnidirectional hydrophones. The wavefronts of target signal and interference are regarded as plane over the dimensions of the receiving array. Since interest centers on the effect of interference, the ambient noise is treated as statistically independent from hydrophone to hydrophone, an assumption that achieves considerable computational simplification and is, in any case, not too unrealistic for hydrophone spacings above a fairly small minimum.

For the purposes of the present investigation the sum of interference and ambient noise may be regarded as the effective noise. Under the assumptions stated above, the effective noise is therefore another stationary Gaussian random process with known spectrum. Thus the problem under investigation differs from that treated in a series of earlier reports¹ only in that the effective noise is strongly anisotropic if the interference exceeds the ambient noise by a substantial amount. The basic analytical techniques developed in the earlier reports remain for the most part applicable with only minor modifications. However, some of the specific results are decidedly different when the anisotropy of the noise is pronounced.

¹In particular Reports No. 2, 3, 6.

The present report addresses itself primarily to the following three problems:

1) The effect of interference on the performance of a conventional (power) detector. The report derives the output signal-to-noise ratio of a conventional detector and shows its dependence on such factors as interference power, number of elements in the array, and angular location of the interference relative to the target.

2) Improvements in detectability attainable through use of optimal procedures. If one assumes that the angular location of the interference is known or can be measured quite accurately (which is a reasonable assumption when the interference is strong), one feels that it should be possible to achieve improvements in detection by "mulling out" the interference by proper operations on the various hydrophone signals. Such a procedure will, of course, also tend to diminish the desired signal so that a compromise is called for. The report investigates the performance of a likelihood ratio detector which automatically achieves the best compromise. The results of earlier studies on likelihood ratio detectors have indicated that the gains to be made by using this generally rather complicated instrumentation are slight unless knowledge concerning important distinguishing features of signal and noise is available at the receiver. The results of the present report suggest that noise anisotropy may be precisely such a feature.

3) Detection from clipped hydrophone data. It is convenient for a number of reasons to clip the output of each hydrophone (i.e., in effect to reduce it to a binary number) before attempting to form beams or engage in other data processing procedures. There is evidence to suggest that such

a procedure may be undesirable when the effective noise consists primarily of interference. The report attempts to give at least a partial assessment of the cost of clipping in the presence of interference.

Nomenclature. The following symbols will be used throughout this report:

$s_j(t)$ = signal component of the output from the j^{th} hydrophone

$i_j(t)$ = interference component of the output from the j^{th} hydrophone

$n_j(t)$ = ambient noise component of the output from the j^{th} hydrophone

τ_{jk} = signal delay from j^{th} to k^{th} hydrophone

τ_{jk} = interference delay from j^{th} to k^{th} hydrophone

S = average signal power at each hydrophone

I = average interference power at each hydrophone

N = average ambient noise power at each hydrophone

$S(\omega)$ = signal spectrum

$I(\omega)$ = interference spectrum

$N(\omega)$ = ambient noise spectrum

$\rho_s(\tau) = \frac{1}{S} \overline{s_j(t) s_j(t+\tau)}$ = normalized autocorrelation of the signal at each hydrophone

$\rho_i(\tau) = \frac{1}{I} \overline{i_j(t) i_j(t+\tau)}$ = normalized autocorrelation of the interference at each hydrophone

$\rho_n(\tau) = \frac{1}{N} \overline{n_j(t) n_j(t+\tau)}$ = normalized autocorrelation of the ambient noise at each hydrophone

M = number of hydrophones

T = observation (smoothing) time

II. The Effect of Interference on the Performance of a Conventional Detector

This section is concerned with the output signal-to-noise ratio of the conventional detector shown in Fig. 1. As in several earlier reports, output signal-to-noise ratio is here defined as the change in DC output due to the appearance of a target signal divided by the rms fluctuation of the output. With the array electrically or mechanically trained on the target location, the change in DC output due to signal is

$$\Delta(\text{DC output}) = M^2 S \quad (1)$$

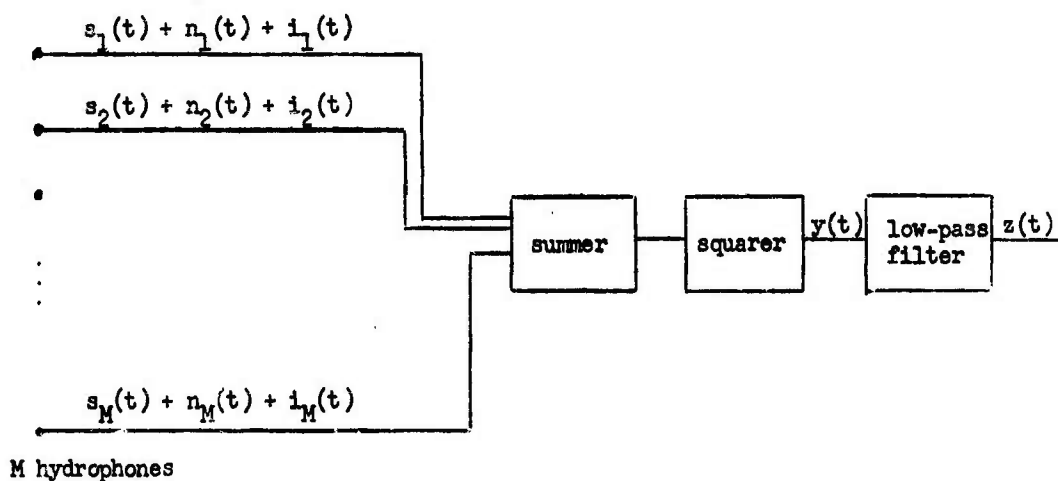


Figure 1

Assuming low input signal-to-noise ratio at each hydrophone, the output variance can be written down immediately from Report No. 3, Eq. (46):

$$N^2(z) = \frac{2I^2}{T} \sum_{j=1}^M \sum_{h=1}^M \sum_{k=1}^M \sum_{\ell=1}^M \int_{-\infty}^{\infty} \rho_1(\tau_{jh} + \tau) \rho_1(\tau_{k\ell} + \tau) d\tau + \frac{2N^2}{T} M^2 \int_{-\infty}^{\infty} \rho_n^2(\tau) d\tau \quad (2)$$

T is the smoothing time of the low-pass filter, which consists of a device averaging $y(t)$ over the past T seconds, $\rho_n(\tau)$ is the normalized autocorrelation function of the ambient noise.

It is probably not unreasonable to assume that the autocorrelation functions of interference and ambient noise are simple exponentials. Furthermore, the bandwidths of both processes are apt to be comparable in many cases of practical interest.¹ Hence it appears permissible for purposes of rough approximation to make the relatively simple assumption

$$\rho_1(\tau) = \rho_n(\tau) = e^{-\omega_0 |\tau|} \quad (3)$$

ω_0 is the effective bandwidth of interference and noise.

Since the hydrophone array is linear and equally spaced it follows that

$$\tau_{jh} = (j - h)\tau_0 \quad (4)$$

where τ_0 is the delay of the interference from hydrophone to hydrophone.

Hence

$$\rho_1(\tau_{jh} + \tau) = e^{-\omega_0 |(j-h)\tau_0 + \tau|} \quad (5)$$

¹One would certainly not process a band very much larger than that of the signal, so that one may rule out the case of an effective interference bandwidth broad compared to the signal bandwidth. On the other hand, if the interference were extremely narrow in bandwidth compared to the signal, one could effectively eliminate it by filtering. Thus the case of primary interest is that of signal and interference at least roughly equal in bandwidth. A similar argument applies to the relative bandwidths of signal and ambient noise.

Thus the indices j, h, k, ℓ in Eq. (2) appear only in the combinations $j-h$ and $k-\ell$. For further manipulation it is convenient to define

$$\int_{-\infty}^{\infty} \rho_1(\tau_{jh} + \tau) \rho_1(\tau_k + \tau) d\tau = C_{j-h, k-\ell} \quad (6)$$

Then the fourfold sum can be reduced to a double sum by the following procedure.

The change of variable $j-h = r$ yields

$$\begin{aligned} \sum_{j=1}^M \sum_{h=1}^M \sum_{k=1}^M \sum_{\ell=1}^M C_{j-h, k-\ell} &= \\ &= M \sum_{k=1}^M \sum_{\ell=1}^M C_{0, k-\ell} + \sum_{k=1}^M \sum_{\ell=1}^M \sum_{r=1}^{M-1} (M-r) C_{r, k-\ell} + \sum_{k=1}^M \sum_{\ell=1}^M \sum_{r=-1}^{-(M-1)} (M+r) C_{r, k-\ell} \\ &= M \sum_{k=1}^M \sum_{\ell=1}^M C_{0, k-\ell} + \sum_{k=1}^M \sum_{\ell=1}^M \sum_{r=1}^{M-1} (M-r) (C_{r, k-\ell} + C_{-r, k-\ell}) \end{aligned} \quad (7)$$

The further change of variable $k-\ell = s$ leads to the form

$$\begin{aligned} \sum_{j=1}^M \sum_{h=1}^M \sum_{k=1}^M \sum_{\ell=1}^M C_{j-h, k-\ell} &= M^2 C_{0,0} + M \sum_{s=1}^{M-1} (M-s) (C_{0,s} + C_{0,-s}) \\ &+ M \sum_{r=1}^{M-1} (M-r) (C_{r,0} + C_{-r,0}) + \sum_{r=1}^{M-1} \sum_{s=1}^{M-1} (M-r)(M-s) (C_{r,s} + C_{-r,s} + C_{r,-s} + C_{-r,-s}) \end{aligned} \quad (8)$$

From symmetry conditions it is clear that

$$\begin{aligned} c_{0,s} &= c_{0,-s} = c_{r,0} = c_{-r,0} \\ c_{r,s} &= c_{-r,-s} \\ c_{-r,s} &= c_{r,-s} \end{aligned} \quad (9)$$

Hence

$$\begin{aligned} \sum_{j=1}^M \sum_{h=1}^M \sum_{k=1}^M \sum_{\ell=1}^M c_{j-h,k-\ell} &= M^2 c_{0,0} + 4M \sum_{s=1}^{M-1} (M-s) c_{0,s} \\ &+ 2 \sum_{r=1}^{M-1} \sum_{s=1}^{M-1} (M-r)(M-s) (c_{r,s} + c_{-r,s}) \end{aligned} \quad (10)$$

The required coefficients are determined by a straightforward computation from Eqs. (5) and (6).

$$c_{0,0} = \frac{1}{\omega_0} \quad (11)$$

$$c_{0,s} = \frac{1}{\omega_0} (1 + s\omega_0\tau_0) e^{-s\omega_0\tau_0} \quad (12)$$

$$c_{r,s} = \frac{1}{\omega_0} (1 + |r-s|\omega_0\tau_0) e^{-|r-s|\omega_0\tau_0} \quad (13)$$

$$c_{-r,s} = \frac{1}{\omega_0} \left[1 + (r+s)\omega_0\tau_0 \right] e^{-(r+s)\omega_0\tau_0} \quad (14)$$

Substitution of Eqs. (11) through (14) into Eq. (10) yields

$$\sum_{j=1}^M \sum_{h=1}^M \sum_{k=1}^M \sum_{\ell=1}^M C_{j-h,k-\ell} =$$

$$\frac{1}{\omega_o} \left\{ M^2 + 4M \sum_{s=1}^{M-1} (M-s)(1+s\omega_o\tau_o) e^{-s\omega_o\tau_o} + 2 \sum_{s=1}^{M-1} (M-s)^2 \left[1 + (1+2s\omega_o\tau_o) e^{-2s\omega_o\tau_o} \right] \right.$$

$$\left. + 4 \sum_{r=2}^{M-1} \sum_{s=1}^{r-1} (M-r)(M-s) \left(\left[1 + (r-s)\omega_o\tau_o \right] e^{-(r-s)\omega_o\tau_o} + \left[1 + (r+s)\omega_o\tau_o \right] e^{-(r+s)\omega_o\tau_o} \right) \right\} \quad (15)$$

Use of Eqs. (1), (2) and (15) now gives the desired output signal-to-noise ratio

$$\frac{(\text{DC output})}{D(\text{output})} =$$

$$\sqrt{\frac{T\omega_o}{2}} \frac{MS}{\left[N^2 + I^2 \left\{ 1 + \frac{4}{M} \sum_{s=1}^{M-1} (M-s)(1+s\omega_o\tau_o) e^{-s\omega_o\tau_o} + \frac{2}{M^2} \sum_{s=1}^{M-1} (M-s)^2 \left[1 + (1+2s\omega_o\tau_o) e^{-2s\omega_o\tau_o} \right] \right. \right.} \right.}$$

$$\left. \left. + \frac{4}{M^2} \sum_{r=2}^{M-1} \sum_{s=1}^{r-1} (M-r)(M-s) \left(\left[1 + (r-s)\omega_o\tau_o \right] e^{-(r-s)\omega_o\tau_o} + \left[1 + (r+s)\omega_o\tau_o \right] e^{-(r+s)\omega_o\tau_o} \right) \right\} \right]^{\frac{1}{2}} \quad (16)$$

Useful insight into the meaning of this result can be obtained by considering the special case

$$e^{-s\omega_o\tau_o} \approx 0 \quad \text{f.r.} \quad s \geq 1$$

This corresponds to a reasonably broad-band interference sufficiently remote from the target in bearing so that the cross-correlation between the interference received at adjacent hydrophones (at the same instant of time) is negligible. An equivalent condition would be that the autocorrelation function of the interference vanishes for values of its argument equal to or larger than the interference delay from hydrophone to hydrophone.

If, under this hypothesis, the exponential terms in Eq. (16) are set equal to zero, one obtains

$$\frac{\Delta(\text{DC output})}{D(\text{output})} = \sqrt{\frac{T\omega_o}{2}} \frac{M S}{\sqrt{N^2 + I^2 \left[1 + \frac{2}{M^2} \sum_{s=1}^{M-1} (M-s)^2 \right]}} \quad (17)$$

The remaining summation can be carried out without difficulty, the result being

$$\frac{\Delta(\text{DC output})}{D(\text{output})} = \sqrt{\frac{T\omega_o}{2}} \frac{M S}{\sqrt{N^2 + \frac{I^2}{3} \left(2M + \frac{1}{M} \right)}} \quad (18)$$

In the absence of interference, Eq. (16) reduces to

$$\frac{\Delta(\text{DC output})}{D(\text{output})} = \sqrt{\frac{T\omega_o}{2}} M \frac{S}{N} \quad (19)$$

In this case the output signal-to-noise ratio varies linearly with the number of hydrophones. Comparison with Report No. 3, Eq. (80), indicates that this basic linear dependence on M is retained even if the isotropic ambient noise is not independent from hydrophone to hydrophone.¹

¹Under the assumption that the spacing between hydrophones remains fixed as M varies.

In the presence of interference (non-isotropic noise), on the other hand, Eq. (18) indicates an increase of output signal-to-noise ratio with only \sqrt{M} once $(I^2/3) \times 2M \gg N^2$. If the interference power is smaller than the ambient noise power, an increase in the number of hydrophones will therefore initially achieve a linear improvement in the output signal-to-noise ratio. In this range the effective input noise power is approximately N . Beyond a certain value of M , however, further improvement depends only on \sqrt{M} and the effective input noise power becomes approximately I . It will be shown in the next section that optimal detection procedures can preserve the first power relation and at the same time achieve an effective input noise power of the order of N for all values of M .

It may, at first glance, appear surprising that interference should result in a different detector performance than isotropic noise when the interference is uncorrelated from hydrophone to hydrophone. It must, however, be remembered that this lack of correlation applies only to the hydrophone outputs at the same instant of time. Since the interference comes from a single source, there exists some value of relative delay for which the interference components of any pair of hydrophone outputs are perfectly correlated. If, as was implicitly assumed in the computations, the smoothing time T is much larger than the travel time of the interference wavefront across the array, then this coherence can and does produce fluctuation in excess of the isotropic noise result at the receiver output.

Since all terms in the denominator of Eq. (16) are non-negative, Eq. (18) provides an upper bound on the output signal-to-noise ratio for any value of $\omega_0 \tau_0$. A lower bound is provided by the case of interference aligned in bearing with the target ($\tau_0 = 0$), in which case Eq. (16) reduces to

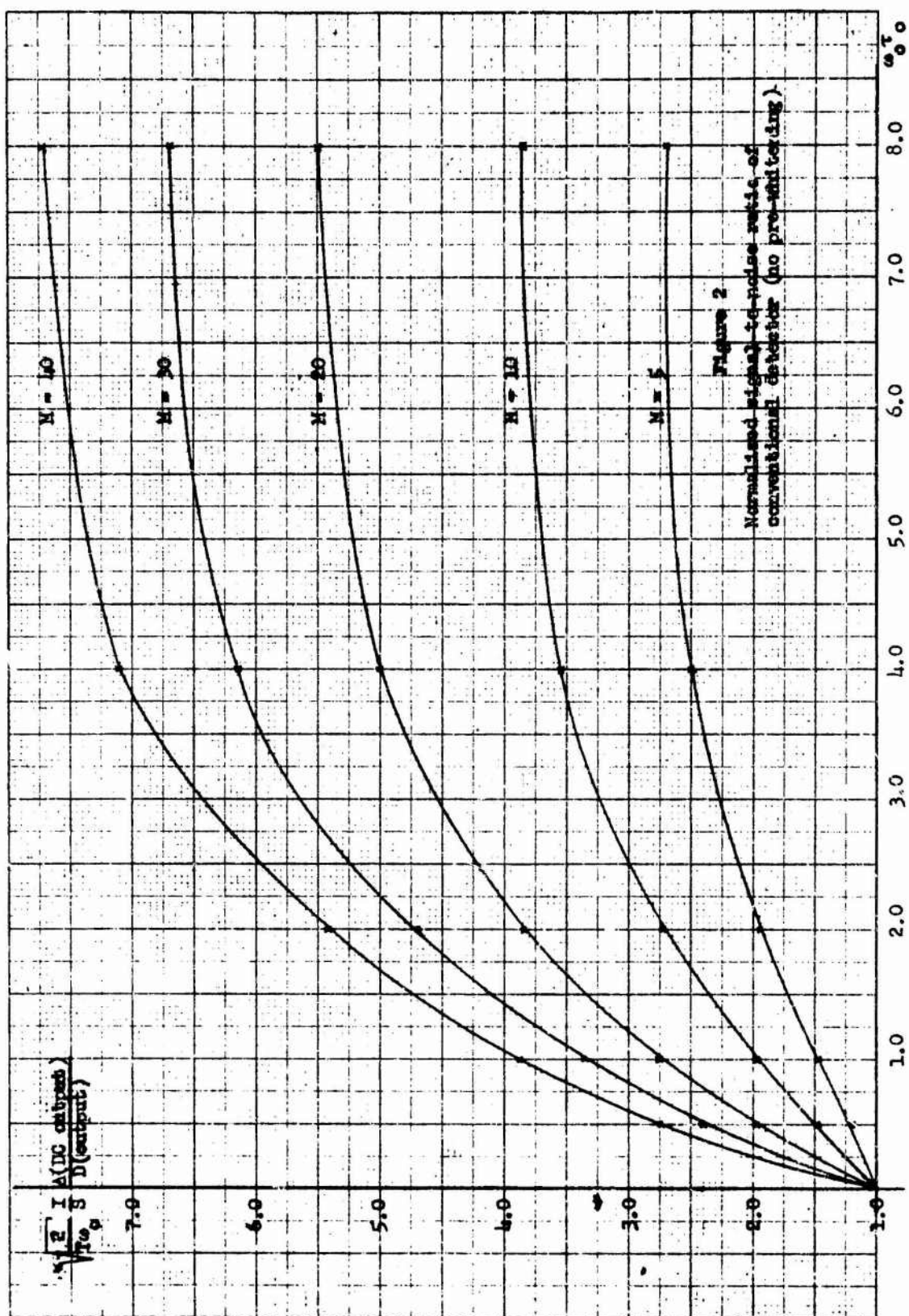
$$\frac{\Delta(\text{DC output})}{D(\text{output})} = \sqrt{\frac{T\omega_0}{2}} \frac{MS}{\sqrt{N^2 + M^2 I^2}} \quad (20)$$

The upper bound is, of course, attained only if $e^{-j\omega_0 \tau_0} \approx 0$ for some value of the bearing angle of the interference relative to the target.

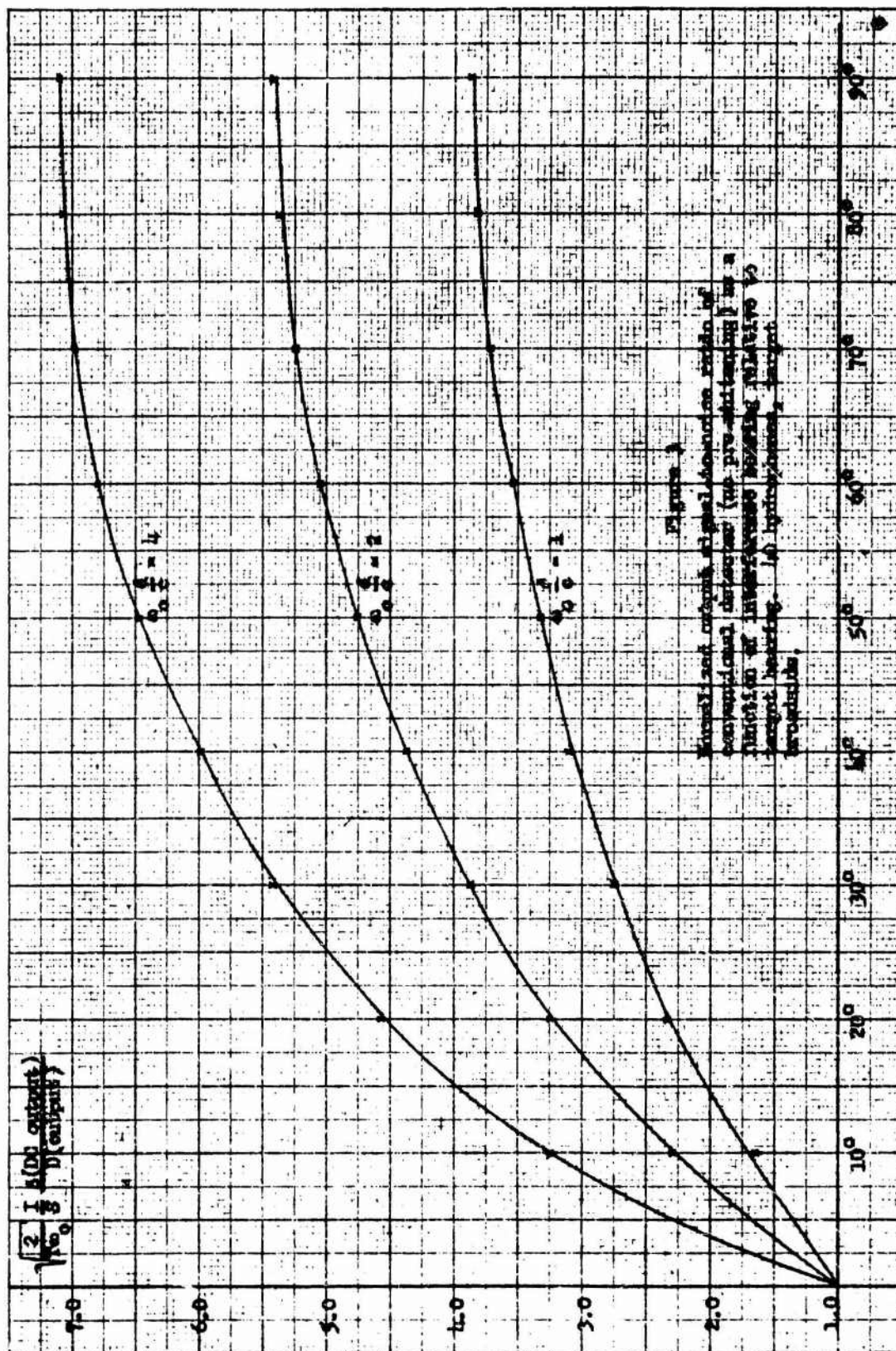
In Fig. 2 the output signal-to-noise ratio [Eq. (16)] is plotted in normalized form as a function of $x = \omega_0 \tau_0$ for the case of primary interest here, $I \gg N$. The number of hydrophones M is a parameter in this computation.

In order to exhibit the actual dependence of output signal-to-noise ratio on interference bearing θ relative to target bearing, the curve for 40 hydrophones is replotted in Fig. 3 as a function of θ for the target in broadside position.¹ In that case $\omega_0 \tau_0 = \omega_0 \frac{d}{c} \sin \theta$, where d is the spacing between hydrophones and c is the velocity of sound in water. With 2-ft hydrophone spacing, the values of $\omega_0 \frac{d}{c} = 1, 2$, and 4 chosen for the plot correspond to interference bandwidths of approximately 400 cps, 800 cps and 1600 cps respectively.

¹With the target in endfire position, the angular discrimination is substantially poorer because of the slower variation of τ_0 with θ . See discussion in Section III.



STUFFEL & ESSER CO., N. Y. MC. 289-11
20 x 20 in. sheet



III. Improvements in Detectability Through Use of Optimal Procedures

The basic theory of the likelihood ratio detector for Gaussian signals and noise is discussed in Report No. 3. Most of the general developments of that report remain applicable to the present problem. Thus if one writes the output of the j^{th} hydrophone as

$$e_j(t) = \sum_n A_j(n) \cos \omega_n t + B_j(n) \sin \omega_n t \quad (21)$$

then the $A_j(n)$ and $B_j(n)$ are independent Gaussian random variables with zero mean. If one writes

$$x_i(n) = \begin{cases} \frac{A_{\frac{i+1}{2}}(n)}{2} & i \text{ odd} \\ B_{\frac{i}{2}}(n) & i \text{ even} \end{cases} \quad (22)^1$$

and defines

$$\langle x_i(n) x_h(n) \rangle_S = p_{ih}(n) \quad (23)^2$$

$$\langle x_i(n) x_h(n) \rangle_N = q_{ih}(n) \quad (24)^2$$

then the output signal-to-noise ratio can be written simply in terms of the matrices $P(n)$ and $Q(n)$ whose elements are $p_{ih}(n)$ and $q_{ih}(n)$ respectively.

Thus one obtains

¹Note that the sequence x_1, x_2, \dots is here defined to correspond to $A_1, B_1, A_2, B_2, \dots$ rather than to $A_1, A_2, \dots, A_M, B_1, B_2, \dots, B_M$ as was done in Report No. 3. This is strictly a matter of computational convenience.

²In Report No. 3 p_{ih} and q_{ih} are normalized with respect to the signal and noise spectra. This is inconvenient here because ambient noise and interference may have different spectral functions.

$$\frac{\Delta(\text{DC output})}{D(\text{output})} = \frac{1}{\sqrt{2}} \sqrt{\sum_n \text{Tr} \left\{ \left[P(n) Q^{-1}(n) \right]^2 \right\}} \quad (25)$$

This expression follows directly from Report No. 3, Eqs. (11), (21) and (23). However, the simplification achieved in the earlier report by expressing the trace of the square of $P(n) Q^{-1}(n)$ in terms of the square of the trace is not applicable here since it depended on symmetry properties in the noise matrix that are present only in the isotropic case.

The primary computational problem is the inversion of the noise matrix. Since ambient noise and interference are independent, the Q matrix is actually the sum of a diagonal matrix (the ambient noise matrix) and a non-diagonal matrix (the interference matrix) which is the signal matrix for a target located in a direction other than that to which the array is steered. The ambient noise matrix has the diagonal elements $N(\omega_n)\Delta\omega$, where $N(\omega)$ is the ambient noise spectrum. Designating the interference spectrum by $I(\omega)$, it is a simple matter to write down the interference matrix (and hence the complete noise matrix) from Bryn's¹ expression for the elements of the signal matrix. The result is

¹F. Bryn, "Optimal signal processing of three-dimensional arrays operating on Gaussian signals and noise," J.A.S.A. 34, No. 3, pp. 289-297, March 1962.

$$Q(n) = I(\omega_n) \Delta \omega \times$$

	A_1	B_1	A_2	E_2	A_3	B_3	A_M	B_M
A_1	$1 + \frac{N(\omega_n)}{I(\omega_n)}$	0	$\cos \omega_n \tau_n$	$\sin \omega_n \tau_n$	$\cos 2\omega_n \tau_n$	$\sin 2\omega_n \tau_n$	$\cos(M-1)\omega_n \tau_n$	$\sin(M-1)\omega_n \tau_n$
B_1	0	$1 + \frac{N(\omega_n)}{I(\omega_n)}$	$-\sin \omega_n \tau_n$	$\cos \omega_n \tau_n$	$-\sin 2\omega_n \tau_n$	$\cos 2\omega_n \tau_n$	$-\sin(M-1)\omega_n \tau_n$	$\cos(M-1)\omega_n \tau_n$
A_2	$\cos \omega_n \tau_n$	$-\sin \omega_n \tau_n$	$1 + \frac{N(\omega_n)}{I(\omega_n)}$	0	$\cos \omega_n \tau_n$	$\sin \omega_n \tau_n$	$\cos(M-2)\omega_n \tau_n$	$\sin(M-2)\omega_n \tau_n$
B_2	$\sin \omega_n \tau_n$	$\cos \omega_n \tau_n$	0	$1 + \frac{N(\omega_n)}{I(\omega_n)}$	$-\sin \omega_n \tau_n$	$\cos \omega_n \tau_n$	$-\sin(M-2)\omega_n \tau_n$	$\cos(M-2)\omega_n \tau_n$
A_3	$\cos 2\omega_n \tau_n$	$-\sin 2\omega_n \tau_n$	$\cos \omega_n \tau_n$	$-\sin \omega_n \tau_n$	$1 + \frac{N(\omega_n)}{I(\omega_n)}$	0	$\cos(M-3)\omega_n \tau_n$	$\sin(M-3)\omega_n \tau_n$
B_3	$\sin 2\omega_n \tau_n$	$\cos 2\omega_n \tau_n$	$\sin \omega_n \tau_n$	$\cos \omega_n \tau_n$	0	$1 + \frac{N(\omega_n)}{I(\omega_n)}$	$-\sin(M-3)\omega_n \tau_n$	$\cos(M-3)\omega_n \tau_n$
\vdots	\vdots	\vdots						
A_M	$\cos(M-1)\omega_n \tau_n$	$-\sin(M-1)\omega_n \tau_n$	$\cos(M-2)\omega_n \tau_n$	$-\sin(M-2)\omega_n \tau_n$	$\cos(M-3)\omega_n \tau_n$	$-\sin(M-3)\omega_n \tau_n$	$1 + \frac{N(\omega_n)}{I(\omega_n)}$	0
B_M	$\sin(M-1)\omega_n \tau_n$	$\cos(M-1)\omega_n \tau_n$	$\sin(M-2)\omega_n \tau_n$	$\cos(M-2)\omega_n \tau_n$	$\sin(M-3)\omega_n \tau_n$	$\cos(M-3)\omega_n \tau_n$	0	$1 + \frac{N(\omega_n)}{I(\omega_n)}$

The inversion of this matrix is accomplished in Appendix A. The result is

$$Q^{-1}(u) = \frac{1}{N(\omega_n)\Delta\omega} \frac{1}{M + \frac{N(\omega_n)}{I(\omega_n)}} \times$$

$\frac{N(\omega_n)}{(M-1) + \frac{N(\omega_n)}{I(\omega_n)}}$	0	$-\cos \omega_n \tau_0$	$-\sin \omega_n \tau_0$	$-\cos 2\omega_n \tau_0$	$-\sin 2\omega_n \tau_0$...	$-\cos(M-1)\omega_n \tau_0$	$-\sin(M-1)\omega_n \tau_0$
0	$\frac{N(\omega_n)}{(M-1) + \frac{N(\omega_n)}{I(\omega_n)}}$	$\sin \omega_n \tau_0$	$-\cos \omega_n \tau_0$	$\sin 2\omega_n \tau_0$	$-\cos 2\omega_n \tau_0$...	$\sin(M-1)\omega_n \tau_0$	$-\cos(M-1)\omega_n \tau_0$
$-\cos \omega_n \tau_0$	$\sin \omega_n \tau_0$	$\frac{N(\omega_n)}{(M-1) + \frac{N(\omega_n)}{I(\omega_n)}}$	0	$-\cos \omega_n \tau_0$	$-\sin \omega_n \tau_0$...	$-\cos(M-2)\omega_n \tau_0$	$-\sin(M-2)\omega_n \tau_0$
$-\sin \omega_n \tau_0$	$-\cos \omega_n \tau_0$	0	$\frac{N(\omega_n)}{(M-1) + \frac{N(\omega_n)}{I(\omega_n)}}$	$\sin \omega_n \tau_0$	$-\cos \omega_n \tau_0$		$\sin(M-2)\omega_n \tau_0$	$-\cos(M-2)\omega_n \tau_0$
$-\cos 2\omega_n \tau_0$	$\sin 2\omega_n \tau_0$	$-\cos \omega_n \tau_0$	$\sin \omega_n \tau_0$	$\frac{N(\omega_n)}{(M-1) + \frac{N(\omega_n)}{I(\omega_n)}}$	0		$-\cos(M-3)\omega_n \tau_0$	$-\sin(M-3)\omega_n \tau_0$
$-\sin 2\omega_n \tau_0$	$-\cos 2\omega_n \tau_0$	$-\sin \omega_n \tau_0$	$\cos \omega_n \tau_0$	0	$\frac{N(\omega_n)}{(M-1) + \frac{N(\omega_n)}{I(\omega_n)}}$		$\sin(M-3)\omega_n \tau_0$	$-\cos(M-3)\omega_n \tau_0$
.
$-\cos(M-1)\omega_n \tau_0$	$\sin(M-1)\omega_n \tau_0$	$-\cos(M-2)\omega_n \tau_0$	$\sin(M-2)\omega_n \tau_0$	$-\cos(M-3)\omega_n \tau_0$	$\sin(M-3)\omega_n \tau_0$		$\frac{N(\omega_n)}{(M-1) + \frac{N(\omega_n)}{I(\omega_n)}}$	0
$-\sin(M-1)\omega_n \tau_0$	$-\cos(M-1)\omega_n \tau_0$	$-\sin(M-2)\omega_n \tau_0$	$\cos(M-2)\omega_n \tau_0$	$-\sin(M-3)\omega_n \tau_0$	$\cos(M-3)\omega_n \tau_0$		0	$\frac{N(\omega_n)}{(M-1) + \frac{N(\omega_n)}{I(\omega_n)}}$

With the array steered on target¹ the signal matrix is

$$P(n) = S(\omega_n) \Delta \omega \begin{bmatrix} 1 & 0 & 1 & 0 & 1 & 0 \\ 0 & 1 & 0 & 1 & 0 & 1 \\ 1 & 0 & 1 & 0 & 1 & 0 \\ 0 & 1 & 0 & 1 & 0 & 1 \\ 1 & 0 & 1 & 0 & 1 & 0 \\ 0 & 1 & 0 & 1 & 0 & 1 \end{bmatrix} \quad (28)^2$$

The computation of $\text{Tr} \left\{ [P(n) Q^{-1}(n)]^2 \right\}$ is tedious but basically straightforward. Details are given in Appendix B. The result is

$$\text{Tr} \left\{ [P(n) Q^{-1}(n)]^2 \right\} = \frac{S^2(\omega_n)}{N^2(\omega_n)} \frac{2}{\left[M + \frac{N(\omega_n)}{I(\omega_n)} \right]^2} \left\{ M \left[M-1 + \frac{N(\omega_n)}{I(\omega_n)} \right] - 2 \sum_{\ell=1}^{M-1} (M-\ell) \cos \ell \omega_n \tau_0 \right\}^2 \quad (29)$$

Substitution into Eq. (25) yields the output signal-to-noise ratio

$$\frac{\Delta(\text{DC output})}{D(\text{output})} = \sqrt{\sum_n \left\{ \frac{S(\omega_n)}{N(\omega_n)} \frac{M \left[M-1 + \frac{N(\omega_n)}{I(\omega_n)} \right] - 2 \sum_{\ell=1}^{M-1} (M-\ell) \cos \ell \omega_n \tau_0}{M + \frac{N(\omega_n)}{I(\omega_n)}} \right\}^2} \quad (30)$$

¹Steering may be mechanical or electrical. In the latter case the parameter τ_0 of the noise matrix must be interpreted as the difference between the interference delay and signal delay from hydrophone to hydrophones. Electrical steering implies the insertion of delay at the output of each hydrophone. Since no information is destroyed by this operation, the performance of the likelihood ratio detector is not affected by it. Hence with proper interpretation of τ_0 the results obtained here are valid for any target bearing relative to the τ_0 array axis.

²Note this is simply Eq. (26) with $\tau_0 = 0$, $N(\omega_n) = 0$ and $I(\omega_n) = S(\omega_n)$.

If the observation time $T = \frac{2\pi}{\Delta\omega}$ is sufficiently large so that none of the ω_n -dependent terms in Eq. (30) change significantly over an interval $\Delta\omega$, the output signal-to-noise ratio can be written in integral form [see Report No. 3, Eq. (29)].

$$\frac{\Delta(\text{DC output})}{D(\text{output})} = \sqrt{\frac{T}{2\pi}} \sqrt{\int_{\omega_1}^{\omega_2} \left\{ \frac{S(\omega)}{N(\omega)} \frac{M \left[M-1 + \frac{N(\omega)}{I(\omega)} \right] - 2 \sum_{\ell=1}^{M-1} (M-\ell) \cos \ell \omega \tau_0}{M + \frac{N(\omega)}{I(\omega)}} \right\}^2 d\omega} \quad (31)$$

$\omega_1 \leq \omega \leq \omega_2$ is the frequency range (in rad/sec) processed by the detector.

If $\frac{N(\omega)}{I(\omega)} \gg M$ for all ω in $\omega_1 \leq \omega \leq \omega_2$, i.e., if the dominant noise is ambient noise, then Eq. (31) reduces to

$$\frac{\Delta(\text{DC output})}{D(\text{output})} \approx \sqrt{\frac{T}{2\pi}} M \sqrt{\int_{\omega_1}^{\omega_2} \left[\frac{S(\omega)}{N(\omega)} \right]^2 d\omega} \quad (32)$$

Comparison with Report No. 3, Eq. (32), indicates that this is simply the output signal-to-noise ratio of a likelihood ratio detector operating in an isotropic Gaussian noise field uncorrelated from hydrophone to hydrophone.

On the other hand, if $\frac{N(\omega)}{I(\omega)} \ll M-1$ for all ω in $\omega_1 \leq \omega \leq \omega_2$ (and $\tau_0 \neq 0$), Eq. (31) becomes

$$\frac{\Delta(\text{DC output})}{D(\text{output})} \approx \sqrt{\frac{T}{2\pi}} \sqrt{\int_{\omega_1}^{\omega_2} \left[\frac{S(\omega)}{N(\omega)} \right]^2 \left[M-1 - \frac{2}{M} \sum_{\ell=1}^{M-1} (M-\ell) \cos \ell \omega \tau_0 \right]^2 d\omega} \quad (33)$$

Eqs. (32) and (33) clearly show two important differences between the likelihood ratio detector and the conventional detector [characterized by Eq. (18)]:

- 1) The effective input signal-to-noise ratio of the likelihood ratio detector is $\frac{S(\omega)}{N(\omega)}$ for high as well as low levels of interference. For the conventional detector the effective input noise power is I when the interference becomes dominant.
- 2) The output signal-to-noise ratio of the likelihood ratio detector increases with M for high as well as low levels of interference. For the conventional detector the output signal-to-noise ratio varies only as \sqrt{M} once the interference becomes dominant.

In the special case $\tau_0 = 0$ (interference aligned in bearing with the target)

$$\sum_{l=1}^{M-1} (M-l) \cos l\omega\tau_0 = \frac{M(M-1)}{2} \quad (34)$$

Thus the terms independent of $\frac{N(\omega)}{I(\omega)}$ in the numerator of Eq. (31) cancel and one obtains

$$\frac{\Delta(\text{DC output})}{D(\text{output})} = \sqrt{\frac{T}{2\pi}} \sqrt{\int_{\omega_1}^{\omega_2} \left[\frac{M \frac{S(\omega)}{I(\omega)}}{M + \frac{N(\omega)}{I(\omega)}} \right]^2 d\omega} \quad (35)$$

In this case, as one would expect, the likelihood ratio detector shows the same type of behavior as the conventional detector (i.e., dependence of output signal-to-noise ratio on $\frac{S(\omega)}{N(\omega)}$ and M for $\frac{N(\omega)}{I(\omega)} \gg M$ and on $\frac{S(\omega)}{I(\omega)}$ and \sqrt{M} for $\frac{N(\omega)}{I(\omega)} \ll M$).¹ Any advantage it may still possess over the conventional detector depends strictly on its ability to discriminate between the spectral properties of signal, noise and interference, rather than on spatial anisotropy of the noise field. If $\tau_0 \neq 0$ but small, i.e., if the interference is located at a bearing close to but not identical with that of the target, the cancellation leading to Eq. (35) will not be

¹See Eq. (20).

perfect. Since the now no longer perfectly cancelled terms in the numerator of Eq. (31) depend on M^2 , they will eventually dominate. However, in this case the inequality $\frac{N(\omega)}{I(\omega)} \ll M-1$ may have to be quite strong before the asymptotic expression of Eq. (33) becomes valid.

In order to compare the ability of the likelihood ratio detector and conventional detector to resolve in angle a weak target from a nearby strong interference, it will be of interest to construct a curve similar to Fig. 2 for the likelihood-ratio detector. For that purpose let $S(\omega) = \frac{S}{N} N(\omega) = \frac{S}{I} I(\omega)$ over the band processed, i.e. assume that signal, noise and interference have spectral functions of the same form though not necessarily of the same power level.

With $\omega_1 = 0$ Eq. (31) now assumes the form

$$\begin{aligned} \frac{\Delta(\text{DC output})}{D(\text{output})} &= \sqrt{\frac{T}{2\pi}} \frac{\frac{S}{N}}{M + \frac{N}{I}} \sqrt{\int_0^{\omega_2} \left[M \left(M-1 + \frac{N}{I} \right) - 2 \sum_{\ell=1}^{M-1} (M-\ell) \cos \ell \omega \tau_0 \right]^2 d\omega} \\ &= \sqrt{\frac{T\omega_2}{2\pi}} \frac{\frac{S}{N}}{M + \frac{N}{I}} \left\{ M^2 \left(M-1 + \frac{N}{I} \right)^2 - 4M \left(M-1 + \frac{N}{I} \right) \sum_{\ell=1}^{M-1} (M-\ell) \frac{\sin \ell \omega_2 \tau_0}{\ell \omega_2 \tau_0} \right. \\ &\quad \left. + 2 \sum_{\ell=1}^{M-1} \sum_{r=1}^{M-1} (M-\ell)(M-r) \left[\frac{\sin(\ell-r)\omega_2 \tau_0}{(\ell-r)\omega_2 \tau_0} + \frac{\sin(\ell+r)\omega_2 \tau_0}{(\ell+r)\omega_2 \tau_0} \right] \right\}^{1/2} \quad (36) \end{aligned}$$

The asymptotic form ($\omega_2 \tau_0 \gg 1$) of Eq. (36) corresponding to Eq. (18) is

$$\begin{aligned} \frac{\Delta(\text{DC output})}{D(\text{output})} &= \sqrt{\frac{T\omega_2}{2\pi}} \frac{\frac{S}{N} M(M-1 + \frac{N}{I})}{M + \frac{N}{I}} \sqrt{1 + \frac{1}{3} \frac{(M-1)(2M-1)}{M(M-1 + \frac{N}{I})^2}} \\ &\approx \sqrt{\frac{T\omega_2}{2\pi}} \frac{\frac{S}{N} M(M-1 + \frac{N}{I})}{M + \frac{N}{I}} = \sqrt{\frac{T\omega_2}{2\pi}} \frac{S}{N} (M-1) \frac{1 + \frac{1}{M-1} \frac{N}{I}}{1 + \frac{1}{M} \frac{N}{I}} \\ &\text{for } M \gg 1 \quad (37)^1 \end{aligned}$$

If $\frac{N}{I} \ll M-1$ this reduces to

$$\frac{\Delta(\text{DC output})}{D(\text{output})} \approx \sqrt{\frac{T\omega_2}{2\pi}} \frac{S}{N} (M-1) \quad (38)$$

In the absence of interference the output signal-to-noise ratio of the likelihood-ratio detector is [from Report No. 3, Eq. (32)]

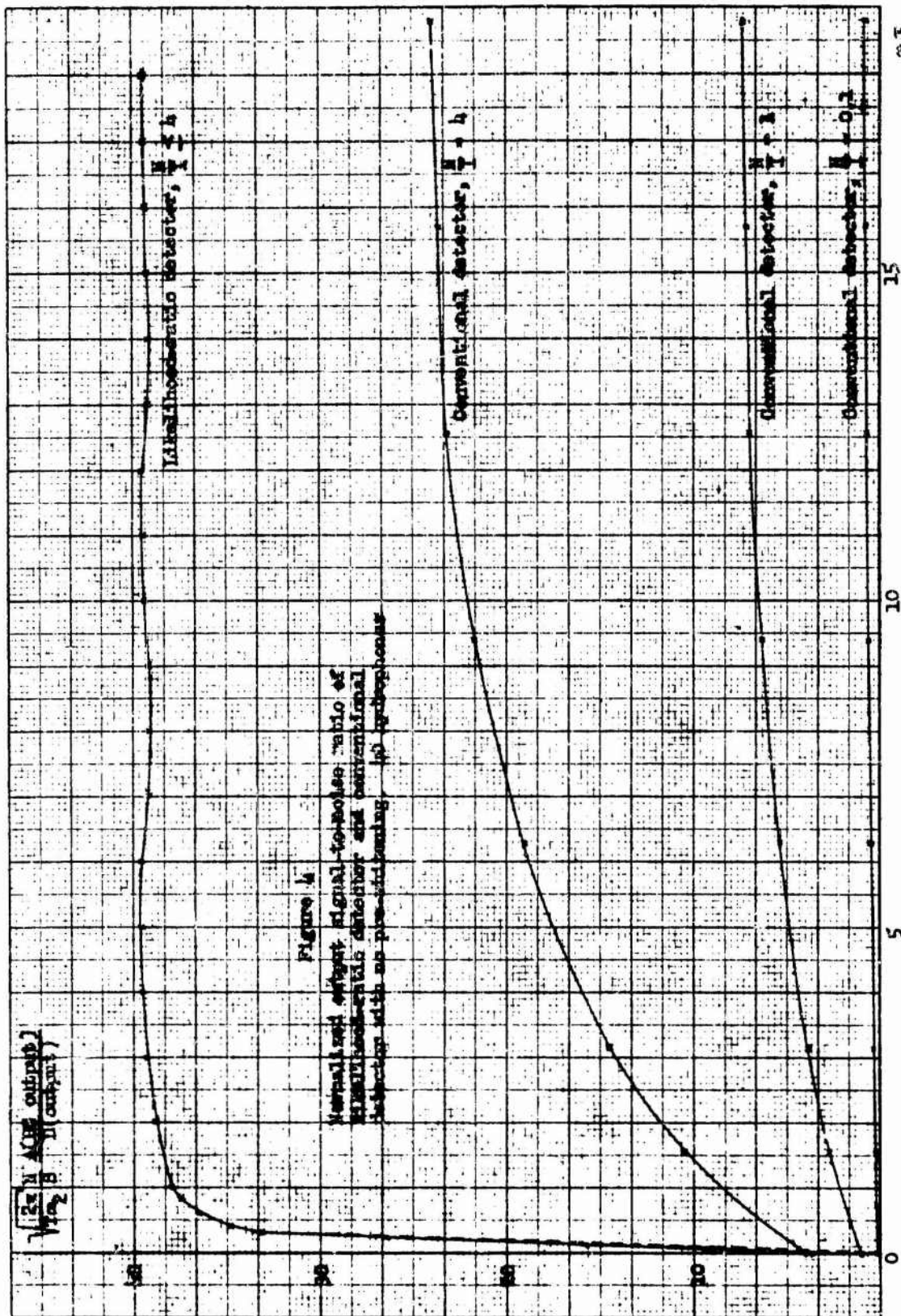
$$\frac{\Delta(\text{DC output})}{D(\text{output})} = \sqrt{\frac{T\omega_2}{2\pi}} \frac{S}{N} M \quad (39)$$

Comparison of Eqs. (38) and (39) suggests that complete elimination of the interference is accomplished at the expense of one degree of freedom, i.e. the performance of the detector in the presence of strong interference as well as ambient noise is the same as that of a similar array (same hydrophone spacing) operating in ambient noise only but having one less hydrophone. The last version of Eq. (37) indicates that for $\frac{N}{I}$ not very small compared with $M-1$ the output signal-to-noise ratio is somewhat larger than the figure given by Eq. (38). The radical in the first form of Eq. (37) can only increase the result. Thus the elimination of interference is actually accomplished at a cost of somewhat less than one degree of freedom. Whether these statements are true under other than the asymptotic conditions considered here remains to be investigated.

¹It is clear from Figs. 4 and 5 that this approximation becomes very good for values of $\omega_2 \tau_0$ exceeding unity by only a relatively small amount.

Figure 4 shows Eq. (36), normalized with respect to $\sqrt{\frac{T\omega_2}{2\pi}} \frac{S}{N}$, plotted as a function of $\omega_2\tau_0$ for $M = 40$. For $\frac{N}{I} \leq 4$ the variation in output signal-to-noise ratio with $\frac{N}{I}$ is too small to be observable on the scale of this graph, except near $\omega_2\tau_0 = 0$. Figure 5 gives the equivalent picture for $M = 10$. Comparison with the conventional detector [Eq. (16)] is complicated by the fact that Eq. (16) depends on $\omega_0\tau_0$, not on the variable $\omega_2\tau_0$ appearing in Eq. (36). ω_0 is the frequency at which signal, noise and interference spectra reach half of their low-frequency values. ω_2 , on the other hand, is a rather arbitrary limitation on the frequency band processed by the likelihood-ratio detector.¹ Since the analysis of the conventional detector implies the absence of any band-limitation imposed by the detector, a reasonable comparison demands that one choose ω_2 appreciably larger than ω_0 . An acceptable value might be $\omega_2 = \pi \omega_0$, which makes the multiplying constants of Eqs. (16) and (36) equal. For the signal bandwidths mentioned in Section III (400 cps - 1600 cps) this corresponds to detector bandwidths of 1250 cps - 5000 cps, which certainly does not appear excessive. Hence the conventional detector curves for $\frac{N}{I} = 0.1, 1$ and 4 appearing on Figs. 4 and 5 were derived from Eq. (16) by choosing $\omega_2 = \pi \omega_0$ and normalizing with respect to $\sqrt{\frac{T\omega_2}{2\pi}} \frac{S}{N}$. It is clear from comparison of the curves that the likelihood-ratio detector exhibits distinctly superior angular discrimination near the interference location. In addition, of course, there is the expected improvement in detectability for targets remote in

¹In practice it is determined by the fact that, counter to the assumption $S(\omega) = \frac{S}{N} N(\omega) = \frac{S}{I} I(\omega)$, the input signal-to-noise ratio becomes negligible above some finite frequency. See discussion in Report No. 3.



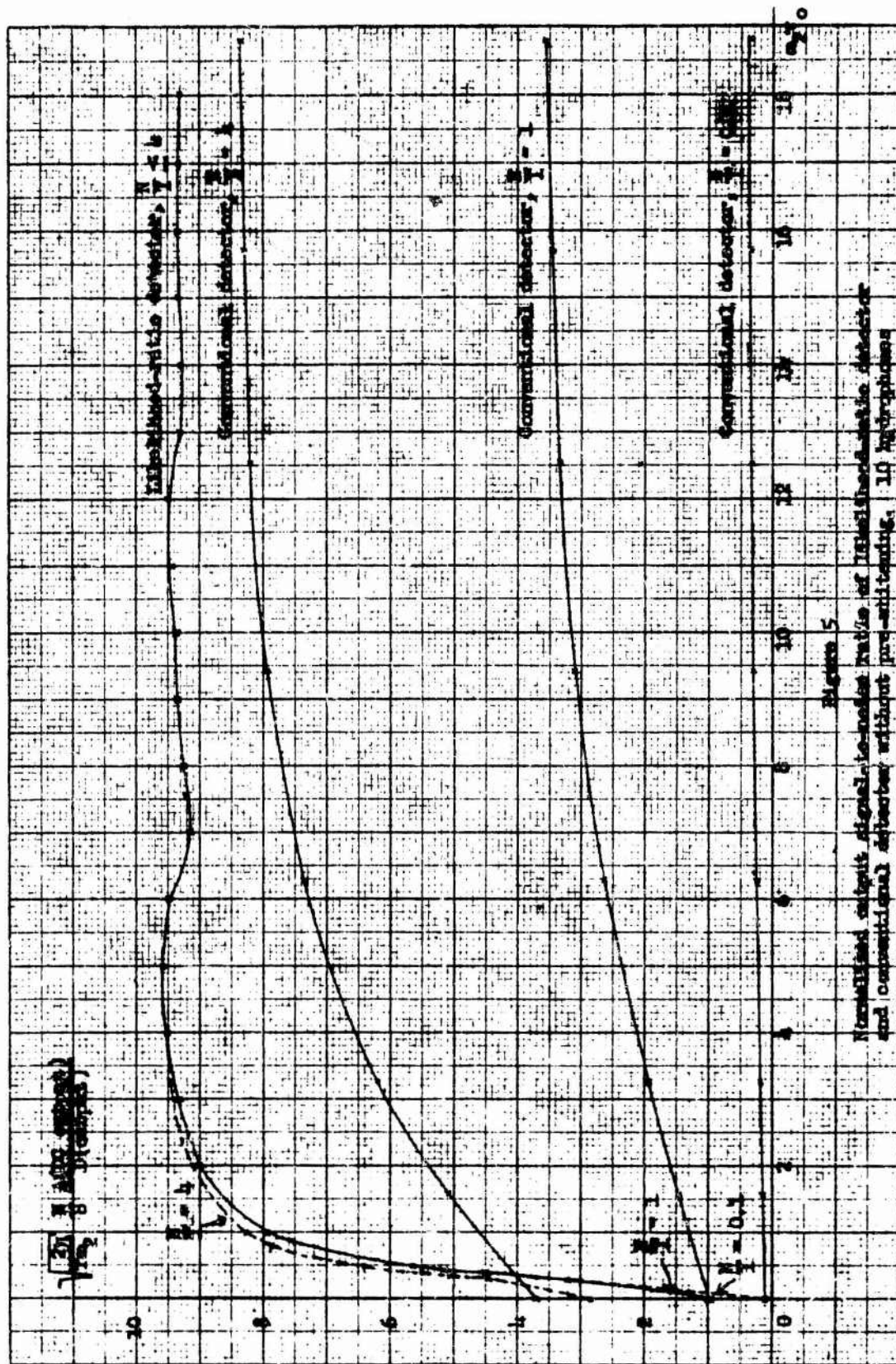


Figure 5
Normalized output signal-to-noise ratio of threshold detector
and conventional detector without pre-whitening, 10 hydrophones

bearing from the interference. Both advantages remain significant even for $\frac{N}{I} \geq 1$, as long as the number of hydrophones is sufficiently large.¹

In order to avoid misinterpretation of Figs. 4 and 5, one should keep in mind that the postulated "conventional detector" is a very simple device: It consists exclusively of delay (beam formation) addition, squaring and smoothing. For the case under study here - signal, ambient noise and interference spectra of the same shape - one could obviously improve system performance by the very simple procedure of introducing a pre-whitening (Eckart) filter. This is not in general the optimum linear filter, but it is simple and previous work suggests² that it realizes most of the gain available through linear filtering techniques. With such a pre-whitening filter the normalized autocorrelation functions corresponding to Eq. (3) are

$$\rho_1(\tau) = \rho_n(\tau) = \frac{\sin \omega_2 \tau}{\omega_2 \tau} \quad (40)$$

where ω_2 is the upper end of the frequency ranged processed by the detector. Then from Eq. (6)

$$C_{r,s} = \int_{-\infty}^{\infty} \frac{\sin \omega_2 (r\tau_0 + \tau)}{\omega_2 (r\tau_0 + \tau)} \frac{\sin \omega_2 (s\tau_0 + \tau)}{\omega_2 (s\tau_0 + \tau)} d\tau \quad (41)$$

With the change of variable $x = \omega_2 (r\tau_0 + \tau)$ this becomes

$$C_{r,s} = \frac{1}{\omega_2} \int_{-\infty}^{\infty} \frac{\sin x}{x} \frac{\sin [\omega_2 (r-s)\tau_0 - x]}{\omega_2 (r-s)\tau_0 - x} dx \quad (42)$$

¹The fact that the conventional detector curve falls somewhat above that of the likelihood-ratio detector at $\omega_2 \tau_0 = 0$ (particularly for $N/I = 4$, $M = 10$) may be attributed to the assumption that the conventional detector is not bandlimited whereas the likelihood-ratio detector completely discards all frequencies above ω_2 .

²C. Kapp, "A Power detector with optimal prefiltering for detecting directional Gaussian signals in Gaussian noise fields," GD/EB Report U417-64-009, February 1964.

Equation (42) is of the form

$$C_{r,s}(y) = \frac{1}{\omega_2} \int_{-\infty}^{\infty} f(x) f(y-x) dx \quad (43)$$

where $f(x) = \frac{\sin x}{x}$ and $y = \omega_2(r-s)\tau_0$.

Fourier transforming Eq. (43), one obtains

$$\int_{-\infty}^{\infty} C_{r,s}(y) e^{-j\lambda y} dy = \frac{1}{\omega_2} \left[\int_{-\infty}^{\infty} f(x) e^{-j\lambda x} dx \right]^2 = \begin{cases} \frac{\pi^2}{\omega_2^2} & \text{for } |\lambda| \leq 1 \\ 0 & \text{for } |\lambda| > 1 \end{cases} \quad (44)$$

It follows that

$$C_{r,s}(y) = \frac{1}{2\pi} \frac{\pi^2}{\omega_2} \int_{-1}^1 e^{jy\lambda} d\lambda = \frac{\pi}{\omega_2} \frac{\sin y}{y} \quad (45)$$

Upon reinserting the definition of y ,

$$C_{r,s} = \frac{\pi}{\omega_2} \frac{\sin \omega_2(r-s)\tau_0}{\omega_2(r-s)\tau_0} \quad (46)$$

Equation (46) clearly satisfies conditions (9), so that it can be used directly in Eq. (10). The desired output signal-to-noise ratio follows almost immediately.

$$\frac{A(\text{DC output})}{D(\text{output})} = \sqrt{\frac{T\omega_2}{2\pi N}} \frac{S}{\sqrt{1 + \frac{I^2}{N^2} \left\{ 1 + \frac{1}{M} \sum_{s=1}^{M-1} (M-s) \frac{\sin \omega_2 s \tau_0}{\omega_2 s \tau_0} + \frac{2}{M^2} \sum_{r=1}^{M-1} \sum_{s=1}^{M-1} (M-r)(M-s) \left[\frac{\sin \omega_2(r-s)\tau_0}{\omega_2(r-s)\tau_0} + \frac{\sin \omega_2(r+s)\tau_0}{\omega_2(r+s)\tau_0} \right] \right\}}} \quad (47)^2$$

¹Strictly speaking, the values of S , N and I appearing in Eq. (47) are average powers after pre-whitening. However, since all spectra have the same shape, the filter has the same effect on each, so that the ratios S/N and I/N appearing in Eq. (47) may still be interpreted as input power ratios.

When $\omega_2 \tau_0 \gg 1$, Eq. (47) reduces to

$$\frac{\Delta(\text{DC output})}{D(\text{output})} = \sqrt{\frac{T\omega_2}{2\pi}} \frac{MS}{\sqrt{N^2 + \frac{I^2}{3} \left(2M + \frac{1}{M}\right)}} \quad (48)$$

This is identical with Eq. (18) except for the replacement of ω_0 with $\frac{\omega_2}{\pi}$. Thus with the relation $\omega_2 = \pi\omega_0$ employed in Figs. 4 and 5, the asymptotic value of output signal-to-noise ratio for large angular differences between target and interference is unaffected by pre-whitening.

For $\tau_0 = 0$, Eq. (47) reduces to the expression

$$\frac{\Delta(\text{DC output})}{D(\text{output})} = \sqrt{\frac{T\omega_2}{2\pi}} \frac{MS}{\sqrt{N^2 + I^2 M^2}} \quad (49)$$

For $\omega_2 = \pi\omega_0$ this is identical with Eq. (20), the corresponding expression for the conventional detector without Eckart filter.

Figure 6 shows plots of Eq. (47) normalized with respect to $\sqrt{\frac{T\omega_2}{2\pi}} \frac{S}{N}$ for $M = 40$ and $\frac{N}{I} = 4, 1$ and 0.1 . Corresponding curves for the conventional detector without pre-whitening are also included to indicate the improvement in angular discrimination attainable through pre-whitening.

Figure 7 gives the actual dependence on interference bearing of the normalized output signal-to-noise ratio with the target in broadside location. Curves are given for the likelihood-ratio detector as well as the conventional detector with and without pre-whitening. All curves are based on the parameter values: $M = 40$, $\frac{N}{I} = 4$, $\omega_2 = 2\pi \times 5000$ rad/sec, hydrophone spacing $d = 2$ ft.

Equivalent results for a target in other than broadside location are readily obtained from the following considerations. Suppose the target bearing (relative to the normal to the array axis) is θ_0 and the interference

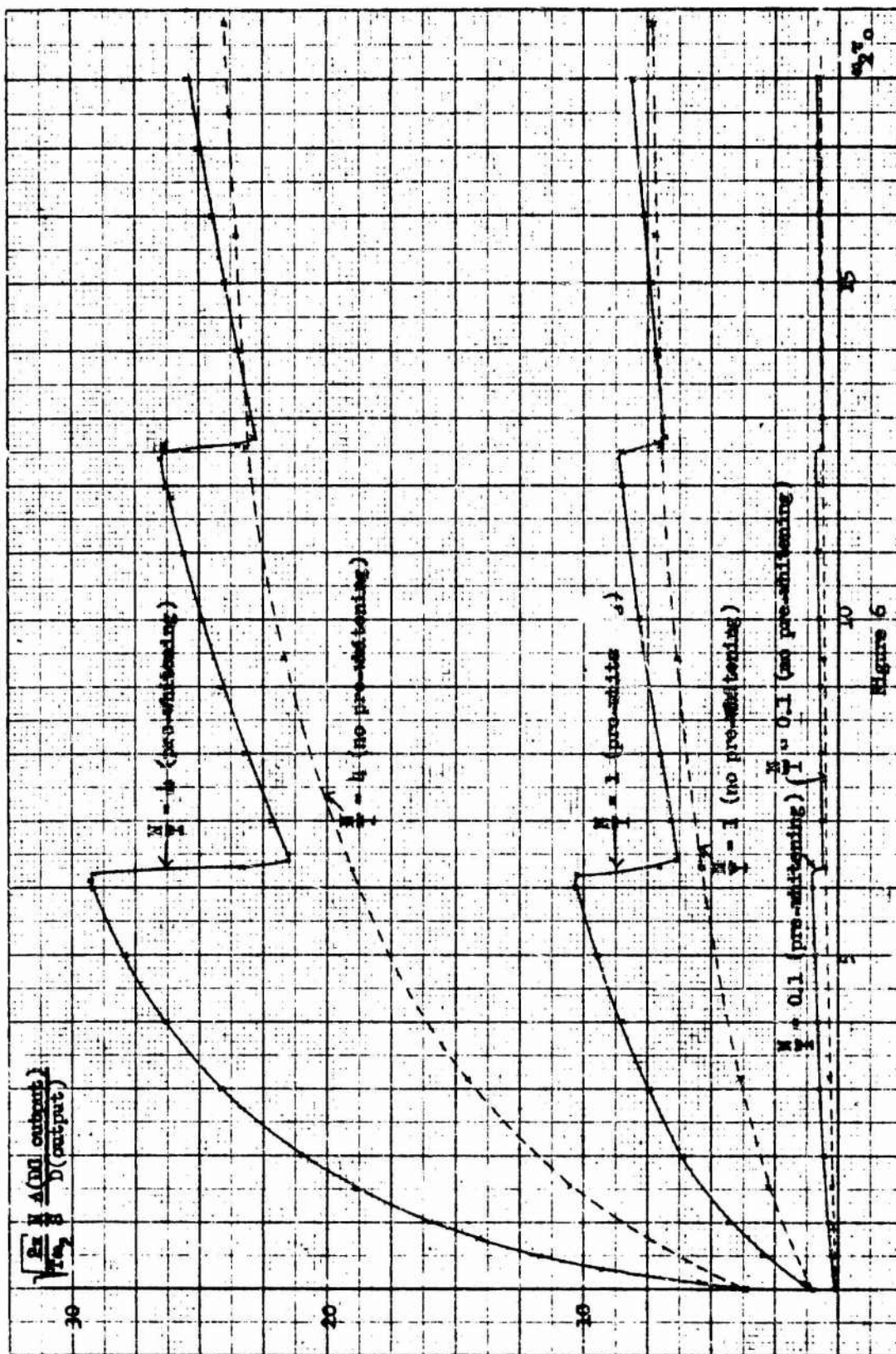


Figure 6

Normalized signal-to-noise ratio of conventional detector with and without pre-whitening. 40 hydrophones.

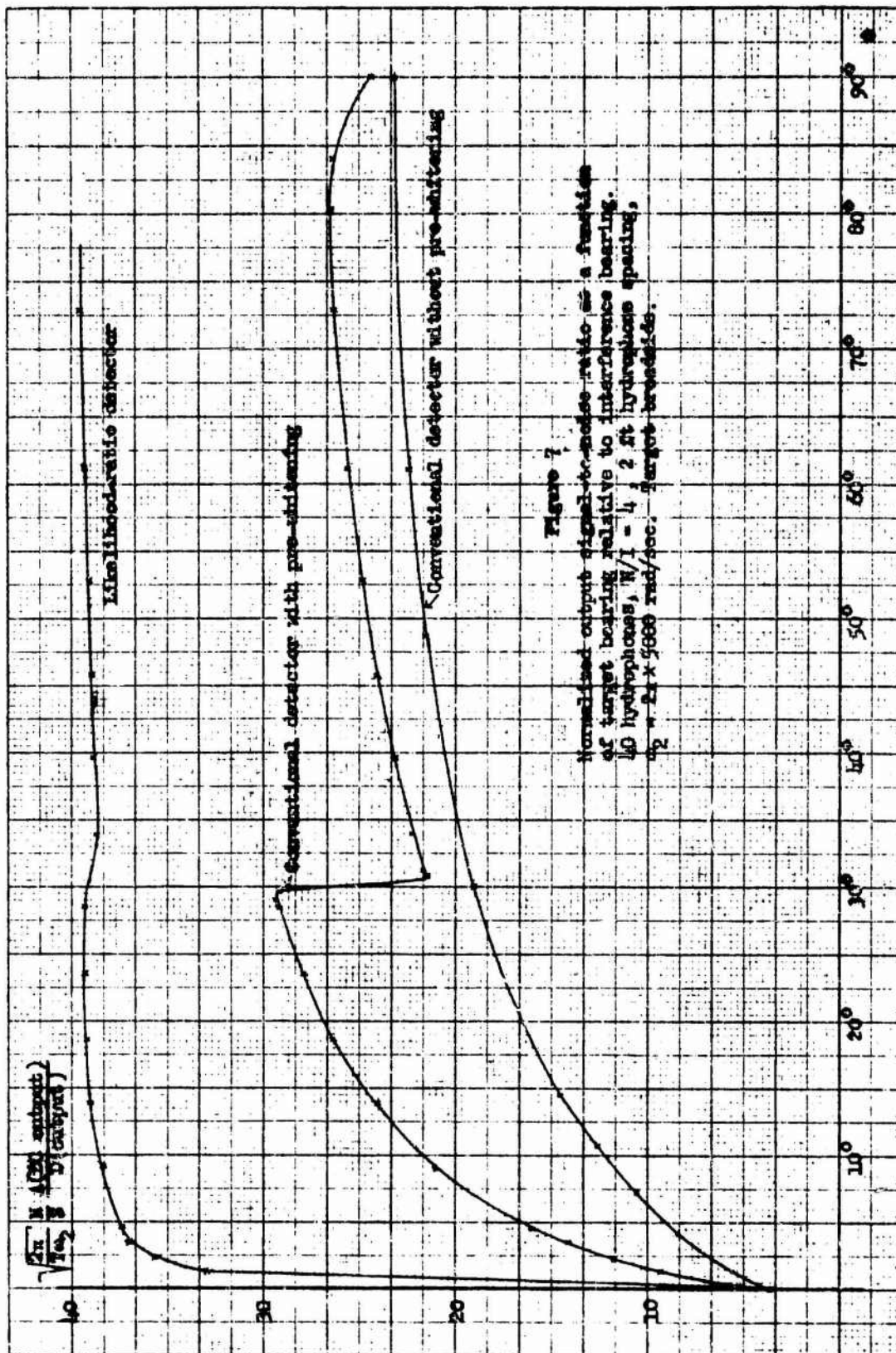


Figure 7
 Normalized output signal-to-noise ratio as a function
 of target bearing relative to interference bearing.
 100 hydrophones, $N/I = 4$; 2 ft hydrophone spacing,
 $\omega_2 = 2\pi \times 5000$ rad/sec. Target broadside.

bearing relative to the target bearing is θ (see Fig. 8). Then the signal delay from hydrophone to hydrophone is $\frac{d}{c} \sin \theta_0$ while the interference delay from hydrophone to hydrophone is $\frac{d}{c} \sin(\theta_0 + \theta)$. As mentioned on page 18 (footnote 1) the parameter τ_0 must be interpreted as the difference between these two delays. Hence

$$\tau_0 = \frac{d}{c} [\sin(\theta_0 + \theta) - \sin \theta_0] \quad (50)$$

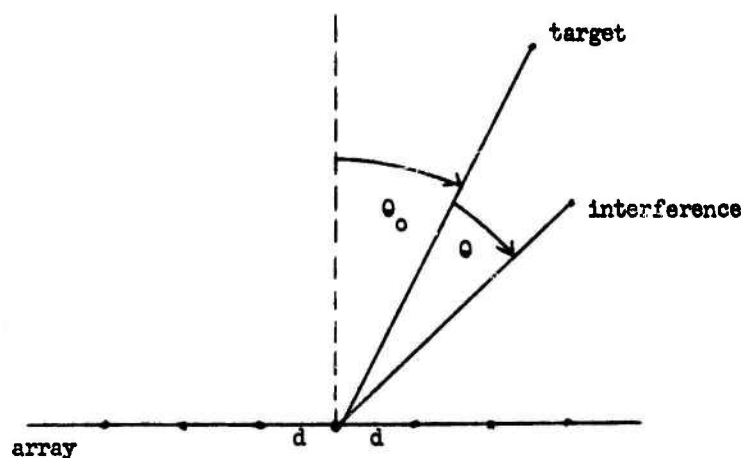


Figure 8

For $\theta_0 = 0$ (broadside condition) this reduces to the expression

$$\tau_0 = \frac{d}{c} \sin \theta \quad (51)$$

used previously. For $\theta_0 = \frac{\pi}{2}$ (endfire condition) one obtains

$$\tau_0 = \frac{d}{c} (\cos \theta - 1) \quad (52)$$

For small values of θ , Eq. (52) varies more slowly with θ than does Eq. (51). Thus the detectability of targets in the presence of interference is poorer in the endfire condition than in the broadside condition. This is illustrated by Fig. 9, which is the equivalent of Fig. 7 with an endfire target. Corresponding curves for other target locations will clearly fall between Figs. 7 and 9.

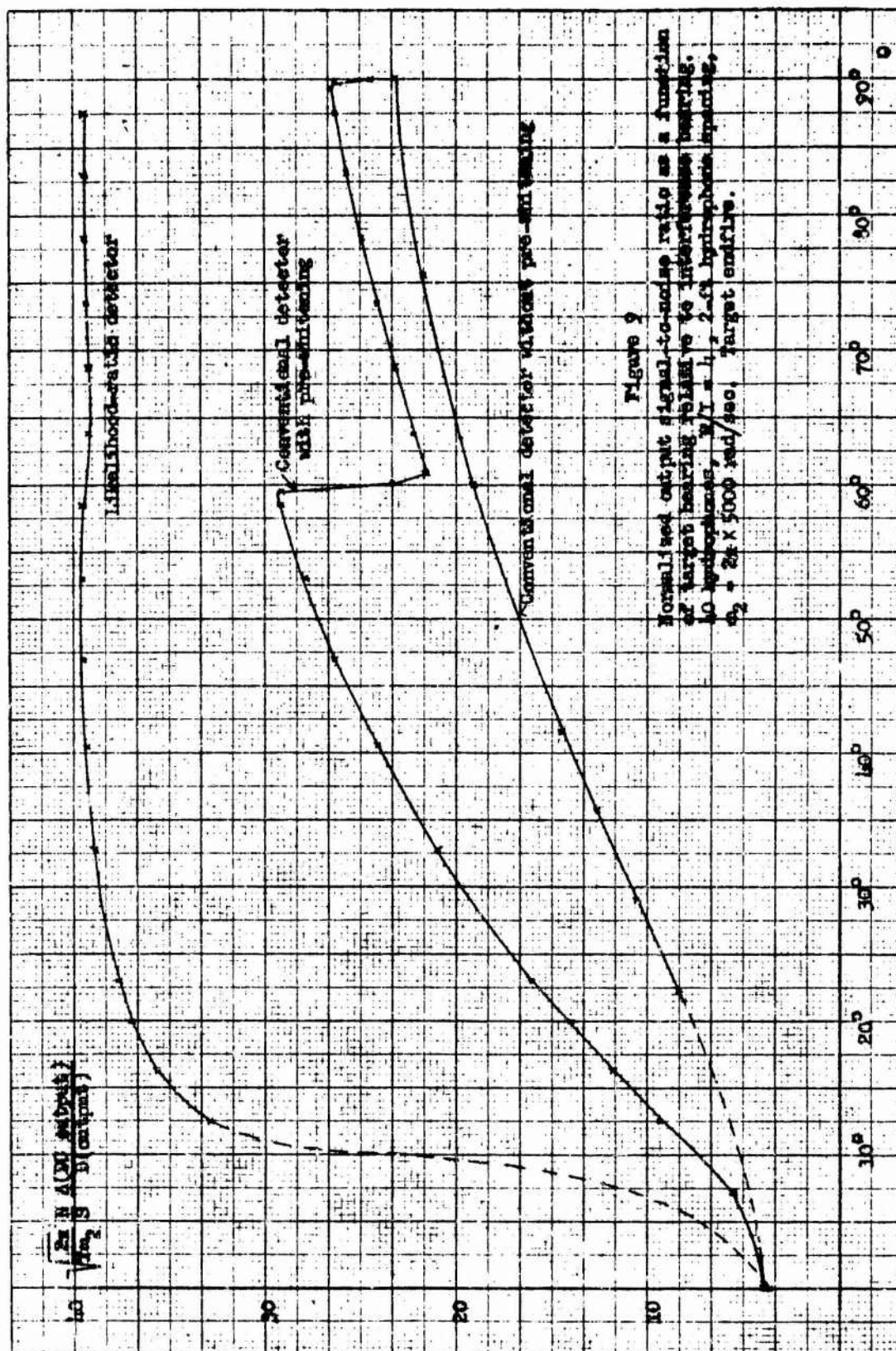


Figure 9

Normalized output signal-to-noise ratio as a function of target bearing relative to interference bearing. 40 hydrophones, $\omega_1 = 1$, $\omega_2 = 2$ kHz hydrophone spacing, $\omega_2 = 2 \times 5000 \text{ rad/sec}$, target endfire.

IV. Error Probabilities

The parameters of ultimate interest in characterizing the performance of a detector are the error probabilities. If the observation time is sufficiently long so that the detector output may be regarded as Gaussian, then it is a simple matter to convert output signal-to-noise ratio into error probabilities. Under this assumption the output probability density of the detector in the presence of signal is

$$f(x/S) = \frac{1}{\sqrt{2\pi} \sigma} e^{-\frac{(x-m_1)^2}{2\sigma^2}} \quad (53)$$

Here σ is the standard deviation of the detector output [D(output) in the nomenclature used earlier in this report] and m_1 is the mean value of the detector output in the presence of signal. In the absence of signal the output probability density is

$$f(x/0) = \frac{1}{\sqrt{2\pi} \sigma} e^{-\frac{(x-m_2)^2}{2\sigma^2}} \quad (54)$$

where m_2 is the mean value of the output in the absence of signal. Strictly speaking, the output standard deviation is not the same in the presence and absence of signal. However, if the input signal-to-noise ratio at each hydrophone is small, the fluctuation power at the output is almost entirely due to noise. Thus the use of the same value of σ in Eqs. (53) and (54) is consistent with the assumption of small input signal-to-noise ratio underlying all other computations in this report.

If a detection threshold K is employed, the false alarm probability α (probability of deciding that signal is present when there is none) is

$$\alpha = \frac{1}{\sqrt{2\pi} \sigma} \int_K^{\infty} e^{-\frac{(x-m_2)^2}{2\sigma^2}} dx \quad (55)$$

With the change of variable $\frac{x-m_2}{\sqrt{2}\sigma} = y$ this becomes

$$\alpha = \frac{1}{\sqrt{\pi}} \int_{\frac{K-m_2}{\sqrt{2}\sigma}}^{\infty} e^{-y^2} dy = \frac{1}{2} \left[1 - \operatorname{erf} \left(\frac{K-m_2}{\sqrt{2}\sigma} \right) \right] \quad (56)$$

where

$$\operatorname{erf} x = \frac{2}{\sqrt{\pi}} \int_0^x e^{-y^2} dy \quad (57)$$

Similarly the miss probability β (probability of deciding signal absent when in fact signal is present) is given by

$$\begin{aligned} \beta &= \frac{1}{\sqrt{2\pi} \sigma} \int_{-\infty}^K e^{-\frac{(x-m_1)^2}{2\sigma^2}} dx \\ &= \frac{1}{2} \left[1 + \operatorname{erf} \frac{K-m_1}{\sqrt{2}\sigma} \right] \end{aligned} \quad (58)$$

The threshold K can be eliminated between Eqs. (56) and (58). Thus from Eq. (56)

$$K = m_2 + \sqrt{2} \sigma \operatorname{erf}^{-1}(1-2\alpha) \quad (59)$$

where erf^{-1} is the inverse of the error function defined by Eq. (57).

Substituting Eq. (59) into Eq. (58), one obtains

$$\beta = \frac{1}{2} \left\{ 1 + \operatorname{erf} \left[\operatorname{erf}^{-1}(1-2\alpha) - \frac{m_2 - m_1}{\sqrt{2} \sigma} \right] \right\} \quad (60)$$

The quantity $\frac{m_2 - m_1}{\sigma}$ is easily recognized as the output signal-to-noise ratio $\frac{\Delta(\text{DC output})}{D(\text{output})}$. Hence Eq. (60) becomes

$$\beta = \frac{1}{2} \left\{ 1 + \operatorname{erf} \left[\operatorname{erf}^{-1}(1-2\alpha) - \frac{1}{\sqrt{2}} \frac{\Delta(\text{DC output})}{D(\text{output})} \right] \right\} \quad (61)$$

Figures 10 and 11 show plots of β versus α for various values of the parameter $x = \frac{\Delta(\text{DC output})}{D(\text{output})}$.

A specific example of the application of Eq. (61) to the detection problem considered in this report is given in Fig. 12. It shows the miss probability β as a function of the signal-to-ambient-noise ratio (in db) at each hydrophone for a fixed false-alarm rate of 1%. The calculations assume $M = 40$, $\omega_2 = 2\pi \times 5000$ rad/sec, $d = 2$ ft, $T = 4$ sec, and a broadside target. Curves are shown for the likelihood-ratio detector (essentially independent of $\frac{N}{I}$ for $\frac{N}{I} \leq 4$) and for the conventional detector without pre-whitening with values of $\frac{N}{I} = 4, 1$ and 0.1 . Each curve is labelled with the bearing in degrees of the interference relative to the target. Figure 13 shows an equivalent set of curves for a conventional detector with pre-whitening filter. It is interesting to observe that for $\frac{N}{I} \leq 4$ and for interference bearings no less than 3° from target bearing, the performance of the likelihood-ratio detector is almost entirely independent of the interference. The performance of the conventional detector depends to a very considerable extent on the strength of the interference.

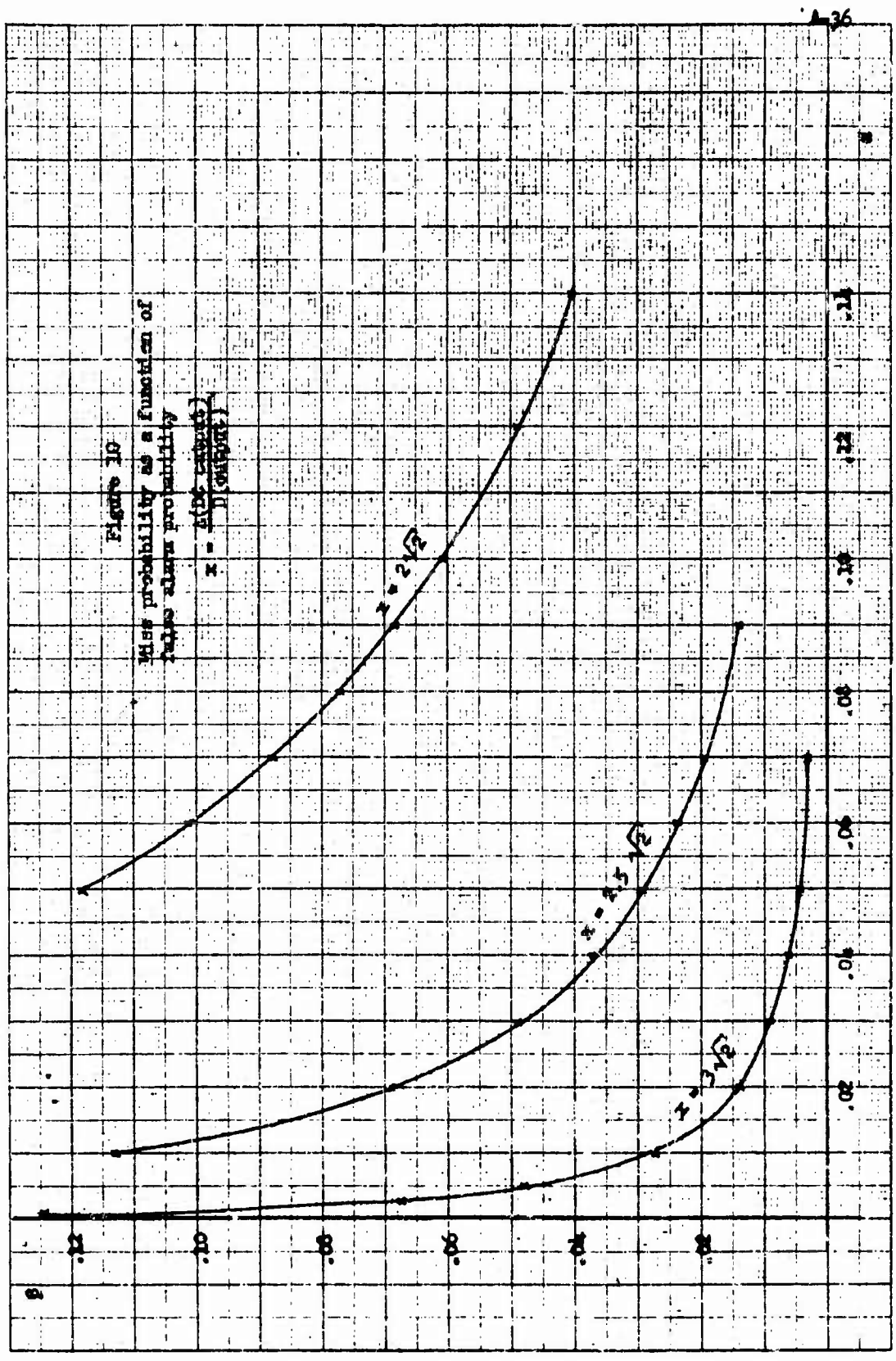
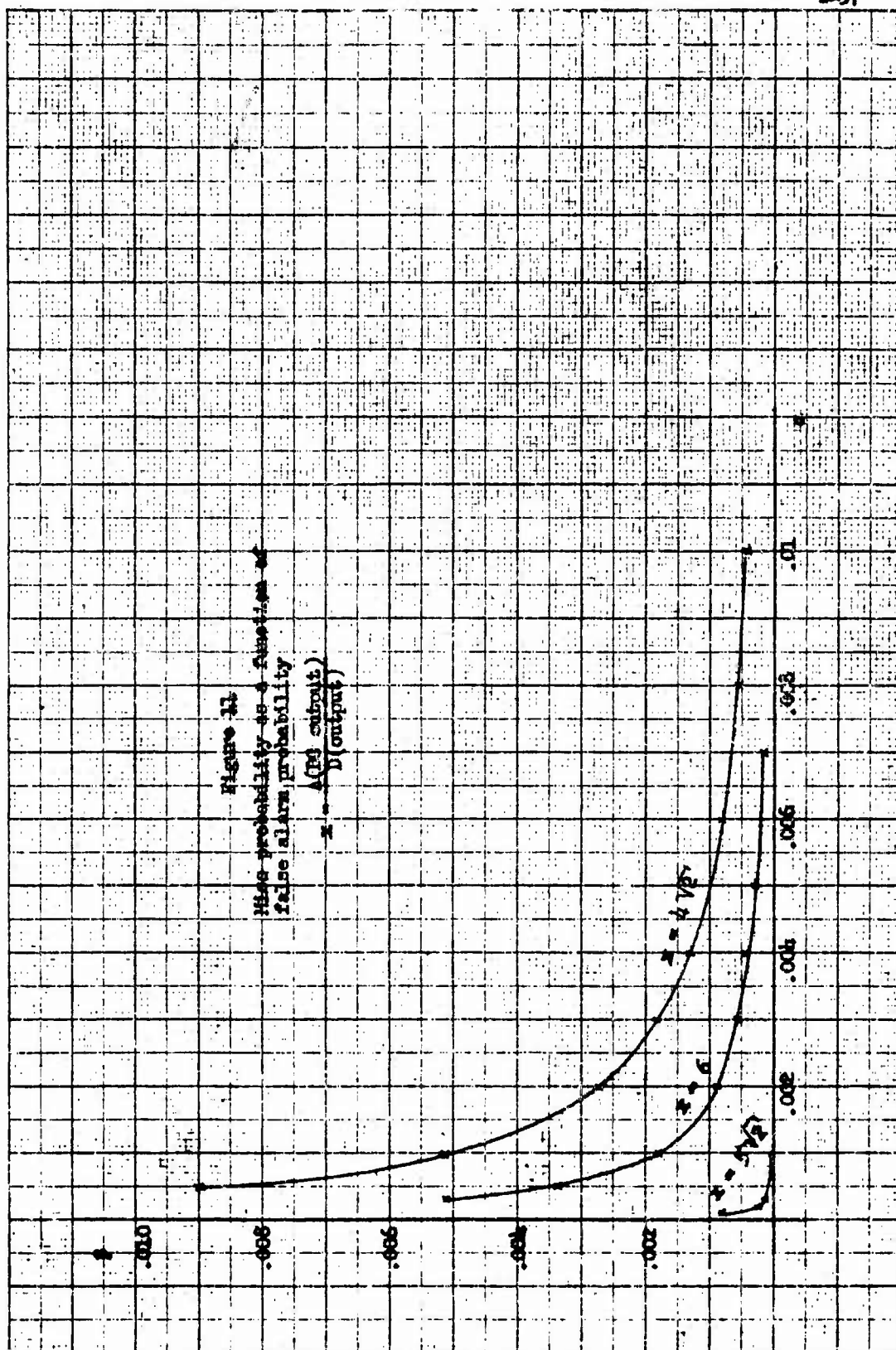
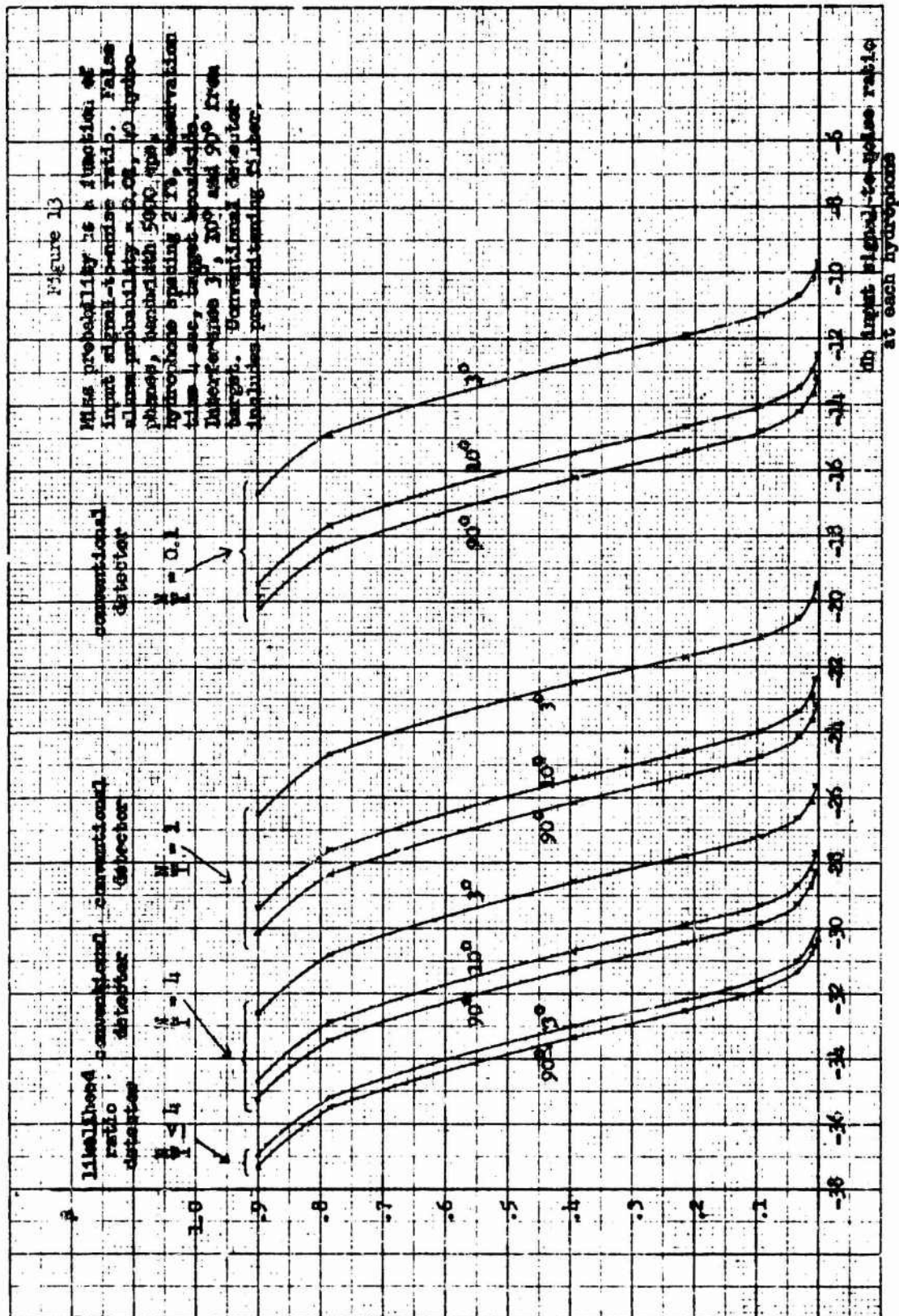


Figure 11
 Miss probability as a function of
 false alarm probability

$$z = \frac{\Delta(PD \text{ output})}{D(\text{output})}$$





In the absence of pre-whitening there is also a substantial dependence on interference bearing, but this effect becomes much less pronounced when pre-whitening is used. No computations have been made for a conventional detector employing optimum linear pre-filtering, but in the light of Knapp's results¹ it appears reasonable to expect further improvement in bearing discrimination from such a procedure. The curves for 90° interference bearing relative to target bearing are virtually identical in Figs. 12 and 13. and there is no reason to expect any different behavior in this respect with optimum pre-filtering.

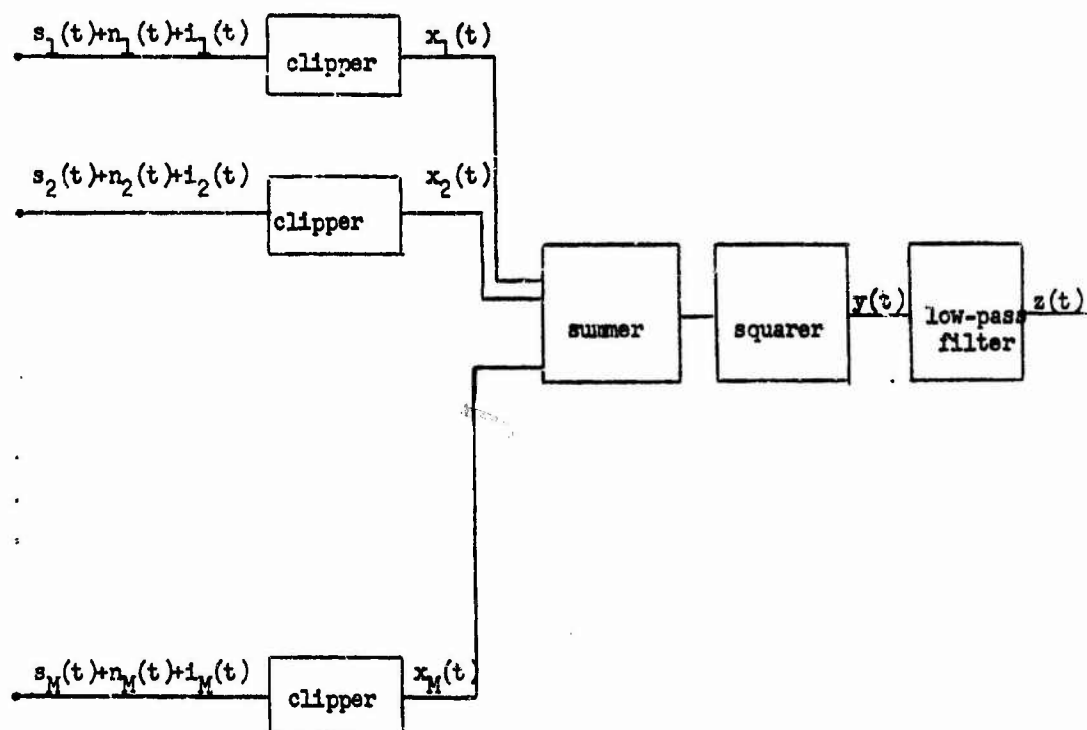
A change in smoothing time T simply shifts all curves of Figs. 12 and 13 horizontally by a fixed amount. Since the output signal-to-noise ratio varies as $\sqrt{T} \frac{S}{N}$ it is clear that an increase by a factor of 2 in smoothing time is equivalent to an increase of 1.5 db in input signal-to-ambient-noise ratio $\left(\frac{S}{N}\right)$ at each hydrophone.

A simple relabelling of the curves yields the corresponding results for a target in locations other than broadside. Thus for an endfire target a straightforward computation from Eqs. (51) and (52) indicates that the 3° curves should be relabelled $18\frac{1}{2}^\circ$, the 10° curves should be relabelled 34°, while the 90° curves remain unchanged.

¹See p. 26, footnote 2.

V. Detection with Clipped Hydrophone Data

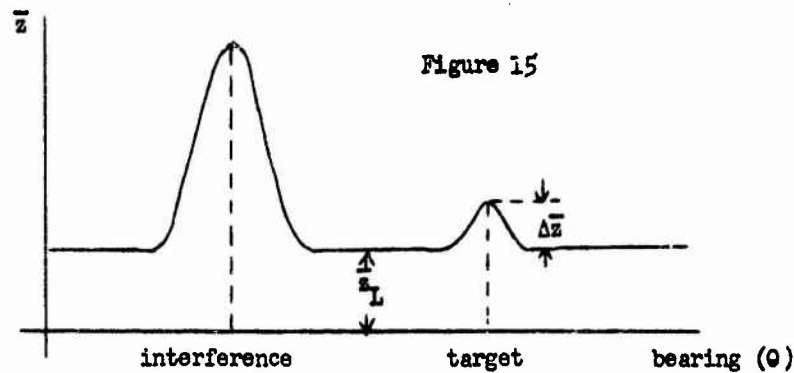
The clipping problem in the presence of interference is here approached by comparing the average bearing response pattern of a conventional detector with and without clipping. Consider the block diagram shown in Fig. 14.



M hydrophones

Figure 14

In accordance with Report No. 2 the average bearing response pattern $\bar{z}(\theta)$ is defined as the average value of the output $z(t)$ as a function of the target bearing θ relative to the bearing angle of the major lobe of the array pattern. If target and interference are well separated in bearing, the bearing response pattern would take the general form shown in Fig. 15. As



in Report No. 2 the excess $\Delta \bar{z}$ of the on-target value over the lowest value \bar{z}_L , normalized with respect to \bar{z}_L , will be used as a figure of merit. The computation of this quantity is quite straightforward. In the absence of clipping

$$\bar{z}(\theta) = \bar{y}(\theta) = \sum_{j=1}^M \sum_{k=1}^M \overline{[e_j(t) + n_j(t) + i_j(t)] [e_k(t) + n_k(t) + i_k(t)]} \quad (62)$$

Since the signal components at each hydrophone are the same except for delays,

$$\overline{s_j(t) e_k(t)} = S \rho_e(\gamma_{jk}) \quad (63)^1$$

Similarly for the interference

$$\overline{i_j(t) i_k(t)} = I \rho_i(\tau_{jk}) \quad (64)^1$$

¹See page 3 for definition of terms.

Finally, because the ambient noise is assumed to be independent from hydrophone to hydrophone,

$$\overline{n_j(t) n_k(t)} = \begin{cases} N & \text{for } j = k \\ 0 & \text{for } j \neq k \end{cases} \quad (65)^2$$

Substituting Eqs. (63), (64) and (65) into Eq. (62), one obtains

$$\bar{z}(\theta) = S \sum_{j=1}^M \sum_{k=1}^M \rho_s(\gamma_{jk}) + M N + I \sum_{j=1}^M \sum_{k=1}^M \rho_i(\tau_{jk}) \quad (66)$$

The delay times γ_{jk} and τ_{jk} are trigonometric functions of the bearing angle θ .

If target and interference are well separated in bearing and both are fairly broadband processes, it appears reasonable to assume that the interference is uncorrelated from hydrophone to hydrophone in the "on target" condition, i.e.,

$$\rho_i(\tau_{jk}) \Big|_{\text{on target}} = \begin{cases} 1 & \text{for } j = k \\ 0 & \text{for } j \neq k \end{cases} \quad (67)$$

For the target signal one obtains analogously

$$\rho_s(\gamma_{jk}) \Big|_{\text{on target}} = 1 \quad \text{for all } j \text{ and } k \quad (68)$$

$$\rho_s(\gamma_{jk}) \Big|_{\text{off target}} = \begin{cases} 1 & \text{for } j = k \\ 0 & \text{for } j \neq k \end{cases} \quad (69)$$

¹See page 3 for definitions of terms.

Hence

$$\bar{z}(0) \Big|_{\text{on target}} = S M^2 + M(N + I) \quad (70)$$

$$\bar{z}_L = M(S + N + I) \quad (71)^1$$

It follows that

$$\frac{\Delta \bar{z}}{\bar{z}_L} = (M-1) \frac{S}{S + N + I} \quad (72)$$

If a perfect clipper (with output $v_j(t) = \pm 1$) is inserted after each hydrophone, the average bearing response becomes

$$\bar{z}(0) = \sum_{j=1}^M \sum_{k=1}^M \overline{v_j(t) v_k(t)} \quad (73)$$

From Report No. 2, Eqs. (6) and (8),

$$\overline{v_j(t) v_k(t)} = \frac{2}{\pi} \arcsin \frac{[s_j(t) + n_j(t) + i_j(t)][s_k(t) + n_k(t) + i_k(t)]}{S + N + I} \quad (74)$$

Hence

$$\bar{z}(0) = \frac{2}{\pi} \sum_{j=1}^M \sum_{k=1}^M \arcsin \left\{ \frac{S \rho_s(\tau_{jk}) + N \delta_{jk} + I \rho_i(\tau_{jk})}{S + N + I} \right\} \quad (75)$$

¹The plateau value \bar{z}_L of $\bar{z}(0)$ is indeed the minimum value, as suggested by Fig. 15, if the autocorrelation functions of signal and interference are non-negative. In practice an exponential function is apt to be a fairly good approximation for both autocorrelation functions so that this hypothesis is not entirely unrealistic. On the other hand, if the detector processes only a relatively narrow frequency band, both autocorrelation functions tend to be oscillatory and one could obtain values of $\bar{z}(0)$ smaller than the \bar{z}_L given by Eq. (71). Whether this would aid in target detection depends on the relative location of the minima and the peak due to the target. In any case the value of \bar{z}_L used here is representative for the important case of target and interference well separated in bearing.

where

$$\delta_{jk} = \begin{cases} 1 & \text{for } j = k \\ 0 & \text{for } j \neq k \end{cases} \quad (76)$$

Now, using the symmetry properties of the correlation function $[\rho_s(\gamma_{jk}) = \rho_s(\gamma_{kj}), \rho_1(\tau_{jk}) = \rho_1(\tau_{kj})]$,

$$\bar{z}(0) = M + \frac{1}{\pi} \sum_{j=1}^M \sum_{k=j+1}^M \arcsin \left\{ \frac{S \rho_s(\gamma_{jk}) + I \rho_1(\tau_{jk})}{S + N + I} \right\} \quad (77)$$

Therefore, if again target and interference are sufficiently separated in bearing so that $\rho_1(\tau_{jk})|_{\text{on target}} = 0$ for $j \neq k$,

$$\begin{aligned} \bar{z}(0)|_{\text{on target}} &= M + \frac{1}{\pi} \sum_{j=1}^M \sum_{k=j+1}^M \arcsin \frac{S}{S + N + I} \\ &= M + \frac{2}{\pi} (M^2 - M) \arcsin \frac{S}{S + N + I} \end{aligned} \quad (78)$$

and

$$\bar{z}_L = M \quad (79)$$

Therefore

$$\frac{\Delta \bar{z}}{\bar{z}_L} = \frac{2}{\pi} (M-1) \arcsin \frac{S}{S + N + I} \quad (80)$$

Comparison with Eq. (72) reveals that for the case of primary interest, that of low input signal-to-noise ratio $\left(\frac{S}{S+N+I} \ll 1 \right)$, the degradation in performance is given by the factor of $\frac{2}{\pi}$, the same as in the absence of interference (see Report No. 2). Thus the presence of interference does

not alter the cost of clipping as measured by average bearing response if a conventional detector is used. This leaves open the question whether the effect of clipping might not be more serious under a measure of performance such as output signal-to-noise ratio or error probability. In Report No. 2 the output signal-to-noise ratio has been computed for the case of isotropic noise only and the resulting figure of merit turns out to be simply a constant (not very different from unity) times the figure of merit $\frac{\Delta \bar{z}}{\bar{z}_L}$.

The corresponding calculation for non-isotropic noise is quite tedious and has not been carried out to date. Also left open is the question whether the inherent cost of clipping may not be substantially greater when the detection procedure is not confined to the conventional arrangement of Fig. 14.

VI. Concluding Remarks

The results of Sections II to IV suggest that significant gains in detectability can be made in certain cases of strong interference by going to some instrumentation more nearly optimal than a simple power detector. No analysis has been made to date of the equipment required to implement the likelihood-ratio detector, but experience with other likelihood-ratio detectors suggests that it may be rather complex. Therefore it becomes important to answer two questions:

- 1) Can one find a simple modification of the conventional power detector that will attain a performance comparable to that of the likelihood-ratio detector?
- 2) Are the assumptions underlying the analysis sufficiently realistic to make the predicted improvement practically meaningful? The deviations from the analytical assumptions which inevitably occur in practice will almost certainly degrade the performance of the likelihood-ratio detector relative to that of the conventional detector. Will the remaining improvement be sufficiently large to justify the increased complexity in instrumentation?

Further study is required to resolve each of these questions. The direction which such an effort should take is indicated in part by the following comments.

It appears that the likelihood-ratio detector combines the outputs of various hydrophones in such a manner as to achieve an at-least-approximate null in the effective array pattern in the direction of the interference while still maintaining as much gain as possible in the target direction. With $\frac{N}{I} = 0$ the null would be perfect. For finite values of $\frac{N}{I}$ a compromise is made between interference rejection and sensitivity to target

signal. Future work will have to determine whether these ideas can lead to a simple but effective suboptimal instrumentation.

As far as the realism of the analytical assumptions is concerned, the following points certainly deserve attention:

- 1) The analysis assumes that the power level and spectral properties of signal, interference and ambient noise are known. Lack of precise knowledge concerning spectral properties may not be crucial. Interference and ambient noise power, on the other hand, are apt to be quite critical and would have to be measured. Since an array is available and the interference is assumed to be quite strong (so that it is easy to locate in bearing), it would not be difficult to make power measurements. However, the accuracy of such measurements in the finite observation time T cannot be perfect, and the resulting degradation of detector performance should be investigated.
- 2) The analysis assumes that the interference bearing is known. If the interference is strong, its bearing can be determined quite accurately. Nevertheless, the measurement is subject to some error, so that the location of the detector "null" will be inaccurate. The degradation of target detectability caused by this imperfection requires investigation.
- 3) The analysis assumes isotropic ambient noise. Since interference elimination is accomplished at the expense of reducing sensitivity to target signals, the question arises whether moderate anisotropy in the ambient noise field could give rise to false target indications.

- 4) The analysis assumes that both target and interference are sufficiently remote so that the resulting wavefronts at the receiving array are essentially plane. This might not be true for a very strong, and hence nearby, interference. There is no reason to expect that the "nulling out" of interference could not be accomplished in this case, but the computational procedure required to determine the output signal-to-noise ratio would be more complicated.
- 5) There is, of course, the very basic underlying assumption that signal, interference and ambient noise are stationary Gaussian random processes. For relatively short smoothing times the assumption of stationarity should be quite satisfactory. Whether deviations from Gaussian statistics would seriously degrade the likelihood-ratio detector relative to the conventional detector is difficult to foresee, but the possibility cannot be ruled out because of the generally rather critical dependence of optimal instrumentations on analytical assumptions.

Finally, it should be stressed that the development of Section V represents only a very partial treatment of the clipping problem in multiple-target situations. At the very least one should obtain error probability curves comparable to those contained in Section IV for a conventional detector with clipping. Also of considerable interest would be the evaluation of a likelihood-ratio detector operating on clipped data. Such a computation would resolve the question whether or not the inherent cost of clipping is the same in the presence and absence of interference.

Appendix A Inversion of the $Q(n)$ Matrix

The derivation of Eq. (27) from Eq. (26) is carried out by induction.

A trivial computation verifies that the result is correct for $M = 1$.

Now assume that $Q^{-1}(n)$ is given by Eq. (27) for $M = M$ and deduce the corresponding inverse for $M+1$.

For greater compactness the argument ω_n of the spectral functions is omitted in subsequent manipulations and $\omega_n \tau_0$ is replaced by x . Then the noise matrix $Q(n)$ for $M+1$ hydrophones is given by

$$Q(n) = I \Delta \omega \times$$

$1 + \frac{N}{I}$	0	cos x	sin x	cos 2x	sin 2x	...	cos(M-1)x	sin(M-1)x	cos Mx	sin Mx
0	$1 + \frac{N}{I}$	-sin x	cos x	-sin 2x	cos 2x	...	-sin(M-1)x	cos(M-1)x	-sin Mx	cos Mx
cos x	-sin x	$1 + \frac{N}{I}$	0	cos x	sin x	...	cos(M-2)x	sin(M-2)x	cos(M-1)x	sin(M-1)x
sin x	cos x	0	$1 + \frac{N}{I}$	-sin x	cos x	...	-sin(M-2)x	cos(M-2)x	-sin(M-1)x	cos(M-1)x
cos 2x	-sin 2x	cos x	-sin x	$1 + \frac{N}{I}$	0	...	cos(M-3)x	sin(M-3)x	cos(M-2)x	sin(M-2)x
sin 2x	cos 2x	sin x	cos x	0	$1 + \frac{N}{I}$...	-sin(M-3)x	cos(M-3)x	-sin(M-2)x	cos(M-2)x
:	:	:	:	:	:	...	:	:	:	:
cos(M-1)x	-sin(M-1)x	cos(M-2)x	-sin(M-2)x	cos(M-3)x	-sin(M-3)x	...	$1 + \frac{N}{I}$	0	cos x	sin x
sin(M-1)x	cos(M-1)x	sin(M-2)x	cos(M-2)x	sin(M-3)x	cos(M-3)x	...	0	$1 + \frac{N}{I}$	-sin x	cos x
cos Mx	-sin Mx	cos(M-1)x	-sin(M-1)x	cos(M-2)x	-sin(M-2)x	...	cos x	-sin x	$1 + \frac{N}{I}$	0
sin Mx	cos Mx	sin(M-1)x	cos(M-1)x	sin(M-2)x	cos(M-2)x	...	sin x	cos x	0	$1 + \frac{N}{I}$

(A-1)

The matrix will be treated as partitioned by the dotted lines into the form

$$Q(n) = \begin{bmatrix} A & B \\ B^T & C \end{bmatrix} \quad (A-2)^1$$

The inverse of this partitioned matrix is given by

$$Q^{-1}(n) = \begin{bmatrix} A^{-1} + A^{-1}B[C - B^T A^{-1}B]^{-1} B^T A^{-1} & -A^{-1}B[C - B^T A^{-1}B]^{-1} \\ -[C - B^T A^{-1}B]^{-1} B^T A^{-1} & [C - B^T A^{-1}B]^{-1} \end{bmatrix} \quad (A-3)^2$$

A^{-1} is given by Eq. (27) (hypothesis). Since $C - B^T A^{-1}B$ is only a 2×2 matrix the inversion becomes quite simple. The primary difficulty is the computation of $B^T A^{-1}B$.

The elements r_{ij} of $B^T A^{-1}B$ are obtained by straightforward computation. Thus for j odd

$$\begin{aligned} \frac{N}{I} \left(M + \frac{N}{I} \right) r_{1j} = & -\cos Mx \cos \frac{j-1}{2} x - \sin Mx \sin \frac{j-1}{2} x - \cos(M-1)x \cos \left(\frac{j-1}{2} - 1 \right) x \\ & - \sin(M-1)x \sin \left(\frac{j-1}{2} - 1 \right) x \dots - \cos \left(M - \frac{j+1}{2} \right) x \cos x \\ & - \sin \left(M - \frac{j+1}{2} \right) x \sin x + \left(M-1 + \frac{N}{I} \right) \cos \left(M - \frac{j-1}{2} \right) x \\ & - \cos \left(M - \frac{j+1}{2} \right) x \cos x + \sin \left(M - \frac{j+1}{2} \right) x \sin x \dots \\ & - \cos x \cos \left(M - \frac{j+1}{2} \right) x + \sin x \sin \left(M - \frac{j+1}{2} \right) x \end{aligned}$$

¹Note that the multiplier $I\omega$ is included in the definitions of A,B,C.

²See, for instance, Hohn

$$\begin{aligned}
&= -\frac{1-l}{2} \cos\left(M - \frac{1-l}{2}\right)x + \left(M-1 + \frac{N}{I}\right) \cos\left(M - \frac{1-l}{2}\right)x \\
&\quad - \left(M - \frac{1+l}{2}\right) \cos\left(M - \frac{1-l}{2}\right)x \\
&= \frac{N}{I} \cos\left(M - \frac{1-l}{2}\right)x
\end{aligned} \tag{A-4}$$

In completely similar fashion

$$\frac{N}{I} \left(M + \frac{N}{I}\right) r_{1j} = -\frac{N}{I} \sin\left(M + 1 - \frac{1}{2}\right)x \quad \text{for } j \text{ even} \tag{A-5}$$

$$\frac{N}{I} \left(M + \frac{N}{I}\right) r_{2j} = \frac{N}{I} \sin\left(M - \frac{1-l}{2}\right)x \quad \text{for } j \text{ odd} \tag{A-6}$$

$$\frac{N}{I} \left(M + \frac{N}{I}\right) r_{2j} = \frac{N}{I} \cos\left(M + 1 - \frac{1}{2}\right)x \quad \text{for } j \text{ even} \tag{A-7}$$

Hence

$$B^T A^{-1} B = I \Delta\omega \frac{1}{M + \frac{N}{I}} X$$

$$\begin{bmatrix} \cos Mx & -\sin Mx & \cos(M-1)x & -\sin(M-1)x & \dots & \cos x & -\sin x \\ \sin Mx & \cos Mx & \sin(M-1)x & \cos(M-1)x & \dots & \sin x & \cos x \end{bmatrix} X \begin{bmatrix} \cos Mx & \sin Mx \\ -\sin Mx & \cos Mx \\ \cos(M-1)x & \sin(M-1)x \\ -\sin(M-1)x & \cos(M-1)x \\ \vdots & \vdots \\ \cos x & \sin x \\ -\sin x & \cos x \end{bmatrix}$$

$$= I \Delta\omega \frac{M}{M + \frac{N}{I}} \begin{bmatrix} 1 & 0 \\ 0 & 1 \end{bmatrix} \tag{A-8}$$

Therefore

$$\begin{aligned}
 C - B^T A^{-1} B &= I \Delta \omega \left\{ 1 + \frac{N}{I} \right\} - \frac{M}{M + \frac{N}{I}} \begin{bmatrix} 1 & 0 \\ 0 & 1 \end{bmatrix} \\
 &= N \Delta \omega \frac{M + 1 + \frac{N}{I}}{M + \frac{N}{I}} \begin{bmatrix} 1 & 0 \\ 0 & 1 \end{bmatrix} \quad (A-9)
 \end{aligned}$$

It follows that

$$\left[C - B^T A^{-1} B \right]^{-1} = \frac{1}{N \Delta \omega} \frac{M + \frac{N}{I}}{M + 1 + \frac{N}{I}} \begin{bmatrix} 1 & 0 \\ 0 & 1 \end{bmatrix} \quad (A-10)$$

The various components of Eq. (A-3) are now easily computed.

$$A^{-1} B \left[C - B^T A^{-1} B \right]^{-1} B^T A^{-1} = \frac{1}{N \Delta \omega} \frac{M + \frac{N}{I}}{M + 1 + \frac{N}{I}} \frac{1}{\left(M + \frac{N}{I} \right)^2} X$$

$$\begin{bmatrix} \cos Mx & \sin Mx \\ -\sin Mx & \cos Mx \\ \cos(M-1)x & \sin(M-1)x \\ -\sin(M-1)x & \cos(M-1)x \\ \vdots & \vdots \\ \cos x & \sin x \\ \sin x & \cos x \end{bmatrix} X \begin{bmatrix} \cos Mx & -\sin Mx & \cos(M-1)x & -\sin(M-1)x & \dots & \cos x & \sin x \\ \sin Mx & \cos Mx & \sin(M-1)x & \cos(M-1)x & \dots & \sin x & \cos x \end{bmatrix}$$

$$= \frac{1}{N \Delta \omega} \frac{1}{M + \frac{N}{I}} \frac{1}{M + 1 + \frac{N}{I}} X$$

1	0	cos x	sin x	...	cos(M-1)x	sin(M-1)x
0	1	-sin x	cos x	...	-sin(M-1)x	cos(M-1)x
cos x	-sin x	1	0	...	cos(M-2)x	sin(M-2)x
sin x	cos x	0	1	...	-sin(M-2)x	cos(M-2)x
cos 2x	-sin 2x	cos x	-sin x	1	...	cos(M-3)x
sin 2x	cos 2x	sin x	cos x	0	...	-sin(M-3)x
:	:	:	:	:	:	:
cos(M-1)x	-sin(M-1)x	cos(M-2)x	-sin(M-2)x	...	1	0
sin(M-1)x	cos(M-1)x	sin(M-2)x	cos(M-2)x	...	0	1

(A-11)

$$\text{Hence } A^{-1} + A^{-1}B[C - B^T A^{-1}B]^{-1} B^T A^{-1} = \frac{1}{N \Delta \omega} \frac{1}{M+1} \frac{N}{I} X$$

$M + \frac{N}{I}$	0	$-\cos x$	$-\sin x$	$-\cos 2x$	$-\sin 2x$...	$-\cos Mx$	$-\sin Mx$
0	$M + \frac{N}{I}$	$\sin x$	$-\cos x$	$\sin 2x$	$-\cos 2x$...	$\sin Mx$	$-\cos Mx$
$-\cos x$	$\sin x$	$M + \frac{N}{I}$	0	$-\cos x$	$-\sin x$...	$-\cos(M-1)x$	$-\sin(M-1)x$
$-\sin x$	$-\cos x$	0	$M + \frac{N}{I}$	$\sin x$	$-\cos x$...	$\sin(M-1)x$	$-\cos(M-1)x$
$-\cos 2x$	$\sin 2x$	$-\cos x$	$\sin x$	$M + \frac{N}{I}$	0	...	$-\cos(M-2)x$	$-\sin(M-2)x$
$-\sin 2x$	$-\cos 2x$	$-\sin x$	$-\cos x$	0	$M + \frac{N}{I}$...	$\sin(M-2)x$	$-\cos(M-2)x$
.
.
.
$-\cos Mx$	$\sin Mx$	$-\cos(M-1)x$	$\sin(M-1)x$	$-\cos(M-2)x$	$\sin(M-2)x$...	$M + \frac{N}{I}$	0
$-\sin Mx$	$-\cos Mx$	$-\sin(M-1)x$	$-\cos(M-1)x$	$-\sin(M-2)x$	$-\cos(M-2)x$...	0	$M + \frac{N}{I}$

(A-12)

This coincides with the first $2M$ rows and columns of Eq. (27) if one replaces M with $M+1$ in the latter expression. With the same substitution Eq. (A-10) goes over into the 2×2 matrix in the lower right corner of Eq. (27). Thus there remains only

$$- \left[C - B^T A^{-1} B \right]^{-1} B^T A^{-1} = \frac{1}{N \Delta \omega} \chi \frac{1}{M+1 + \frac{N}{I}} \chi$$

$$\begin{bmatrix} -\cos Mx & \sin Mx & -\cos(M-1)x & \sin(M-1)x & -\cos(M-2)x & \sin(M-2)x & \dots & -\cos x & \sin x \\ -\sin Mx & -\cos Mx & -\sin(M-1)x & -\cos(M-1)x & -\sin(M-2)x & -\cos(M-2)x & \dots & -\sin x & -\cos x \end{bmatrix}$$

(A-13)

This corresponds to the first $2M$ columns of the last two rows of Eq. (27) with M replaced by $M+1$. With the same substitution the transpose of Eq. (A-13) yields the first $2M$ rows of the last two columns of Eq. (27). Thus the proof of Eq. (27) is complete.

Appendix B Computation of $\text{Tr}\{[P(n)Q^{-1}(n)]^2\}$

It is apparent from Eq. (28) that $P(n)Q^{-1}(n)$ consists of M identical pairs of rows. Thus it is necessary to compute only one such pair, say rows 1 and 2.

For M even the two rows are

$$\frac{S}{N} \frac{1}{M+1} \begin{bmatrix} a_1 & b_1 & a_2 & b_2 & \dots & a_{M/2} & b_{M/2} & a_{M/2} & -b_{M/2} & \dots & a_2 & -b_2 & a_1 & -b_1 \\ -b_1 & a_1 & -b_2 & a_2 & \dots & -b_{M/2} & a_{M/2} & b_{M/2} & a_{M/2} & \dots & b_2 & a_2 & b_1 & a_1 \end{bmatrix} \quad (\text{B-1})$$

where

$$a_j = M - 1 + \frac{N}{1} - \sum_{\ell=1}^{M-j} \cos \ell x - \sum_{\ell=1}^{j-1} \cos \ell x \quad (\text{B-2})^1$$

and

$$b_j = \sum_{\ell=j}^{M-j} \sin \ell x \quad (\text{B-3})$$

The equivalent expression for odd M is

$$\frac{S}{N} \frac{1}{M+1} \times \begin{bmatrix} a_1 & b_1 & a_2 & b_2 & \dots & \frac{a_{M-1}}{2} & \frac{b_{M-1}}{2} & \frac{a_{M+1}}{2} & 0 & \frac{a_{M-1}}{2} & -\frac{b_{M-1}}{2} & \dots & a_2 & -b_2 & a_1 & -b_1 \\ -b_1 & a_1 & -b_2 & a_2 & \dots & -\frac{b_{M-1}}{2} & \frac{a_{M-1}}{2} & 0 & \frac{a_{M+1}}{2} & \frac{b_{M-1}}{2} & \frac{a_{M-1}}{2} & \dots & b_2 & a_2 & b_1 & a_1 \end{bmatrix} \quad (\text{B-4})$$

¹The last sum of this expression is to be interpreted as zero for $j = 1$.

where a_j and b_j are still given by Eqs. (B-2) and (B-3). Since each b_j occurs both with positive and negative sign in each row of Eqs. (B-1) and (B-4), it is clear that the b 's make no contribution to $\text{Tr} \left\{ \left[P(n) Q^{-1}(n) \right]^2 \right\}$. Hence $\text{Tr} \left\{ \left[P(n) Q^{-1}(n) \right]^2 \right\}$ depends on the a 's only and a simple computation yields

$$\text{Tr} \left\{ \left[P(n) Q^{-1}(n) \right]^2 \right\} = \left(\frac{S}{N} \right)^2 \frac{1}{\left(M + \frac{N}{I} \right)^2} \begin{cases} 8(a_1 + a_2 + \dots + a_{M/2})^2 & \text{for } M \text{ even} \\ 2(2a_1 + 2a_2 + \dots + 2a_{\frac{M-1}{2}} + a_{\frac{M+1}{2}})^2 & \text{for } M \text{ odd} \end{cases} \quad (\text{B-5})$$

Going back to the definition of a_j [Eq. (B-2)], it is a simple matter to count the number of terms of the form $M-1+\frac{N}{I}$, $\cos x$, $\cos 2x \dots$ in the sums of Eq. (B-5). One finds for even M

$$a_1 + a_2 + \dots + a_{M/2} = \frac{M}{2} \left(M-1 + \frac{N}{I} \right) - \sum_{\ell=1}^{M-1} (M-\ell) \cos \ell x \quad (\text{B-6})$$

and for odd M

$$2a_1 + 2a_2 + \dots + 2a_{\frac{M-1}{2}} + a_{\frac{M+1}{2}} = M - 2 \sum_{\ell=1}^{M-1} (M-\ell) \cos \ell x \quad (\text{B-7})$$

Hence for both even and odd M

$$\text{Tr} \left\{ \left[P(n) Q^{-1}(n) \right]^2 \right\} = \left(\frac{S}{N} \right)^2 \frac{2}{\left(M + \frac{N}{I} \right)^2} \left[M \left(M-1 + \frac{N}{I} \right) - 2 \sum_{\ell=1}^{M-1} (M-\ell) \cos \ell x \right]^2 \quad (\text{B-8})$$

This agrees with Eq. (29) and the derivation is therefore complete.



OPTIMAL DETECTION OF SIGNALS
IN A NOISE BACKGROUND OF UNKNOWN STRENGTH

by

F. B. Tuteur

Progress Report No. 18
General Dynamics/Electric Boat Research
(53-00-10-0231)
January 1965

DEPARTMENT OF ENGINEERING
AND APPLIED SCIENCE
YALE UNIVERSITY

ABSTRACT

The problem of detecting modulated Gaussian directional signals is reconsidered under the condition that the noise level is unknown. It appears that results obtained in previous analyses of this problem are essentially unaffected by the added uncertainty as long as detection is by arrays with a large number of elements. It is also found that in general the cost of not knowing the precise noise level is approximately equivalent to the loss of one half of a hydrophone from a large array.

I. Introduction

In previous analyses of the detectability of underwater signals, it has generally been assumed that the background noise was a stationary Gaussian random process with zero mean and known power spectrum. Although this assumption may be unjustified on several different counts, the only aspect considered in this report is that the noise is nonstationary. Furthermore, the nonstationarity is assumed to be slow, so that in a relatively short observation interval the noise level is essentially constant.

The signal is assumed to be a Gaussian random process with zero mean which is distinguished from the noise mainly by the fact that it is directional, while the noise is assumed to be isotropic. It is also possible that the signal is amplitude modulated with a known modulating function whose frequency is high relative to the time over which the noise level can be assumed to be constant.

Under these conditions the detection problem becomes the problem of finding a Gaussian signal in a Gaussian noise of unknown level. The optimum detector in this case depends on what is known about the noise level, and it is discussed in some detail in the next section.

II. Optimum Detectors for Signals in Noise of Unknown Level

If it is assumed that the probability density functions $p_S(S)$ and $p_N(N)$ of the signal and of the noise level are known, then one can in principle compute an averaged likelihood ratio:

$$L(\underline{x}) = \frac{\int_0^\infty p_N(N) \int_0^\infty p_S(S) f_1(\underline{x}/S, N) dS dN}{\int_0^\infty p_N(N) f_0(\underline{x}/N) dN} \quad (1)$$

where $\underline{x} = [x_1, \dots, x_n]^T$ is the sample vector representing the received signal $x(t)$, and $f_1(\underline{x}/S, N)$ and $f_0(\underline{x}/N)$ are the probability density functions of \underline{x} given that the signal is or is not present, respectively, and that the signal and noise levels are, respectively, S and N . (The prime indicates matrix transposition.)

Although it generally is not reasonable to assume that $p_S(S)$ or $p_N(N)$ is known, Eq. (1) furnishes a clue concerning the form of the optimum detector. If it is assumed that $f_1(\underline{x}/S, N)$ and $f_0(\underline{x}/N)$ are Gaussian density functions, and if the signal-to-noise ratio is small, Eq. (1) can be written in the approximate form⁽¹⁾:

$$L(\underline{x}) = \frac{\int_0^\infty p_N(N) N^{-n/2} \exp \left\{ \frac{u_1 - B_1}{2N^2} - \frac{u_2 + B_2}{2N} \right\} dN}{\int_0^\infty p_N(N) N^{-n/2} \exp \left(- \frac{u_2}{2N} \right) dN} \quad (2)$$

where

$$u_1 = \bar{S} \underline{x}' \underline{Q}^{-1} \underline{P} \underline{Q}^{-1} \underline{x},$$

$$u_2 = \underline{x}' \underline{Q}^{-1} \underline{x},$$

$$\bar{S} = \int_0^\infty S p_S(S) dS,$$

$\underline{Q} = \frac{1}{N} \langle \underline{x} \underline{x}' \rangle_N$ is the normalized covariance matrix of \underline{x} if $\underline{x}(t)$ consists of noise only, and

$\underline{P} = \frac{1}{S} \langle \underline{x} \underline{x}' \rangle_S$ is the normalized covariance matrix of \underline{x} if $\underline{x}(t)$ consists of signal only. A convenient normalization, which, in effect, defines S and N is $\text{tr } \underline{P} = \text{tr } \underline{Q} = n$.

$B_1 = \frac{S^2}{2} \text{tr}(\underline{P} \underline{Q}^{-1})^2$ and $B_2 = S \text{tr } \underline{P} \underline{Q}^{-1}$ are constant bias terms.*

From Eq. (2) it can be seen that u_1 and u_2 are sufficient statistics in the sense that they contain all the relevant information about the signal. Hence the basic function of the optimum detector must be the computation of u_1 and u_2 given the received signal $\underline{x}(t)$. Also it can be seen that if the decision rule is to accept the signal hypothesis when $L(\underline{x})$ exceeds the threshold K , there is an equivalent decision rule that accepts the signal hypothesis when

*The derivation of Eq. (2) involves the expansion of the matrix expression $\left(\underline{I} + \frac{S}{N} \underline{P} \underline{Q}^{-1} \right)^{-1}$ in a binomial series of the form

$\underline{I} + \sum_{m=1}^{\infty} (-1)^m \left(\frac{S}{N} \right)^m (\underline{P} \underline{Q}^{-1})^m$ and retaining only the first term in the summation. This procedure is permissible if $\left| \frac{S}{N} \lambda_1 \right| \ll 1$ where λ_1 is

the eigenvalue of $\underline{P} \underline{Q}^{-1}$ having the largest absolute value. For instance, if detection is by means of an array of M elements, if the array is steered on target, and if signal and noise spectra are white, $\lambda_1 = M$ and therefore it is necessary that $\frac{S}{N} \ll \frac{1}{M}$ for Eq. (2) to be a good approximation.

$g(u_1, u_2) > 0$, where $g(u_1, u_2)$ is a function depending on $p_N(N)$ and on the type of detection characteristic that is desired.

In the absence of any information about the noise level, it is often desirable to employ a detector with a constant false-alarm rate,⁽²⁾ a CFAR detector. It is easily seen that such a detector results if

$$g(u_1, u_2) = u_1 - au_2 \quad (3)$$

where a is a constant. In order to demonstrate this we compute the false-alarm rate for a detector with this characteristic. The statistics u_1 and u_2 are random variables, and if the number n of elements in \underline{x} is very large, as is usually the case, the distribution of u_1 and u_2 approaches the Gaussian form by the Central Limit Theorem. Hence $u_1 - au_2$ is also Gaussian. Under the hypothesis that $x(t)$ consists of noise only, it is easily shown⁽³⁾ that the mean and variance of $u_1 - au_2$ are given by

$$\mu_0 = \langle u_1 - au_2 \rangle_N = N(\text{tr } \underline{P} \underline{Q}^{-1} - an) \quad (4)$$

and

$$\sigma_0^2 = \langle (u_1 - au_2)^2 \rangle_N - \langle u_1 - au_2 \rangle_N^2 = 2N^2 \left[\text{tr}(\underline{P} \underline{Q}^{-1})^2 - 2a \text{tr } \underline{P} \underline{Q}^{-1} + a^2 n \right] \quad (5)$$

The false-alarm probability is the probability that $u_1 - au_2 > 0$ when $x(t)$ consists of noise only, and in view of Eqs. (4) and (5) it is given by

$$\alpha = \frac{1}{2} \text{erfc} \left(\frac{\mu_0}{\sigma_0} \right) = \frac{1}{2} \text{erfc} \left\{ \frac{an - \text{tr } \underline{P} \underline{Q}^{-1}}{\left[2 \left[\text{tr}(\underline{P} \underline{Q}^{-1})^2 - 2a \text{tr } \underline{P} \underline{Q}^{-1} + a^2 n \right]^{1/2}} \right\} \quad (6)$$

where

$$\operatorname{erfc}(x) = \frac{2}{\sqrt{\pi}} \int_x^{\infty} e^{-y^2} dy$$

It is seen that the noise level N cancels out in this expression so that the detector has, in fact, a CFAR characteristic. It is not completely obvious, however, that it is the optimum CFAR detector, since it is easily shown that any quadratic form $\underline{x}' \underline{A} \underline{x}$ used instead of u_2 would also result in a CFAR characteristic. A further discussion of this point is given in Appendix A. The general form of the detector is shown in Fig. 1. The upper channel forming the test statistic u_1 is equivalent to a likelihood-ratio detector for noise level known precisely, and it is generally a nonlinear filter matched to the expected signal structure. The lower channel is basically an estimator of the noise level.

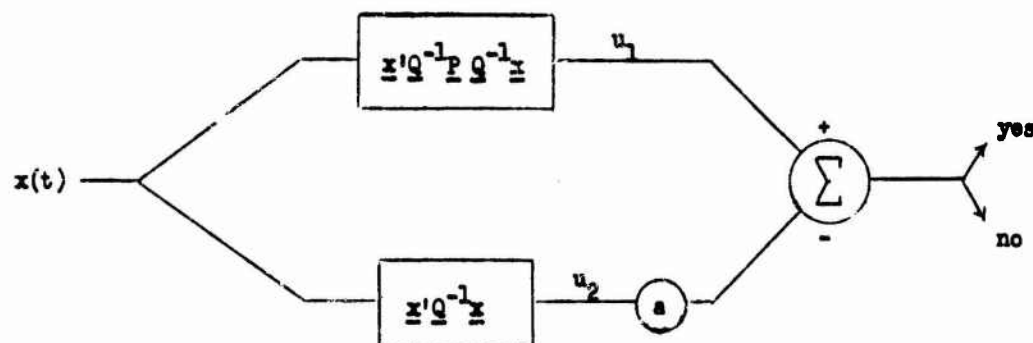


Figure 1 Optimum CFAR Detector

If the false-alarm probability α is specified, the argument of erfc in Eq. (6) is a constant, K_α , and therefore Eq. (6) can be solved for a . The result is

$$a = \frac{1}{n} \text{tr}(\underline{P} \underline{Q}^{-1}) \left[1 + \sqrt{1 - \left(\frac{n}{n - 4K_\alpha^2} \right) \left(1 - 4K_\alpha^2 \frac{\text{tr}(\underline{P} \underline{Q}^{-1})^2}{(\text{tr} \underline{P} \underline{Q}^{-1})^2} \right)} \right] \quad (7)$$

For large n this simplifies to

$$a \approx \frac{1}{n} \text{tr}(\underline{P} \underline{Q}^{-1}) \quad (8)$$

which is seen to be independent of the false-alarm probability. The reason for this is that for large n the error function in Eq. (6) approaches a unit step function, and therefore any value of α other than zero or one will result in approximately the same argument for erfc .

In order to compute the detection probability $1 - \beta$ the mean and variance of the output statistic $u_1 - au_2$ under the hypothesis that $x(t)$ consists of signal and noise must be found. Under the assumption that signal and noise are independent, the mean is

$$\mu_1 = \langle u_1 - au_2 \rangle_{S+N} = S \left[\text{tr}(\underline{P} \underline{Q}^{-1})^2 - a \text{tr}(\underline{P} \underline{Q}^{-1}) \right] + \mu_0 \quad (9)$$

and if the signal-to-noise ratio is very small, then the variance $\sigma_1^2 \approx \sigma_0^2$. Then

$$1 - \beta = \text{erfc} \left\{ K_\alpha - \frac{S}{2N} \frac{\text{tr}(\underline{P} \underline{Q}^{-1})^2 - a \text{tr}(\underline{P} \underline{Q}^{-1})}{\left[\text{tr}(\underline{P} \underline{Q}^{-1})^2 - 2a \text{tr} \underline{P} \underline{Q}^{-1} + a^2 n \right]^{1/2}} \right\} \quad (10)$$

If the value of a from Eq. (7) is substituted into this expression, the result is

$$1 - \beta = \operatorname{erfc} \left\{ K_a - \frac{S}{2N} \left[\sqrt{\left\{ \operatorname{tr}(\underline{P} \underline{Q}^{-1})^2 - \frac{1}{n} [\operatorname{tr}(\underline{P} \underline{Q}^{-1})]^2 \right\} \left[1 - \frac{4K_a^2}{n} \right]} - \frac{2K_a}{n} \operatorname{tr}(\underline{P} \underline{Q}^{-1}) \right] \right\} \quad (11)$$

For large n this can again be simplified to

$$1 - \beta = \operatorname{erfc} \left\{ K_a - \frac{S}{2N} \sqrt{\operatorname{tr}(\underline{P} \underline{Q}^{-1})^2 - \frac{1}{n} [\operatorname{tr}(\underline{P} \underline{Q}^{-1})]^2} \right\} \quad (12)$$

The detection probability obviously depends on the signal-to-noise ratio $\frac{S}{N}$, but since the detector structure does not, the detector is "uniformly optimum."

It is clear from Eq. (12) that the detection probability is determined by the magnitude of the quantity

$$\frac{d}{\sqrt{2}} = \frac{S}{2N} \sqrt{\operatorname{tr}(\underline{P} \underline{Q}^{-1})^2 - \frac{1}{n} (\operatorname{tr} \underline{P} \underline{Q}^{-1})^2} \quad (13)$$

By Eqs. (4) and (9), d is also seen to be the "output signal-to-noise ratio" $(\mu_1 - \mu_0)/\sigma_0$. Thus d is the usual figure of merit for evaluating the detection system. For an optimum detector where the background noise level is known, d is given by the well-known relation⁽⁴⁾

$$d_0 = \frac{S}{\sqrt{2} N} \sqrt{\operatorname{tr}(\underline{P} \underline{Q}^{-1})^2} \quad (14)$$

This can be seen, for instance, by setting $a = 0$ in Eq. (10). Comparison of Eqs. (13) and (14) therefore furnishes a convenient indication of the cost of the uncertainty in the noise level.

III. Evaluation of the CFAR Detector

The figure of merit d of Eq. (13) is now evaluated for some special cases. In all cases considered, detection is by means of an array consisting of M elements properly phased so that the array is steered "on target." The signal consists of amplitude-modulated noise, i.e.,

$$s(t) = f(t) y(t) \quad (15)$$

where $y(t)$ is a stationary Gaussian noise with mean-square value S , and where $f^2(t) = 1 + b \cos \omega_0 t$. The modulation frequency is known, and it is low compared to ω_m , the bandwidth of $y(t)$.

Suppose first that the power spectrum of $y(t)$ and $n(t)$ is uniform (white) up to a frequency ω_m and zero above this frequency. For large ω_m it can be shown⁽⁵⁾ that this implies that there is zero correlation between the noise received on different hydrophones.

According to the sampling theorem,⁽⁶⁾ the signal received by any one hydrophone can be represented by m time samples during an observation interval T , where $m = \omega_m T / \pi$. Then for detection by an array of M elements one can use the convention that the first m samples of \underline{x} represent the signal on the first hydrophone, the next m represent the signal on the second hydrophone, etc. Then the dimension of the sample vector is $n = Mm$.

The fact that the array is steered on target implies that the signal components at the different hydrophones are 100 per cent correlated. Hence the \underline{P} matrix consists of M^2 identical submatrices, which are diagonal if $y(t)$ is a white noise. As a result of the additional factor of amplitude modulation, the general element of the \underline{P} matrix is given by

$$P_{ij} = f_k^2 \quad \text{for } |i-j| = mr; r=0,1,2,\dots,M-1$$

$$0 \quad \text{otherwise} \quad (16)$$

where for $mr < i \leq m(r+1)$, $k = i - mr$; and where $f_k^2 = f^2(t_k) = 1 + b \cos \omega_0 t_k$. Furthermore, the assumption concerning the noise implies that $\underline{Q} = \underline{I}$, the n -dimensional unit matrix. Then it follows directly that

$$\text{tr } \underline{P} \underline{Q}^{-1} = M \sum_{k=1}^m f_k^2 \approx Mm = n \quad (17)$$

where the approximation is valid by the Riemann-Lebesgue lemma if the observation time $T = m(t_k - t_{k-1}) \gg 2\pi/\omega_0$. Similarly,

$$\text{tr}(\underline{P} \underline{Q}^{-1})^2 = M^2 \sum_{k=1}^m f_k^4 \approx M^2 m \left(1 + \frac{b^2}{2}\right) \quad (18)$$

Hence the figure of merit d becomes

$$d = \frac{S}{\sqrt{2} N} \sqrt{m \left[M^2 \left(1 + \frac{b^2}{2}\right) - M \right]} \quad (19)$$

If the signal were unmodulated, $b = 0$, and therefore the ratio of figures of merit for the cases of modulated and unmodulated signals is

$$\frac{d_m}{d_u} = \sqrt{\frac{M \left(1 + \frac{b^2}{2}\right) - 1}{M - 1}} \rightarrow \sqrt{1 + \frac{b^2}{2}} \quad \text{for } M \gg 1 \quad (20)$$

If the noise level had been assumed to be precisely known, then, by Eqs. (14) and (18), the ratio of d 's for modulated and unmodulated signals would have been

$$\frac{d_{cm}}{d_{ou}} = \sqrt{1 + \frac{b^2}{2}} \quad (21)$$

for all M . This is the result that has been obtained previously.⁽⁷⁾ Since b cannot exceed unity, the increase in d caused by modulation is less than 25 per cent. This is equivalent to saying that the reduction in $\frac{S}{N}$ permitted for equivalent performance is less than .9 db if modulation is present.

It is clear that for large arrays the effect of the lack of knowledge of the noise level becomes negligible. In fact, if the square-root factor in Eq. (19) is expanded by means of the binomial formula, the result for large M is approximately

$$d = \frac{S}{\sqrt{2} N} \cdot \sqrt{M} \left[M \left(1 + \frac{b^2}{2} \right)^{1/2} - \frac{1}{2} \right] \quad (22)$$

whereas, by Eq. (14), for precisely known noise level,

$$d_o = \frac{S}{\sqrt{2} N} \sqrt{M} \left(1 + \frac{b^2}{2} \right)^{1/2} \quad (23)$$

Thus for large M the cost of not knowing the noise level is approximately one half of a hydrophone.

The situation is clearly different when M is small. As an extreme case, consider $M = 1$. Then with modulation and unknown noise level

$$d = \frac{S}{\sqrt{2} N} b \sqrt{\frac{M}{2}} \quad (24)$$

Without modulation $d = 0$, leading to the obvious result that an unmodulated signal is not detectable by a single hydrophone if the noise

level is completely unknown. Thus modulation plays a very crucial role in this case. On the other hand, if $M = 2$, the ratio d_m/d_u is already less than $\sqrt{2}$; hence the limiting case of large M is approached very rapidly.

IV. Nonuniform Signal and Noise Spectra

The results of the previous section may be extended to nonuniform signal and noise spectra if the assumption of negligible noise correlation between hydrophones is retained. The general effect of modulation with nonuniform spectra has been considered previously⁽⁸⁾ and the general conclusion was that for a modulating frequency very much lower than the frequency for which the spectrum of $y(t)$ begins to drop off, the effects of modulation on detectability are unaffected by the shape of either the signal or the noise spectrum. Thus in this section we consider only unmodulated signals.

Let the signal spectrum be $S_0 S(\omega)$, where S_0 is zero-frequency spectrum level and $S(\omega)$ the normalized spectrum, defined such that $\lim_{\omega \rightarrow 0} S(\omega) = 1$. Similarly, let the noise spectrum be given by $N_0 N(\omega)$.^{*} Then it has been shown in previous reports⁽⁹⁾ that

$$\text{tr}(\underline{P} \underline{Q}^{-1})^2 = 2 \sum_{i=1}^m \frac{S_0^2}{N_0^2} \left[\frac{S(\omega_i)}{N(\omega_i)} G(\omega_i) \right]^2 \quad (25)$$

where $G(\omega_i)$ is the array gain.⁽¹⁰⁾ As is shown in Reference (9), if the observation time T is sufficiently large so that the signal and noise spectra are essentially constant over a frequency interval of $\Delta\omega = \frac{2\pi}{T}$ rad/sec, Eq. (25) can be expressed in the integral form:

^{*}It is assumed that $S(\omega)$ and $N(\omega)$ have finite values as $\omega \rightarrow 0$.

$$\text{tr}(\underline{P} \underline{Q}^{-1})^2 = \frac{T}{\pi} \frac{S_o^2}{N_o^2} \int_0^{\omega_m} \left[\frac{S(\omega)}{N(\omega)} G(\omega) \right]^2 d\omega \quad (26)$$

Similarly, it can be shown that

$$\text{tr}(\underline{P} \underline{Q}^{-1}) = \frac{T}{\pi} \frac{S_o}{N_o} \int_0^{\omega_m} \left[\frac{S(\omega)}{N(\omega)} G(\omega) \right] d\omega \quad (27)$$

Finally, since there are $\frac{\omega_m \pi}{\pi}$ frequency samples in time T,

$$n = \frac{M \omega_m T}{\pi} \quad (28)$$

Substituting Eqs. (26), (27), and (28) into Eq. (13) results in the figure of merit

$$d = \sqrt{\frac{T}{2\pi}} \frac{S_o}{N_o} \sqrt{\int_0^{\omega_m} \left[\frac{S(\omega)}{N(\omega)} G(\omega) \right]^2 d\omega} - \frac{1}{M \omega_m} \left[\int_0^{\omega_m} \left[\frac{S(\omega)}{N(\omega)} G(\omega) \right] d\omega \right]^2 \quad (29)$$

If the noise correlation between different hydrophones is negligible,⁽¹¹⁾ then $G(\omega) \approx M$. Also, it is often true that the signal and noise spectra are sufficiently similar so that approximately $S(\omega) = N(\omega)$. Using this results in

$$d = \sqrt{\frac{T \omega_m}{2\pi}} \frac{S_o}{N_o} \sqrt{M^2 - M} \quad (30)$$

This equation is identical to Eq. (19) with $b = 0$ since the number of samples m in Eq. (19) can be equated to $\frac{T \omega_m}{\pi}$. Also we find that the figure of merit for noise level known precisely is given by

$$d = \sqrt{\frac{T\omega_m}{2\pi}} \frac{S_o}{N_o} M \quad (31)$$

Hence the argument of Eq. (22) can be applied here again to show that the cost of ignorance about the noise level is approximately $\frac{1}{2}$ hydrophone when M is large.

In order to consider a case where $S(\omega)$ and $N(\omega)$ are not identical, suppose that

$$\frac{S(\omega)}{N(\omega)} = \frac{\omega_o^2}{\omega^2 + \omega_o^2} \quad (32)$$

A possible combination of signal and noise spectral densities leading to this result might be

$$S(\omega) = \frac{\omega_1^2}{\omega_1^2 + \omega^2} \quad (33)$$

$$N(\omega) = \frac{\omega_1^2(\omega^2 + \omega_o^2)}{\omega_o^2(\omega^2 + \omega_1^2)} \quad (34)$$

Thus both signal and noise spectra have essentially the same form at low frequencies, but at frequencies above ω_o the noise spectrum levels off. Then, from Eqs. (26) and (27),

$$\text{tr}(\underline{P} \underline{Q}^{-1})^2 = \frac{\omega_o}{2} \left[\frac{\frac{\omega_m \omega_o}{2}}{\frac{\omega_m^2}{2} + \omega_o^2} + \tan^{-1} \frac{\omega_m}{\omega_o} \right] \quad (35)$$

and

$$\text{tr}(\underline{P} \underline{Q}^{-1}) = \omega_o \tan^{-1} \frac{\omega_m}{\omega_o} \quad (36)$$

and therefore

$$d = \sqrt{\frac{T}{2\pi}} \frac{S_0}{N_0} \sqrt{\frac{\omega_0}{2} \left[\frac{\omega_m \omega_0}{\omega_m^2 + \omega_0^2} + \tan^{-1} \frac{\omega_m}{\omega_0} \right] M^2 - \frac{\omega_0^2}{\omega_m} \left(\tan^{-1} \frac{\omega_m}{\omega_0} \right)^2 M} \quad (37)$$

For $\omega_m \ll \omega_0$ this reduces to the result obtained above [Eq. (30)].

However, for $\omega_m \gg \omega_0$

$$d \approx \sqrt{\frac{T\omega_0}{2\pi}} \frac{S_0}{N_0} \sqrt{\frac{\pi}{4} M^2 - \frac{\omega_0}{\omega_m} M} \longrightarrow \sqrt{\frac{T\omega_0}{8}} \frac{S_0}{N_0} M \quad (38)$$

as $\omega_m/\omega_0 \rightarrow \infty$. The limiting value of d is the same as the value obtained when the noise level is known precisely. Thus the cost of not knowing the noise level is less than 1/2 hydrophone for large M , and it approaches zero for large ω_m/ω_0 . Detection by a single hydrophone also becomes feasible under this condition.

This result does not depend critically on the precise form of

$\frac{S(\omega)}{N(\omega)}$, but only on the fact that $\int_0^\infty \frac{S(\omega)}{N(\omega)} G(\omega) d\omega$ is finite. This

will always be true if the signal spectrum falls off more rapidly with increasing frequency than the noise spectrum, and it is true particularly for narrow-band signals. Under these conditions the received signal at very high frequencies consists almost exclusively of noise, and it is theoretically possible, therefore, for the high-frequency noise level to be quite accurately established. Then, if the form of the noise spectral density is precisely known, the high-frequency level can be extrapolated down to low frequencies, and the noise level at all frequencies would be precisely known.

In practice this sort of extrapolation is not always feasible. Thus, in the example noise spectrum of Eq. (34), the frequency ω_0 might be the frequency at which the locally generated white noise begins to dominate the sea noise. This frequency depends on the low-frequency level of the sea noise as well as on the level of the white noise. Hence in this case the high-frequency noise level does not necessarily contain very much information about the low-frequency noise.

It can be seen by means of Schwartz's inequality that

$$\int_0^{\omega_m} \left[\frac{S(\omega)}{N(\omega)} G(\omega) \right]^2 d\omega \geq \frac{1}{\omega_m} \left[\int_0^{\omega_m} \frac{S(\omega)}{N(\omega)} G(\omega) d\omega \right]^2 \quad (39)$$

where the equality holds only when the integrand is a constant.⁽¹²⁾ Thus for non-constant $\frac{S(\omega)}{N(\omega)}$ the figure of merit d is always somewhat larger than the value given by Eq. (30). This indicates that the optimum CFAR detector can always make use of known differences between signal and noise spectra to improve the detectability. This is of course particularly important if detection is by a single omnidirectional hydrophone, since in this case differences in spectral shape provide the only possibility for detection. On the other hand, for large M the improvement cannot exceed the $\frac{1}{2}$ hydrophone loss that results when $\frac{S(\omega)}{N(\omega)} = 1$. Moreover, it is shown in the next section that even for fairly large variations in $\frac{S(\omega)}{N(\omega)}$ the two sides of Eq. (39) are approximately equal.

VI. The Approximate Effect of Noise Correlation Between Hydrophones

Noise correlation between hydrophones results in a reduction in the array gain with decreasing frequency. This has been studied in some detail in previous reports,⁽¹³⁾ and the exact relation between $G(\omega)$ and ω was found to be fairly complex. A typical curve of $G(\omega)$ vs. ω is

shown in Fig. 2. For zero frequency, the noise correlation approaches 100 per cent, and therefore, if there is some self-noise, $\lim_{\omega \rightarrow 0} G(\omega) = G_0 = 1$. (In the absence of self-noise G_0 may differ from unity, but this is a singular case which is of little practical interest.)

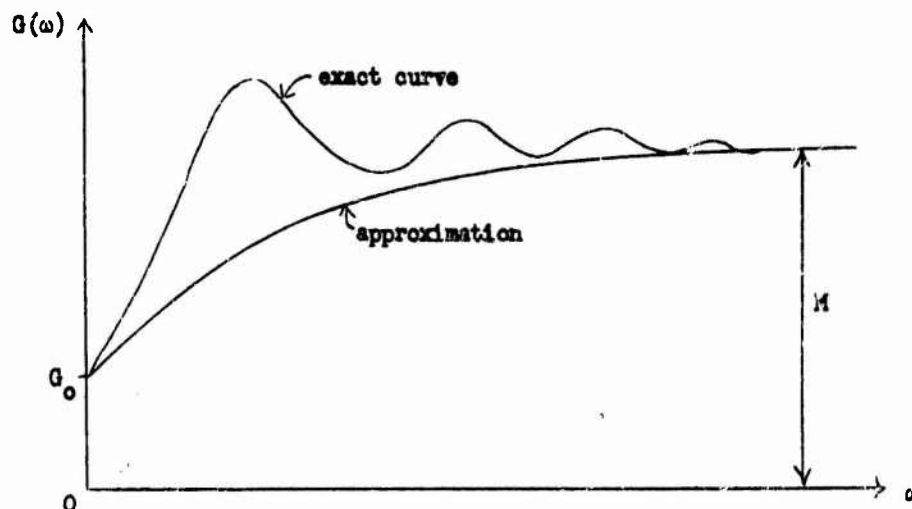


Figure 2 Typical Array Gain

In order to obtain an estimate of the effect of noise correlation, we approximate $G(\omega)$ by

$$G(\omega) = M - (M - G_0) e^{-c\omega} \quad (40)$$

where c is a constant chosen to approximate the true $G(\omega)$. A typical curve of approximate $G(\omega)$ vs. ω is also shown in Fig. 2. Furthermore, since it is desired to observe only the effect of $G(\omega)$, it is assumed that $\frac{S(\omega)}{N(\omega)} = 1$. Substitution of Eq. (40) into Eq. (29) and performing the integration yields

$$d = \sqrt{\frac{-\omega_m}{2\pi} \frac{S_0}{N_0}} \left\{ M^2 - M - \frac{2(M - G_0)(M - 1)}{c\omega_m} \left(1 - e^{-c\omega_m} \right) + \frac{(M - G_0)^2}{2c\omega_m} \left(1 - e^{-2c\omega_m} \right) - \frac{(M - G_0)^2}{Mc^2\omega_m^2} \left(1 - e^{-c\omega_m} \right)^2 \right\}^{1/2} \quad (41)$$

For noise level precisely known the result would be

$$d_o = \sqrt{\frac{T\omega_m}{2\pi}} \frac{S_o}{N_o} \left\{ M^2 - \frac{2M(M-G_o)}{c\omega_m} \left(1 - e^{-c\omega_m}\right) + \frac{(M-G_o)^2}{2c\omega_m} \left(1 - e^{-2c\omega_m}\right) \right\}^{1/2} \quad (42)$$

For $\omega_m \rightarrow 0$, limiting forms for d and d_o are

$$d = \sqrt{\frac{T\omega_m}{2\pi}} \frac{S_o}{N_o} G_o \left(1 - \frac{1}{M}\right)^{1/2} \quad (43)$$

$$d_o = \sqrt{\frac{T\omega_m}{2\pi}} \frac{S_o}{N_o} G_o$$

and for $\omega_m \rightarrow \infty$,

$$d = \sqrt{\frac{T\omega_m}{2\pi}} \frac{S_o}{N_o} M \left(1 - \frac{1}{M}\right)^{1/2} \quad (44)$$

$$d_o = \sqrt{\frac{T\omega_m}{2\pi}} \frac{S_o}{N_o} M$$

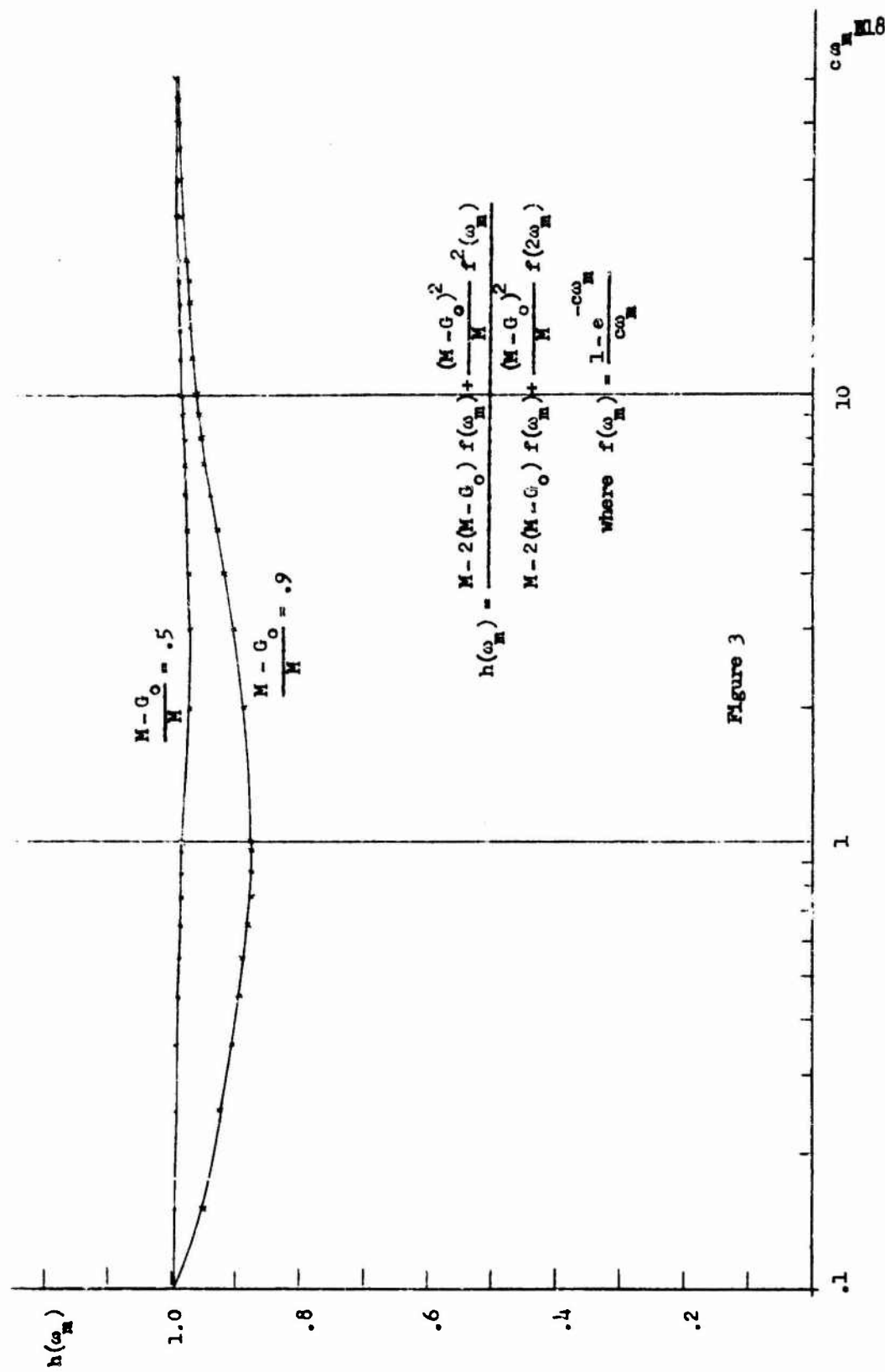
For intermediate values of ω_m , the Schwartz inequality again indicates that

$$\sqrt{1 - \frac{1}{M}} \leq \frac{d}{d_o} \leq 1 \quad (45)$$

If we let $\left(\frac{1 - e^{-c\omega_m}}{c\omega_m}\right) = f(\omega_m)$, then

$$\left(\frac{d}{d_o}\right)^2 = 1 - \frac{1}{M} \left[\frac{M - 2(M-G_o)f(\omega_m) + \frac{(M-G_o)^2}{M} f^2(\omega_m)}{M - 2(M-G_o)f(\omega_m) + \frac{(M-G_o)^2}{M} f(2\omega_m)} \right] \quad (46)$$

The bracketed term is plotted in Fig. 3 for several values of $\frac{(M-G_o)}{M}$, and is seen to be approximately equal to unity for all values of ω . Hence



$$\frac{d}{d_0} \approx \sqrt{1 - \frac{1}{M}} \quad (47)$$

for all ω_m . Thus it can be concluded that noise correlation does not have any significant effect on the cost of not knowing the precise noise level. Although this conclusion is based on a particular expression for the array gain, it can be seen by inspection of the basic relation [Eq. (29)] that it actually depends on the fact that

$$\int_0^{\omega_m} G^2(\omega) d\omega \approx \frac{1}{\omega_m} \left[\int_0^{\omega_m} G(\omega) d\omega \right]^2 \quad (48)$$

This equation is obviously not true in general, as shown, in fact, by Eq. (39). However, if $G(\omega)$ had been approximated more closely, as for instance by $M - (M - G_0) e^{-c\omega} \cos(k\omega + \phi)$, which simulates the oscillations in $G(\omega)$ better than Eq. (40), Eq. (48) would still have been approximately correct. One may be justified, therefore, in assuming the conclusion of this section to be generally true. Also, it can be seen by inspection of Eq. (39) that variation of $\frac{S(\omega)}{N(\omega)}$ with frequency would generally have the same kind of result.

VII. Conclusions

If the noise level is not known, it is desirable to employ a detector having a CFAR characteristic. Such a detector can be represented as a two-channel device in which one channel is a standard likelihood-ratio detector, and the other channel consists of a noise level estimator. When a detector of this type is employed in the detection of a Gaussian directional signal, the following results are obtained:

- a) The improvement in detectability resulting from amplitude modulation by means of a known time function depends on the number of

elements in the receiving array. If there is only a single element in the array, amplitude modulation is crucial to detection, an unmodulated signal being essentially undetectable if the noise level is not known. However, if there are many hydrophones in the array, the improvement approaches that obtained when the noise level is known, and modulation permits a reduction in signal-to-noise ratio of at most .9 db for a sinusoidal modulation. Even with two hydrophones in the array, the effect is equivalent only to about 1.5 db of signal-to-noise ratio.

b) The effect of the unknown noise level on the detectability by large arrays is generally equivalent to the loss of $\frac{1}{2}$ hydrophone from the array. This figure is relatively unaffected by noise correlation between hydrophones or by the shape of the signal or noise spectrum, so long as the signal and noise cover essentially the same band. However, if the signal band is narrower than the noise band, the cost of ignorance about the noise level becomes further reduced, and approaches zero as the ratio of signal bandwidth to noise bandwidth approaches zero.

It is interesting to note that a DDMUS detecting system approximates the operation of the optimum CFAR detector quite closely, since it displays off-target as well as on-target information simultaneously. The difference between the on-target and off-target indications is very similar to the difference between upper and lower channels of the CFAR detector considered in this report.

Appendix A Optimality of the CFAR Detector for Detection of a Gaussian
Signal in Gaussian Noise

It is well known that if the signal and noise power levels, S and N , are known, the optimum detector is the likelihood-ratio detector. It can be shown⁽¹⁴⁾ that this detector generally minimizes the quantity $\beta + K\alpha$, where β and α are respectively the conditional miss and false-alarm probabilities, and K is the likelihood-ratio threshold. When S and N are not known, and if it is not reasonable to assume that probability density functions for S and N can be defined, then a conditional likelihood ratio must be employed. It has the form

$$L(\underline{x}/S,N) = \frac{f_1(\underline{x}/S,N)}{f_0(\underline{x}/N)} \quad (A-1)$$

where $f_1(\underline{x}/S,N)$ is the conditional probability density of \underline{x} given that signal is present, and that signal and noise power are respectively S and N ; and where $f_0(\underline{x}/N)$ is the conditional probability density of \underline{x} given that there is no signal and that the noise power is N . Also under these conditions the error probabilities α and β become $\alpha(N)$ and $\beta(S,N)$; i.e., they are conditional on the signal and noise levels S and N respectively. The conditional likelihood-ratio detector is then optimum in the sense that it minimizes the quantity $\beta(N,S) + K\alpha(N)$ relative to other detectors.

In formulating the conditional likelihood ratio one assumes that S and N take on particular, known values. Hence if the signal and noise are independent Gaussian processes, and if it is assumed that the signal-to-noise ratio is very small (See footnote, page 3), the expression for the conditional likelihood ratio has the usual form:⁽¹⁵⁾

$$L(\underline{x}/S, N) = \exp \left\{ -\frac{S}{2N^2} \underline{x}' \underline{Q}^{-1} \underline{P} \underline{Q}^{-1} \underline{x} - \frac{S}{2N} \text{tr} \underline{P} \underline{Q}^{-1} - \frac{S^2}{4N^2} \text{tr}(\underline{P} \underline{Q}^{-1})^2 \right\} \quad (\text{A-2})$$

The conditional false-alarm probability $\alpha(N)$ is the probability that $u_1 = \underline{x}' \underline{Q}^{-1} \underline{P} \underline{Q}^{-1} \underline{x}$ exceeds the threshold u_0 when $\underline{x}(t)$ consists of noise only. For large sample size, u_1 is approximately Gaussian by the Central Limit Theorem, and its mean and variance for $\underline{x}(t)$ consisting of noise only are given by

$$\mu_0(N) = \langle u_1 \rangle_N = N \text{tr}(\underline{P} \underline{Q}^{-1}) \quad (\text{A-3})$$

$$\sigma_0^2(N) = \langle u_1^2 \rangle_N - \langle u_1 \rangle_N^2 = 2N^2 \text{tr}(\underline{P} \underline{Q}^{-1})^2 \quad (\text{A-4})$$

Hence

$$\alpha(N) = \frac{1}{2} \text{erfc} \left[\frac{N \text{tr}(\underline{P} \underline{Q}^{-1}) - u_0}{2N \sqrt{\text{tr}(\underline{P} \underline{Q}^{-1})^2}} \right] \quad (\text{A-5})$$

By Eq. (A-2)

$$u_0 = \frac{2N}{S} \log K + \text{tr} \underline{P} \underline{Q}^{-1} + \frac{S}{2N} \text{tr}(\underline{P} \underline{Q}^{-1})^2 \quad (\text{A-6})$$

It must be re-emphasized that in this formulation S and N are given values, and therefore if K is fixed, u_0 is also fixed. But with fixed u_0 it is clear from Eq. (A-5) that α will change as N changes. Thus, to obtain a CFAR characteristic it is necessary that u_0 be made proportional to N . However, since N is not known, this is not directly possible, and the best that can be done is to make u_1 proportional to an unbiased estimate \hat{N} of N ; i.e., to let

$$u_0 = a \hat{N} \quad (\text{A-7})$$

A simple way of estimating the noise level is to measure the power in the received signal; i.e.,

$$\hat{N} = \sum_{i=1}^n x_i^2 = \underline{x}' \underline{x} \quad (\text{A-8})$$

A more general form of estimator is the quadratic form

$$\hat{N} = \underline{x}' \underline{A} \underline{x} \quad (\text{A-9})$$

The matrix \underline{A} is an arbitrary $n \times n$ symmetric matrix, except that it is convenient to require that it satisfy

$$\text{tr}(\underline{A} \underline{Q}) = n \quad (\text{A-10})$$

This is merely a normalization that specifies a particular value of a in Eq. (A-7). It is clear that Eq. (A-8) is a special case of Eq. (A-9) with $\underline{A} = \underline{I}$.

For large n the estimate \hat{N} is approximately Gaussian by the Central Limit Theorem. Its mean value, when $x(t)$ consists of noise only, is

$$\langle \hat{N} \rangle_N = N \text{tr} \underline{A} \underline{Q} = Nn \quad (\text{A-11})$$

Thus the estimate is unbiased, as required. Also, the variance of \hat{N} (for $x(t)$ consisting of noise only) is easily shown to be

$$\sigma_{\hat{N}}^2 = 2N^2 \text{tr}(\underline{A} \underline{Q})^2 \quad (\text{A-12})$$

It is clear that the threshold u_0 is also a Gaussian random variable. Thus, depending on the value of u_0 that actually emerges from the noise-level estimator, the false-alarm probability is different from observation to observation, and it can therefore be represented by $\alpha(N, u_0)$.

Since one is usually interested in an overall false-alarm rate rather than the false-alarm probability for a particular observation, one would presumably want the average of the false-alarm probabilities over u_o . This would, for instance, yield the expected number of false alarms in a long period of time in which a large number of disjoint observations had been made. Without getting involved in the details of the computation of this average false-alarm probability, it is fairly clear that the effect of the variable threshold is to broaden the curve of α vs. a , as shown in Fig. A-1. In this figure $\alpha(\bar{N}, \bar{u}_o)$ represents a particular false-alarm probability evaluated with an average noise level \bar{N} and with $\bar{u}_o = a \bar{N}$, a deterministic quantity. The average $\langle \alpha(N, u_o) \rangle_{u_o}$ is essentially the weighted sum of curves of this type with different \bar{N} 's.

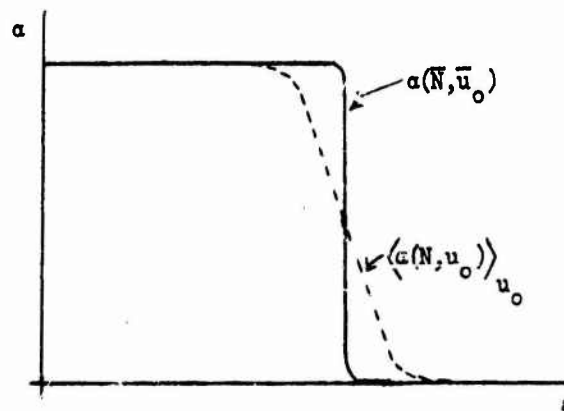


Figure A-1

From heuristic reasoning of this sort it can be concluded that the smaller the variance of u_o , the steeper the curve of $\langle \alpha(N, u_o) \rangle_{u_o}$ vs. a would be.

Therefore, the value of a needed to obtain a given small value of α decreases as the variance of u_o decreases. But the smaller a is, the

higher the detection probability will be. Hence it is concluded that the optimum system results when the variance of u_0 is a minimum.

As a result of Eqs. (A-7) and (A-12), the variance of u_0 is $2a^2N^2 \text{tr}(\underline{A} \underline{Q})^2$. Consider the non-negative quantity

$$\begin{aligned} \text{tr}[\underline{A} \underline{Q} - \underline{I}]^2 &= \text{tr}(\underline{A} \underline{Q})^2 - 2 \text{tr} \underline{A} \underline{Q} + n \\ &= \text{tr}(\underline{A} \underline{Q})^2 - n \geq 0 \end{aligned} \quad (\text{A-13})$$

where the second step follows by use of Eq. (A-10). The equality holds for $\underline{A} = \underline{Q}^{-1}$, and therefore the minimum-variance estimate of \hat{N} is

$$\hat{N}_{m.v.} = u_2 = \underline{x}' \underline{Q}^{-1} \underline{x} \quad (\text{A-14})$$

The optimum detector that emerges from this discussion is then the one shown in Fig. 1.

List of Symbols

\underline{A}	arbitrary symmetric matrix
a	constant that determines false-alarm rate
B_1	$\frac{1}{2} \overline{S^2} \text{tr}(\underline{P} \underline{Q}^{-1})^2$
B_2	$\overline{S} \text{tr}(\underline{P} \underline{Q}^{-1})$
b	modulation index
c	constant
d	figure of merit
d_o	figure of merit for known noise level
d_m	figure of merit with modulation present
d_u	figure of merit for unmodulated signal
d_{om}	same as d_m , except for known noise level
d_{ou}	same as d_u , except for known noise level
$f(t)$	modulating function
f_k	$f(t_k)$
$f_1(\underline{x}/S, N)$	probability density of \underline{x} , given that signal is present
$f_o(\underline{x}/N)$	probability density of \underline{x} , given that signal is absent
$G(\omega)$	array gain
G_o	zero-frequency array gain
\underline{I}	unit matrix
K	likelihood-ratio threshold

K_α	argument of false-alarm probability
$L(\underline{x})$	likelihood ratio
M	number of elements in array
m	number of samples per array element
N	noise level
n	dimension of sample vector
$N(\omega)$	normalized noise spectral density
N_0	zero-frequency noise spectral level
\underline{P}	normalized signal covariance matrix
$P_N(N)$	probability density function of noise level
$P_S(S)$	probability density function of signal level
\underline{Q}	normalized noise covariance matrix
S	signal level
S_0	zero-frequency signal spectral level
$S(\omega)$	normalized signal spectral density
$s(t)$	signal
T	observation time
$\text{tr}()$	trace of matrix
u_1	test statistic
u_2	noise estimate
u_0	threshold value of u_1

$x(t)$	received signal
\underline{x}	received-signal sample vector
$y(t)$	unmodulated signal
α	conditional false-alarm probability
β	conditional miss probability
λ_1	eigenvalue of $\underline{P} \underline{Q}^{-1}$ having largest absolute value
μ_0	mean value of statistic when signal is absent
μ_1	mean value of statistic when signal is present
σ_0	variance of statistic when signal is absent
ω_0	modulation frequency, also high-frequency break frequency in noise spectrum
ω_1	break frequency
ω_m	maximum frequency

List of References

- (1) D. Middleton, Introduction to Statistical Communication Theory, McGraw-Hill Book Company, Inc., 1960, p. 840.
- (2) W. M. Siebert, "Some Applications of Detection Theory to Radar," IRE National Convention Record, March 1958, p. 5.
- (3) R. A. McDonald, P. M. Schultheiss, F. B. Tuteur, T. Usher, Jr., "Processing of Data from Sonar Systems," General Dynamics/Electric Boat Research and Development Department, Groton, Connecticut, Report No. UH17-63-045 (September 1, 1963), pp. 45-6,7.
- (4) Ibid., p. A5-8.
- (5) Ibid., p. A5-13.
- (6) Middleton, op. cit., p. 201.
- (7) McDonald et al., op. cit., p. A5-14.
- (8) Ibid., pp. A5-15 to A5-20.
- (9) Ibid., pp. A3-11,12.
- (10) Ibid.
- (11) Ibid., p. A3-14.
- (12) H. Margenau and G. M. Murphy, The Mathematics of Physics and Chemistry, D. Van Nostrand Company, Inc., Princeton, New Jersey, 1956, p. 134.
- (13) P. M. Schultheiss, "Evaluation of a Suboptimal Procedure for Detecting Directional Gaussian Signals in Isotropic Gaussian Noise," General Dynamics/Electric Boat Research, Progress Report No. 10, December 1963.
- (14) D. Middleton, Topics in Communication Theory, McGraw-Hill Book Company, Inc., 1965, Chapter 2.
- (15) Middleton, Introduction to..., op. cit., p. 840.



DETECTION OF SIGNALS OF UNKNOWN FREQUENCY

by

Allen H. Levesque

Progress Report No. 20

General Dynamics / Electric Boat Research

(53-00-10-0231)

June 1965

DEPARTMENT OF ENGINEERING
AND APPLIED SCIENCE

YALE UNIVERSITY

CHAPTER III DETECTION OF A NARROWBAND GAUSSIAN SIGNAL OF UNKNOWN
CENTER FREQUENCY - PART I. WEAK SIGNALS

III.1	Introduction	C-52
III.2	Detection of a Stochastic Signal of Unknown Center Frequency	C-53
III.3	Narrowband Gaussian Signal of Unknown Center Frequency	C-59
III.4	Signal Detectability in the Weak-Signal Case	
a)	Error Probabilities	C-72
b)	First Approximation - Non-overlapping Filters ($b = r$)	C-74
c)	Second Approximation - Overlapping Filters ($b = 2r$)	C-81
III.5	Experimental Verification	C-97

CHAPTER IV DETECTION OF A NARROWBAND GAUSSIAN SIGNAL OF UNKNOWN
CENTER FREQUENCY - PART II. STRONG SIGNALS

IV.1	Detection Analysis in the Strong-Signal Case	C-106
IV.2	Detection for Short Observation Times ($B_S T \ll 1$)	
a)	Detector Structure	C-108
b)	Signal Detectability	C-117
IV.3	Detection for Long Observation Times ($B_S T \gg 1$)	C-146

CHAPTER V CONCLUSION C-160

APPENDIX A DEFLECTIONS OF TERMS IN THE POWER SERIES FOR $\log \lambda(\underline{v})$ C-165

APPENDIX B A SMALL-SIGNAL APPROXIMATION TO THE OPTIMUM
DETECTOR FOR THE CASE OF COHERENT DETECTION C-169

APPENDIX C ERROR PROBABILITIES FOR A BAND-SPLITTING DETECTOR
WITH INDEPENDENT OUTPUTS C-173

APPENDIX D CORRELATION COEFFICIENT RELATING Q_1 AND Q_2 C-176

APPENDIX E DIAGRAMS FOR THE EXPERIMENTAL DETECTOR C-182

LIST OF PRINCIPAL SYMBOLS C-184

REFERENCES C-186

CONTENTS

SUMMARY	C- iv
CHAPTER I INTRODUCTION	
I.1 Preliminary Remarks	C-1
I.2 Optimum Detection of Signals with Unknown Parameters	
a) The Likelihood Ratio Detector	C-2
b) Detection in Gaussian Noise	C-6
c) Signals with Unknown Parameters	C-7
I.3 Description of the Problem	C-9
I.4 A Power Series Approach and Its Limitations	C-10
CHAPTER II DETECTION OF A COHERENT SINUSOID OF UNKNOWN FREQUENCY	
II.1 Introduction	C-14
II.2 Likelihood Ratio Detection of a Signal of Unknown Frequency	C-14
II.3 Detection of a Coherent Sinusoid - Two-Frequency Case	
a) The Decision Plane	C-16
b) Detection in Gaussian Noise	C-19
c) Detection Probabilities - Two-Frequency Case	C-29
II.4 Detection of a Coherent Sinusoid - m-Frequency Case	
a) The Decision Space	C-34
b) Detection Probabilities - m-Frequency Case	C-37
II.5 Detection of a Sinusoid of Random Phase and Unknown Frequency in Gaussian Noise	C-47
II.6 Comments	C-51

The major result of the work of Chapters III and IV is that in the case of low pre-detection SNR, the detectability of a stochastic signal of unknown center frequency is governed primarily by the pre-detection SNR R_g in a band of the width of the signal, even though the frequency location of the signal may be unknown within the wider processing band. Thus if the signal spectrum and the observation time are fixed and the processing band is gradually widened, the signal detectability (for a fixed false-alarm probability) will gradually decrease, but the decrease will be slight when compared with the increase in noise power which results from widening of the processing band.

From another point of view the processing band and the observation time may be regarded as fixed. Then, if the signal power is confined to a frequency band r times narrower than the processing band instead of being uniformly spread over the processing band, the pre-detection SNR is increased by a factor r and signal detectability is accordingly increased in spite of the signal frequency uncertainty. The work of Chapters III and IV indicates that substantial improvement in detectability can be achieved in this manner only up to the point where the pre-detection SNR R_g becomes on the order of unity.

SUMMARY

This investigation is concerned with the detection of signals of unknown frequency in the presence of broadband additive gaussian noise. Several signal models are considered and in each case the structure of the optimum detector is determined and the signal detectability is calculated.

Chapter I presents the background and description of the problem to be considered. A power series approach to the problem which was investigated in earlier work is described and its limitations are discussed.

In Chapter II the signal to be detected is taken to be a sinusoid with known amplitude and phase but unknown frequency, the frequency having a discrete probability distribution. The results show that as the post-detection SNR is made large the optimum detector becomes equivalent to a band-splitting detector in which a test quantity is generated and threshold-tested at each possible value of the unknown signal frequency. The performance of this detector is analyzed and is compared with that of a sub-optimum detector in which the test quantities are summed before the threshold test. Finally, some work is described in which the results of the present investigation were extended to the problem of detecting a sinusoid of known amplitude but unknown phase and frequency, with the frequency again being given by a discrete probability distribution.

Chapters III and IV are concerned with the detection of a gaussian stochastic signal of unknown center frequency. The signal power is assumed to be confined to a frequency band which is r times narrower than the overall frequency band being processed and the signal spectrum is assumed to lie anywhere within the processing band with uniform probability. The optimum detector structure in this case is conjectured to be a band-sweeping detector, the limiting form of the band-splitting detector derived in Chapter II. A suitable engineering approximation to the band-sweeping detector is then found and its performance is evaluated.

The analysis of Chapter III is based upon the assumption of low pre-detection SNR. Experimental data is presented which corroborates some of the theoretical results obtained in this chapter. When the pre-detection SNR R_S (defined in a band of the width of the signal spectrum) is on the order of or larger than unity, the analysis of Chapter III must be modified; this strong-signal situation is considered in Chapter IV.

CHAPTER I

INTRODUCTION

I.1 Preliminary Remarks

This report deals with the detection of sinusoidal or narrowband signals of unknown frequency in a background of noise having known statistical properties. Much of this work has been reported in a series of earlier progress reports. In particular, most of Chapter II has previously been submitted as Progress Report No. 15, while Chapters III and IV were largely covered by Progress Report No. 19. Some portions of Chapter I were contained in Progress Reports No. 8 and 14. The purpose of the present report is primarily to collect all the material on this topic in one place, to put some of the earlier work on the subject into proper perspective in the light of the later results, and, where appropriate, to make a number of extensions of the work already reported.

Motivation for the investigations described in this report was derived from the knowledge that signals received from passive sonar targets often contain a number of low frequency sinusoidal or quasi-sinusoidal components. These are believed to originate at the target vessel as rotating-machinery noises and upon reception are observed in the spectrum of the received data as lines of some small but non-zero bandwidth. Although some existing sonar systems make use of these low frequency components, no analysis has been made to date to determine the ultimate detectability of such signals. Hence this investigation was undertaken.

The frequencies of these narrowband signals are related to the operating speeds of various machines on board the target vessel and cannot be known a priori; however, the signals do appear in predictable regions of the spectrum. The frequencies of the individual signals are

observed to vary with time, but these variations appear to be relatively slow with respect to the processing times which are typical of sonar detection systems. Therefore the signal frequencies may reasonably be regarded as constant, though unknown, throughout the observation time of the received signal.

For the purposes of analysis, some reasonable assumptions can be made regarding other characteristics of these signals, i.e., statistical parameters, bandwidths and spectral shapes. Thus the problem to be considered is one of detecting a narrowband signal with given statistical properties, whose frequency is unknown but may be characterized by a statistical distribution over some prescribed range of the spectrum. One would also like to know the structure of the detector which provides maximum detectability for such signals, the optimum detector.

In general several such narrowband signals as have been described appear simultaneously in the received data at a number of frequencies, but for simplicity this investigation will consider the detection of a target characterized by only one such signal.

The problem which has thus been outlined in physical terms belongs to a broad class of problems which will be discussed in the next section, namely, the optimum detection of signals having unknown parameters. The specific problem to be considered will then be described mathematically in Section I.3.

I.2 Optimum Detection of Signals with Unknown Parameters

a) The Likelihood Ratio Detector

The detection of a signal in the presence of noise may be described as follows: A received signal $v(t)$ is observed during some interval of time $0, T$ and on the basis of this observation one of the following two decisions is made. Either 1) the received

data consists of noise only, and $v(t) = n(t)$; or 2) the received data consists of signal and noise, and $v(t) = s(t) + n(t)$, where the noise is assumed to be additive.

Since the noise (and perhaps the signal as well) is a random process, these decisions are statistical in nature and are subject to errors of false alarm and false dismissal. The conditional probabilities of these two types of error are defined in the following manner: The conditional probability of false alarm α is the probability of deciding that a signal is present when the received data actually contains only noise. The conditional probability of false dismissal β is the probability of deciding that only noise is present when the received data contains a signal and noise.

The central problem of signal detection is then one of designing detectors which make these decisions in an efficient manner. In order to design detectors which are in some sense optimum, one must know the statistical properties of the noise and the description (a statistical description if the signal is stochastic) of the signal to be detected or be able to make estimates of these characteristics. If in addition a criterion of goodness is selected, by which the performance of detectors may be compared, then one may in principle find a detector which yields the best performance with respect to this criterion. Such a detector is termed an optimum detector.

In the literature on detection theory several approaches have been taken to this question of selecting an optimum detector. Two representative approaches will be mentioned briefly. One is based on the theory of hypothesis testing as originally outlined by Neyman

and Pearson,[†] who proposed the use of hypothesis tests which minimize the conditional probabilities of error. In terms of the detection problem, this corresponds to using a criterion of goodness which requires that the detector minimize the conditional false dismissal probability for some pre-assigned value of conditional false alarm probability.

A second approach was developed by Middleton,^{††} who analyzed the signal detection problem from the point of view of statistical decision theory. In this type of analysis the detector is required to make decisions in such a way that a certain average "risk" is minimized.

The use of either of these criteria leads to a Likelihood Ratio (hereafter LR) detector as an optimum detector structure.^{†††} When the statistical properties of the noise are known and the signal is a known function, the optimum detector processes the received signal by forming the LR

$$L(\underline{v}) = \frac{f(\underline{v}/\underline{s})}{f(\underline{v}/\underline{0})} \quad (I-1)$$

where \underline{v} and \underline{s} represent sample-vector forms of $v(t)$ and $s(t)$ respectively, and where $f(\underline{v}/\underline{s})$ and $f(\underline{v}/\underline{0})$ are the probability density functions (hereafter p. d. f. 's) of \underline{v} conditioned on the

[†] See Neyman and Pearson (I). The Neyman-Pearson theory is discussed in many books; see for example Cramer (I, Chap. 35) and Lehmann (I).

^{††} See Middleton (II, Part 4). This reference also presents discussions of several other decision criteria in relation to detection systems.

^{†††} Derivations of the LR detector can be found in many references. See for example Davenport and Root (I, Chap. 14), Helstrom (I) and Middleton (II, Part 4).

presence of signal and noise and on the presence of noise only, respectively. When the signal $s(t)$ depends upon parameters which are unknown but have known statistical distributions, then the optimum detector must generate a LR as follows:

$$l(y) = \frac{\langle f(y/s) \rangle_s}{f(y/0)} \quad (I-2)$$

where the average indicated by $\langle \rangle_s$ represents a statistical average taken over all values of the unknown signal parameters. Since only the numerator in Eq. (I-2) depends upon the signal parameters, the average $\langle \rangle_s$ may equivalently be taken over the entire right side of Eq. (I-2) and thus $l(y)$ may be regarded as an average LR.

The optimum detector makes a decision by comparing the average LR with a preset threshold k . This threshold test is indicated by

$$\frac{\langle f(y/s) \rangle_s}{f(y/0)} \geq k \quad (I-3)$$

If the threshold is exceeded the decision is made that signal and noise are present in the received data y ; otherwise the decision is made that only noise is present.

The threshold setting k is determined by the particular criterion which has been selected to evaluate the detector performance.

If for example the Neyman-Pearson criterion had been chosen, k would be set at a level to produce the pre-assigned conditional false alarm probability. The threshold test indicated by Eq. (I-3) would then minimize the conditional false dismissal probability for the pre-assigned false alarm probability.

The LR given by the right side of Eq. (I-2) prescribes the

operations which the optimum detector must perform on the received signal and therefore represents the structure of the optimum detector. This structure clearly depends upon the statistical description of the noise and upon the functional form of the signal and the statistical distributions of its unknown parameters. Attention will now be given to the problem of detection in a background of gaussian noise.

b) Detection in Gaussian Noise

If the noise is a zero-mean gaussian random process, the p.d.f. of the received signal \underline{y} conditioned on the presence of noise only is

$$f(\underline{y}/0) = \frac{1}{(2\pi)^{n/2}(\det \underline{K})^{n/2}} \exp \left[-\frac{1}{2} \underline{y}' \underline{K}^{-1} \underline{y} \right] \quad (I-4)$$

where n is the number of time samples of the received signal taken during the observation interval $0, T$ and \underline{K} is the noise covariance matrix. Since the noise is additive, the p.d.f. for \underline{y} given signal and noise is

$$f(\underline{y}/\underline{s}) = \frac{1}{(2\pi)^{n/2}(\det \underline{K})^{n/2}} \exp \left[-\frac{1}{2} (\underline{y}-\underline{s})' \underline{K}^{-1} (\underline{y}-\underline{s}) \right] \quad (I-5)$$

When Eqs. (I-4) and (I-5) are substituted into Eq. (I-2) the average LR becomes

$$L(\underline{y}) = \left\langle \exp \left[-\frac{1}{2} (\underline{y}-\underline{s})' \underline{K}^{-1} (\underline{y}-\underline{s}) \right] \right\rangle_S \exp \left[\frac{1}{2} \underline{y}' \underline{K}^{-1} \underline{y} \right] \quad (I-6)$$

or

$$L(\underline{y}) = \left\langle \exp \left[-\frac{1}{2} \underline{s}' \underline{K}^{-1} \underline{s} + \underline{s}' \underline{K}^{-1} \underline{y} \right] \right\rangle_S \quad (I-7)$$

It thus remains to carry out the averaging operation over the values of the unknown signal parameters in specific signal cases.

When the signal is completely known the averaging operation can be dropped and the LR becomes

$$l(\underline{y}) = \exp \left[-\frac{1}{2} \underline{s}' \underline{K}^{-1} \underline{s} + \underline{s}' \underline{K}^{-1} \underline{y} \right] \quad (I-8)$$

It is usually convenient to interpret the detector structure from $\log l(\underline{y})$ rather than from $l(\underline{y})$, therefore

$$\log l(\underline{y}) = -\frac{1}{2} \underline{s}' \underline{K}^{-1} \underline{s} + \underline{s}' \underline{K}^{-1} \underline{y} \quad (I-9)$$

The operation which the optimum detector performs on the received signal in this case is given in Eq. (I-9) by the term $\underline{s}' \underline{K}^{-1} \underline{y}$ which may be interpreted as a generalized cross-correlation of the received signal \underline{y} with a replica of the desired signal \underline{s} . The term $-\frac{1}{2} \underline{s}' \underline{K}^{-1} \underline{s}$ is a constant from one observation to the next and acts as a bias in the threshold test.

c) Signals with Unknown Parameters

When the desired signal is a function of unknown parameters, then the average $\langle \rangle_{\underline{s}}$ in Eq. (I-7) must be carried out. If this average can be carried out analytically, the result is a closed-form expression for the detector structure. Such results can be obtained in certain instances. One example is the important case of a narrow-band signal with unknown phase.

When the signal to be detected has the form

$$s(t) = a e(t) \cos(2\pi f t - \phi) \quad (I-10)$$

with known amplitude factor a , envelope function $e(t)$, and frequency f , but with an unknown phase ϕ whose p.d.f. is uniform over the range $0, 2\pi$, the statistical average over phase can be

carried out analytically, and this leads to a closed-form representation of the detector structure.[†] Furthermore it can be shown that this structure is optimum regardless of the signal amplitude if the amplitude is one sided^{††} (confined to positive values or confined to negative values). That is to say, if, in addition to the phase, the amplitude factor in Eq. (I-10) is unknown and has a one-sided statistical distribution, the detector structure derived for the case of random phase will yield maximum signal detectability for any fixed level of false alarm probability, regardless of the signal amplitude. This point will be discussed more fully in a later chapter, where a specific problem of this type will be considered.

If the frequency f of the narrowband signal is not known a priori, then the development of the average LR, as given by Eq. (I-7) for detection in gaussian noise, requires an averaging with respect to f . Unfortunately such an average cannot be carried out in closed form, and other methods must be used to determine the optimum detector structure in such cases. It is cases of this type with which the work of this dissertation is concerned.

There is one other type of signal for which the optimum detector structure has been obtained analytically: a gaussian stochastic signal having a known spectrum. The detection of such signals in gaussian noise has been investigated in detail by Middleton.^{†††} (A specific case of this type will arise in later chapters). If the center frequency of the signal spectrum is unknown, however, the LR

[†] Derivations of this result are widely available in the literature. See for example Helstrom (I, Chap. V) and Middleton (II, Sec. 20.1-3).

^{††} See Helstrom (I, pp. 157-158) for a discussion of this point.

^{†††} See Middleton (I) and (II, Sec. 20.4-7).

must again be averaged, and this cannot be done in closed form.

For situations in which the signal involves unknown parameters and the average LR cannot be obtained in closed form, one technique which has been proposed for obtaining the detector structure consists of expanding the average LR in a power series and approximating the detector structure by using certain low order terms of the series. This technique will be discussed in Section Y.4, where it will be shown that the technique is not satisfactory in cases of narrowband signals of unknown frequency. First the specific problems to be considered will be discussed.

I.3 Description of the Problem

As has been stated this research is concerned with the optimum detection of a signal of unknown frequency in a background of noise having known statistical properties. Two distinct problems of this type will be considered, corresponding to two different models of the signals to be detected. In each case the noise is assumed to be gaussian with a flat spectral density of level N_0 volt²/cps extending from zero frequency up to some cutoff frequency which is much higher than the highest possible signal frequency. It is assumed that the noise is additive and independent of the signal. The two signal models to be considered are as follows:

- 1) In the first case the signal to be detected is a sinusoid of known amplitude and phase, but unknown frequency. The unknown frequency is assumed to have a discrete probability distribution over m possible values. Since the phase of the signal is assumed to be known for each possible value of the signal frequency, this signal will be termed a "coherent" sinusoid. The structure and performance of the optimum detector for such a signal will be found. This idealized signal model will serve to give insight into the particular

question of finding an optimum structure for the detection of signals of unknown frequency. This case will be analyzed in Chapter II.

2) The second case deals with the detection of a narrowband gaussian stochastic signal of known average power and known bandwidth B_g cps. The center frequency of this signal is not given a priori but is known only to lie somewhere within a wider frequency band of width B cps. It is assumed that $B = rB_g$, $r \geq 1$, where r is called the frequency uncertainty ratio. The form of the optimum detector will be obtained for this case by extending the results obtained for the case in which the signal frequency has a discrete distribution to cases in which the frequency has a p.d.f. over a continuous frequency range.

Of particular interest in this case is the question as to what enhancement in signal detectability can be obtained from the knowledge that the signal power is confined to a band appreciably narrower than overall frequency band B being processed, even though the exact frequency location of this signal is not known in advance. This problem will be treated in Chapters III and IV. Chapter III will deal with the situation of low pre-detection SNR. When the pre-detection SNR is high, the analysis must be modified somewhat; this will be done in Chapter IV.

1.4 A Power Series Approach and Its Limitations

It was pointed out in Section I.2 that there are situations of interest in which the averaging of the LR, as indicated by Eq. (I-2) cannot be carried out in closed form. One approach to this problem

which has been proposed[†] is based on an expansion of the average LR (or some monotone function of the average LR) in a power series involving linear, quadratic and higher order operations on the received signal y . This gives a series representation of the optimum detector structure. Under certain conditions it may then be possible to obtain an accurate approximation of the detector structure from one or more low-order terms in the series, if higher-order terms can safely be neglected. An analysis^{††} was carried out in order to determine the conditions under which such a technique could be applied to the detection of signals of unknown frequency in gaussian noise.

In that analysis three signal cases were considered:

- 1) A broadband gaussian stochastic signal whose spectral density is flat over a band of width B cps and zero outside the band.
- 2) A narrowband gaussian stochastic signal with bandwidth B_g cps and center frequency f_c cps. Here f_c was assumed equally likely to lie anywhere in the band B , and B_g was assumed to be much smaller than B .
- 3) A limiting case of 2) in which $B_g \rightarrow 0$, thus producing a sinusoidal signal of unknown phase and frequency whose amplitude is constant over each observation interval, but considered over all observations, is a random variable with a Rayleigh p.d.f.

[†] See Middleton (II, p. 819ff.).

^{††} See Levesque (I).

[Cases 2) and 3) are essentially identical with those which will be treated by different means in Chapters III and IV of the present investigation.]

An expansion of the detector structure was obtained by first developing the average LR, of the form given in Eq. (I-7), in a power series and then taking the average $\langle \rangle_g$ term by term. Then $\log L(y)$ was expanded in a second power series. For each of the three signal cases described above, the "deflections" of certain terms were calculated. A deflection is defined here as a change in the average value of a term in going from the noise-only situation to a signal-plus-noise situation. In order that any terms in the series be considered negligible in describing the operation of the detector, it is necessary that their deflections be negligible.

The results of the analysis are summarized in Appendix A. They show that in the broadband gaussian signal case higher order terms in the expansion can be neglected on the basis of low pre-detection SNR. For the case of narrowband signals, however, and even more for the sinusoidal signal, the higher-order terms may become significantly large if the post-detection SNR is made large by a long integration time. Thus dropping higher-order terms on the basis of low pre-detection SNR, as is suggested by Middleton[†], is justified only in cases where the post-detection SNR is also small, cases which are not of interest where high signal detectability is required. Thus the application of this power series technique to the problem at hand would involve the use of a number of terms in the power series

[†] See Middleton (II, discussion on p. 821).

representation (a number depending upon the pre-detection SNR and the observation time) in order to adequately describe the detector structure. This procedure is cumbersome and thus a new approach to this problem has been undertaken and will be outlined in the following chapter.

CHAPTER II

DETECTION OF A COHERENT SINUSOID
OF UNKNOWN FREQUENCYII.1 Introduction

The detection of a sinusoid of known amplitude and phase, but unknown frequency, in a background of broadband gaussian noise will now be considered. Since the phase of the signal is assumed to be known for each possible value of the frequency, the signal is termed a "coherent" sinusoid. The unknown frequency is assumed to have a discrete probability distribution over m possible frequency values. A geometric interpretation of $l(y)$, given by Eq. (I-2), and of the threshold test, given by Eq. (I-3), is proposed; from this point of view the structure of the optimum detector will be developed. Then signal detectability will be calculated. Optimum detector performance will also be compared with that of a sub-optimum structure derived from a power series expansion of the average LR.

II.2 Likelihood Ratio Detection of a Signal of Unknown Frequency

Since signal frequency f is the only unknown parameter in this signal case, the average $\langle \rangle_S$ in Eq. (I-2) simply implies $\langle \rangle_f$.

The expression for $L(\underline{v})$ may now be re-written as

$$L(\underline{v}) = \left\langle L(\underline{v}/f) \right\rangle_f \quad (\text{II-1})$$

where

$$L(\underline{v}/f) = \frac{f(\underline{v}/f)}{f(\underline{v}/0)} \quad (\text{II-2})$$

is a LR calculated for a particular value of f .

If the frequency f has a discrete probability distribution over a finite set of values,

$$L(\underline{v}) = \sum_{i=1}^m p_i L(\underline{v}/f_i) \quad (\text{II-3})$$

where m is the total number of possible values of f and p_i is the probability of the i^{th} value. In general the quantities $\log L(\underline{v}/f_i)$ can be generated more conveniently than $L(\underline{v}/f_i)$.

With this in mind the average LR can be written as

$$L(\underline{v}) = \sum_{i=1}^m p_i \exp \left[\log L(\underline{v}/f_i) \right] \quad (\text{II-4})$$

Thus the optimum detector calculates the quantities $\log L(\underline{v}/f_i)$, forms the sum in Eq. (II-4), and compares this with a pre-set threshold k . If the threshold is exceeded, the decision is made that the desired signal is present in the received data. This test is indicated by

$$\sum_{i=1}^m p_i \exp \left[\log L(\underline{v}/f_i) \right] \geq k \quad (\text{II-5}) \quad >$$

The decision scheme can be visualized in geometric terms if the test quantities $\log L(\underline{y}/f_1)$ are taken as coordinates in an m -dimensional hyperspace. The space is divided into two regions, which may be called the "signal" and "no signal" regions. The boundary between these two regions is determined from Eq. (II-5) by the equality

$$\sum_{i=1}^m p_i \exp \left[\log L(\underline{y}/f_i) \right] = k \quad (\text{II-6})$$

For a given received signal \underline{y} , the coordinates $\log L(\underline{y}/f_i)$ define a point in the m -dimensional space. If the point lies in the "signal" region, the decision is made that the desired signal is present with noise. If the point lies in the "no signal" region, the decision is made that noise only is present. A specific case will now be considered.

II.3 Detection of a Coherent Sinusoid - Two-Frequency Case

a) The Decision Plane

If the desired signal is a sinusoid with known amplitude and phase and with a frequency f that can take on any one of m discrete values, then from Eq. (II-4),

$$i(\underline{y}) = \sum_{i=1}^m p_i \exp \left[\log L(\underline{y}/f_i) \right] \quad (\text{II-7})$$

As an example, let $m = 2$ and $p_1 = p_2 = \frac{1}{2}$. Equation (II-7) now gives

$$i(\underline{y}) = \frac{1}{2} \exp \left[\log L(\underline{y}/f_1) \right] + \frac{1}{2} \exp \left[\log L(\underline{y}/f_2) \right] \quad (\text{II-8})$$

Using Eq. (II-6), the boundary between the two decision regions is given by

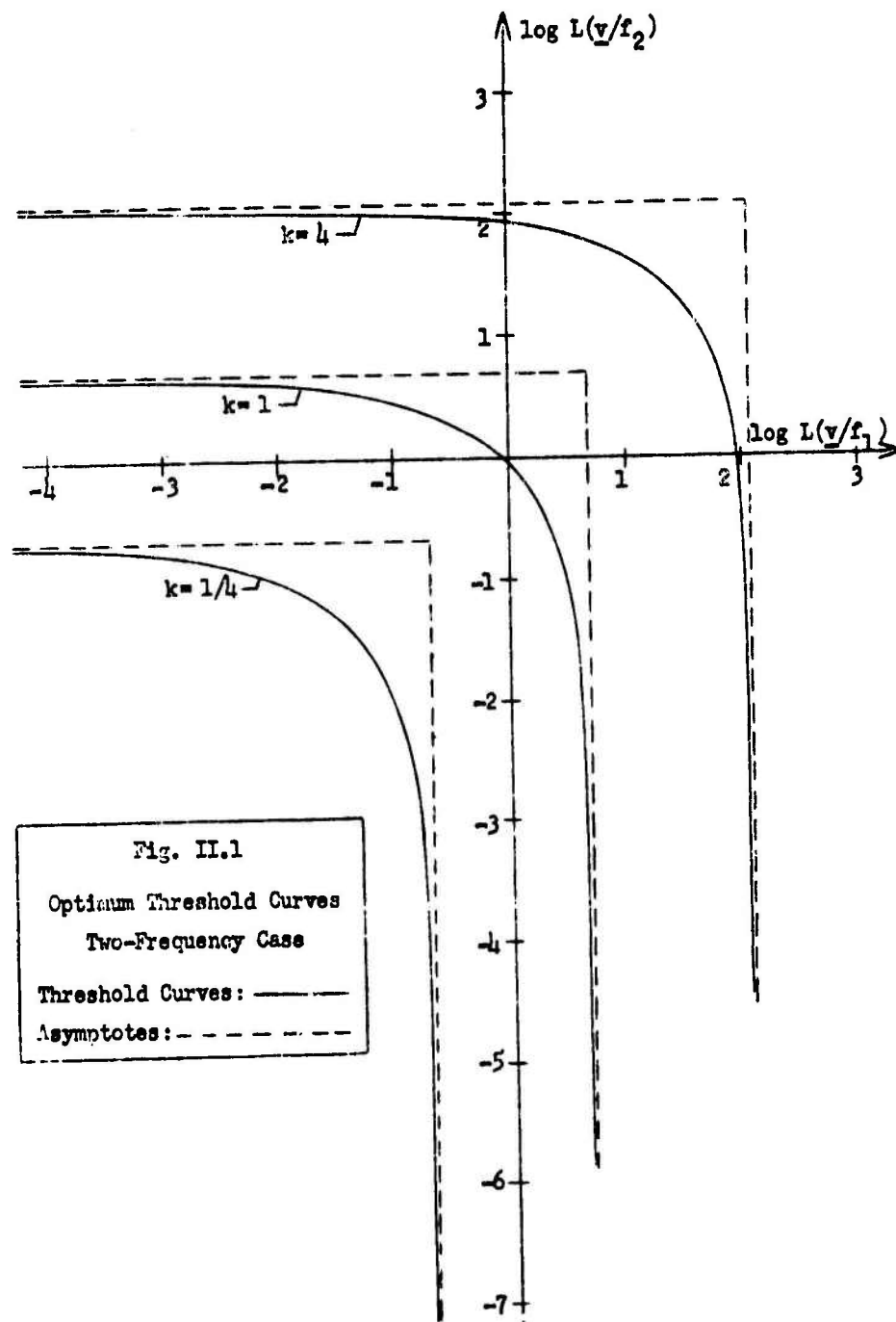
$$\frac{1}{2} \exp \left[\log L(\underline{v}/f_1) \right] + \frac{1}{2} \exp \left[\log L(\underline{v}/f_2) \right] = k \quad (\text{II-9})$$

or

$$\log L(\underline{v}/f_2) = \log \left\{ 2k - \exp \left[\log L(\underline{v}/f_1) \right] \right\} \quad (\text{II-10})$$

Threshold curves given by Eq. (II-10) are plotted in Fig. II.1 for several values of k . It should be noted that the curves all become asymptotically parallel to the coordinate axes. In practice one of these curves is chosen to divide the plane into "signal" and "no signal" decision regions. For a received signal vector \underline{v} , $\log L(\underline{v}/f_1)$ and $\log L(\underline{v}/f_2)$ are calculated and these quantities define a point in this decision plane. If the point lies above or to the right of the chosen threshold curve, the decision is made that the desired signal is present. If the point lies below and to the left of the curve, the decision is made that noise only is present.

If the number of possible values of the frequency is made larger, the decision plane of Fig. II.1 is replaced by an m -dimensional decision space, and the threshold curve is replaced by an m -dimensional decision surface.



b) Detection in Gaussian Noise

If the noise is additive and gaussian with a covariance matrix \underline{K} , then from Eq. (I-8) the LR for a given value of signal frequency is

$$L(\underline{y}/f_1) = \exp \left[-\frac{1}{2} \underline{s}'(f_1) \underline{K}^{-1} \underline{s}(f_1) + \underline{s}'(f_1) \underline{K}^{-1} \underline{y} \right] \quad (\text{II-11})$$

For convenience let

$$L_1 = L(\underline{y}/f_1)$$

and

$$\underline{s}_1 = \underline{s}(f_1)$$

For the case in which the signal frequency may take on one of two discrete values, the test quantities are then given by

$$\log L_1 = -\frac{1}{2} \underline{s}_1' \underline{K}^{-1} \underline{s}_1 + \underline{s}_1' \underline{K}^{-1} \underline{y} \quad (\text{II-12})$$

$$\log L_2 = -\frac{1}{2} \underline{s}_2' \underline{K}^{-1} \underline{s}_2 + \underline{s}_2' \underline{K}^{-1} \underline{y} \quad (\text{II-13})$$

Thus the operation of the optimum detector in this case consists of a general cross-correlation of the received signal with the desired signal at each of the possible signal frequencies.

In order to calculate the detectability of the signal, the conditional p.d.f.'s of $\log L_1$ and $\log L_2$ must be obtained. Since the noise is gaussian and Eqs. (II-12) and (II-13) describe linear operations on the received signal, the quantities $\log L_1$ and $\log L_2$ are gaussian random variables. The required mean values of $\log L_1$ are calculated as follows:

$$\begin{aligned}
 \left\langle \log L_1 \right\rangle_N &= -\frac{1}{2} \underline{s}_1' \underline{K}^{-1} \underline{s}_1 + \left\langle \underline{s}_1' \underline{K}^{-1} \underline{v} \right\rangle_N \\
 &= -\frac{1}{2} \underline{s}_1' \underline{K}^{-1} \underline{s}_1 + \underline{s}_1' \underline{K}^{-1} \left\langle \underline{v} \right\rangle_N \\
 &= -\frac{1}{2} \underline{s}_1' \underline{K}^{-1} \underline{s}_1 \quad (II-14)
 \end{aligned}$$

$$\begin{aligned}
 \left\langle \log L_1 \right\rangle_{S_1 + N} &= -\frac{1}{2} \underline{s}_1' \underline{K}^{-1} \underline{s}_1 + \left\langle \underline{s}_1' \underline{K}^{-1} (\underline{s}_1 + \underline{n}) \right\rangle_{S_1 + N} \\
 &= -\frac{1}{2} \underline{s}_1' \underline{K}^{-1} \underline{s}_1 + \underline{s}_1' \underline{K}^{-1} \underline{s}_1 + \underline{s}_1' \underline{K}^{-1} \underline{n}_N \\
 &= \frac{1}{2} \underline{s}_1' \underline{K}^{-1} \underline{s}_1 \quad (II-15)
 \end{aligned}$$

$$\begin{aligned}
 \left\langle \log L_1 \right\rangle_{S_2 + N} &= -\frac{1}{2} \underline{s}_1' \underline{K}^{-1} \underline{s}_1 + \left\langle \underline{s}_1' \underline{K}^{-1} (\underline{s}_2 + \underline{n}) \right\rangle_N \\
 &= -\frac{1}{2} \underline{s}_1' \underline{K}^{-1} \underline{s}_1 + \underline{s}_1' \underline{K}^{-1} \underline{s}_2 \quad (II-16)
 \end{aligned}$$

The variances of $\log L_1$ are

$$\begin{aligned}
 \text{var}_N \left[\log L_1 \right] &= \left\langle \left[-\frac{1}{2} \underline{s}_1' \underline{K}^{-1} \underline{s}_1 + \underline{s}_1' \underline{K}^{-1} \underline{v} \right]^2 \right\rangle_N - \frac{1}{4} (\underline{s}_1' \underline{K}^{-1} \underline{s}_1)^2 \\
 &= \left\langle \underline{s}_1' \underline{K}^{-1} \underline{v} \underline{v}' \underline{K}^{-1} \underline{s}_1 \right\rangle_N \\
 &= \underline{s}_1' \underline{K}^{-1} \left\langle \underline{v} \underline{v}' \right\rangle_N \underline{K}^{-1} \underline{s}_1 \\
 &= \underline{s}_1' \underline{K}^{-1} \underline{K} \underline{K}^{-1} \underline{s}_1 \\
 &= \underline{s}_1' \underline{K}^{-1} \underline{s}_1 \quad (II-17)
 \end{aligned}$$

$$\begin{aligned}
 \text{var}_{S_1+N}[\log L_1] &= \left\langle \left[-\frac{1}{2} \underline{s}_1' \underline{K}^{-1} \underline{s}_1 + \underline{s}_1' \underline{K}^{-1} (\underline{s}_1 + \underline{n}) \right]^2 \right\rangle_N - \frac{1}{4} (\underline{s}_1' \underline{K}^{-1} \underline{s}_1)^2 \\
 &= \left\langle \left[\frac{1}{2} \underline{s}_1' \underline{K}^{-1} \underline{s}_1 + \underline{s}_1' \underline{K}^{-1} \underline{n} \right]^2 \right\rangle_N - \frac{1}{4} (\underline{s}_1' \underline{K}^{-1} \underline{s}_1)^2 \\
 &= \frac{1}{4} (\underline{s}_1' \underline{K}^{-1} \underline{s}_1)^2 + \underline{s}_1' \underline{K}^{-1} \underline{s}_1 \underline{s}_1' \underline{K}^{-1} \langle \underline{n} \rangle_N \\
 &\quad + \underline{s}_1' \underline{K}^{-1} \langle \underline{n} \underline{n} \rangle_N \underline{K}^{-1} \underline{s}_1 - \frac{1}{4} (\underline{s}_1' \underline{K}^{-1} \underline{s}_1)^2 \\
 &= \underline{s}_1' \underline{K}^{-1} \underline{s}_1 \tag{II-18}
 \end{aligned}$$

$$\begin{aligned}
 \text{var}_{S_2+N}[\log L_1] &= \left\langle \left[-\frac{1}{2} \underline{s}_1' \underline{K}^{-1} \underline{s}_1 + \underline{s}_1' \underline{K}^{-1} (\underline{s}_2 + \underline{n}) \right]^2 \right\rangle_N - \frac{1}{4} (\underline{s}_1' \underline{K}^{-1} \underline{s}_1)^2 \\
 &= -\underline{s}_1' \underline{K}^{-1} \underline{s}_1 \underline{s}_1' \underline{K}^{-1} \underline{s}_2 + (\underline{s}_1' \underline{K}^{-1} \underline{s}_2)^2 + \underline{s}_1' \underline{K}^{-1} \langle \underline{n} \underline{n} \rangle_N \underline{K}^{-1} \underline{s}_1 \\
 &= -\underline{s}_1' \underline{K}^{-1} \underline{s}_1 \underline{s}_1' \underline{K}^{-1} \underline{s}_2 + (\underline{s}_1' \underline{K}^{-1} \underline{s}_2)^2 + \underline{s}_1' \underline{K}^{-1} \underline{s}_1 \tag{II-19}
 \end{aligned}$$

The noise is assumed to have a flat spectrum over a band extending from zero frequency up to a sharp cutoff at W cps. Thus samples of the noise taken at a rate $2W$ are independent, and the noise covariance matrix \underline{K} is diagonal. One can therefore write

$$\underline{s}_1' \underline{K}^{-1} \underline{s}_2 = \frac{1}{N} \sum_{i=1}^N s_1(t_i) s_2(t_i) \tag{II-20}$$

and

$$\underline{s}_1' K^{-1} \underline{s}_2 = \frac{1}{N} \sum_{i=1}^N s_1^2(t_i) \quad (\text{II-21})$$

where N is the variance of the noise.

If the spectral level of the noise is N_0 volt²/cps, then $N = N_0 W$ and, from results of sampling analysis,

$$\frac{1}{N} \sum_{i=1}^N s_1(t_i) s_2(t_i) \approx \frac{2}{N_0} \int_0^T dt s_1(t) s_2(t) \approx 0 \quad (\text{II-22})$$

where T is the observation time of the received signal. The zero result in Eq. (II-22) follows from the fact that $s_1(t)$ and $s_2(t)$ are sinusoids of different frequencies.[†]

Similarly,

$$\frac{1}{N} \sum_{i=1}^N s_1^2(t_i) \approx \frac{2}{N_0} \int_0^T dt s_1^2(t) \quad (\text{II-23})$$

It will be convenient to define a detection index:

$$d \equiv \frac{2}{N_0} \int_0^T dt s^2(t) \quad (\text{II-24})$$

where $s(t)$ may be either $s_1(t)$ or $s_2(t)$, since the signal is assumed to have the same amplitude at either frequency. It should be noted that the detection index is proportional to the power in

[†] [It is assumed that the smallest spacing between possible frequency values is much larger than the reciprocal of T . It can be shown that if $2\pi(f_1 - f_2)T \geq 10$, then the exact value of $\underline{s}_1' K^{-1} \underline{s}_2$ is at most one tenth as large as $\underline{s}_1' K^{-1} \underline{s}_1$].

the received signal and to the observation time and inversely proportional to the spectral level of the noise. This detection index may also be regarded as the post-detection SNR.

With the aid of Eqs. (II-20) through (II-24), the averages in Eqs. (II-14), (II-15) and (II-16) may now be written as

$$\left\langle \log L_1 \right\rangle_N = -\frac{d}{2} \quad (\text{II-25})$$

$$\left\langle \log L_1 \right\rangle_{S_1+N} = -\frac{d}{2} \quad (\text{II-26})$$

$$\left\langle \log L_1 \right\rangle_{S_2+N} = -\frac{d}{2} \quad (\text{II-27})$$

Similarly,

$$\left\langle \log L_2 \right\rangle_N = -\frac{d}{2} \quad (\text{II-28})$$

$$\left\langle \log L_2 \right\rangle_{S_1+N} = -\frac{d}{2} \quad (\text{II-29})$$

$$\left\langle \log L_2 \right\rangle_{S_2+N} = -\frac{d}{2} \quad (\text{II-30})$$

Similarly,

$$\text{var}_N \left[\log L_2 \right] = d \quad (\text{II-31})$$

$$\text{var}_{S_1+N} \left[\log L_2 \right] = d \quad (\text{II-32})$$

$$\text{var}_{S_2+N} \left[\log L_2 \right] = d \quad (\text{II-33})$$

To construct the joint p.d.f.'s for the test quantities, the correlation coefficient is required.

$$\begin{aligned}
 \frac{1}{d} \left\langle \left[\log L_1 + \frac{d}{2} \right] \left[\log L_2 + \frac{d}{2} \right] \right\rangle_N &= \frac{1}{d} \left\langle \underline{s}_1' \underline{K}^{-1} \underline{v} \underline{v}' \underline{K}^{-1} \underline{s}_2 \right\rangle_N \\
 &= \frac{1}{d} \underline{s}_1' \underline{K}^{-1} \left\langle \underline{v} \underline{v}' \right\rangle_N \underline{K}^{-1} \underline{s}_2 \\
 &= \frac{1}{d} \underline{s}_1' \underline{K}^{-1} \underline{s}_2 \\
 &= 0
 \end{aligned} \tag{II-34}$$

Thus the test quantities $\log L_1$ and $\log L_2$ are uncorrelated, and, since they are gaussian random variables, independent. With the following change of variables,

$$x_1 = \log L_1$$

$$x_2 = \log L_2$$

the joint p.d.f.'s can be written as

$$f(x_1, x_2 / Q) = \frac{1}{2^2 d} \exp \left[- \frac{\left(x_1 + \frac{d}{2} \right)^2 + \left(x_2 + \frac{d}{2} \right)^2}{2d} \right] \tag{II-35}$$

$$f(x_1, x_2 / \underline{s}_1) = \frac{1}{2^2 d} \exp \left[- \frac{\left(x_1 - \frac{d}{2} \right)^2 + \left(x_2 + \frac{d}{2} \right)^2}{2d} \right] \tag{II-36}$$

$$f(x_1, x_2 / \underline{s}_2) = \frac{1}{2^2 d} \exp \left[- \frac{\left(x_1 + \frac{d}{2} \right)^2 + \left(x_2 - \frac{d}{2} \right)^2}{2d} \right] \tag{II-37}$$

The centers of these three density functions are plotted in the decision plane of Fig. II.2, together with a typical optimum threshold curve. It is particularly interesting to note that if the threshold curve remains fixed and the detection index d becomes large, the precise shape of the threshold curve near the origin of the decision plane becomes less important with regard to the conditional probabilities of error. This is because the region near the "corner" of the curve becomes a region of steadily smaller probability measure with respect to the three p.d.f.'s as d increases.[†] With this in mind the decision scheme may be simplified when d is large by replacing the optimum threshold curve with its straight-line asymptotes, also shown in Fig. II.2. The decision scheme corresponding to this new threshold curve can be stated as follows: If either $\log L_1$ or $\log L_2$ is above the threshold value $\log 2k$, the decision is made that a signal is present. Thus a threshold test is performed at each of the possible frequencies at which the signal may appear and a final decision about the presence of the signal is made on the basis of the individual tests. This type of decision scheme will be referred to in a general way as a "band-splitting" scheme.^{††} As d is made increasingly large, the region (shown in Fig. II.2) between the optimum threshold curve and the band-splitting threshold curve, makes a steadily smaller contribution to the conditional probabilities

[†] The mean value of each of the test quantities has a magnitude equal to $d/2$, and a standard deviation equal to \sqrt{d} ; thus as d becomes larger, each of the density functions becomes narrower with respect to its mean value.

^{††} The term "band splitting" is more appropriate where a continuous frequency band is being searched for a signal by means of a bank of band-pass filters. For convenience a set of correlation detectors will be regarded as a special case of the filter bank.

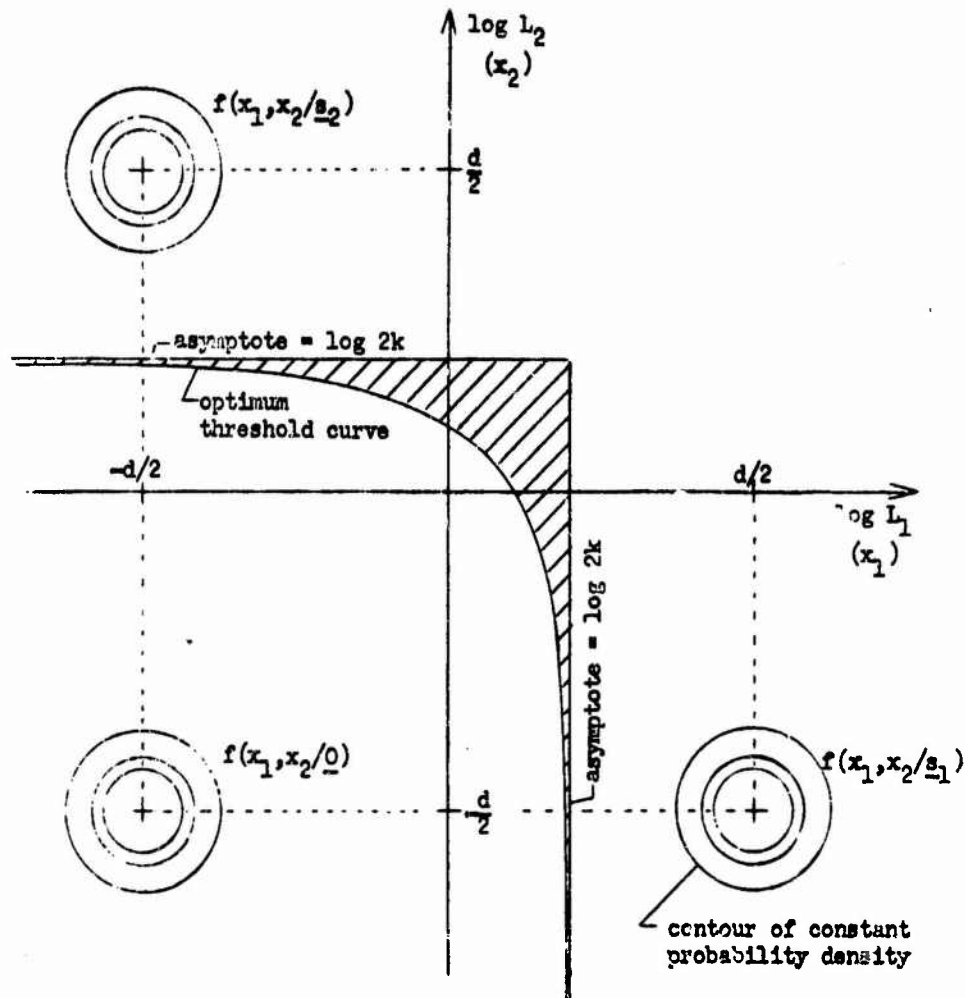


Fig. II.2. Optimum Threshold Curve and Its Band-Splitting Approximation
Two-Frequency Case

of error. Therefore it can be stated that the optimum detector becomes asymptotically a band-splitting detector as the detection index d is made increasingly large.

A different situation prevails as d approaches zero, however. Figure II.3 shows, for a low value of d , the arrangement of centers of the p.d.f.'s with respect to a typical optimum threshold curve. As d is made very small, the shape of the threshold curve for large magnitudes of $\log L_1$ and $\log L_2$ becomes less significant in the determination of the error probabilities. Only the shape of the threshold curve in the region of the closely spaced p.d.f.'s is important, and a straight line with slope -1 can serve as a good approximation to the curve in that region. Such a straight-line threshold is also pictured in Fig. II.3.

It is shown in Appendix B that if $\log \langle L(\underline{v}/f) \rangle_f$ is expanded in a power series and the lowest-order coherent term in the series is used to approximate the operation of the optimum detector, then that approximation corresponds precisely to a straight-line threshold as pictured in Fig. II.3. That is, for this case of a coherent sinusoid having one of two known frequencies, a power series analysis with small-signal approximations leads to the test

$$\log L_1 + \log L_2 \approx 2 \log k - \frac{d}{2} \quad (\text{II-38})$$

It is now clear that the approximation leading to Eq. (II-38) is valid only if the detection index d is much smaller than unity, and it must be noted that it is not sufficient that the pre-detection SNR be small, since d also depends on the integration time, as shown

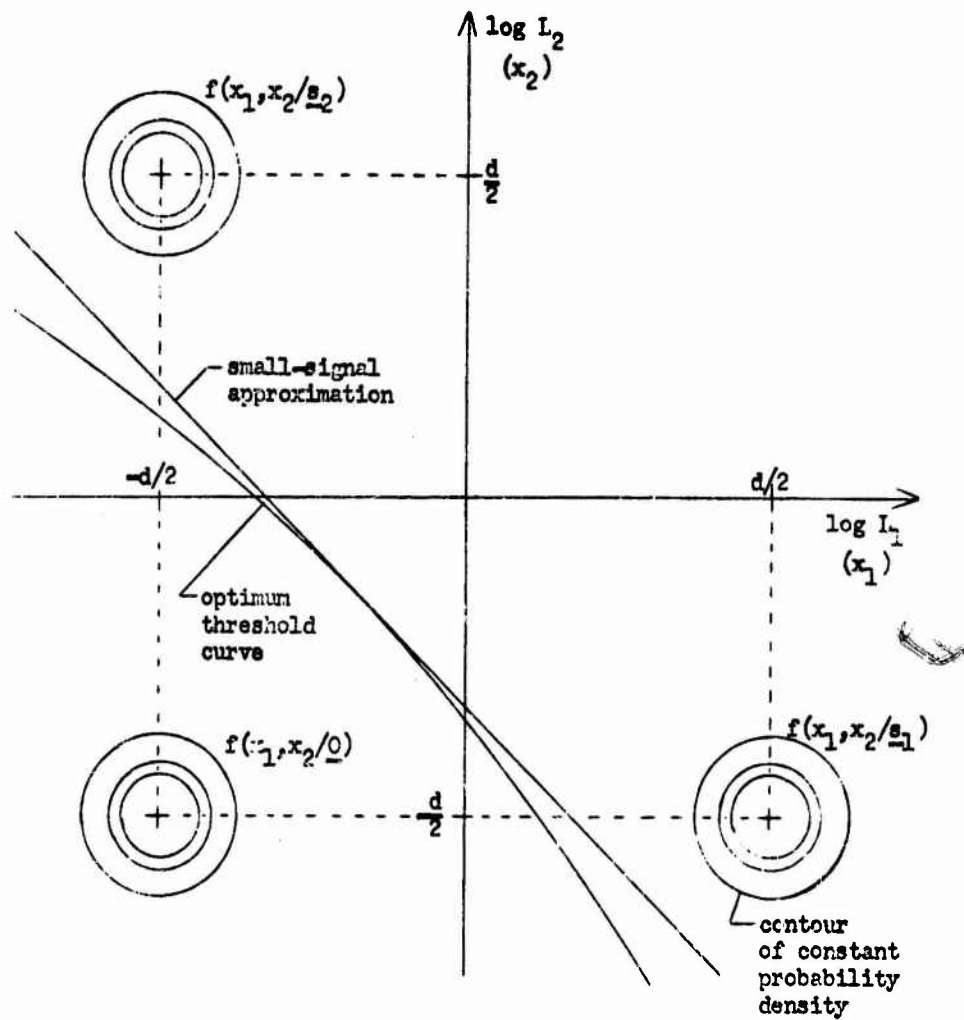


Fig. II.3. Optimum Threshold Curve and Its Small-Signal Approximation
Two-Frequency Case

by Eq. (II-24)[†]. In the weak-signal situation, where d is made much larger than unity by means of a long integration time, the band-splitting detector will provide a better approximation to the optimum detector.

The detector structure implied by Eq. (II-38) will be referred to hereafter as a "sum-and-test" detector.

c) Detection Probabilities - Two-Frequency Case

The conditional false-alarm and false-dismissal probabilities will be calculated for the optimum detector and for the sub-optimum detector derived by the small-signal analysis of Appendix B. Signal detectability curves will then be obtained.

Optimum Detector

The conditional false alarm probability α can be visualized with the aid of Fig. II.2. It is the probability that the point $(\log L_1, \log L_2)$ lies above or to the right of the optimum threshold curve, given that noise only is present. From Eq. (II-35),

$$\alpha = \int_{\log 2k}^{\infty} dx_2 \frac{1}{\sqrt{2\pi d}} \exp \left[-\frac{1}{2d} \left(x_2 + \frac{d}{2} \right)^2 \right] + \int_{-\infty}^{\log 2k} dx_2 \frac{1}{\sqrt{2\pi d}} \exp \left[-\frac{1}{2d} \left(x_2 + \frac{d}{2} \right)^2 \right] \int_{\log [2k - \exp(x_2)]}^{\infty} dx_1 \frac{1}{\sqrt{2\pi d}} \exp \left[-\frac{1}{2d} \left(x_1 + \frac{d}{2} \right)^2 \right] \quad (\text{II-39})$$

[†] It will be recalled that this is the conclusion which was stated in Sec. I.4 in the discussion of the power series technique and its suitability for problems involving the detection of signals of unknown frequency.

After a change of variables,

$$\alpha = \frac{1}{\sqrt{2\pi}} \int_{\sqrt{\frac{d}{k}} + \frac{1}{\sqrt{d}} \log 2k}^{\infty} dv \exp\left(-\frac{v^2}{2}\right) + \frac{1}{\sqrt{2\pi}} \int_{-\infty}^{\sqrt{\frac{d}{k}} + \frac{1}{\sqrt{d}} \log 2k} dv \exp\left(-\frac{v^2}{2}\right) \frac{1}{\sqrt{2\pi}} \int_{\sqrt{\frac{d}{k}} + \frac{1}{\sqrt{d}} \log[2k - \exp(\sqrt{d}v - \frac{d}{2})]}^{\infty} du \exp\left(-\frac{u^2}{2}\right)$$

(II-40)

The double integration in Eq. (II-40) cannot be carried out in closed form, but it may be numerically evaluated to any desired degree of accuracy. To facilitate computations in this report, the optimum threshold curve will be replaced by the band-splitting threshold for large values of d . A graphical estimation of the detectability for low values of d will then be carried out. For the band-splitting approximation, the conditional false alarm probability is given by

$$\alpha \approx \frac{1}{\sqrt{2\pi}} \int_{\sqrt{\frac{d}{k}} + \frac{1}{\sqrt{d}} \log 2k}^{\infty} dv \exp\left(-\frac{v^2}{2}\right) + \frac{1}{\sqrt{2\pi}} \int_{-\infty}^{\sqrt{\frac{d}{k}} + \frac{1}{\sqrt{d}} \log 2k} dv \exp\left(-\frac{v^2}{2}\right) \frac{1}{\sqrt{2\pi}} \int_{\sqrt{\frac{d}{k}} + \frac{1}{\sqrt{d}} \log 2k}^{\infty} du \exp\left(-\frac{u^2}{2}\right)$$

$$\alpha \approx \frac{1}{2} \left[1 - \Phi\left(\sqrt{\frac{d}{k}} + \frac{1}{\sqrt{d}} \log 2k\right) \right] \left[\frac{3}{2} + \frac{1}{2} \Phi\left(\sqrt{\frac{d}{k}} + \frac{1}{\sqrt{d}} \log 2k\right) \right]$$

(II-41)

where

$$\phi(x) = \frac{1}{\sqrt{2\pi}} \int_{-\infty}^x dt \exp\left(-\frac{t^2}{2}\right) \quad (\text{II-42})$$

The function $\phi(x)$ is the Normal Probability Integral, available in tables[†].

The conditional false-dismissal probability is the probability that the point $(\log L_1, \log L_2)$ lies to the left of and below the optimum threshold curve in Fig. II.2 when a signal is present in the received data. Given that the two signal frequencies are equally likely, this probability can be calculated with respect to either one of the signal-plus-noise distributions. Thus

$$\beta = \int_{-\infty}^{\log 2k} dx_2 \frac{1}{\sqrt{2\pi d}} \exp\left[-\frac{1}{2d}\left(x_2 - \frac{d}{2}\right)^2\right] \int_{-\infty}^{\log [2k - \exp(x_2)]} dx_1 \frac{1}{\sqrt{2\pi d}} \exp\left[-\frac{1}{2d}\left(x_1 + \frac{d}{2}\right)^2\right] \quad (\text{II-43})$$

After a change of variables,

$$\beta = \frac{1}{\sqrt{2\pi}} \int_{-\infty}^{\frac{1}{\sqrt{d}} \log 2k} dv \exp\left(-\frac{v^2}{2}\right) \frac{1}{\sqrt{2\pi}} \int_{-\infty}^{\frac{\sqrt{d}}{4} + \frac{1}{\sqrt{d}} \log [2k - \exp(\frac{d}{2} + \sqrt{d} v)]} du \exp\left(-\frac{u^2}{2}\right) \quad (\text{II-44})$$

[†] See National Bureau of Standards (I).

Again, for the band-splitting approximation the false-dismissal probability is approximated by

$$\beta \approx \frac{1}{\sqrt{2\pi}} \int_{-\infty}^{\frac{1}{\sqrt{d}} \log 2k - \sqrt{\frac{d}{4}}} \exp\left(-\frac{v^2}{2}\right) \frac{1}{\sqrt{2\pi}} \int_{-\infty}^{\sqrt{\frac{d}{4}} + \frac{1}{\sqrt{d}} \log 2k} \exp\left(-\frac{u^2}{2}\right) du dv \quad (\text{II-45})$$

$$\beta = \frac{1}{4} \left[1 - \Phi\left(\sqrt{\frac{d}{4}} - \frac{1}{\sqrt{d}} \log 2k\right) \right] \left[1 + \Phi\left(\sqrt{\frac{d}{4}} + \frac{1}{\sqrt{d}} \log 2k\right) \right] \quad (\text{II-46})$$

From Eqs. (II-41) and (II-46), the conditional detection probability $1 - \beta$ is plotted in Fig. II.4 as a function of \sqrt{d} for fixed values of the conditional false-alarm probability α . The curves are estimated for the region of $1 - \beta$ below 80 per cent. Detection probabilities on the order of 99 per cent or better will usually be desired, and this is well within the range where the band-splitting detector provides a very accurate approximation to the optimum detector.[†]

Sum-And-Test Detector

From Eq (II-35) and with the aid of Fig. II.3

$$\alpha = \int_{\frac{1}{\sqrt{2}} (d/2 + \log k)}^{\infty} du \frac{1}{\sqrt{2\pi d}} \exp\left(-\frac{u^2}{2d}\right) \quad (\text{II-47})$$

[†] Eq. (II-44) was evaluated by means of hand computations for a few points in Fig. II.4 in order to check the accuracy of the band-splitting approximation. When Eq. (II-46) gives $\beta = .500$ the exact expression Eq. (II-44) gives $\beta = .485$, an error of approximately 3 per cent. The percentage error falls off rapidly as β decreases.

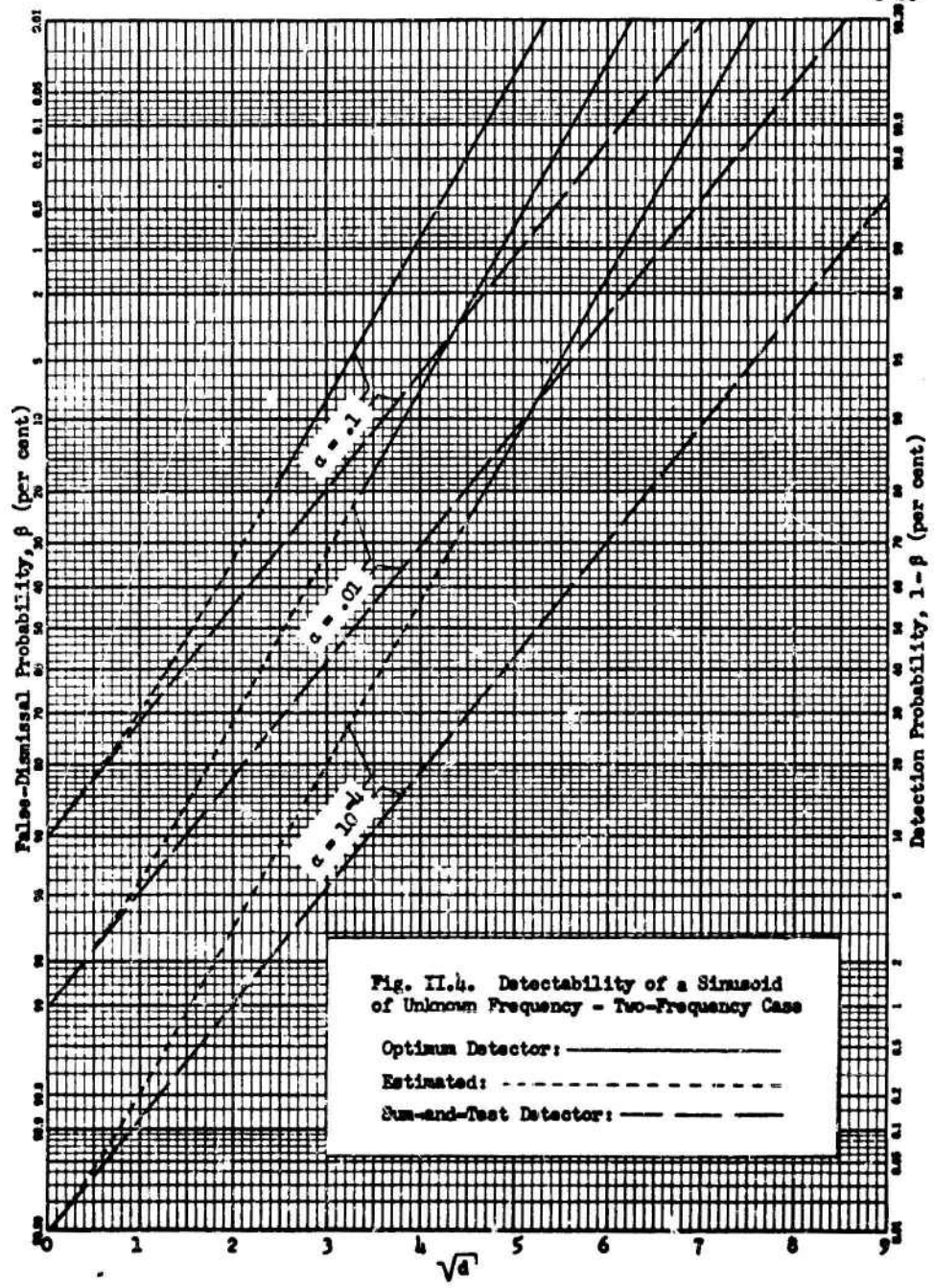


Fig. II.4. Detectability of a Sinusoid of Unknown Frequency - Two-Frequency Case

After a change of variable,

$$\alpha = \frac{1}{\sqrt{2\pi}} \int_{\sqrt{\frac{d}{8}} + \frac{1}{\sqrt{2d}} \log k}^{\infty} dz \exp \left(-\frac{z^2}{2} \right)$$

$$\alpha = \frac{1}{2} \left[1 - \Phi \left(\sqrt{\frac{d}{8}} + \frac{1}{\sqrt{2d}} \log k \right) \right] \quad (\text{II-48})$$

Similarly,

$$\beta = \frac{1}{2} \left[1 - \Phi \left(\sqrt{\frac{d}{8}} - \frac{1}{\sqrt{2d}} \log k \right) \right] \quad (\text{II-49})$$

From Eqs. (II-48) and (II-49), values of $1 - \beta$ are plotted in Fig. II.4 as a function of \sqrt{d} for three fixed false-alarm probabilities. It is seen that the conditional detection probability for this sub-optimum scheme steadily falls away from that of the optimum detector as the detection index increases. As the uncertainty about the frequency of the desired signal is increased to a larger number of possible values, the difference between the performance of the sum-and-test detector and that of the optimum detector becomes more pronounced.

II.4 Detection of a Coherent Sinusoid - m-Frequency Case

a) The Decision Space

The work of the previous section has shown that in the detection of a coherent sinusoid with an unknown frequency which can have one of two values, the optimum detector becomes asymptotically a

band-splitting type of detector as the post-detection SNR becomes large. If the unknown signal frequency is equally likely to have any one of m possible values, the decision space becomes an m -dimensional hyperspace, and the threshold surface dividing the space into "signal" and "no signal" regions is obtained from Eq. (II-6) with $L(\underline{v}/f_1) = L_1$, as

$$\frac{1}{m} \sum_{i=1}^m \exp(\log L_i) = k \quad (\text{II-50})$$

As the detection index is made very large and a received signal is tested, two different situations will occur, depending upon the presence or absence of a signal:

1) If no signal is present, all m of the test quantities $\log L_i$ will have large negative mean values, equal to $-d/2$ [See Eq. (II-25)].

2) If signal is present, $m-1$ of the test quantities will have mean values equal to $-d/2$, and one test quantity will have a mean value equal to $d/2$ [See Eqs. (II-27) and (II-26)].

Thus it is of interest to examine the shape of the threshold surface in regions of the hyperspace where the test quantities have large negative values. If Eq. (II-50) is solved for one of the test quantities in terms of the others,

$$\exp(\log L_1) = mk - \exp(\log L_2) - \dots - \exp(\log L_m) \quad (\text{II-51})$$

or

$$\log L_1 = \log [mk - \exp(\log L_2) - \dots - \exp(\log L_m)] \quad (\text{II-52})$$

When $\log L_2, \dots, \log L_m$ have large negative values, the exponentials in Eq. (II-52) become very small, and

$$\log L_1 \approx \log m k \quad (\text{II-53})$$

Thus the asymptotes of the optimum threshold curve are hyperplanes perpendicular to each of the m coordinate axes of the decision space. These asymptote planes are analogous to the asymptote lines of the two-dimensional case.

It is seen then that as the detection index becomes large the precise shape of the threshold surface near the origin of the decision space becomes less important with respect to error probabilities and the optimum threshold surface may be approximated by a set of m hyperplanes. The decision scheme corresponding to this approximation can be stated as follows: If one or more of the test quantities $\log L_1, \log L_2, \dots, \log L_m$ is above the threshold $\log m k$, the decision is made that a signal is present. If all m test quantities are below $\log m k$, the decision is made that noise only is present. As in the two-frequency case, this detection scheme will be referred to as a "band-splitting" scheme.

It can be stated in general, then, that the optimum detector for the detection of a coherent sinusoid whose unknown frequency is given by a discrete probability distribution becomes asymptotically a band-splitting detector as the detection index d becomes large.

For small values of post-detection SNR, the work of Appendix B shows that the optimum detector can be approximated by a sum-and-test

detector. For the m -frequency case the approximation leads to the test

$$\sum_{i=1}^m \log L_i \geq m \log k - (m-1) \frac{d}{2} \quad (\text{II-54})$$

The threshold surface corresponding to this sub-optimum scheme is given by

$$\sum_{i=1}^m \log L_i = m \log k - (m-1) \frac{d}{2} \quad (\text{II-55})$$

and this is seen to be a hyperplane in the m -dimensional decision space. This is analogous to the straight-line threshold shown in Fig. II.3 for the small-signal approximation in the two-frequency case.

b) Detection Probabilities - m -Frequency Case

Optimum Detector

For large values of d the optimum detector will be approximated by the band-splitting detector to simplify the computation of the error probabilities. For small values of d the detectability will then be estimated.

The conditional false-alarm probability is the probability that one or more of the test quantities exceeds the threshold $\log mk$, given that noise only is present. That is,

$$\begin{aligned} \alpha &= P \text{ [At least one of the test quantities } \log L_i \text{ is} \\ &\quad \text{above its threshold, given that noise only is} \\ &\quad \text{present.]} \\ &= 1 - P \text{ [All the test quantities } \log L_i \text{ are below} \\ &\quad \text{their thresholds, given that noise only is present.]} \end{aligned}$$

The conditional false-dismissal probability is

$$\beta = P \text{ [All the test quantities } \log L_i \text{ are below their thresholds, given that a signal is present at any one of the possible frequencies.]}$$

It is shown in Appendix C that

$$\alpha = 1 - (1 - \alpha_1)^m \quad (\text{II-56})$$

and

$$\beta = \beta_1 (1 - \alpha_1)^{m-1} \quad (\text{II-57})$$

where

$$\alpha_1 = P \text{ [} \log L_1 \text{ is above its threshold, given that no signal is present at the frequency } f_1 \text{.]}$$

$$\beta_1 = P \text{ [} \log L_1 \text{ is below its threshold, given that a signal is present at the frequency } f_1 \text{.]}$$

The probabilities α_1 are assumed equal for all $i = 1, 2, \dots, m$, and the probabilities β_1 are assumed equal for all $i = 1, 2, \dots, m$. The error probabilities α and β can be bounded as follows: From an expansion of Eq. (II-56) one obtains

$$\alpha \leq m \alpha_1 \quad (\text{II-58})$$

and from Eq. (II-57) one obtains

$$\beta \leq \beta_1 \quad (\text{II-59})$$

These bounds are very accurate for $m \alpha_1 \ll 1$. It is seen from Eqs. (II-58) and (II-59) that if the threshold for each $\log L_i$ is held fixed and the number of possible frequencies is increased, the false alarm probability will be approximately proportional to m ,

while the false dismissal probability will remain approximately unchanged.

The conditional p.d.f.'s for $\log L_1$ are needed. Let $x_1 = \log L_1$. Then, from Eqs. (II-25), (II-26), (II-27), (II-31), (II-32) and (II-33),

$$f(x_1/\underline{0} \text{ or } \underline{s}_j) = \frac{1}{\sqrt{2\pi d}} \exp \left[-\frac{1}{2d} \left(x_1 + \frac{d}{2} \right)^2 \right] \quad (II-60)$$

$i \neq j$

and

$$f(x_1/\underline{s}_1) = \frac{1}{\sqrt{2\pi d}} \exp \left[-\frac{1}{2d} \left(x_1 - \frac{d}{2} \right)^2 \right] \quad (II-61)$$

If the threshold for each test quantity is $\log mk$,

$$\left\{ \begin{matrix} \alpha_1 \\ \beta_1 \end{matrix} \right\} = \frac{1}{2} \left[1 - \Phi \left(\frac{\sqrt{A}}{\sqrt{d}} \pm \frac{1}{\sqrt{d}} \log mk \right) \right] \quad (II-62)$$

From Eqs. (II-56), (II-57) and (II-62), the conditional detection probability $1 - \beta$ can be calculated as a function of \sqrt{d} for a fixed value of the conditional false alarm probability α and for any number m of signal frequencies. Results of these calculations for $\alpha = .01$ and $m = 1, 2, 4, 8$ and 128 are shown in Fig. II.5. It can be seen from the figure that the set of detection curves for different values of m becomes a set of parallel straight lines as d becomes large, with the detectability becoming poorer as m increases, as would be expected. The asymptotic form of the detectability curves for small error probabilities can easily be derived using the bounds of Eqs. (II-58) and (II-59). For small values of $m\alpha_1$

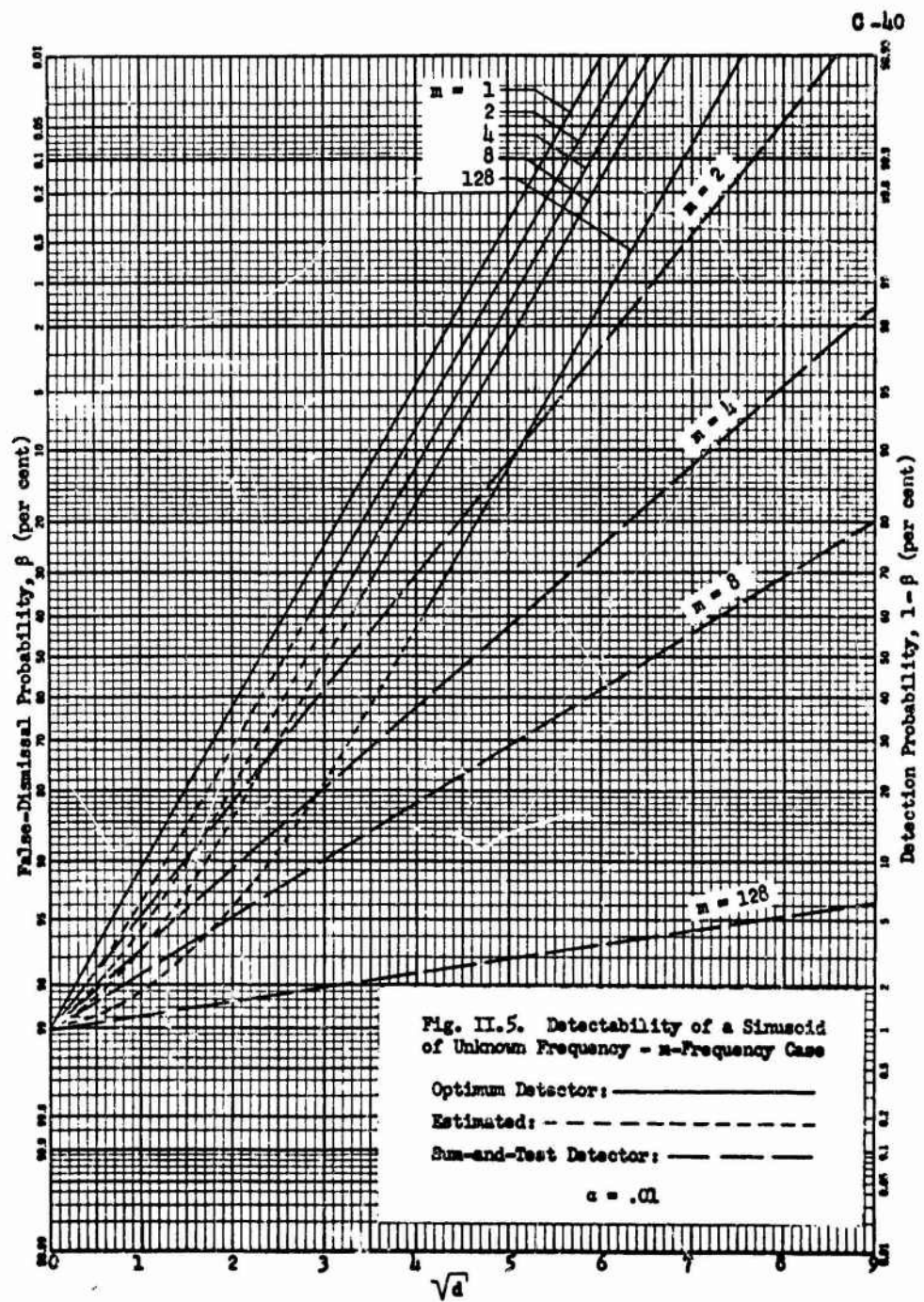


Fig. II.5. Detectability of a Sinusoid of Unknown Frequency - n -Frequency Case

the bounds become very good approximations and using Eq. (II-58) together with Eq. (II-62), one can write

$$\alpha \approx \frac{m}{2} \left[1 - \Phi \left(\sqrt{\frac{E}{4}} + \frac{1}{\sqrt{d}} \log m k \right) \right] \quad (\text{II-63})$$

The conditional detectability $1 - \beta$ is to be calculated as a function of \sqrt{d} for a fixed value of α , therefore let $\alpha = \alpha^*$ where α^* is the chosen fixed false-alarm rate. Now, from Eq. (II-63),

$$\frac{1}{\sqrt{d}} \log m k = \Phi^{-1} \left(1 - \frac{2\alpha^*}{m} \right) - \sqrt{\frac{E}{4}} \quad (\text{II-64})$$

where $\Phi^{-1}(z)$ denotes the "inverse Normal Probability Integral", that is, the number x for which $z = \Phi(x)$ [See Eq. (II-42)].

From Eqs. (II-59) and (II-62), an approximation is obtained for the conditional false-dismissal probability as

$$\beta \approx \frac{1}{2} \left[1 - \Phi \left(\sqrt{\frac{E}{4}} - \frac{1}{\sqrt{d}} \log m k \right) \right] \quad (\text{II-65})$$

Inserting Eq. (II-64) into Eq. (II-65), one obtains

$$\beta \approx \frac{1}{2} \left\{ 1 - \Phi \left[\sqrt{\frac{E}{4}} - \Phi^{-1} \left(1 - \frac{2\alpha^*}{m} \right) \right] \right\} \quad (\text{II-66})$$

The conditional detection probability is then approximately

$$1 - \beta \approx \frac{1}{2} \left\{ 1 + \Phi \left[\sqrt{\frac{E}{4}} - \Phi^{-1} \left(1 - \frac{2\alpha^*}{m} \right) \right] \right\} \quad \sqrt{d} \gg 1 \quad (\text{II-67})$$

The right-hand side of Eq. (II-67) is seen to be of the general form

$$C_1 \Phi \left[C_2 \sqrt{d} + C_3 \right] + C_4 \quad (\text{II-68})$$

where C_1, C_2, C_3 and C_4 are constants. This general form represents a linear function of \sqrt{d} on the normal probability scale of Fig. II.5. Thus the asymptotes of the detectability curves for the optimum detector, given by Eq. (II-67), plotted for various values of m or various values of α^* are a family of parallel straight lines, the horizontal displacement of each line being determined by the quantity $\Phi^{-1}(1 - 2\alpha^*/m)$. If α^* is held fixed and m is increased,

$$\Phi^{-1} \left(1 - \frac{2\alpha^*}{m} \right) \rightarrow \infty \quad \text{as } m \rightarrow \infty$$

$\alpha^* = \text{const.}$

Thus the detection curve moves steadily to the right as m increases, representing steadily poorer detectability with increasing uncertainty about the signal frequency, as is seen in Fig. II.5. The same trend is observed if m is held fixed and α^* is decreased; that is,

$$\Phi^{-1} \left(1 - \frac{2\alpha^*}{m} \right) \rightarrow \infty \quad \text{as } \alpha^* \rightarrow 0$$

$m = \text{const.}$

This is the trend exhibited by the optimum detector curves in Fig. II.4 for the two-frequency case.

Sum-And-Test Detector

For the sum-and-test detector, the test quantity is

$$y = \sum_{i=1}^m \log L_i \quad (\text{II-69})$$

When noise only is present, each of the quantities $\log L_1$ has a mean value $-d/2$ and a variance d . Thus

$$f(y/0) = \frac{1}{\sqrt{2\pi md}} \exp \left[-\frac{1}{2md} \left(y + \frac{md}{2} \right)^2 \right] \quad (\text{II-70})$$

When a signal is present at one of the m possible frequencies, $m-1$ of the quantities $\log L_1$ will have a mean value $-d/2$ and one will have a mean value $d/2$. Thus

$$f(y/s_1) = \frac{1}{\sqrt{2\pi md}} \exp \left\{ -\frac{1}{2md} \left[y + (m-2) \frac{d}{2} \right]^2 \right\} \quad (\text{II-71})$$

If y is compared with a threshold $m \log k - (m-1) \frac{d}{2}$, the conditional error probabilities are given by

$$\left\{ \begin{array}{l} \alpha \\ \beta \end{array} \right\} = \frac{1}{2} \left[1 - \Phi \left(\sqrt{\frac{d}{4m}} \pm \sqrt{\frac{m}{d}} \log k \right) \right] \quad (\text{II-72})$$

Curves of conditional detection probability $1-\beta$ as a function of \sqrt{d} are shown in Fig. II.5 for the sum-and-test detector. The curves are plotted for $\alpha = .01$ and values of $m = 1, 2, 4, 8$, and 128 . As was seen for the optimum detector, the signal detectability with the sum-and-test detector becomes poorer as m increases. An expression for $1-\beta$ as a function of \sqrt{d} and any fixed false-alarm rate $\alpha = \alpha^*$ and for any value of m can be found as follows: From Eq. (II-72),

$$\alpha^* = \frac{1}{2} \left[1 - \Phi \left(\sqrt{\frac{d}{4m}} + \sqrt{\frac{m}{d}} \log k \right) \right] \quad (\text{II-73})$$

Thus

$$\sqrt{\frac{m}{d}} \log k = \phi^{-1}(1 - 2\alpha^*) - \sqrt{\frac{d}{4m}} \quad (\text{II-74})$$

From Eqs. (II-72) and (II-74),

$$1 - \beta = \frac{1}{2} \left\{ 1 + \phi \left[\sqrt{\frac{d}{m}} - \phi^{-1}(1 - 2\alpha^*) \right] \right\} \quad (\text{II-75})$$

where $\phi^{-1}(\)$ has the same meaning as in Eq. (II-64). The right-hand side of Eq. (II-75) is seen to be of the general form of expression (II-68) and thus represents a linear function of \sqrt{d} on the normal probability scale of Fig. II.5. Since \sqrt{d} enters Eq. (II-75) in the form $\sqrt{d/m}$, the slope of the detectability curve will vary with m , decreasing as m increases. Thus if a family of detectability curves for the sum-and-test detector is plotted for a fixed value of α , the slope of each curve will approach zero as m becomes increasingly large, as is seen in Fig. II.5. The horizontal displacement of the curves is governed by $\phi^{-1}(1 - 2\alpha^*)$ and thus a family of curves plotted for a fixed value of m consists of a set of parallel lines, with the detectability becoming steadily poorer as α^* is made smaller; this is seen in Fig. II.4.

Fig. II.5 shows that as the uncertainty about signal frequency increases, the performance of the sum-and-test detector declines more rapidly than that of the optimum detector. In the operation of the sum-and-test detector, an increase in the number of possible values of the signal frequency requires an identical increase in the number of noisy correlator outputs to be summed before the

threshold test; thus the post-detection SNR varies inversely with m , as is seen in Eq. (II-72). However, the optimum detector, when visualized in terms of its asymptotic form, the band-splitting detector, effectively searches out the "best" (that is, the largest) of the m outputs and then uses this in the threshold test. Increasing m simply increases the number of test quantities among which the detector must search, but the detector will still seek out the "best" output for use in the threshold test. As more outputs are to be examined, the conditional false alarm probability increases, therefore the threshold must be adjusted slightly upward to maintain the same false alarm rate; this change in threshold level leads to a slightly lower conditional detection probability.

A useful basis for comparison of the optimum detector with the sum-and-test detector is that of pre-detection SNR or integration time required for a desired level of performance. This comparison is made in Fig. II.6 in a plot of $d_{\text{sum}}/d_{\text{opt}}$ vs. m , for $\alpha = .01$, and $\beta = .50$; where

d_{sum} = detection index required with the sum-and-test detector for error probabilities $\alpha = .01$ and $\beta = .50$.

d_{opt} = detection index required with the optimum detector for error probabilities $\alpha = .01$ and $\beta = .50$.

Since the detection index d is seen from Eq. (II-24) to depend linearly upon the pre-detection SNR and linearly upon the integration time, the ratio $d_{\text{sum}}/d_{\text{opt}}$ may be interpreted as either a ratio of required input SNR for a fixed integration time or a ratio of required integration times for a fixed input SNR. It is seen from

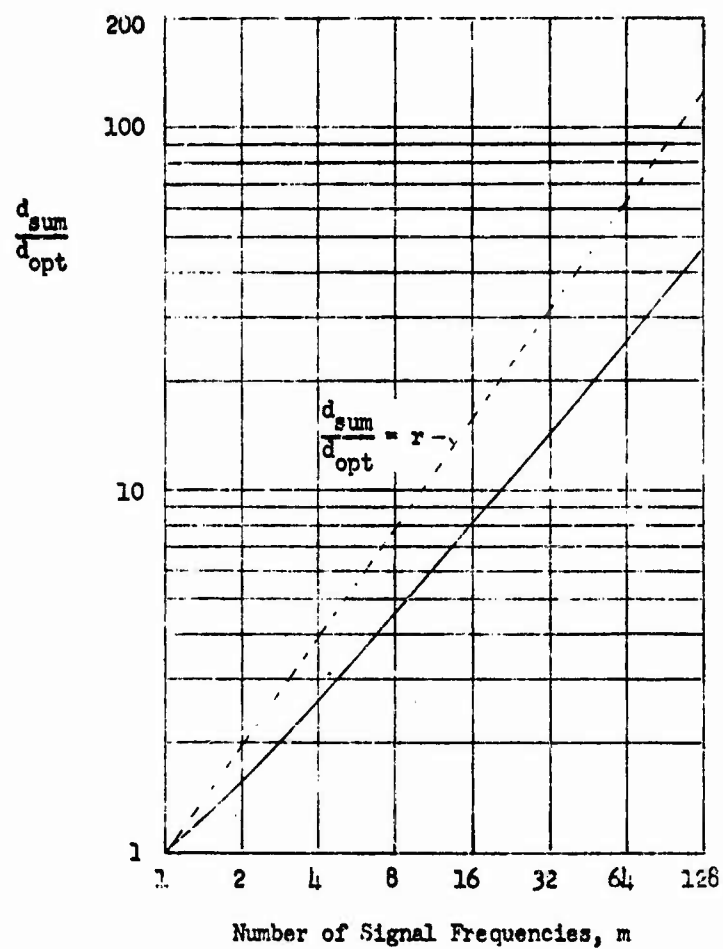


Fig. II.6. Comparison of Optimum Detector with Sum-and-Detector -
Ratio of Required Detection Indices for $\alpha = .01$, $\beta = .50$

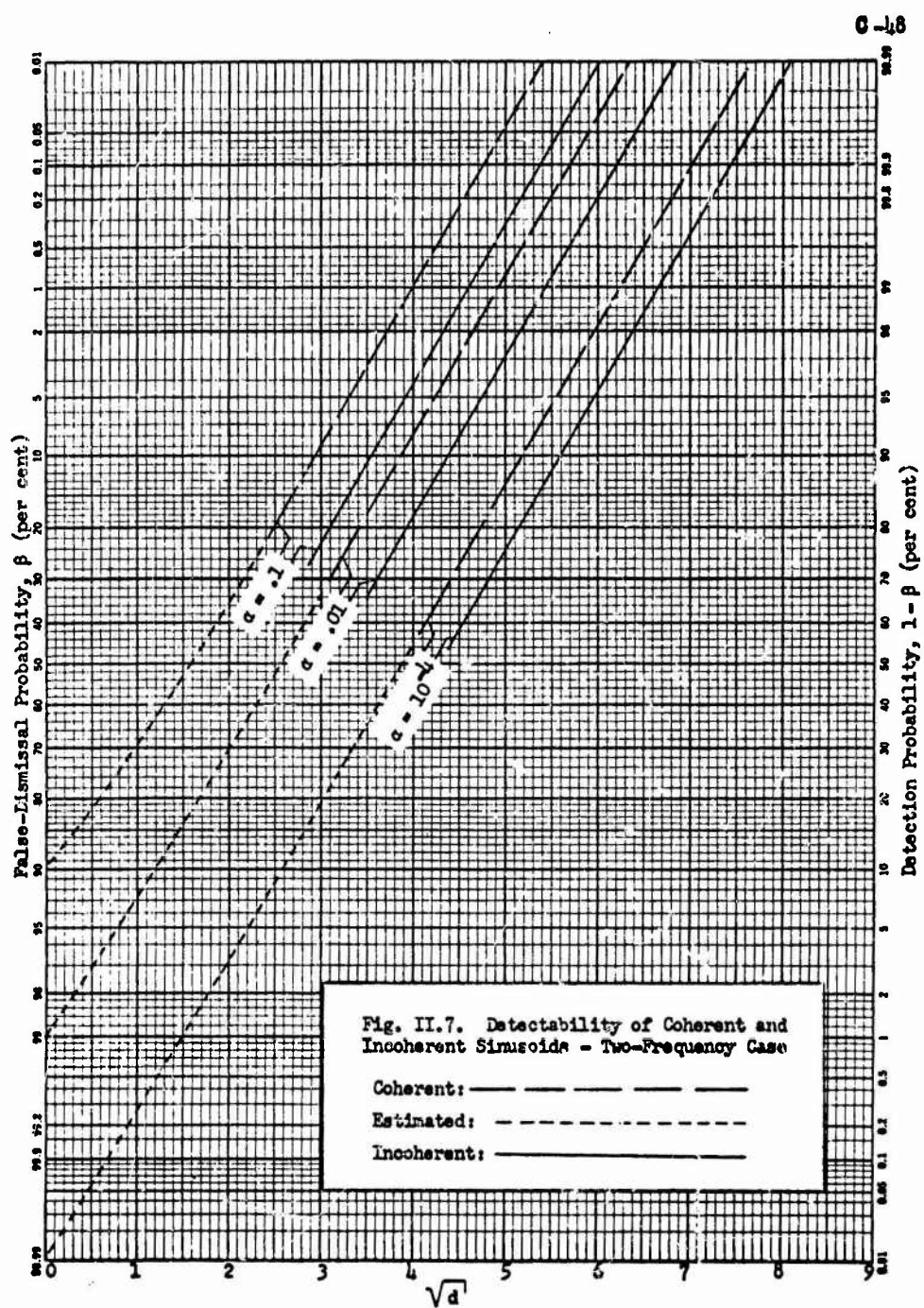
the figure that the logarithm of this ratio increases in an approximately linear fashion with the logarithm of m .

II.5 Detection of a Sinusoid of Random Phase and Unknown Frequency in Gaussian Noise

After the results presented in this chapter were originally reported[†], they were extended by Hill^{††} to the problem of detecting a sinusoid of known amplitude but unknown phase and unknown frequency in broadband gaussian noise. The signal frequency was assumed to have a discrete probability distribution over m possible values as was assumed in the present investigation, but the phase was assumed to be unknown with a uniform p.d.f. over the range $0, 2\pi$. This signal was termed an incoherent sinusoid. Hill employed the geometric decision-space approach developed here and showed that in the case of unknown phase the optimum detector again becomes a band-splitting detector as the post-detection SNR is made large. Signal detectability curves were computed and compared with the corresponding results obtained for the coherent-sinusoid case. Detectability curves are presented in Fig. II.7 for both the coherent and incoherent signals, for the 2-frequency case ($m = 2$). Conditional detection probability is plotted as a function of the detection index \sqrt{d} for several values of the false alarm probability α . The curves for coherent signals are those previously shown in Fig. II.4. It is seen from Fig. II.7 that for each value of α the detectability curves corresponding to coherent and incoherent signals, respectively, become parallel

[†] See Levesque (II)

^{††} Hill, F. S., Jr., unpublished research, January, 1965.

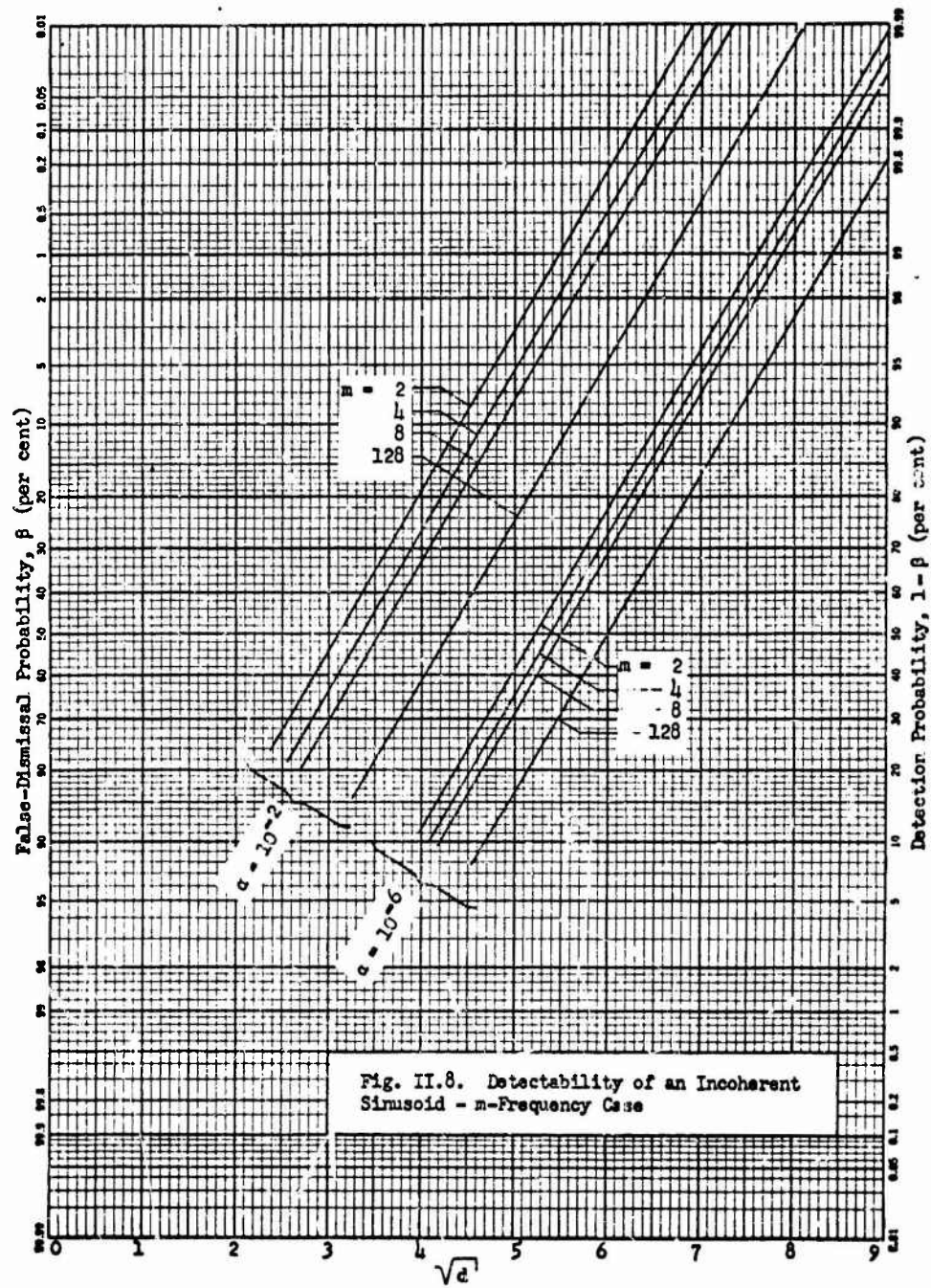


straight lines as \sqrt{d} increases. Thus the randomness of the phase results in an approximately constant "cost" in \sqrt{d} in the region of high detectability. This is the same trend which is exhibited in a single-frequency analysis[†].

In Fig. II.8 are plotted detectability curves for the incoherent case with $m = 2, 4, 8$, and 128, and for $\alpha = 10^{-2}$ and 10^{-6} . It can be seen by comparing the curves for $\alpha = 10^{-2}$ with Fig. II.5 that the curves for the incoherent case once again become parallel to the corresponding curves for the coherent case.

A useful measure of the loss in detectability due to unknown phase is the increase in pre-detection SNR required to achieve a desired level of performance with the observation time T assumed fixed. For $\alpha = .01$ and $\beta = .50$ the required increase in SNR varies from 1.5 db to 1.0 db as m varies from 2 to 128. Similar losses in pre-detection SNR are exhibited at $\alpha = 10^{-6}$.

[†] See for example Helstrom (I, discussion on pp. 155-156).



II.6 Comments

The results obtained in this chapter have shown that the optimum structure for the detection of a coherent sinusoid with a discrete frequency distribution becomes a band-splitting detector as the post-detection SNR is made large. This work could be extended directly to the detection of any incoherent signal whose frequency is given by a discrete probability distribution. For such a case the threshold test would again be given by Eq. (II-5) and the threshold surface by Eq. (II-6). The major departure from the foregoing analysis would be the non-gaussian statistics of the test quantities $\log L(\underline{y}/f_1)$. However, regardless of the precise form of the distributions of $\log L(\underline{y}/f_1)$, these distributions would again move away from the n -dimensional "corner" of the decision threshold surface, and the surface could again be accurately approximated by its asymptote planes. Thus once again the band-splitting detector should emerge as an accurate representation of the optimum detector structure.

The next two chapters will consider a somewhat more generalized problem, one of detecting a narrowband signal whose frequency is given by a p.d.f. over a continuous frequency range.

CHAPTER III

DETECTION OF A NARROWBAND GAUSSIAN SIGNAL
OF UNKNOWN CENTER FREQUENCY - PART I
WEAK SIGNALSIII.1 Introduction

This chapter and the following chapter will deal with the problem of detecting, in broadband gaussian noise, a narrowband gaussian signal of bandwidth B_g . The center frequency of this signal is not known in advance but is assumed to lie within a frequency band of width B , where $B = rB_g$ and $r \geq 0$. The quantity r will be referred to as the frequency uncertainty ratio. The optimum structure for the detection of such a signal will be determined and a satisfactory engineering approximation to the optimum detector will be found.

The signal detectability will also be determined. Of particular interest is the question as to what improvement in detectability is obtained when the signal power is confined to a band r times narrower than the frequency band B being processed rather than being uniformly spread over the band B . This improvement in detectability will be determined for several values of r . Experimental data on optimum detector performance will be presented and compared with theoretical results.

The signal detectability will be seen to depend upon signal strength through R_g , the SNR in a narrow band of width B_g . This chapter will be concerned with the situation in which R_g is $\ll 1$, that is, the weak-signal case. When the signal is strong with respect to the noise in a band of width B_g , and $R_g \gg 1$, then the analysis must be modified; the strong-signal case will be taken up in Chapter IV.

III.2 Detection of a Stochastic Signal of Unknown Center Frequency

When the signal to be detected is a stochastic signal with a spectrum of known shape but unknown center frequency f_c , the optimum detector must compute the average LR.

$$l(\underline{y}) = \left\langle L(\underline{y}/f_c) \right\rangle_{f_c} \quad (\text{III-1})$$

where

$$L(\underline{y}/f_c) = \frac{f(\underline{y}/s, f_c)}{f(\underline{y}/0)} \quad (\text{III-2})$$

is a LR calculated for a particular value of the center frequency.

When $l(\underline{y})$ is expressed in terms of $\log L(\underline{y}/f_c)$,

$$l(\underline{y}) = \left\langle \exp [\log L(\underline{y}/f_c)] \right\rangle_{f_c} \quad (\text{III-3})$$

If the unknown center frequency has a probability distribution over a discrete set of m values, Eq. (III-3) becomes

$$l(\underline{y}) = \sum_{i=1}^m p_i \exp [\log L(\underline{y}/f_{c,i})] \quad (\text{III-4})$$

where p_i is the probability that the center frequency has the value f_{ci} . The optimum detector forms the sum in Eq. (III-4) and compares the sum with a preset threshold k :

$$\sum_{i=1}^m p_i \exp [\log L(\underline{y}/f_{ci})] \geq k \quad (\text{III-5})$$

The average LR given by Eq. (III-4) and the threshold test given by Eq. (III-5) are analogous to Eq. (II-4) and (II-5) derived in the preceding chapter for the detection of a coherent sinusoid whose frequency was given by a discrete probability distribution. In that chapter a geometric interpretation of the average LR and of the threshold test was proposed and that interpretation was used to derive the asymptotic form of the detector structure. A slightly different approach will be taken here.

Suppose that the stochastic signal is narrowband and the discrete center-frequency values f_{ci} are separated by frequency intervals at least as large as the signal bandwidth. Then when the observation time is long, i.e., several times as large as the reciprocal of the signal bandwidth, test quantities $\log L(\underline{y}/f_{ci})$ and $\log L(\underline{y}/f_{cj})$ will be independent for $i \neq j$ [†]. If the post-detection SNR is made large in order to insure high detectability, and if a signal of center frequency f_{ck} is present in the received data, the test quantity $\log L(\underline{y}/f_{ck})$ will on the average have a

[†] It will be seen in the next section that the formation of a test quantity $\log L(\underline{y}/f_{ci})$ requires three basic operations: filtering of the received signal with a pre-detection filter matched to the signal spectrum and centered at frequency f , followed by a nonlinear operation and finally integration. If the pre-detection filters centered at f_{ci} and f_{cj} have non-overlapping frequency responses and if the observation time is long with respect to the reciprocal of the filter bandwidths, then the filter outputs, and hence $\log L(\underline{y}/f_{ci})$ and $\log L(\underline{y}/f_{cj})$ are independent.

high value. The remaining $m-1$ of the test quantities will on the average have small values. The exponential operation in Eq. (III-5) suppresses low values of $\log L(\underline{v}/f_{ci})$ and emphasizes high values. Therefore when a signal is present in the received data the dominant term in the summation in Eq. (III-5) is that corresponding to the actual center frequency of the signal to be detected. As the separation is increased between the average value of $\log L(\underline{v}/f_{ci})$ with only noise present and the average value with signal of center frequency f_{ci} and noise present, the threshold test on $l(\underline{v})$ can be closely approximated by a test on the largest term in the summation, that is,

$$\max_i [\log L(\underline{v}/f_{ci}) + \log p_i] \geq \log k \quad (\text{III-6})$$

A test of this form is referred to as a maximum likelihood test.

If at least one of the m quantities $[\log L(\underline{v}/f_{ci}) + \log p_i]$ exceeds the threshold, the maximum of the quantities will have exceeded the threshold. Hence the test prescribed by Eq. (III-6) can be accomplished by a band-splitting detector, in which $\log L(\underline{v}/f_{ci})$ is generated at each of the m possible center frequencies and is compared with a threshold as follows:

$$\log L(\underline{v}/f_{ci}) \geq \log k - \log p_i \quad (\text{III-7})$$

If one or more of the test quantities exceeds its threshold, the decision is made that a signal is present in the received data[†]. This band-splitting detector is precisely the detector structure which was derived in Chapter II using the geometric interpretation of the average LR and the threshold test.

The foregoing argument has made use of the assumed independence of the test quantities $\log L(\underline{y}/f_{c_i})$ in order to state that when a signal is present and the post-detection SNR is high, one of the terms in the summation in Eq. (III-4) will dominate and the remaining terms may be ignored. If the number m of possible locations of the signal center frequency in a fixed frequency range is steadily increased, test quantities generated at neighboring frequency values will become correlated. Then, when a signal is present, two or more test quantities will on the average have high values. However the test quantity $\log L(\underline{y}/f_{c_k})$, where f_{c_k} is the true signal center frequency, will have a higher average value than any other test quantity $\log L(\underline{y}/f_{c_i})$. The exponential operation in Eq. (III-4) will cause the average difference between $\exp [\log L(\underline{y}/f_{c_k})]$ and $\exp [\log L(\underline{y}/f_{c_i})]$, $i \neq k$, to be of exponential order in the difference between the average values of $\log L(\underline{y}/f_{c_k})$ and $\log L(\underline{y}/f_{c_i})$, the difference between these latter average values increasing with the post-detection SNR. Thus as the post-detection

[†] Since it is not required in the detection problem that the actual center frequency of the detected signal be identified, it does not matter that on some occasions the threshold will be exceeded at more than one frequency, though a signal can be present at only one possible center frequency.

SNR is made very large the test quantity $\log L(\underline{y}/f_{ck})$ will again dominate in the summation which represents $l(\underline{y})$ and the threshold test in Eq. (III-5) may be accurately approximated by a test on the largest term in the summation, a test which is implemented by a band-splitting detector, as was found in the case of independent test quantities.

Thus it may be concluded that the optimum detector for the detection of a stochastic signal whose center frequency is given by a discrete probability distribution asymptotically becomes a band-splitting detector as the post-detection SNR becomes increasingly large, regardless of the spacing of the possible values of the signal center frequency.

If the number m of frequency values in a fixed range is increased indefinitely, a limiting situation will be reached in which the center frequency of the stochastic signal is unknown over a continuous frequency band. If this frequency band has a width B cps, the average LR as given by Eq. (III-3) may be written as

$$l(\underline{y}) = \int_B df_c p(f_c) \exp[\log L(\underline{y}/f_c)] \quad (\text{III-8})$$

The optimum detector now generates $\exp[\log L(\underline{y}/f_c)]$ as a continuous function of frequency and averages this over the band B with respect to the p.d.f. of the signal center frequency. As in the case of a discrete frequency distribution, the exponential operation in Eq. (III-8) emphasizes large values of $\log L(\underline{y}/f_c)$ and suppresses low values so that if a signal is present in the received data and the post-detection SNR is made large, the function

$\exp[\log L(\underline{v}/f_c)]$ will on the average have a large peak near the true value of the signal center frequency, and this peak will provide the major contribution to the integral in Eq. (III-8). Thus it can again be seen that if the post-detection SNR is made very large, a test on $L(\underline{v})$ can be closely approximated by a test on the peak value of $p(f_c)$ times $\exp[\log L(\underline{v}/f_c)]$ or equivalently by a test on $[\log p(f_c) + \log L(\underline{v}/f_c)]$. This test can be implemented by means of a "band-sweeping" detector, in which $\log L(\underline{v}/f_c)$ is generated as a continuous function of frequency[†] and the following test is made:

$$\log L(\underline{v}/f_c) \geq \log k - \log p(f_c) \quad (\text{III-9})$$

If the threshold is exceeded anywhere in the band B, a decision is made that a signal is present. The foregoing discussion does not constitute a proof of the asymptotic optimality of the band-sweeping detector, but is simply an extension of the similar result, obtained for the case of a discrete frequency distribution, to the limiting case of a continuous distribution. Since the asymptotic optimality of a band-splitting detector can be demonstrated for any discrete distribution of signal frequencies however dense, it seems reasonable that the limiting form of the band-splitting detector, the

[†] Elsewhere the term "sweeping" is often used to describe a filter or other electronic device some parameter of which is continuously varied as a function of time while the device is processing a signal. It must be emphasized that the band-sweeping detector described here does not operate in this fashion. Rather, the detector generates the function $\log L(\underline{v}/f_c)$ simultaneously for all frequencies f_c in the band B, and $\log L(\underline{v}/f_c)$ at each frequency is generated from the same set of samples of $v(t)$, taken in the time interval $0, T$.

band-sweeping detector, is also asymptotically optimum as the post-detection SNR is made increasing large. Thus, the asymptotic optimality of the band-sweeping detector will be conjectured without further attempt at a rigorous proof.

The performance of the band-sweeping detector will now be analyzed to determine the detectability of a narrowband gaussian signal of unknown center frequency in regions of high signal detectability. In regions of low detectability, where the analysis of the optimum detector is not tractable, the signal detectability can be estimated. This is no loss, however, since the only situations of real interest are those where high detectability is obtained.

A practical implementation of the band-sweeping detector would employ a densely spaced bank of narrowband filters, each matched to the expected signal band, spanning the overall band of frequency uncertainty. It is clear that as more filters are added to the filter bank, the instrumentation approaches the band-sweeping detector. It is thus of practical interest to determine how densely the filters must be spaced in order to achieve satisfactory performance. The question will be answered by considering successive band-splitting approximations to the band-sweeping detector.

III.3 Narrowband Gaussian Signal of Unknown Center Frequency

The problem to be considered is as follows: A narrowband gaussian random signal is to be detected in the presence of broadband gaussian noise. The spectral level of the noise is assumed to be known, as are the signal power and the signal bandwidth B_s cps.

The center frequency of the signal is not known however, except that it lies somewhere in the frequency band being processed, a band of width B , where $B \geq B_s$. In various situations the signal bandwidth B_s may be narrower than B by varying amounts. Thus it is of interest to determine the signal detectability as a function of the relative magnitudes of B and B_s , as well as a function of signal and noise powers and the integration time.

For convenience of analysis, the following assumptions will be made:

1) The background noise has a flat spectral density of level N_0 volt²/cps from zero frequency up to a cutoff frequency W cps, where W is much higher than the highest possible signal frequency. The noise may thus be considered white with respect to the narrow-band signal.

2) The signal is assumed to have a rectangular spectrum of width B_s centered at some frequency f_c . The total average signal power will be $A^2/2$.

3) The p.d.f. for the signal center frequency is assumed to be uniform over the band B , and the band B is an integral number of times wider than the signal bandwidth, that is

$$B = r B_s \quad (\text{III-10})$$

where r , the frequency uncertainty ratio, is assumed to take on integer values.

The assumed model of the signal spectrum is shown in Fig. III.1.

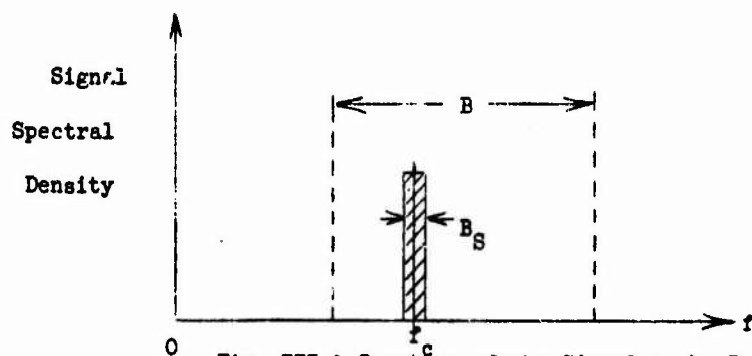


Fig. III.1 Spectrum of the Signal to be Detected

As was stated in Section III.2, the optimum detector will be approximated by a band-sweeping detector. It was conjectured that this detector becomes asymptotically optimum as the signal detectability is increasingly improved. Thus the detector must calculate $\log L(\underline{v}/f_c)$ for values of f_c in the band B . The quantity $L(\underline{v}/f_c)$ is the LR calculated for a gaussian signal in gaussian noise given that the center frequency of the signal spectrum is known to be f_c . $L(\underline{v}/f_c)$ is easily derived. When a signal is present, the received sample vector \underline{v} is

$$\underline{v} = \underline{s} + \underline{n} \quad (\text{III-11})$$

where \underline{s} is a sample vector from the gaussian signal process and \underline{n} a sample vector from the gaussian noise process. If the signal and noise processes are independent, then \underline{v} is a sample vector from a gaussian process with covariance matrix $\underline{P} + \underline{K}$ where \underline{P} is the signal covariance matrix for a given value of the narrowband

center frequency f_c , and \underline{K} is the noise covariance matrix. Thus, given that signal is present, the p.d.f. of the received signal \underline{v} is

$$f(\underline{v}/\underline{s}, f_c) = \frac{1}{(2\pi)^{n/2} [\det(\underline{P} + \underline{K})]^{1/2}} \exp \left\{ -\frac{1}{2} \underline{v}' (\underline{P} + \underline{K})^{-1} \underline{v} \right\} \quad (\text{III-12})$$

where n is the total number of samples.

When noise only is present in the received signal, the p.d.f. for \underline{v} is

$$f(\underline{v}/0) = \frac{1}{(2\pi)^{n/2} (\det \underline{K})^{1/2}} \exp \left\{ -\frac{1}{2} \underline{v}' \underline{K}^{-1} \underline{v} \right\} \quad (\text{III-13})$$

Hence the LR evaluated for a given value of the narrowband center frequency is

$$L(\underline{v}/f_c) = \left[\frac{\det \underline{K}}{\det (\underline{P} + \underline{K})} \right]^{1/2} \exp \left\{ -\frac{1}{2} \underline{v}' [(\underline{P} + \underline{K})^{-1} - \underline{K}^{-1}] \underline{v} \right\} \quad (\text{III-14})$$

It is necessary at this point to establish the precise structure of the vector and matrix forms \underline{v} , \underline{P} and \underline{K} used in Eq. (III-14). Since the assumption is being made that the signal spectrum is rectangular with width B_S centered at f_c , then in forming the quantity $L(\underline{v}/f_c)$ for a particular value of f_c , none of the noise spectrum outside the corresponding band B_S centered at f_c need be considered. Thus if the received signal $v(t)$ is ideally pre-filtered to the band B_S , \underline{v} represents a vector of samples of a band-pass signal $v(t)$ taken during the observation time T . Sampling analysis indicated that for $B_S T \gg 1$,

the signal $v(t)$ can be completely described by complex samples taken every $1/B_S$ seconds. Each complex sample $z(t_1)$ consists of a sample of the received signal $v(t)$ and a sample of its Hilbert Transform $\hat{v}(t)$, that is,

$$z(t_1) = v(t_1) + j \hat{v}(t_1) \quad (\text{III-15})$$

For $B_S T \gg 1$ the following properties of a function $x(t)$ and its Hilbert Transform $\hat{x}(t)$ can be demonstrated. These two statements will not be proven here, but follow directly from the properties of the Hilbert Transformation.[†]

1) The mean-squared value of a function $x(t)$ is equal to the mean-squared value of its Hilbert Transform $\hat{x}(t)$.^{††}

2) When the function $x(t)$ is a bandpass function strictly limited to a band of width W cps, samples of the Hilbert Transform $\hat{x}(t)$ taken at intervals of $\frac{1}{W}$ sec. are uncorrelated, as are samples of $x(t)$. Also, samples of $x(t)$ and of $\hat{x}(t)$ are uncorrelated at the same instant of time or at instants separated by intervals of $\frac{1}{W}$ sec., that is

$$\overline{x(t_1) \hat{x}(t_j)} = 0, \quad t_1 - t_j = 0, \frac{1}{W}, \frac{2}{W}, \dots \quad (\text{III-16})$$

Thus it is seen that when the received signal $v(t)$ is a gaussian process strictly band-limited to a band of width B_S cps and when $B_S T \gg 1$, $v(t)$ can be represented by a vector \underline{v} of $2B_S T$ independent samples. Furthermore, the matrices \underline{P} and \underline{K} can be written as diagonal matrices (of order $2B_S T$), that is,

$$\underline{P} = \frac{A^2}{2} \underline{I} \quad (\text{III-17})$$

[†] See Deutsch (I, Chap. 1).

^{††} This property can be stated either in terms of time averages or in terms of ensemble averages, the only requirement being that the process $x(t)$ be wide sense stationary. See the previous reference for a discussion of this point and for further references.

and

$$\underline{K} = N \underline{I} \quad (\text{III-18})$$

where \underline{I} is the identity matrix and

$$N = N_0 B_s \quad (\text{III-19})$$

is the total noise power in the narrow signal band. The determinants appearing in Eq. (III-14) then become

$$\det \underline{K} = N^n \quad (\text{III-20})$$

$$\det(\underline{P} + \underline{K}) = \left(\frac{A^2}{2} + N \right)^n \quad (\text{III-21})$$

Now Eq. (III-14) can be written more simply as

$$\begin{aligned} L(\underline{v}/f_c) &= \left[\frac{N}{\frac{A^2}{2} + N} \right]^{n/2} \exp \left\{ -\frac{1}{2} \left[\frac{1}{\frac{A^2}{2} + N} - \frac{1}{N} \right] \underline{v}' \underline{I} \underline{v} \right\} \\ &= \left[\frac{1}{\frac{A^2}{2N} + 1} \right]^{n/2} \exp \left\{ -\frac{1}{2} \left[\frac{1}{\frac{A^2}{2N} + 1} \right] \frac{A^2}{2N^2} \underline{v}' \underline{I} \underline{v} \right\} \end{aligned} \quad (\text{III-22})$$

The test quantity $\log L(\underline{v}/f_c)$ is given by

$$\log L(\underline{v}/f_c) = -\frac{n}{2} \log \left[\frac{A^2}{2N} + 1 \right] - \frac{1}{2} \left[\frac{1}{\frac{A^2}{2N} + 1} \right] \frac{A^2}{2N^2} \underline{v}' \underline{I} \underline{v} \quad (\text{III-23})$$

The operation on the received signal is seen to be a linear function of the quadratic form $\underline{y}'\underline{I}\underline{y}$, and it is clear that any linear function of $\underline{y}'\underline{I}\underline{y}$ would serve as an equivalent test quantity. For purposes of analysis and computation, it will be convenient to take as a test quantity[†]

$$Q(f) = \frac{A^2}{4N^2} \underline{y}'\underline{I}\underline{y} - \frac{n}{2} \left[\frac{A^2}{2N} + \frac{1}{2} \left(\frac{A^2}{2N} \right)^2 \right] \quad (\text{III-24})$$

At this point an input or pre-detection SNR will be defined as

$$\begin{aligned} R_S &\triangleq \frac{A^2}{2N} \\ &= \frac{A^2}{2N_0 B_S} \end{aligned} \quad (\text{III-25})$$

and is simply the signal-to-noise power ratio in a band B_S containing the desired signal. An input SNR may also be defined with respect to the overall band to be processed:

$$R \triangleq \frac{A^2}{2N_0 B} \quad (\text{III-26})$$

In the work immediately following, R_S as given by Eq. (III-25) will be more useful, but at certain later points in this work, R will also be a convenient measure of SNR. The distinction will always be made clear by the subscript S .

[†] Since the test quantity is specifically a function of center frequency, it should be written as $Q(f_c)$; however, for simplicity $Q(f)$ will be used.

From the definition of R_B , Eq. (III-24) may be rewritten

as

$$Q(f) = \frac{A^2}{4N^2} \underline{v}' \underline{I} \underline{v} - \frac{n}{2} \left[R_B + \frac{1}{2} R_B^2 \right] \quad (\text{III-27})$$

For small values of input SNR R_B , Eq. (III-27) represents a close approximation to the right side of Eq. (III-23), but $Q(f)$ is always a valid test statistic, being a monotone function of $\log L(\underline{v}/f_c)$, regardless of the size of R_B . Hence if the received signal is ideally pre-filtered to a band B_B cps wide centered at $f = f_c$, the calculation of the test quantity simply requires the formation of the vector product of \underline{v} with itself, $\underline{v}' \underline{I} \underline{v}$. From the discussions following Eqs. (III-14) and (III-15), the vector product becomes

$$\underline{v}' \underline{I} \underline{v} = \sum_{i=1}^{B_B T} v_i^2 + \psi_i^2 \quad (\text{III-28})$$

From property 1) stated in that discussion, one can write that for $B_B T \gg 1$,

$$\sum_{i=1}^{B_B T} v_i^2 \approx \sum_{i=1}^{B_B T} \psi_i^2 \quad (\text{III-29})$$

and thus Eq. (III-28) may be written approximately as

$$\underline{v}' \underline{I} \underline{v} \approx \sum_{i=1}^{2B_B T} v_i^2 \quad (\text{III-30})$$

If the summation in Eq. (III-30) is approximated by an integration, the operation on the filtered received signal $v(t)$ is

$$\underline{v}' \underline{I} \underline{v} = 2B_S \int_0^T dt v^2(t) \quad (\text{III-31})$$

Thus for long observation times ($B_S T \gg 1$) the formation of the test quantity $Q(f)$ at a particular value of center frequency $f = f_c$ requires a filtering of the received signal $v(t)$ to a band of width B_S cps centered at f_c , followed by squaring and integrating operations. This set of operations simply represents a measurement of the energy in the received signal in the corresponding band B_S during the interval T .

Since \underline{v} is a vector of samples from a gaussian random process, the quadratic form $\underline{v}' \underline{I} \underline{v}$ has a Chi-Squared p.d.f. with n degrees of freedom. However, in a weak-signal situation n is made very large, corresponding to a large time-bandwidth product; and as n is made large, the Chi-Squared p.d.f. becomes gaussian.

Thus only the mean and variance of $Q(f)$ are required, and they are calculated as follows: With only noise present,

$$\begin{aligned} E_N[Q(f)] &= \frac{A^2}{4N^2} \langle \underline{v}' \underline{I} \underline{v} \rangle_N = \frac{n}{2} \left[R_S + \frac{1}{2} R_S^2 \right] \\ &= \frac{A^2}{4N^2} \text{tr } \underline{K} = \frac{n}{2} \left[R_S + \frac{1}{2} R_S^2 \right] \\ &= n \frac{A^2}{4N} - \frac{n}{2} \left[R_S + \frac{1}{2} R_S^2 \right] \\ &= -\frac{n}{4} R_S^2 \end{aligned} \quad (\text{III-32})$$

$$\begin{aligned}
\text{var}_N [Q(f)] &= \left(\frac{A^2}{4N^2} \right)^2 \text{var}_N [\underline{v}' \underline{I} \underline{v}] \\
&= \left(\frac{A^2}{4N^2} \right)^2 \left[\langle \underline{v}' \underline{I} \underline{v} \underline{v}' \underline{I} \underline{v} \rangle - n^2 N^2 \right] \\
&= \left(\frac{A^2}{4N^2} \right)^2 \left[\text{tr}^2 \underline{K} + 2 \text{tr} \underline{K}^2 - n^2 N^2 \right] \\
&= \left(\frac{A^2}{4N^2} \right)^2 \left[n^2 N^2 + 2nN^2 - n^2 N^2 \right] \\
&= \frac{n}{2} R_S^2 \quad (\text{III-33})
\end{aligned}$$

When a signal is present in the received data, the mean and variance of $Q(f)$ depend upon the relative frequency positions of the band-sweeping filter and the narrowband signal spectrum. When the filter is centered at a frequency f separated from the true signal center frequency by at least B_S cps, then the filter does not overlap the signal spectrum, and the mean and variance of $Q(f)$ are given by Eqs. (III-32) and (III-33). When the filter is exactly aligned with the signal spectrum at $f = f_c$, the mean and variance of $Q(f)$ are easily shown to be

$$E_{S+N}[Q(f)] = \frac{n}{4} R_S^2 \quad (\text{III-34})$$

and

$$\text{var}_{S+N}[Q(f)] = \frac{n}{2} R_S^2 [1 + R_S]^2 \quad (\text{III-35})$$

In any intermediate situation, where the pass-band of the band-sweeping filter overlaps a fraction σ of the narrowband signal spectrum, the total average signal (desired signal) power in the filter output is $\frac{\sigma A^2}{2}$. Thus it can easily be shown that the mean and variance of $Q(f)$ are

$$E_{S+N}[Q(f)] = \frac{n}{4} R_S^2 (2\sigma - 1), \quad 0 \leq \sigma \leq 1 \quad (\text{III-36})$$

and

$$\text{var}_{S+N}[Q(f)] = \frac{n}{2} R_S^2 [1 + \sigma R_S]^2, \quad 0 \leq \sigma \leq 1 \quad (\text{III-37})$$

When $\sigma = 0$, representing no overlap, Eqs (III-36) and (III-37) give the results of Eqs (III-32) and (III-33); and when $\sigma = 1$, corresponding to alignment of the filter with the signal spectrum, Eqs. (III-36) and (III-37) become identical to Eqs. (III-34) and (III-35).

From results of sampling analysis the number of time samples n in the time interval T is

$$n = 2 B_S T \quad (\text{III-38})$$

where T is the observation time of the received signal. When Eq. (III-38) is substituted into Eqs. (III-32), (III-33), (III-36) and (III-37),

$$E_N[Q(f)] = -\frac{1}{2} R_S^2 B_S T \quad (\text{III-39})$$

$$\text{var}_N[Q(f)] = R_S^2 B_S T \quad (\text{III-40})$$

$$E_{S+N}[Q(f)] = \frac{1}{2} (2\sigma - 1) R_S^2 B_S T, \quad 0 \leq \sigma \leq 1 \quad (\text{III-41})$$

$$\text{var}_{S+N}[Q(f)] = R_S^2 [1 + \sigma R_S]^2 B_S T, \quad 0 \leq \sigma \leq 1 \quad (\text{III-42})$$

Thus, when the time-bandwidth product $B_S T$ is made much larger than unity, as will always be true if small received signals are to be enhanced to a detectable level by long integration time, the test quantity $Q(f)$ calculated at each possible value of signal center frequency will become a gaussian random variable. Its parameters are given above, and depend upon the presence or absence of desired signal and the degree of overlap of the band-sweeping filter with the signal spectrum. The detectability of the narrow-band gaussian signal with unknown center frequency can now be considered.

At this point it is convenient to define a detection index D as

$$D = R_S^2 B_S T \quad (\text{III-43})$$

which may also be regarded as a measure of post-detection or output SNR. Since $Q(f)$ can be treated as a gaussian random variable, the signal detectability will be a function of the deflection of $Q(f)$ and the variance of $Q(f)$ in the noise-only case and in the signal-plus-noise case. The deflection of $Q(f)$ is simply the difference between the averages in Eqs. (III-39) and (III-41); using Eq. (III-43) this becomes

$$\begin{aligned}\Delta E [Q(f)] &= \frac{1}{2} (2\sigma) R_S^2 B_S T \\ &= \sigma D, \quad 0 \leq \sigma \leq 1\end{aligned}\quad (\text{III-44})$$

The variance of $Q(f)$ given noise only becomes

$$\text{var}_N[Q(f)] = D \quad (\text{III-45})$$

and given that signal and noise are present,

$$\text{var}_{S+N}[Q(f)] = [1 + \sigma R_S]^2, \quad 0 \leq \sigma \leq 1 \quad (\text{III-46})$$

Inspection of Eq. (III-46) shows that if the pre-detection SNR R_S is much smaller than unity, then

$$\text{var}_{S+N}[Q(f)] \approx D \quad (\text{III-47})$$

which is equal to the variance given by Eq. (III-45), indicating that if the input SNR is very small, the variance of the p.d.f. for $Q(f)$ is essentially unchanged with the arrival of a signal. In such cases, the input SNR and the integration time determine the detectability only through the detection index D (the spectrum overlap σ will disappear when the average detectability is computed), which means that the signal detectability can be presented as a function of the single variable D for various values of the frequency uncertainty ratio r . When R_S is on the order of unity or greater, it is seen from Eq. (III-46) that detectability will then be a function of two variables, D and R_S (or, equivalently, $B_S T$ and R_S). Advantage will be taken of the compactness of presentation afforded by low input SNR by treating this case separately in the following section. The strong-signal case will be treated in Chapter IV.

III.4 Signal Detectability in the Weak-Signal Case

a) Error Probabilities

In this section attention will be turned to the calculation of the detectability of a gaussian stochastic signal of total average power $\frac{A^2}{2}$ having a rectangular spectrum of bandwidth B_s centered at an unknown frequency f_c . Here the assumption will be made that the pre-detection SNR is small, that is,

$$R_s = \frac{A^2}{2N_0 B_s} \ll 1 \quad (\text{III-48})$$

As was indicated earlier, the signal detectability will be calculated by analyzing the performance of a band-sweeping detector, since it is conjectured that this detector becomes asymptotically optimum as the post-detection SNR is made very large. The band-sweeping detector would generate $Q(f)$, given by Eq. (III-24), as a continuous function of frequency f within a band B cps wide which is known to contain the center frequency f_c of the signal when a signal is indeed present. It has been assumed that the p.d.f. for f_c is uniform over the uncertainty band B so that $Q(f)$ is to be compared with a uniform threshold:

$$Q(f) \geq \kappa' \quad (\text{III-49})$$

A practical approximation to this detector consists of discrete set of densely spaced (possible overlapping) filters covering the B -band, each of bandwidth B_s . The discussion following Eq. (III-27) showed that the output of each of these filters is to be squared and

then integrated over the observation interval $0, T$. Each of these integrator outputs, $Q(f_i)$, is then compared with the constant threshold k' ; and if one or more of these outputs exceeds its threshold, a decision is made that signal is present. Such a detector may be referred to as a band-splitting approximation to the band-sweeping detector. As the number of filters placed in the B-band is increased, the performance will approach that of the band-sweeping detector. It is of practical interest therefore to determine how densely the band-splitting filters must be spaced in order to achieve detection performance reasonably close to optimum.

Let the number of filters in a given band-splitting detector be given by b . If each of the integrator outputs $Q(f_i)$ is tested against the threshold k' , the conditional false alarm probability, given that only noise is present, is

$$\begin{aligned} \alpha &= P [\text{at least one } Q(f_i) > k' / \text{noise only}] , i = 1, 2, \dots, b \\ &= 1 - P [\text{all } Q(f_i) < k' / \text{noise only}] , i = 1, 2, \dots, b \end{aligned}$$

(III-50)

Given that signal and noise are present, the conditional false dismissal probability is

$$\beta = P [\text{all } Q(f_i) < k' / \text{signal and noise}] , i = 1, 2, \dots, b$$

(III-51)

Two successive approximations to the band-sweeping detector will be considered, each employing rectangular filters of width B_g . In the first approximation the number of uniformly spaced filters b

will be equal to r , where r is the ratio of signal frequency uncertainty. It can be seen that this describes a set of non-overlapping rectangular filters completely covering the band B . In the second approximation, b will equal $2r$. In each case the conditional detection probability, $1-\beta$, is to be calculated as a function of the detection index D for a fixed conditional false alarm probability.

b) First Approximation - Non-overlapping Filters ($b = r$)

When the frequency responses of the band-splitting filters do not overlap, then under the assumption of long observation time ($B_s T \gg 1$) being made in this chapter, their outputs are linearly independent, and any two test quantities $Q(f_i)$ and $Q(f_j)$, $i \neq j$, are independent.[†] The conditional false alarm rate given by Eq. (III-50) can then be written as^{††}

$$\alpha = 1 - \prod_{i=1}^b P [Q(f_i) < k' / \text{noise only}] \quad (\text{III-52})$$

Each of the terms in the product in Eq. (III-52) can be interpreted as the complement of a false alarm rate for the i^{th} output $Q(f_i)$, that is,

$$\alpha = 1 - \prod_{i=1}^b [1 - \alpha_i] \quad (\text{III-53})$$

where

$$\alpha_i = P [Q(f_i) > k' / \text{noise only}] , i = 1, 2, \dots, b \quad (\text{III-54})$$

[†] See Appendix D, which deals with the correlation properties of test quantities $Q(f_i)$.

^{††} See Appendix C.

When the integration time is long, $Q(f_i)$ is a gaussian random variable with mean and variance obtained from Eqs. (III-39), (III-43), and (III-45) as

$$E_N[Q(f_i)] = -\frac{1}{2} D, \quad i = 1, 2, \dots, b \quad (\text{III-55})$$

$$\text{var}_N[Q(f_i)] = D, \quad i = 1, 2, \dots, b \quad (\text{III-56})$$

The conditional p.d.f. for $Q(f_i)$, given noise only, is then

$$f(x/0) = \frac{1}{\sqrt{2\pi D}} \exp \left[-\frac{1}{2D} \left(x + \frac{D}{2} \right)^2 \right] \quad (\text{III-57})$$

where $x = Q(f_i)$. The false alarm probability for the i^{th} output α_i is then

$$\alpha_i = \frac{1}{\sqrt{2\pi D}} \int_{k'} dx \exp \left[-\frac{1}{2D} \left(x + \frac{D}{2} \right)^2 \right]$$

After a change of variable,

$$\alpha_i = \frac{1}{\sqrt{2\pi}} \int_{\sqrt{\frac{D}{4}} + \frac{k'}{\sqrt{D}}}^{\infty} du \exp \left(-\frac{u^2}{2} \right)$$

$$\alpha_i = \frac{1}{2} \left[1 - \Phi \left(\sqrt{\frac{D}{4}} + \frac{k'}{\sqrt{D}} \right) \right] \quad (\text{III-58})$$

where $\Phi(x)$ is the Normal Probability Integral, given by

$$\Phi(x) = \frac{1}{\sqrt{2\pi}} \int_{-x}^x dt \exp \left(-\frac{t^2}{2} \right) \quad (\text{III-59})$$

When signal and noise are present, signal power will in general appear in the outputs of two adjacent band-splitting filters, a fraction σ of the total average signal power appearing in one and the remaining fraction $1 - \sigma$ appearing in the other. This situation is indicated in Fig. III.2. When signal is present, two of the filters will share the total signal power, as shown, and $b - 2$ of the filter outputs will contain noise power only. Therefore the conditional false dismissal probability is

$$\beta = P[2 \text{ outputs } Q(f_i) < k', \text{ given that signal spectrum overlaps the corresponding frequency bands, and } b - 2 \text{ outputs } Q(f_i) < k', \text{ given that only noise is present in these bands.}]$$

Since none of the filter responses overlap one another, the b outputs $Q(f_i)$ are independent and β may be calculated as

$$\beta = \beta_{1(\sigma)} \beta_{1(1-\sigma)} (1 - \alpha_1)^{b-2}, \quad b = r \quad (\text{III-60})$$

Under the assumption being made in this section that the input SNR is low, as indicated in Eq. (III-48), the mean and variance of $Q(f_i)$ in a filter band containing a fraction σ of the total signal power are

$$E_{S+N}[Q(f_i)] = (2\sigma - 1) \frac{D}{2}, \quad 0 \leq \sigma \leq 1 \quad (\text{III-61})$$

$$\text{var}_{S+N}[Q(f_i)] = D \quad (\text{III-62})$$

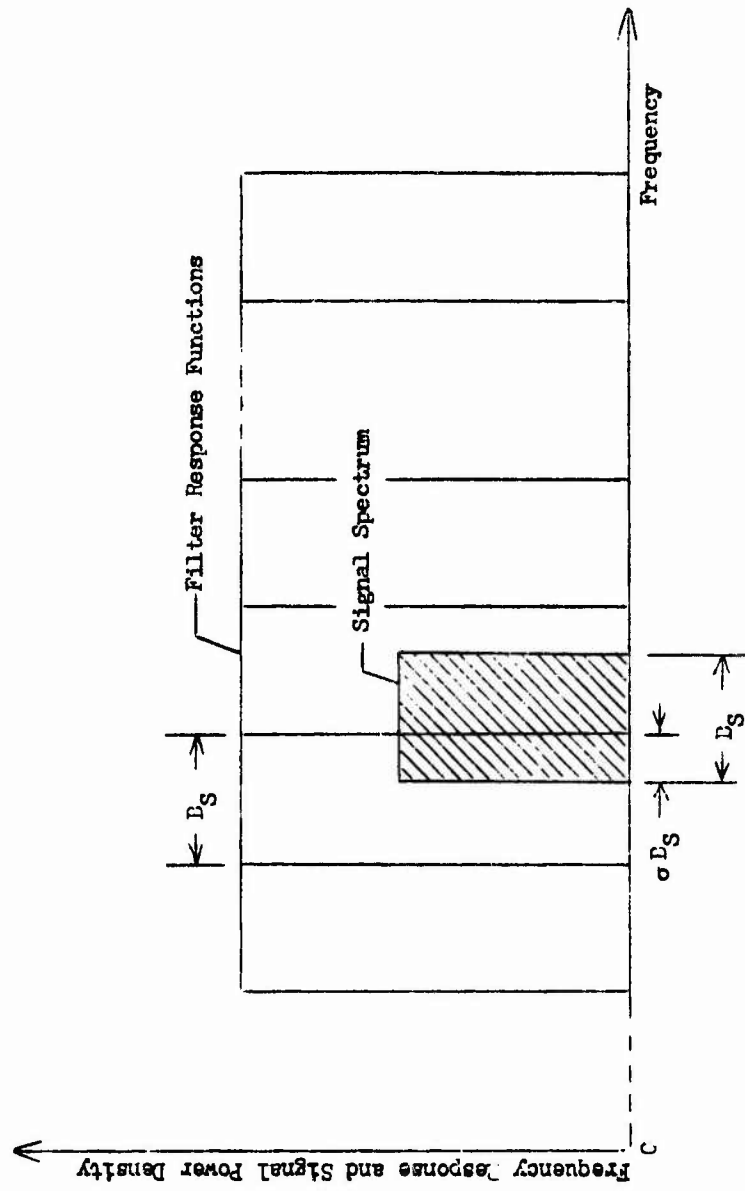


Fig. III.2. Non-overlapping Filter Response Functions and a Typical Signal Spectrum

The p.d.f.'s for $Q(f_1)$ in the bands containing signal power are thus

$$f(x/\sigma) = \frac{1}{\sqrt{2\pi D}} \exp \left\{ -\frac{1}{2D} \left[x - (2\sigma - 1) \frac{D}{2} \right]^2 \right\} \quad (\text{III-63})$$

and

$$f(x/1 - \sigma) = \frac{1}{\sqrt{2\pi D}} \exp \left\{ -\frac{1}{2D} \left[x + (2\sigma - 1) \frac{D}{2} \right]^2 \right\} \quad (\text{III-64})$$

From the above distributions,

$$\begin{aligned} B_{1(\sigma)} &= \int_{-\infty}^{k'} dx f(x/\sigma) \\ &= \frac{1}{\sqrt{2\pi D}} \int_{-\infty}^{k'} dx \exp \left\{ -\frac{1}{2D} \left[x - (2\sigma - 1) \frac{D}{2} \right]^2 \right\} \\ &= \frac{1}{\sqrt{2\pi}} \int_{-\infty}^{\sqrt{\frac{D}{4}} - (2\sigma - 1)\sqrt{\frac{D}{4}} - \frac{k'}{\sqrt{D}}} du \exp \left\{ -\frac{u^2}{2} \right\} \end{aligned}$$

$$B_{1(\sigma)} = \frac{1}{2} \left\{ 1 - \Phi \left[(2\sigma - 1) \sqrt{\frac{D}{4}} - \frac{k'}{\sqrt{D}} \right] \right\}, \quad 0 \leq \sigma \leq 1 \quad (\text{III-65})$$

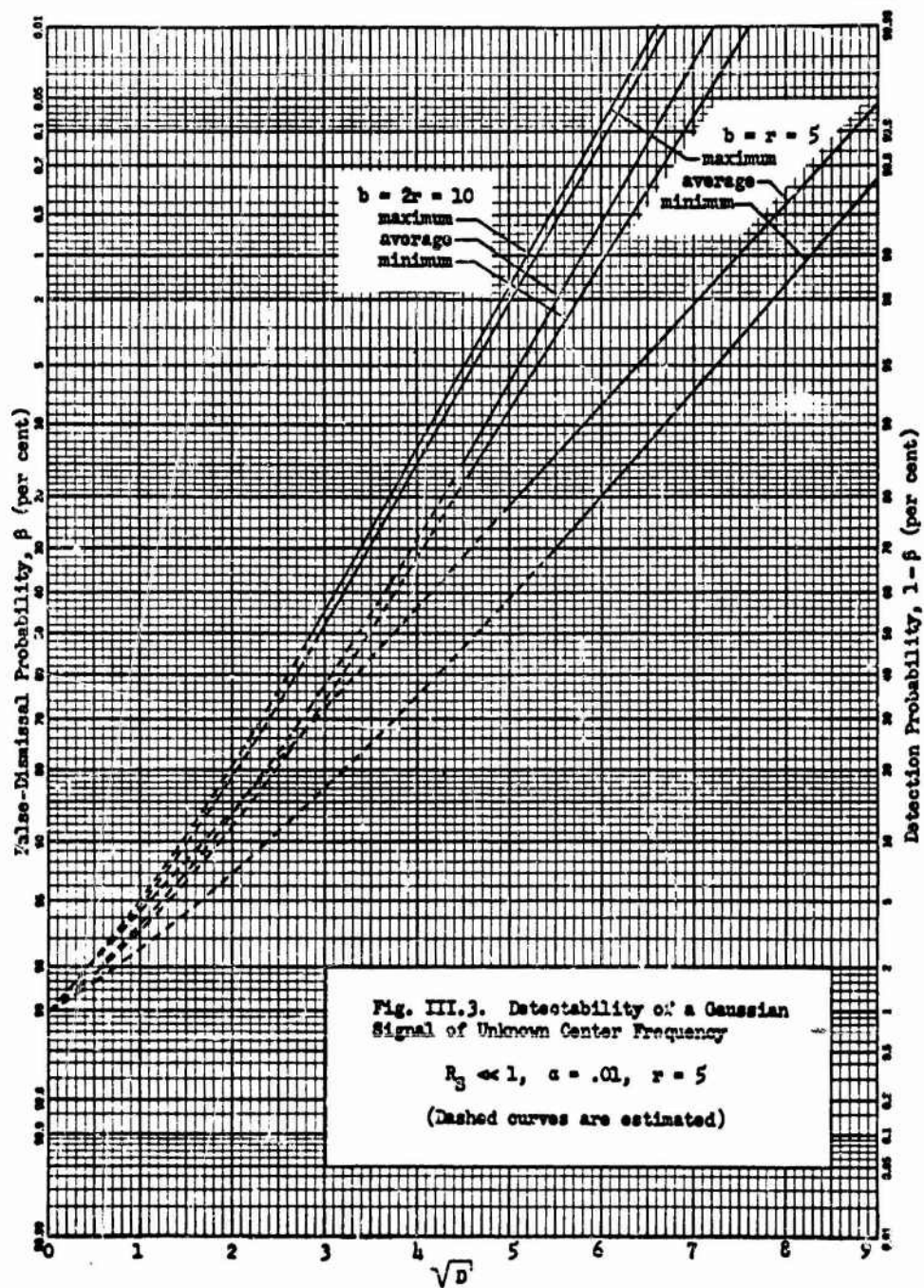
Similarly,

$$B_{1(1-\sigma)} = \frac{1}{2} \left\{ 1 + \Phi \left[(2\sigma - 1) \sqrt{\frac{D}{4}} + \frac{k'}{\sqrt{D}} \right] \right\}, \quad 0 \leq \sigma \leq 1 \quad (\text{III-66})$$

With Eqs. (III-53), (III-58), (III-60), (III-65) and (III-66) the conditional detection probability $1 - \beta$ can be calculated as a function of the detection index D for a fixed value of false alarm probability, which determines the threshold k' , and a prescribed value of the frequency uncertainty ratio r . At each value of D , of course, the detectability is a function of the signal spectrum overlap σ . It has been assumed that over the ensemble of all observations of the received signal, the narrow-band signal spectrum will be centered at all possible frequencies in the band B with uniform probability density. Therefore, ignoring end effects near the edges of the band B , the signal overlap σ will take on all values in the range $0,1$ with uniform probability density. Thus at each value of detection index D the average signal detectability may be computed, representing an average detectability over all possible locations of the signal spectrum within the band of signal frequency uncertainty.

Signal detectability has been calculated for a case in which $r = 5$, that is, a case in which the band of signal frequency uncertainty is five times as wide as the signal bandwidth[†]. Figure III.3 shows the detectability obtainable with a first-approximation detector as analyzed in this section, a detector employing a bank of five non-overlapping rectangular filters covering the entire band being processed. The pertinent curves are those labelled " $b = r = 5$ ". The curve denoted as "maximum"

[†] Where r is as low as 5, end effects are not really negligible in the calculation of error probabilities. Nevertheless, end effects were ignored. In this way the results obtained for $r = 5$ can be generalized to higher values of r , where end effects indeed become negligible.



indicates signal detectability obtainable when the spectrum of the narrowband signal happens to be precisely aligned with any one of the five filters, that is, when $\sigma = 1$. The curve denoted as "minimum" refers to the least favorable frequency location of the signal, when the signal power is divided equally between two adjacent filters, that is, when $\sigma = \frac{1}{2}$. The "average" curve gives average detectability over all values of σ , as discussed in the previous paragraph. All curves in Fig. III.3 have been derived for a fixed value of conditional false alarm probability $\alpha = .01$.

It is evident from Fig. III.3 that if a bank of non-overlapping filters is to be used in detection, the performance is very sensitive to the actual location of the signal center frequency, a wide variation in detectability resulting from the range of values of σ . Thus a second and better approximation to the band-sweeping detector will next be considered.

c) Second Approximation - Overlapping Filters ($b = 2r$)

A detector will now be considered which employs a bank of $b = 2r$ uniformly spaced rectangular filters covering the entire processing band B . Since each filter has a bandwidth B_g , and since $B = rB_g$, the centers of the filters are spaced at frequency intervals of $\frac{1}{2} B_g$. The outputs of the filters and consequently the test quantities $Q(f_i)$ are no longer independent, and from Eq. (III-50), the conditional false alarm probability is now

$$\begin{aligned}
 a &= 1 - P[\text{all } Q_i < k' / \text{noise only}] \\
 &= 1 - P[Q_1 < k' / \text{noise only}] \\
 &\quad \cdot P[Q_2 < k' / Q_1 < k', \text{noise only}] \\
 &\quad \cdot P[Q_3 < k' / Q_1 < k', Q_2 < k', \text{noise only}] \\
 &\quad \dots P[Q_b < k' / Q_1 < k', Q_2 < k', \dots, Q_{b-1} < k', \text{noise only}]
 \end{aligned}$$

(III-67)

where for simplification $Q_i \equiv Q(f_i)$.

When $b = 2r$, the output of each filter is correlated with that of each of the two (except for end effects, which shall be ignored) nearest-neighboring filters but not with that of any more remote filter. Thus Q_i and Q_j are partially correlated for $|i - j| = 1$, but uncorrelated for $|i - j| > 1$. With this fact, the false alarm probability can be written as

$$\begin{aligned}
 a &= 1 - \left\{ P[Q_1 < k' / \text{noise only}] \right. \\
 &\quad \cdot P[Q_2 < k' / Q_1 < k', \text{noise only}] \\
 &\quad \cdot P[Q_3 < k' / Q_2 < k', \text{noise only}] \\
 &\quad \left. \dots P[Q_b < k' / Q_{b-1} < k', \text{noise only}] \right\} \\
 &= 1 - \left[P[Q_1 < k' / \text{noise only}] \right. \\
 &\quad \left. \cdot \left\{ P[Q_2 < k' / Q_1 < k', \text{noise only}] \right\}^{b-1} \right]
 \end{aligned}$$

(III-68)

If end effects near the edges of the processing band are ignored, the false alarm probability becomes approximately

$$\alpha \approx 1 - \left\{ P[Q_2 < k' / Q_1 < k', \text{ noise only}] \right\}^b \quad (\text{III-69})$$

The joint p.d.f. for Q_1 and Q_2 is needed. From Section III.3,

$$E_N[Q_1] = E_N[Q_2] = -\frac{D}{2} \quad (\text{III-70})$$

$$\text{var}_N[Q_1] = \text{var}_N[Q_2] = D \quad (\text{III-71})$$

The calculation of the correlation coefficient relating Q_1 and Q_2 is not carried out here, but is left to Appendix D. The derivation is straightforward and for the case at hand, in which $b = 2r$, the correlation coefficient is

$$\rho = \frac{\text{covariance}_N[Q_1 \text{ and } Q_2]}{\sqrt{\text{var}_N[Q_1]} \sqrt{\text{var}_N[Q_2]}} = \frac{1}{2} \quad (\text{III-72})$$

The joint p.d.f. for Q_1 and Q_2 given noise only can now be written. If $Q_1 = x$ and $Q_2 = y$, then from Eqs. (III-70), (III-71) and (III-72),

$$f(x, y/Q) = \frac{1}{2\pi D \sqrt{1 - (\frac{1}{2})^2}} \exp \left\{ -\frac{1}{2D \left[1 - (\frac{1}{2})^2 \right]} \left[\left(x + \frac{D}{2} \right)^2 - 2 \left(\frac{1}{2} \right) \left(x + \frac{D}{2} \right) \left(y + \frac{D}{2} \right) + \left(y + \frac{D}{2} \right)^2 \right] \right\} \quad (\text{III-73})$$

From Eq. (III-69),

$$a = 1 - \left\{ P[y < k' / x < k', \text{ noise only}] \right\}^b$$

$$= 1 - \left\{ \frac{P[y < k', x < k' / \text{ noise only}]}{P[x < k' / \text{ noise only}]} \right\}^b \quad (\text{III-74})$$

and then from Eq. (III-73)

$$P[y < k', x < k' / \text{ noise only}]$$

$$= \frac{1}{2\pi D \sqrt{1 - (\frac{1}{2})^2}} \int_{-\infty}^{k'} dx \int_{-\infty}^{k'} dy \exp \left\{ \frac{-1}{2D \left[1 - (\frac{1}{2})^2 \right]} \left[\left(x + \frac{D}{2} \right)^2 - 2\left(\frac{1}{2}\right)\left(x + \frac{D}{2}\right)\left(y + \frac{D}{2}\right) + \left(y + \frac{D}{2}\right)^2 \right] \right\}$$

$$= \frac{1}{2\pi \sqrt{1 - (\frac{1}{2})^2}} \int_{-\infty}^{\sqrt{\frac{D}{4}} + \frac{k'}{\sqrt{D}}} du \int_{-\infty}^{\sqrt{\frac{D}{4}} + \frac{k'}{\sqrt{D}}} dv \exp \left\{ \frac{-1}{2 \left[1 - (\frac{1}{2})^2 \right]} \left[u^2 - 2\left(\frac{1}{2}\right)uv + v^2 \right] \right\} \quad (\text{III-75})$$

The integral in Eq. (III-75) is of the form

$$L(h, k, \rho) = \int_h^{\infty} du \int_k^{\infty} dv \frac{1}{2\pi \sqrt{1 - \rho^2}} \exp \left[- \frac{1}{2(1 - \rho^2)} (u^2 - 2\rho uv + v^2) \right]$$

$$(\text{III-76})$$

This integral has been tabulated[†] for various values of the limits h and k and the correlation coefficient ρ . If Eq. (III-76) is substituted into Eq. (III-75),

[†] See National Bureau of Standards (II).

$$P[y < k', x < k' / \text{noise only}] = L \left[-\left(\sqrt{\frac{D}{4}} + \frac{k'}{\sqrt{D}}\right), -\left(\sqrt{\frac{D}{4}} + \frac{k'}{\sqrt{D}}\right), \frac{1}{2} \right] \quad (\text{III-77})$$

The denominator in Eq. (III-74) is simply

$$P[x < k' / \text{noise only}] = \frac{1}{2} \left[1 + \Phi \left(\sqrt{\frac{D}{4}} + \frac{k'}{\sqrt{D}} \right) \right] \quad (\text{III-78})$$

From Eqs (III-74), (III-77) and (III-78)

$$\alpha \approx 1 - \frac{\left(L \left[-\left(\sqrt{\frac{D}{4}} + \frac{k'}{\sqrt{D}}\right), -\left(\sqrt{\frac{D}{4}} + \frac{k'}{\sqrt{D}}\right), \frac{1}{2} \right] \right)^b}{\frac{1}{2} \left[1 + \Phi \left(\sqrt{\frac{D}{4}} + \frac{k'}{\sqrt{D}} \right) \right]} \quad (\text{III-79})$$

The conditional probability of false dismissal will now be calculated. When a signal is present, the remarks following Eq. (III-67) regarding pair-wise statistical dependence of the test quantities Q_1 still hold, and from Eq. (III-51) the false dismissal probability is

$$\begin{aligned} \beta &= P[Q_1 < k' / S + N] \\ &\quad \cdot P[Q_2 < k' / Q_1 < k', S + N] \\ &\quad \cdot P[Q_3 < k' / Q_2 < k', S + N] \\ &\quad \cdots P[Q_b < k' / Q_{b-1} < k', S + N] \quad (\text{IXI-80}) \end{aligned}$$

When a narrowband signal is present, the signal spectrum will in general overlap the pass bands of four of the band-splitting filters, (see Fig. III.4) thereby increasing the average power in the outputs of these four adjacent filters, and the mean values of the four corresponding test quantities Q_i will accordingly be increased. Since the pre-detection SNR is assumed to be low, the presence of signal will not affect the variances of these four Q_i 's, nor will the correlation coefficient ρ relating adjacent Q_i 's be affected. The remaining $1 - 4$ quantities Q_i will have statistics unchanged from the noise-only condition.

Let the filters be numbered consecutively starting from the low-frequency end of the band B. Let the lowest numbered filter which passes part of the signal spectrum be the j^{th} filter. Then the j^{th} filter and the next three filters along the frequency scale share the signal power as follows:

$$\left. \begin{aligned} j^{\text{th}} \text{ filter: } & \sigma \left(\frac{A^2}{2} \right) \\ (j+1)^{\text{th}} \text{ filter: } & (\sigma + .5) \left(\frac{A^2}{2} \right) \\ (j+2)^{\text{th}} \text{ filter: } & (1 - \sigma) \left(\frac{A^2}{2} \right) \\ (j+3)^{\text{th}} \text{ filter: } & (.5 - \sigma) \left(\frac{A^2}{2} \right) \end{aligned} \right\} 0 \leq \sigma \leq .5 \quad (\text{III-81})$$

Thus the mean values of the four corresponding test quantities are obtained from Eq. (III-61) as

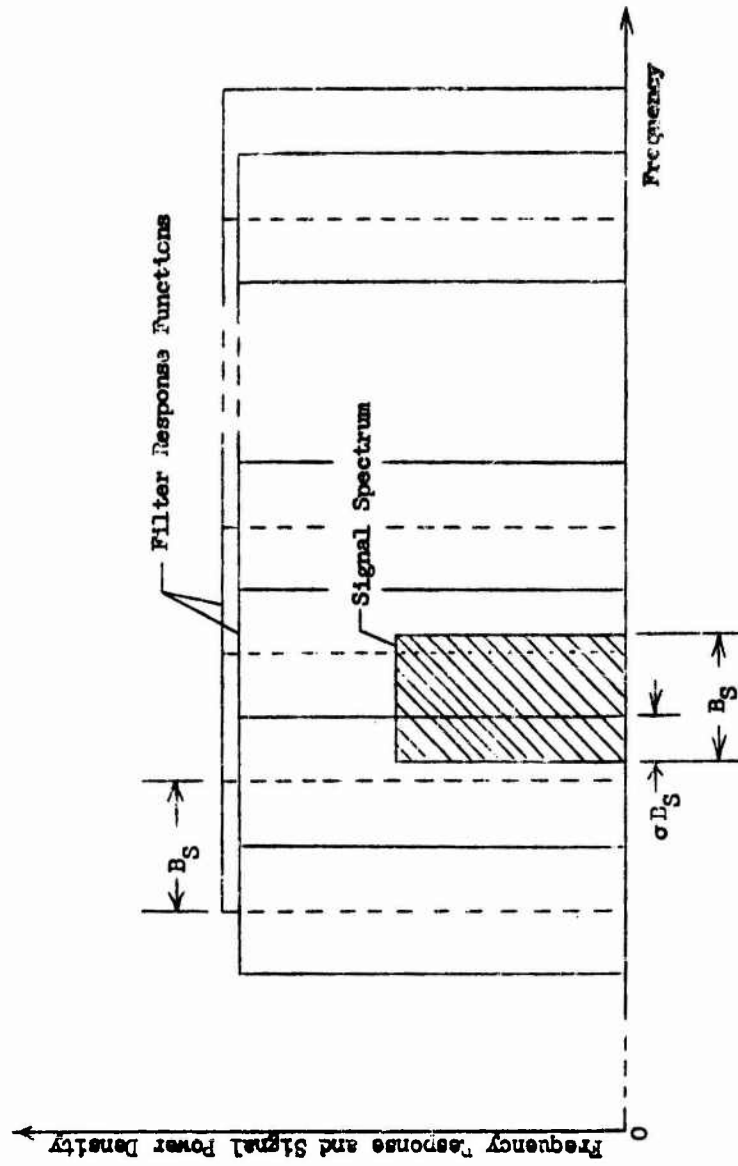


Fig. III.4. Overlapping Filter Response Functions and a Typical Signal Spectrum

$$\left. \begin{aligned} E_{S+N}[Q_j] &= (2\sigma - 1) \frac{D}{2} \\ E_{S+N}[Q_{j+1}] &= (2\sigma) \frac{D}{2} \\ E_{S+N}[Q_{j+2}] &= -(2\sigma - 1) \frac{D}{2} \\ E_{S+N}[Q_{j+3}] &= -(2\sigma) \frac{D}{2} \end{aligned} \right\} \quad \begin{aligned} 0 \leq \sigma \leq .5 \\ (III-82) \end{aligned}$$

A total of five of the conditional probabilities in Eq. (III-80) will be affected by the presence of signal: The j^{th} through $(j+3)^{\text{th}}$ terms indicated above and also the $(j+4)^{\text{th}}$ term, since Q_{j+4} is correlated with Q_{j+3} . Therefore if end effects are ignored, the false dismissal rate as given by Eq. (III-80) is the product of b terms, $b-5$ of them of the form

$$P(Q_2 < k' / Q_1 < k', N) = \frac{L \left[-\left(\sqrt{\frac{D}{k}} + \frac{k'}{\sqrt{D}}\right), -\left(\sqrt{\frac{D}{k}} + \frac{k'}{\sqrt{D}}\right), \frac{1}{2} \right]}{\frac{1}{2} \left[1 + \Phi \left(\sqrt{\frac{D}{k}} + \frac{k'}{\sqrt{D}} \right) \right]} \quad (III-83)$$

The five remaining terms in the product are

$$P(Q_j < k' / Q_{j-1} < k', S+N) = \frac{L \left[\left((2\sigma - 1) \sqrt{\frac{D}{k}} - \frac{k'}{\sqrt{D}} \right), -\left(\sqrt{\frac{D}{k}} + \frac{k'}{\sqrt{D}}\right), \frac{1}{2} \right]}{\frac{1}{2} \left[1 + \Phi \left(\sqrt{\frac{D}{k}} - \frac{k'}{\sqrt{D}} \right) \right]} \quad (III-84)$$

$$P [Q_{j+1} < k' / Q_j < k, S + N] = \frac{L \left[- \left(2\sigma \sqrt{\frac{D}{4}} - \frac{k'}{\sqrt{D}} \right), - \left((2\sigma - 1) \sqrt{\frac{D}{4}} - \frac{k'}{\sqrt{D}} \right), \frac{1}{2} \right]}{\frac{1}{2} \left[1 - \Phi \left((2\sigma - 1) \sqrt{\frac{D}{4}} - \frac{k'}{\sqrt{D}} \right) \right]}$$

(III-85)

$$P [Q_{j+2} < k' / Q_{j+1} < k', S + N] = \frac{L \left[- \left((2\sigma - 1) \sqrt{\frac{D}{4}} + \frac{k'}{\sqrt{D}} \right), \left(2\sigma \sqrt{\frac{D}{4}} - \frac{k'}{\sqrt{D}} \right), \frac{1}{2} \right]}{\frac{1}{2} \left[1 + \Phi \left(2\sigma \sqrt{\frac{D}{4}} - \frac{k'}{\sqrt{D}} \right) \right]}$$

(III-86)

$$P [Q_{j+3} < k' / Q_{j+2} < k', S + N] = \frac{L \left[- \left(2\sigma \sqrt{\frac{D}{4}} + \frac{k'}{\sqrt{D}} \right), - \left((2\sigma - 1) \sqrt{\frac{D}{4}} + \frac{k'}{\sqrt{D}} \right), \frac{1}{2} \right]}{\frac{1}{2} \left[1 + \Phi \left((2\sigma - 1) \sqrt{\frac{D}{4}} + \frac{k'}{\sqrt{D}} \right) \right]}$$

(III-87)

$$P [Q_{j+4} < k' / Q_{j+3} < k', S + N] = \frac{L \left[- \left(\sqrt{\frac{D}{4}} + \frac{k'}{\sqrt{D}} \right), - \left(2\sigma \sqrt{\frac{D}{4}} + \frac{k'}{\sqrt{D}} \right), \frac{1}{2} \right]}{\frac{1}{2} \left[1 + \Phi \left(2\sigma \sqrt{\frac{D}{4}} + \frac{k'}{\sqrt{D}} \right) \right]}$$

(III-88)

Thus, if the first term in Eq. (III-80) is approximated by the right-hand side of Eq. (III-83) in order to eliminate end effects, the conditional false dismissal probability is obtained from the above equations by

$$S = [\text{Eq. (III-83)}]^{b-5} [\text{Eq. (III-84)}] [\text{Eq. (III-85)}] [\text{Eq. (III-86)}] \\ \cdot [\text{Eq. (III-87)}] [\text{Eq. (XII-88)}], \\ b = 2r$$

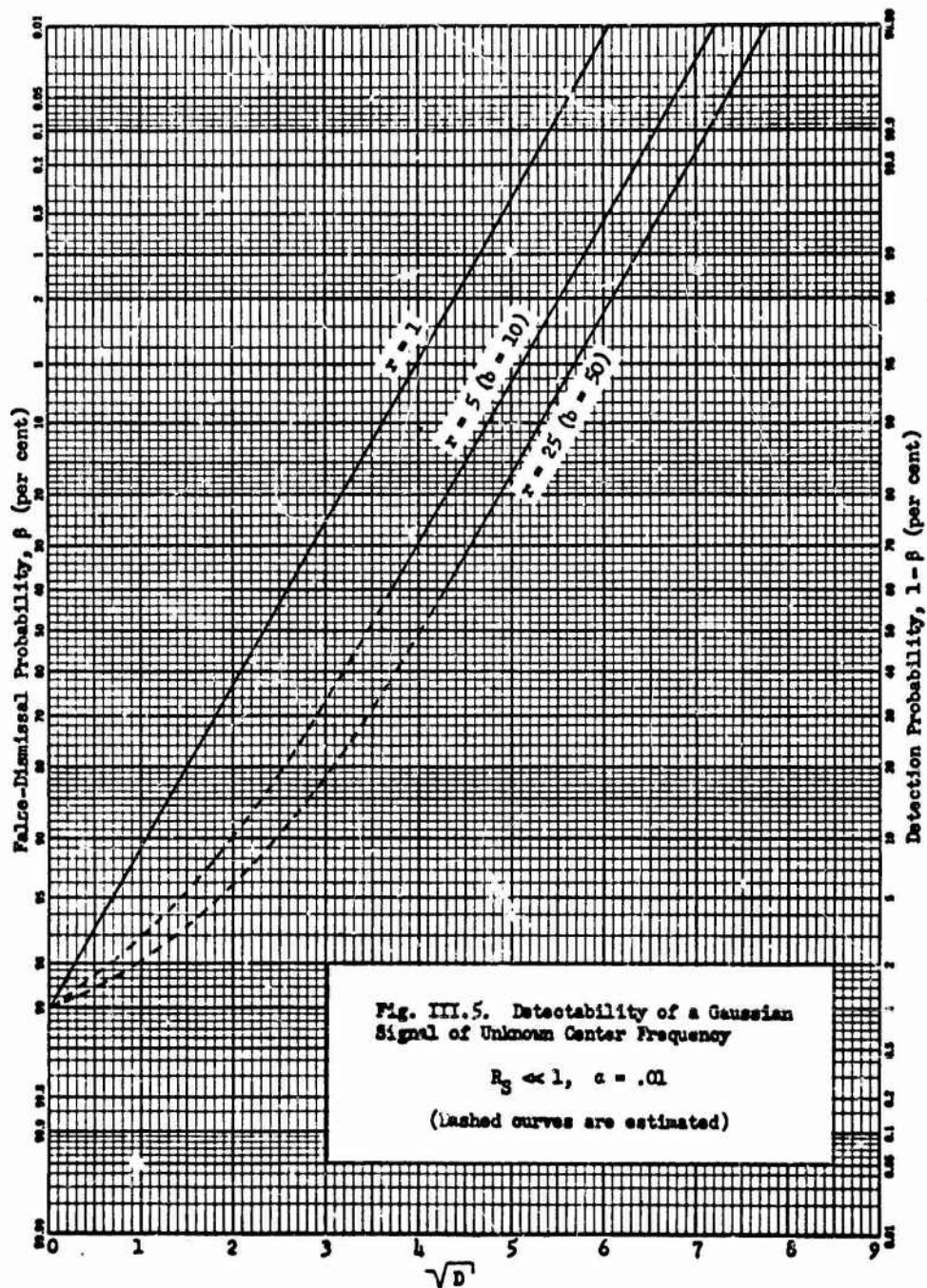
(III-89)

As in the analysis of the first-approximation detector, signal detectability may be calculated as a function of the detection index D for a fixed value of false alarm probability α and a fixed value of the frequency uncertainty ratio r , using Eqs. (III-79) and (III-89). At each value of D signal detectability must be averaged with respect to the signal spectrum overlap σ . These computations have been carried out for the case in which $r = 5$, and the resulting curves of average detectability at a false alarm probability $\alpha = .01$ are plotted in Fig. III.3, labelled as " $b = 2r = 10$ ". It is seen from the figure that when the number of band-splitting filters is twice the frequency uncertainty ratio, the variation in signal detectability due to the randomness in the frequency location of the narrowband signal is greatly reduced from the corresponding variation with the first-approximation detector. It is clear that a third and better approximation to the optimum detector, say a 15-band or 20-band detector, would further improve detectability, but only marginally. Since the ultimate optimum detectability curve would lie above the "average" curve obtained for $b = 2r = 10$ and below the "maximum" curve for the same value of b , it is seen from Fig. III.3 that for values of $1 - \delta$ in excess

of 95 per cent, this detector will yield an average signal detectability which is within 3 per cent of the optimum. It may thus be concluded that a band-splitting detector with a number of filters equal to twice the frequency uncertainty ratio represents a very satisfactory compromise between complexity of implementation and efficient signal detectability.

With this result at hand, Eqs. (III-79) and (III-89) may be used to derive detectability curves for various values of the signal frequency uncertainty ratio r . In Fig. III.5 signal detectability is plotted for a fixed false alarm rate $\alpha = .01$ for values of $r = 1, 5$ and 25 . The curve for $r = 1$ is obtained from Eqs. (III-58) and (III-65) with $\sigma = 1$ and represents the most favorable situation with regard to detecting the narrowband signal, that in which the center frequency is known a priori. For $r = 5$ and 25 , $b = 2\pi$ as indicated, and these two curves give average detectability with respect to all possible values of signal spectrum overlap. It is seen that the curves for $r = 5$ and 25 become parallel to that for $r = 1$ as \sqrt{D} increases and are displaced further to the right as r increases. If the curves are compared at a given value of detection probability, this trend may be interpreted as meaning that the initial uncertainty regarding the center frequency of the narrowband signal results in a fixed "cost" in \sqrt{D} for a particular value of r as \sqrt{D} becomes large. Since

$$\sqrt{D} = R_B \sqrt{B_S T} \quad (\text{III-90})$$



The cost in \sqrt{D} may be regarded as a cost in pre-detection SNR for a fixed value of the time-bandwidth product $B_g T$. Similarly, if the curves are compared at a given value of \sqrt{D} , an increase in the uncertainty ratio r is seen to produce a decrease in signal detectability.

From another point of view, let the total signal power and the overall bandwidth B be given. If the signal power were spread uniformly across the band B being processed, signal detectability would depend upon the pre-detection SNR R , where

$$R = \frac{A^2}{2N_0 B} \quad (\text{III-91})$$

If, however, the same signal power is confined to a narrower band of width B_g , it has been shown that detectability depends upon R_g as a pre-detection SNR, thus

$$\begin{aligned} R_g &= \frac{A^2}{2N_0 B_g} \\ &= \frac{rA^2}{2N_0 B} \\ &= r R \end{aligned} \quad (\text{III-92})$$

Thus knowledge that the signal bandwidth is r times narrower than the band being processed leads to an increase in the pre-detection SNR by the factor r and a resulting increase in detectability for a fixed false alarm probability.

The uncertainty regarding the actual frequency location of the signal makes necessary the use of a bank of band-splitting filters

which in effect search the overall band B . As the frequency uncertainty ratio r increases, the number of filters required also increases and if a constant false alarm probability is to be maintained, the threshold level must be raised, which tends to offset somewhat the increase in detectability. The net result, however, is a gain in signal detectability.

A useful measure of this gain in detectability can be obtained as follows: Suppose that the bandwidth B and the observation time T are fixed and that prescribed values of false alarm probability α and false dismissal probability β are required. One can then calculate the pre-detection SNR R required to achieve this performance in each of the following two cases:

- 1) In one case assume that the signal power is uniformly distributed over the band B .
- 2) In the second case assume that the signal power is confined to a band of width $B_s = \frac{1}{r} B$, and that the signal lies at some unknown frequency within the band B .

Let R_1 and R_2 be the values of pre-detection SNR R [given by Eq. (III-91)] required to produce the prescribed values of α and β in cases 1) and 2), respectively. The ratio R_1/R_2 then represents the net increase in effective pre-detection SNR for a fixed level of performance achieved when the signal spectrum is r times narrower than the overall band being processed.

Figure III.6 shows the ratio R_1/R_2 as a function of r for false alarm probability $\alpha = .01$ and false dismissal probability $\beta = .50$. The dashed line in the figure corresponds to the ratio

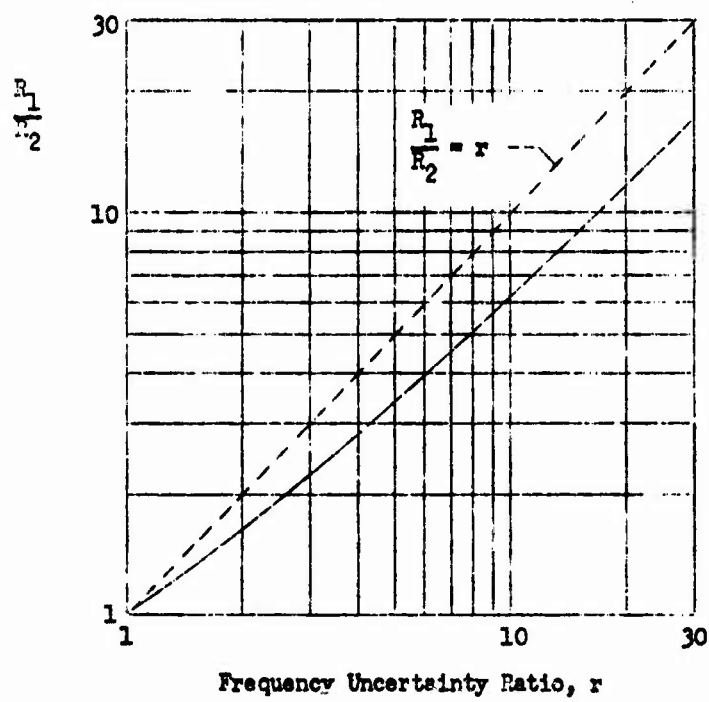


Fig. III.6. Ratio of Required Input SNR's for $\alpha = .01$, $\theta = .50$

$R_1/R_2 = r$ and represents the gain in pre-detection SNR which could be obtained by narrowing the signal spectrum by the factor r is the frequency location if the signal spectrum were known in advance. Thus the vertical displacement of the curve for R_1/R_2 from this dashed line represents the loss in pre-detection SNR due to frequency uncertainty. It can be seen that this loss is fairly constant at approximately 2db for values of r between 5 and 30.

Therefore it may be concluded that in the weak-signal case, most of the enhancement in pre-detection SNR, achieved when the signal spectrum is appreciably narrower than the processing band, is retained in spite of the frequency uncertainty.

The work of this chapter has been a weak-signal, long-observation-time analysis. The assumption of a long observation interval has been rather heavily relied upon at certain points, notably in representing the pre-detection filtering operation by a rectangular frequency response curve. Without this device the calculation of detection probabilities would have been vastly more complicated, if possible at all. The assumption of long observation time is of course quite reasonable when high detectability is to be achieved in a weak-signal situation. In Chapter IV the assumption of a weak input signal will be dropped.

Before proceeding to the next chapter, the results of some experimental work, related to the work of this chapter, will be presented.

III.5 Experimental Verification

Experimental work was carried out to obtain a check on some of the theoretical results obtained in Section III.4. A band-splitting detector was constructed employing a bank of five band-pass pre-detection filters, each filter being followed by a full-wave rectifier and a low-pass filter. Each of the pre-detection filters had a half-power bandwidth of 50 cps and rolloffs of ± 18 db per octave. The filter responses were aligned in such a way that the upper half-power frequency of one filter coincided with the lower half-power frequency of the adjacent filter. The five filters covered the frequency range from 1,000 cps to 1,250 cps. Each low-pass filter consisted of a simple RC pi-section. Diagrams of the detector circuits are shown in Appendix E.

The detector was operated in two different configurations:

1) In the first configuration, a threshold test was made on the output of each individual low-pass filter, a decision being made in favor of the presence of a signal whenever at least one filter output exceeded its threshold. This system is shown diagrammatically in Fig. III.7.

2) In the second configuration the five low-pass filter outputs were summed, and a threshold test was made on this sum. This system is shown in Fig. III.8 and will be termed a sum-and-test detector.

The first configuration represents an approximation to the idealized band-splitting detector described and analyzed in the work of this chapter. The second configuration is analogous to the suboptimum sum-and-test detector discussed in Chapter II in connection

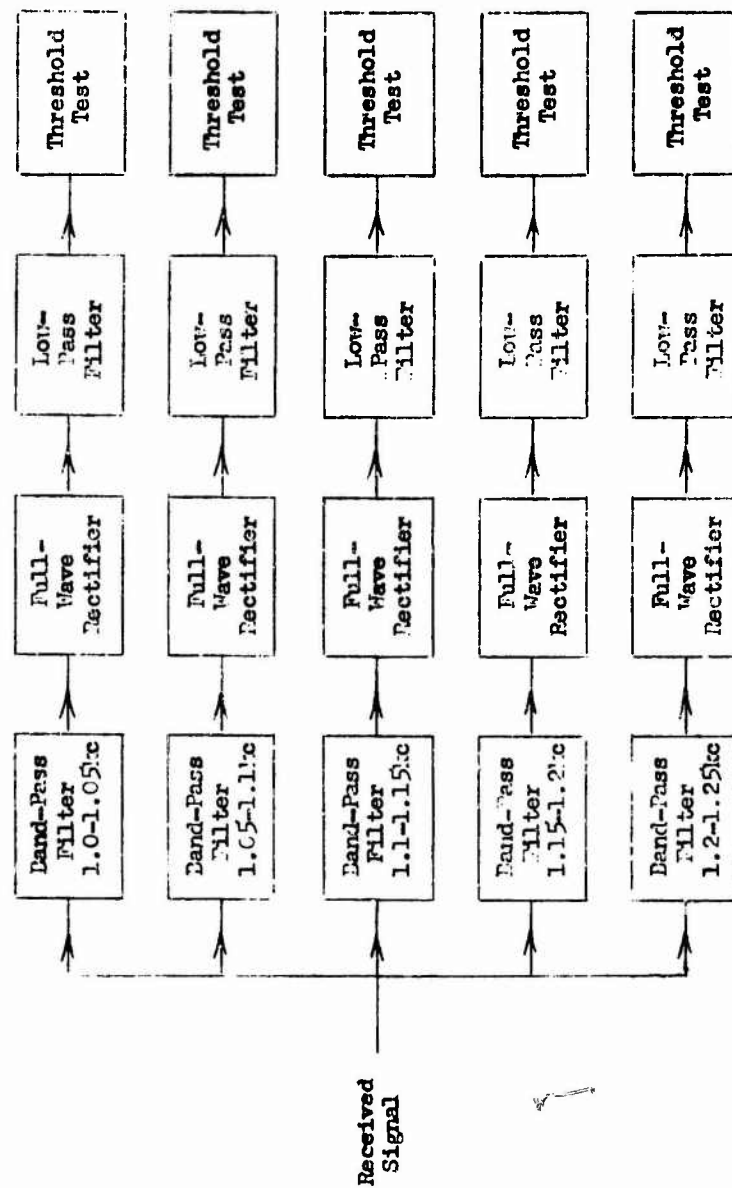


Fig. III.7. An Experimental Band-Splitting Detector

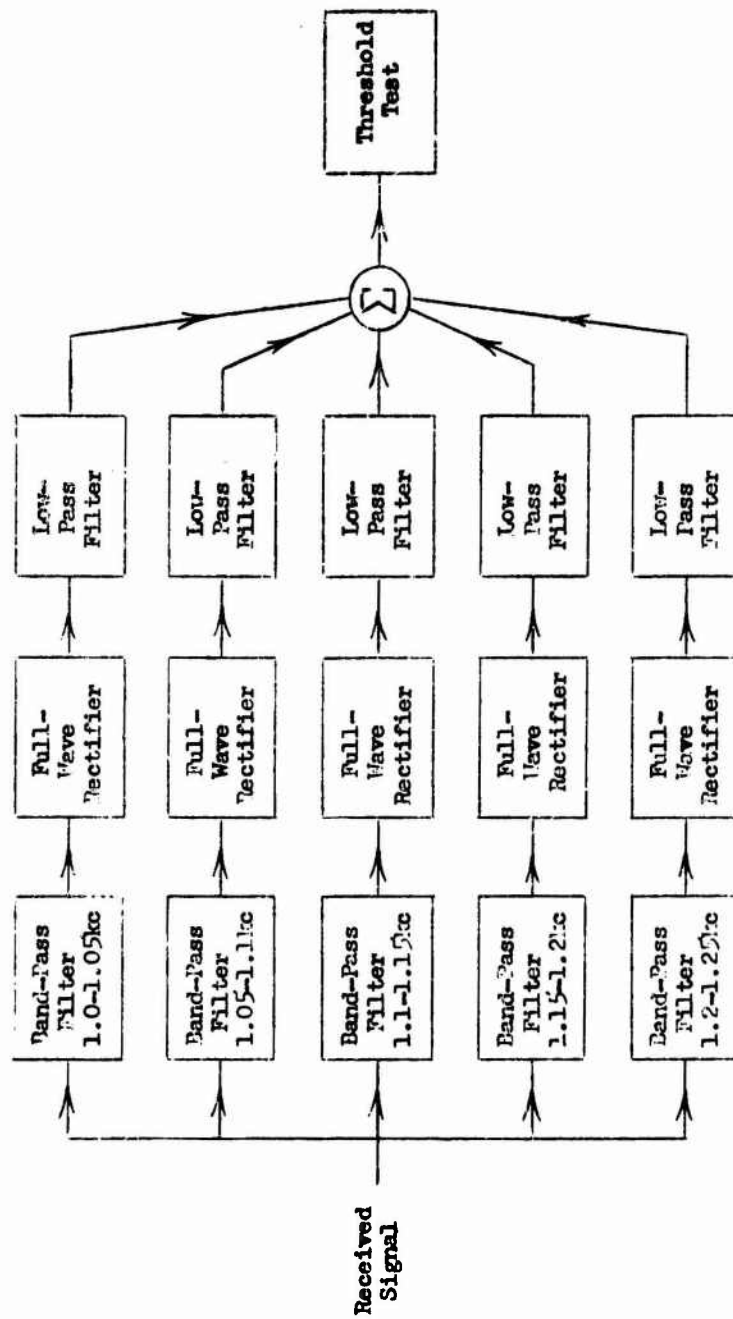


Fig. III.8. An Experimental Sum-and-Test Detector

with the detection of a coherent sinusoid of unknown frequency.

The sum-and-test detector effectively processes in toto the frequency band covered by the five pre-detection filters, since the enhancement in SNR provided by band splitting is offset by the summation of the five low-pass filter outputs.

These two detector structures were used to detect a sinusoid of unknown frequency in broadband gaussian noise.

The additive noise was generated by means of a standard CR noise source. Statistical measurements of the noise output indicated that the noise exhibited a gaussian distribution out to amplitudes equal to four times the standard deviation.

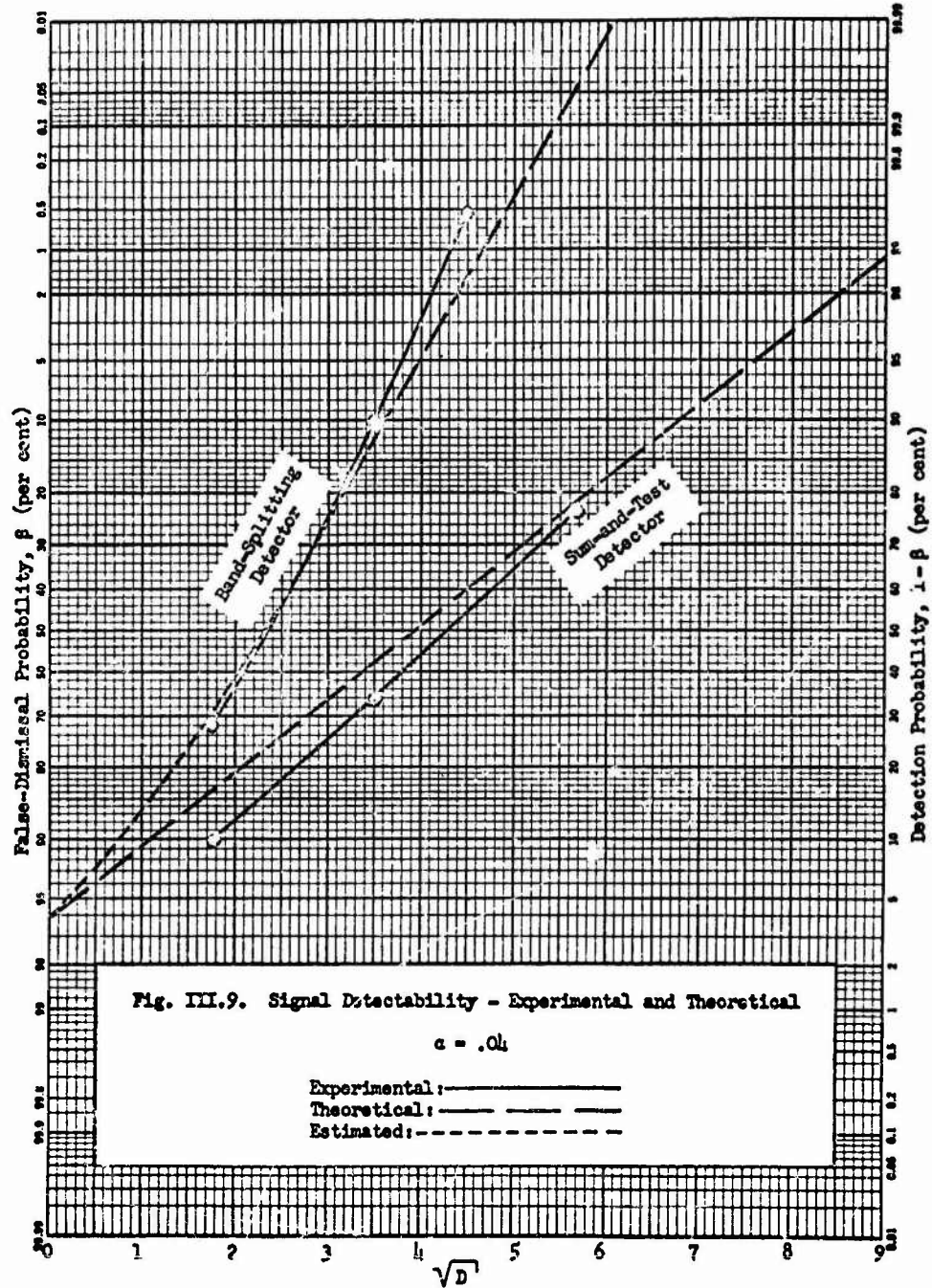
The detection of the sinusoid using the band-splitting detector is equivalent to the detection of any weak signal of the same power when the signal frequency is such that all the signal power appears in the pass band of one of the pre-detection filters. That is, only the average signal power is of consequence in determining the detectability. Thus the detection of the sinusoid with this detector configuration is approximately equivalent to the upper-bound situation analyzed in Section III.4, Article b, where non-overlapping pre-detection filters were considered and where the gaussian signal was assumed to be exactly aligned with the pass band of one of the filters.

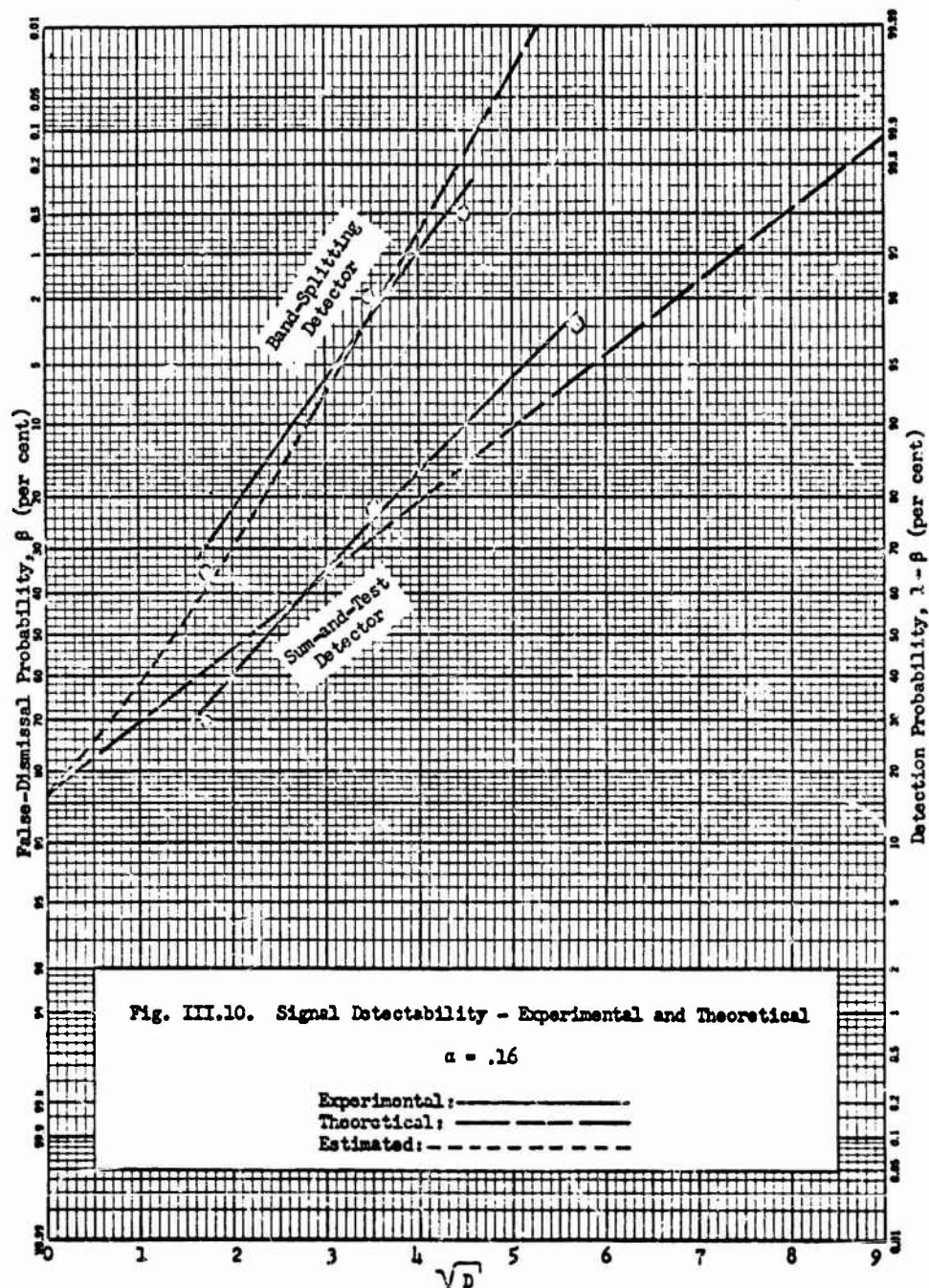
When the second detector configuration, the sum-and-test detector, is used, the performance should be comparable with a power detector processing the overall frequency band 1,000 - 1,250 cps to detect a weak signal in that band. This can be seen as follows: If each of the pre-detection filters had an ideal rectangular frequency response function and if each were followed by a squarer and then an ideal

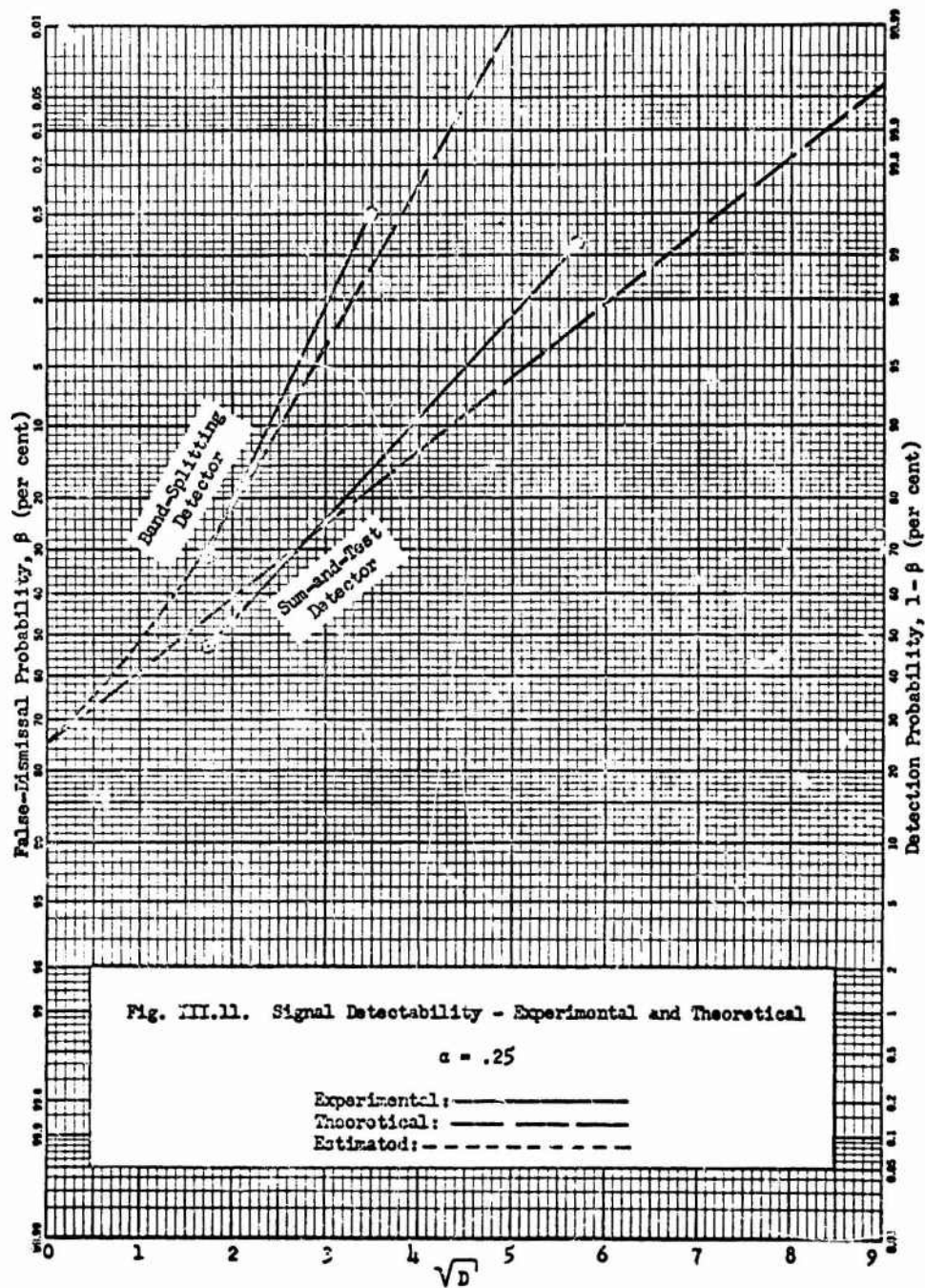
integrator, this detector would simply be measuring the energy in each of the five bands and then summing these energy measurements. Since this sum is equal to the total energy in the overall band, the operation of the detector would be equivalent to measuring this total energy directly. The sum-and-test detector which was actually built represents an approximation to this idealized detector.

Experimental data was obtained with the two detector structures described, giving signal detectability as a function of the pre-detection SNR and the integration time for several fixed values of the false alarm probability. A block diagram of the instrumentation used is shown in Appendix E.

The results are presented in Figs. III.9 through III.11. The acquisition of data was of necessity confined to a restricted range of error probabilities. Level drift in the high-gain d.c. amplifier made it difficult to run the large numbers of tests which would have been necessary in order to obtain reliable statistics at low error rates. Together with the experimental data are plotted pertinent curves obtained from the theoretical analysis of Section III.4. The data obtained with the band-splitting configuration are to be compared with the upper bound on detectability obtained in Section III.4, Article b, for the specific case $b = r = 5$. The data obtained with the sum-and-test configuration are to be compared with the theoretical detectability based upon the SNR in the overall frequency band being processed, that is detectability for the case $b = r = 1$. It is seen from the figures that the experimental results are in reasonably close agreement with the theoretical results. The







enhancement in detectability obtained with the band-splitting detector is clearly evidenced.

It is seen that the measured detectability curves are almost consistently steeper than the theoretical. This seems to be due to two factors: First, the electronic noise source used in these measurements produces noise with an amplitude distribution which is truncated at some finite amplitude. Thus the rare but intense noise peaks which would contribute to errors at low probability levels are simply not produced. Second, the level crossings counter does not respond to threshold crossings which are arbitrarily short in duration. That is to say, the instrumentation introduces additional post-detection smoothing.

CHAPTER IV

DETECTION OF A NARROWBAND GAUSSIAN SIGNAL
 OF UNKNOWN CENTER FREQUENCY - PART II
 STRONG SIGNALS

IV.1 Detection Analysis in the Strong-Signal Case

In Chapter III the pre-detection SNR R_g , defined in the narrow band B_g containing the signal spectrum was assumed to be much smaller than unity; in this chapter the assumption will be dropped. When R_g becomes on the order of or greater than unity, the analysis of Chapter III must be modified in two ways, one which affects the form of the optimum detector for short observation times and another which affects the signal detectability when the observation time is very long:

1) The signal detectability is always a monotone increasing function of the pre-detection SNR R_g and the time-bandwidth product $B_g T$. When R_g is small, as was assumed in Chapter III, $B_g T$ must of necessity be large in order that high detectability can be achieved. This requires that $B_g T$ be $\gg 1$, which implies that the observation time is many times longer than the correlation time of the narrowband signal. In such a situation the optimum detector can only perform energy measurements on the received signal, and the analysis of Chapter III is applicable. If, however,

R_S is made arbitrarily large, $B_S T$ is not necessarily required to be $\gg 1$ in order for high detectability to be obtained. If $B_S T$ is on the order of unity, then the signal is highly coherent over the observation interval $0, T$, and in view of this coherency the form of the optimum detector must be re-examined. It should be noted, however, that if $B_S T$ is made much larger than unity, the optimum detector will process the received signal in the purely incoherent fashion described in Chapter III, regardless of the magnitude of the pre-detection SNR R_S .

2) When the time-bandwidth product $B_S T$ is $\gg 1$, the signal to be detected must be regarded as completely incoherent. However when R_S is large, the variance of the test quantity $Q(f)$ given signal and noise cannot be accurately given by Eq. (III-47). Instead, the variance must be calculated using Eq. (III-42), which is repeated here as

$$\text{var}_{S+N}[Q(f)] = (1 + \sigma R_S)^2 R_S^2 B_S T, \quad 0 \leq \sigma \leq 1 \quad (\text{IV-1})$$

where σ is the fraction of the signal spectrum which appears in the pass band of the rectangular filter, centered at frequency f , used in generating $Q(f)$. (For example, when the signal spectrum is precisely aligned with the pass band of the filter, $\sigma = 1$.)

It can be seen by comparing Eqs. (IV-1) and (III-40) that the effect of high input SNR is to increase the variance of the signal-and-noise distribution of $Q(f)$. It can be shown that this growth in the variance of $Q(f)$ has the effect of making the gaussian

assumption for $Q(f)$ in the signal-and-noise situation inaccurate as R_S becomes $\gg 1$. For this reason an exact Chi-squared distribution for the test quantity will be used. It must also be noted that in the strong-signal case detectability cannot be calculated in terms of a detection index alone, but rather R_S and $B_S T$ must both be specified.

The case of short observation time, i.e., $B_S T \ll 1$, will be considered first.

IV.2 Detection for Short Observation Times ($B_S T \ll 1$)

a) Detector Structure

The signal to be detected has been described as having total average power $A^2/2$ in a rectangular spectrum of width B_S centered at some frequency f_c . The a.c.f. for this signal is given by

$$R_S(\tau) = \frac{A^2}{2} \text{sinc } B_S \tau \cos 2\pi f_c \tau \quad (\text{IV-2})$$

where

$$\text{sinc } x \triangleq \frac{\sin \pi x}{\pi x}$$

When the observation time T of the signal is long compared with the correlation time, that is, when $B_S T \gg 1$, then the signal may be accurately represented by complex samples taken at a rate B_S , as was discussed in Section III.3. That discussion showed that under the assumption of long observation time, the signal covariance matrix \underline{P} could be written as a diagonal matrix. However, when $B_S T$ is on the order of unity, the narrowband signal can no longer be accurately described by samples taken at the rate B_S , and the

signal must instead be sampled at a much higher rate.

It has been assumed that the background noise is gaussian with a flat spectrum extending up to frequencies much higher than the highest possible signal frequency. Let it be assumed that the noise spectrum extends from zero frequency and is sharply cut off at a frequency W cps, which is chosen so that

$$2WT \gg 1$$

The signal may now be represented by real time samples taken at a rate $2W$, so that samples of the noise are independent. From Eq. (IV-2) the sampled a.c.f. of the desired signal is now

$$R_S(t_1 - t_j) = \frac{A^2}{2} \text{sinc } B_S(t_1 - t_j) \cos 2\pi f(t_1 - t_j) \quad (\text{IV-3})$$

For very short observation times, when $B_S T \ll 1$, then the envelope of $R_S(\tau)$ is approximately constant and

$$R_S(t_1 - t_j) \approx \frac{A^2}{2} \cos 2\pi f_c(t_1 - t_j) \quad , B_S T \ll 1 \quad (\text{IV-4})$$

which is the a.c.f. for a sinusoid of frequency f_c with a mean-squared value of $A^2/2$, or equivalently, an r.m.s. amplitude A . Since the signal $s(t)$ is a gaussian random process, the moments of $s(t)$ can be written in general as

$$\langle s^p(t) \rangle = \begin{cases} 1 \cdot 3 \cdot 5 \dots (p-1) \left(\frac{A^2}{2} \right)^{p/2} & , p \text{ even} \\ 0 & , p \text{ odd} \end{cases} \quad (\text{IV-5})$$

It will now be shown that for $B_g T \ll 1$, $s(t)$ can be represented by a sinusoid of unknown phase ϕ and unknown amplitude a . The phase, considered over the ensemble of all observations of length T , has the p.d.f.

$$f(\phi) = \begin{cases} \frac{1}{2\pi} & 0 \leq \phi \leq 2\pi \\ 0 & \text{elsewhere} \end{cases} \quad (\text{IV-6})$$

The amplitude of the sinusoid is constant over the duration of each observation interval (as is the phase), and its p.d.f. is

$$f(a) = \begin{cases} \frac{2a}{A^2} \exp\left(-\frac{a^2}{A^2}\right) & a \geq 0 \\ 0 & a < 0 \end{cases} \quad (\text{IV-7})$$

If this representation is valid, then all the moments of this sinusoidal signal should agree with Eq. (IV-5). The sinusoid is written as

$$s(t) = a \cos(2\pi f_c t - \phi) \quad (\text{IV-8})$$

The variance is

$$\begin{aligned} \langle s^2(t) \rangle_{\phi, a} &= \left\langle \frac{a^2}{2} [1 + \cos 2(2\pi f_c t - \phi)] \right\rangle_{\phi, a} \\ &= \frac{1}{2} \langle a^2 \rangle \\ &= \int_0^\infty da \frac{a^3}{A^2} \exp\left(-\frac{a^2}{A^2}\right) \\ &= \frac{A^2}{2} \end{aligned} \quad (\text{IV-9})$$

Similarly, $\langle s^4(t) \rangle_{\phi, a} = 3 \left(\frac{A^2}{2} \right)^2$ (IV-10)

$$\langle s^6(t) \rangle_{\phi, a} = 15 \left(\frac{A^2}{2} \right)^3 \quad (\text{IV-11})$$

and in general

$$\langle s^p(t) \rangle_{\phi, a} = \begin{cases} 1 \cdot 3 \cdot 5 \dots (p-1) \left(\frac{A^2}{2} \right)^{p/2} & , p \text{ even} \\ 0 & , p \text{ odd} \end{cases} \quad (\text{IV-12})$$

which agrees with Eq. (IV-5). According to a theorem regarding moments,[†] if $v_p, p = 0, 1, 2, \dots$, are the moments (assumed finite) of a probability distribution function, and if the series

$$\sum_{p=0}^{\infty} \frac{v_p}{p!} t^p$$

is absolutely convergent for some $t > 0$, then the stated probability distribution function is uniquely defined by the moments $v_p, p = 0, 1, 2, \dots$. Letting

$$v_p = \langle s^p(t) \rangle_{\phi, a} \quad (\text{IV-13})$$

in the above summation, and using Eq. (IV-12), one may easily verify that

$$\sum_{p=0}^{\infty} \frac{\langle s^p(t) \rangle_{\phi, a}}{p!} t^p = \exp \left(\frac{A^2}{4} t^2 \right) \quad (\text{IV-14})$$

p even

[†] See Cramer (I, pp. 176-177).

for any finite value of t . Thus the series converges, and the moments given by Eq. (IV-5) and (IV-12) must define the same p.d.f.. Therefore, when the observation time T is much shorter than the correlation time of the narrowband signal, the signal is equivalent to a sinusoid of unknown phase with a random amplitude given by a Rayleigh p.d.f.. It should also be noted that this representation would be exact for any observation time T if the signal bandwidth B_s were allowed to go to zero, since the signal correlation time would then be infinite.

The sinusoidal signal model as described above will now be used to analyze the form of the optimum detector and the signal detectability when the observation time is short. The argument put forth in Section III.2 to explain the asymptotic optimality of a band-sweeping detector is equally valid for any narrowband signal of unknown frequency. The argument relies upon the fact that as the post-detection SNR becomes very large, then when a signal is present the LR, generated as a function of frequency, will have a large peak in the vicinity of the actual signal frequency and will lie near some low average value at other points in the band of signal frequency uncertainty. It then follows that a test on the peak value of the LR, or on the peak value of the logarithm of the LR, becomes optimum as the post-detection SNR becomes very large. The argument can be applied as well to the detection of a sinusoid of unknown phase, amplitude and frequency as to the detection of a narrowband gaussian signal of unknown center frequency.

Thus the band-sweeping detector will again be taken as a close approximation to the optimum detector, and it now becomes necessary

to find the form of the processor which will generate $\log L(\underline{v}/f_c)$, that is, the LR detector for a sinusoidal signal of known frequency but unknown phase and amplitude.

The problem of detecting a sinusoid of unknown phase has been treated in the literature and the analysis leads to the familiar $\log I_0$ detector structure[†]. When written in terms of the variables being used in the present work, this result gives

$$L(\underline{v}/f_c, a) = \exp \left(- \frac{a^2}{4N_0 W} \right) I_0 \left(\sqrt{\underline{v}' \underline{G} \underline{v}} \right) \quad (\text{IV-15})$$

or

$$\log L(\underline{v}/f_c, a) = - \frac{a^2}{4N_0 W} n + \log I_0 \left(\sqrt{\underline{v}' \underline{G} \underline{v}} \right) \quad (\text{IV-16})$$

where

$$\underline{G}_c = \left\{ \frac{a^2}{N_0 2W^2} \cos 2\pi f_c (t_i - t_j) \right\} \quad (\text{IV-17})$$

and

$$n = 2WT \quad (\text{IV-18})$$

and W is the cutoff frequency of the noise spectrum.

In an earlier discussion[†] it was pointed out that the form of the optimum detector for the detection of such a signal does

[†] See earlier discussion in Section I.2, Article c, and the pertinent references.

^{††} From the point of view of hypothesis testing, a threshold test on the right side of Eq. (IV-16) is a "uniformly most powerful test at a fixed level" with respect to all values of the amplitude a . See Lehmann (1) for discussions of uniformly most powerful tests.

not depend upon the signal amplitude a provided only that a has a one-sided p.d.f. . Thus the detector structure prescribed by Eq. (IV-16) will provide maximum probability of detection at any fixed level of false alarm probability . The particular value of the probability of detection at any given false alarm probability will of course depend upon the statistics of a . Thus if both the false alarm probability and the detection probability are to be considered in setting the threshold, the statistics of the signal amplitude would influence the choice of a threshold setting.

With the above discussion in mind, it can be seen that since I_0 is monotone, any monotone function of $\underline{v}' \underline{G}_c \underline{v}$ will serve equally well as a test quantity in this case of unknown phase and amplitude. It will be convenient in this work to use as a test quantity

$$q(f) \triangleq \underline{v}' \underline{G}_c \underline{v} \quad (\text{IV-19})^{\dagger\dagger}$$

where

$$\underline{G}_c \triangleq \left\{ \frac{A^2}{2N_0^2 W^2} \cos 2\pi f_c(t_1 - t_j) \right\} \quad (\text{IV-20})$$

Thus the operation to be performed on the received signal is

[†] See the previous footnote.

^{††} Strictly, this test quantity is a function of the given signal center frequency f_c and thus should be written as $q(f_c)$. However, for simplicity, $q(f)$ will be used.

$$\begin{aligned}
 q(f) &= \frac{A^2}{2N_0 2W^2} \sum_i \sum_j v_i v_j \cos 2\pi f_c (t_i - t_j) \\
 &= \frac{A^2}{2N_0 2W^2} \left[\sum_i \sum_j v_i v_j \cos 2\pi f_c t_i \cos 2\pi f_c t_j \right. \\
 &\quad \left. + \sum_i \sum_j v_i v_j \sin 2\pi f_c t_i \sin 2\pi f_c t_j \right] \\
 &= \frac{A^2}{2N_0 2W^2} \left[\left(\sum_i v_i \cos 2\pi f_c t_i \right)^2 + \left(\sum_i v_i \sin 2\pi f_c t_i \right)^2 \right] \quad (\text{IV-21})
 \end{aligned}$$

where all the summations are taken from 1 to n, the total number of time samples. Sampling relationships may be used to approximate the summations in Eq. (IV-21) by integrals:

$$\begin{aligned}
 q(f) &\approx \frac{A^2}{2N_0 2W^2} \left[\left(2W \int_0^T dt v(t) \cos 2\pi f_c t \right)^2 + \left(2W \int_0^T dt v(t) \sin 2\pi f_c t \right)^2 \right] \\
 q(f) &\approx \frac{2A^2}{N_0} \left[\left(\int_0^T dt v(t) \cos 2\pi f_c t \right)^2 + \left(\int_0^T dt v(t) \sin 2\pi f_c t \right)^2 \right] \quad (\text{IV-22})
 \end{aligned}$$

Thus it is seen from Eq. (IV-22) that the optimum detector processes the received signal $v(t)$ at each possible value of the signal center frequency by correlating $v(t)$ with the quadrature components of the desired signal at that frequency, squaring and then summing the two squared outputs.

This result has followed from the assumption of short observation time ($B_g \ll 1$) made in paragraph 1) on page 106, and indicates that under such an assumption the operation of the optimum detector on the received signal is quite different from the operation required when the observation time is long [Compare Eq. (IV-22) with Eq. (III.23)]. Summarizing briefly, when the observation time is long compared with the correlation time of the narrowband signal, the detector can only measure total received power in each possible narrow band of width B_g . However, when the observation time is short compared with the signal correlation time, the phase of the signal, though unknown, is essentially constant over the observation period and thus a form of correlation detection is to be employed. A complete analysis of the optimum detector in the strong-signal situation then requires analysis of the correlation detector for $B_g T \ll 1$ and analysis of the power detector for $B_g T \gg 1$. In the region where $B_g T \approx 1$, a rigorous analysis of the optimum detection problem in the strong-signal case, without simplifying assumptions regarding the duration of the observation interval, is required. Such an analysis however is outside the scope of this investigation. (Further comments in this regard will be made in the concluding chapter.) Rather, signal detectability in this region will be interpolated from the results which can be obtained analytically for $B_g T \ll 1$ and $B_g T \gg 1$.

b) Signal Detectability

It has been argued earlier that the optimum detector becomes a band-sweeping detector as the post-detection SNR is made large. If $B_S T$ is $\ll 1$ in regions of high output SNR, then the band-sweeping detector must generate the test quantity given by Eq.(IV-22) as a continuous function of center frequency f_c in the overall uncertainty band B . If the test quantity exceeds a preset threshold at any frequency f_c in the band, the decision is made that a signal is present.

A practical approximate form of the optimum detector would consist of a discrete set of correlator pairs, analogous to the bank of band-splitting filters analyzed in Section III.4. Again it is of interest to know how many such correlator pairs are required in an uncertainty band of given width to achieve detectability close to the optimum.

In order to investigate the performance of a given bank of correlator pairs, the joint p.d.f.'s relating test quantities $q(f)$ at different values of the frequency f_c are required. For convenience let the correlator outputs in Eq. (IV-22), generated at a particular frequency value $f_c = f_1$, be denoted by

$$x_{c1} = \int_0^T dt v(t) \cos 2\pi f_1 t \quad (\text{IV-23})$$

$$x_{s1} = \int_0^T v(t) \sin 2\pi f_1 t \quad (\text{IV-24})$$

and let

$$\psi_1^2 = x_{c1}^2 + x_{s1}^2 \quad (\text{IV-25})$$

It is clear that a threshold test on $q(f_1)$ is equivalent to a test on ψ_1^2 or even on ψ_1 . Consider then the joint p.d.f. for ψ_1 and ψ_2 , quantities generated at two different values of frequency f_1 and f_2 . Since $v(t)$ is a sample function of a gaussian random process, x_{c1} and x_{s1} are gaussian random variables, being generated by linear operations on $v(t)$ as seen in Eqs. (IV-23) and (IV-24). Thus a joint p.d.f. can easily be written for the four variables $x_{c1}, x_{s1}, x_{c2}, x_{s2}$ and from this the joint p.d.f. for ψ_1 and ψ_2 can be obtained. The result, adapted from Rice[†], is

$$f(\psi_1, \psi_2) = \frac{\psi_1 \psi_2}{M} I_0 \left[\frac{\psi_1 \psi_2}{M} (\mu_{13}^2 + \mu_{14}^2)^{1/2} \right] \exp \left[-\frac{\mu_{11}}{2M} (\psi_1^2 + \psi_2^2) \right]$$

(IV-26)

where

$$\mu_{11} = \langle x_{c1}^2 \rangle = \langle x_{s1}^2 \rangle = \langle x_{c2}^2 \rangle = \langle x_{s2}^2 \rangle \quad (\text{IV-27})$$

$$\mu_{13} = \langle x_{c1} x_{c2} \rangle = \langle x_{s1} x_{s2} \rangle \quad (\text{IV-28})$$

[†] See Rice (I, Sec. 3.7).

$$\mu_{14} = \langle x_{c1} x_{s2} \rangle = - \langle x_{s1} x_{c2} \rangle \quad (\text{IV-29})$$

and

$$M = \mu_{11}^2 - \mu_{13}^2 - \mu_{14}^2 \quad (\text{IV-30})$$

Thus ψ_1 and ψ_2 are seen to be correlated random variables, their correlation being accounted for in Eq. (IV-26) by μ_{13} and μ_{14} within the argument of the modified Bessel function. Consider for the sake of discussion a simple case in which detection is to be carried out using a bank of correlator pairs, and the correlator frequencies are spaced at intervals such that quantities ψ_1 and ψ_j at adjacent correlator frequencies are correlated but correlations between more remotely separated correlators may be ignored. (This is similar to the situation, described on page 81, involving pair-wise-overlapping band-splitting filters.) In such a case, the calculation of false-alarm probability will involve the evaluation of integrals of the form

$$I = \int_{-\infty}^{k'} d\psi_1 \int_{-\infty}^{k'} d\psi_2 f(\psi_1, \psi_2) \quad (\text{IV-31})$$

where $f(\psi_1, \psi_2)$ is given by Eq. (IV-26). Such integrals with respect to this p.d.f. cannot be carried out in closed form but would have to be evaluated numerically. Thus even a simple case such as pair-wise dependence between test quantities cannot in general be easily handled by analytical methods. If however, both the covariances μ_{13} and μ_{14} are equal to zero, then ψ_1

and ψ_2 are independent and the p.d.f. in Eq. (IV-26) is greatly simplified and integrals of the form of Eq. (IV-31) may be readily evaluated. Thus μ_{13} and μ_{14} will be examined in the case of noise only.

It has been assumed that the background noise is gaussian with a flat spectral density extending from zero frequency up to a cutoff frequency W cps. Thus if W is much higher than the highest possible signal frequency, the a.c.f. for the noise may be written as

$$\langle v(t) v(s) \rangle_N = \frac{N_0}{2} \delta(t-s) \quad (\text{IV-32})$$

where $\delta(x)$ is the Dirac delta function. From Eqs. (IV-23) and (IV-28) the covariance μ_{13} is obtained for the noise-only case as

$$\begin{aligned} \mu_{13} &= \left\langle \int_0^T dt v(t) \cos 2\pi f_1 t \int_0^T ds v(s) \cos 2\pi f_2 s \right\rangle_N \\ &= \int_0^T dt \int_0^T ds \langle v(t) v(s) \rangle_N \cos 2\pi f_1 t \cos 2\pi f_2 s \\ &= \frac{N_0}{2} \int_0^T dt \int_0^T ds \delta(t-s) \cos 2\pi f_1 t \cos 2\pi f_2 s \\ &= \frac{N_0}{2} \int_0^T dt \cos 2\pi f_1 t \cos 2\pi f_2 t \end{aligned}$$

(Continued on next page)

$$\begin{aligned}
&= \frac{N_0}{4} \int_0^T dt [\cos 2\pi(f_1 - f_2)t + \cos 2\pi(f_1 + f_2)t] \\
&= \frac{N_0}{4} \left[\frac{\sin 2\pi(f_1 - f_2)T}{2\pi(f_1 - f_2)} + \frac{\sin 2\pi(f_1 + f_2)T}{2\pi(f_1 + f_2)} \right] \quad (IV-33)
\end{aligned}$$

$$\approx \frac{N_0}{4} \frac{\sin 2\pi(f_1 - f_2)T}{2\pi(f_1 - f_2)} \quad (IV-34)$$

$$= \frac{N_0 T}{4} \frac{\sin 2\pi(f_1 - f_2)T}{2\pi(f_1 - f_2)T} \quad (IV-35)$$

The second term in the right side of Eq. (IV-33) is dropped since $2(f_1 + f_2) \gg 1$.

Similarly, from Eqs. (IV-23), (IV-24) and (IV-29)

$$\mu_{14} \approx \frac{N_0}{4} \frac{1 - \cos 2\pi(f_1 - f_2)T}{2\pi(f_1 - f_2)T} \quad (IV-36)$$

From Eqs. (IV-34) and (IV-36),

$$\begin{aligned}
\mu_{13}^2 + \mu_{14}^2 &= \frac{N_0^2 T^2}{16} \frac{\sin^2 2\pi(f_1 - f_2)T + 1 - 2\pi \cos 2\pi(f_1 - f_2)T + \cos^2 2\pi(f_1 - f_2)T}{4\pi^2(f_1 - f_2)^2 T^2} \\
&= \frac{N_0^2 T^2}{16} \frac{2 - 2 \cos 2\pi(f_1 - f_2)T}{4\pi^2(f_1 - f_2)^2 T^2} \\
&= \frac{N_0^2 T^2}{16} \frac{\sin^2 \pi(f_1 - f_2)T}{\pi^2(f_1 - f_2)^2 T^2}
\end{aligned}$$

$$\boxed{\mu_{13}^2 + \mu_{14}^2 = \frac{N_0^2 T^2}{16} \operatorname{sinc}^2(f_1 - f_2)T} \quad (IV-37)$$

Therefore it is seen from Eq. (IV-37) that $\mu_{13}^2 + \mu_{14}^2 = 0$ when the frequency separation $f_1 - f_2$ is equal to non-zero integral multiples of $\frac{1}{T}$. (The general form of $\mu_{13}^2 + \mu_{14}^2$ has been derived for completeness, but inspection of Eqs. (IV-35) and (IV-36) shows that μ_{13} and μ_{14} each equal zero with the stated frequency separation.) When these zeroes occur, then since $I_1(0) = 1$, the p.d.f. in Eq. (IV-26) becomes

$$\begin{aligned} f(\psi_1, \psi_2) &= \frac{\psi_1 \psi_2}{\mu_{11}^2} \exp \left[-\frac{1}{2\mu_{11}} (\psi_1^2 + \psi_2^2) \right] \\ &= \frac{\psi_1}{\mu_{11}} \exp \left(-\frac{1}{2\mu_{11}} \psi_1^2 \right) \frac{\psi_2}{\mu_{11}} \exp \left(-\frac{1}{2\mu_{11}} \psi_2^2 \right) \end{aligned}$$

(IV-38)

Thus ψ_1 and ψ_2 become statistically independent and Eq. (IV-38) is seen to be the product of two Rayleigh p.d.f.'s. The smallest separation between correlator frequencies for which independence occurs is $f_1 - f_2 = \frac{1}{T}$; therefore the densest spacing of correlators in the band of signal frequency uncertainty which can be conveniently analyzed is that in which the correlator frequencies are set at intervals of $\frac{1}{T}$. If closer correlator spacings were to be considered, then $\mu_{13}^2 + \mu_{14}^2$ as given by Eq. (IV-37) would not equal zero and the p.d.f. in Eq. (IV-26) would have to be used in its general form. Numerical evaluation of integrals of the form of Eq. (IV-31) would then be required in the calculation of error probabilities. For the purposes of this investigation then,

only one detector structure will be considered in evaluating signal detectability for $B_s T \ll 1$, a structure consisting of a bank of correlator pairs whose frequencies are spaced at uniform intervals of $\frac{1}{T}$ in the overall band of frequency uncertainty. The detector will therefore employ BT correlator pairs. This detector structure will be used to obtain upper and lower bounds on signal detectability for $B_s T \ll 1$. The conditional false-alarm probability will first be calculated.

The test quantity generated at a general correlator frequency f_1 is, from Eq. (IV-22),

$$q(f_1) = \frac{2A^2}{B_o^2} \left[\left(\int_0^T dt v(t) \cos 2\pi f_1 t \right)^2 + \left(\int_0^T dt v(t) \sin 2\pi f_1 t \right)^2 \right] \quad (\text{IV-39})$$

The conditional false-alarm probability is the probability that at least one quantity $q(f_1)$ exceeds its threshold, given that only noise is present. If the correlator frequencies are chosen at intervals equal to $\frac{1}{T}$, then from the previous discussion the quantities $q_1 \triangleq q(f_1)$ will be independent random variables, and the conditional false-alarm probability may be written as

$$\begin{aligned} \alpha &= 1 - \prod_{i=1}^{BT} P[q_i < k' / \text{noise only}] \\ &= 1 - [1 - \alpha_1]^{BT} \end{aligned} \quad (\text{IV-40})$$

where

$$\alpha_i = P[q_i > k' / \text{noise only}], i = 1, 2, \dots, BT \quad (\text{IV-41})$$

The p.d.f. for q_i under the assumption of noise only is obtained from the p.d.f. for ψ_i ,

$$f(\psi_i/0) = \begin{cases} \frac{\psi_i}{\nu_{11}} \exp\left(-\frac{1}{2\nu_{11}} \psi_i^2\right) & \psi_i \geq 0 \\ 0 & \psi_i < 0 \end{cases} \quad (\text{IV-42})$$

which is obtained from Eq. (IV-23), (IV-24), (IV-25) and (IV-39) one sees that

$$q_i = \frac{2A^2}{N_0^2} \psi_i^2 \quad (\text{IV-43})$$

and thus one may write the p.d.f. of q_i as

$$f(y/0) = \begin{cases} \frac{N_0^2}{4\nu_{11}A^2} \exp\left(-\frac{N_0^2}{4\nu_{11}A^2} y\right), & y \geq 0 \\ 0 & , y \leq 0 \end{cases} \quad (\text{IV-44})$$

where the variable y stands for q_i .

The variance ν_{11} is calculated for the noise-only case as

$$\begin{aligned}
\mu_{11} &= \left\langle \int_0^T dt v(t) \cos 2\pi f_1 t \int_0^T ds v(s) \cos 2\pi f_1 s \right\rangle_N \\
&= \int_0^T dt \int_0^T ds \left\langle v(t) v(s) \right\rangle_N \cos 2\pi f_1 t \cos 2\pi f_1 s \\
&= \frac{N_0}{2} \int_0^T dt \int_0^T ds \delta(t-s) \cos 2\pi f_1 t \cos 2\pi f_1 s \\
&= \frac{N_0}{2} \int_0^T dt \cos^2 2\pi f_1 t \\
&\approx \frac{N_0}{4} T \quad (\text{IV-45})
\end{aligned}$$

The p.d.f. for q_1 thus becomes

$$f(y/Q) = \begin{cases} \frac{N_0}{A^2 T} \exp \left(- \frac{N_0}{A^2 T} y \right) & , y \geq 0 \\ 0 & , y \leq 0 \end{cases} \quad (\text{IV-46})$$

A detection index d' will now be defined as

$$d' = \frac{A^2}{2N_0} T \quad (\text{IV-47})^\dagger$$

[†] This detection index is seen to be analogous to the detection index d defined in Chapter II for the case of a coherent sinusoid; see Eq. (II-24).

The detection index can also be written as

$$\begin{aligned} d' &= \frac{A^2}{2N_0 B B} B S^T \\ &= R_S B S^T \end{aligned} \quad (\text{IV-48})$$

Thus d' may also be regarded as a post-detection SNR, equal to the input or pre-detection SNR times the normalized observation time, and the p.d.f. for q_1 can be written simply as

$$f(y/Q) = \frac{1}{2d'} \exp\left(-\frac{1}{2d'} y\right), \quad y \geq 0 \quad (\text{IV-49})$$

The conditional probability α_1 that q_1 exceeds its threshold when only noise is present is calculated as

$$\begin{aligned} \alpha_1 &= \int_{k'}^{\infty} dy f(y/Q) = \frac{1}{2d'} \int_{k'}^{\infty} dy \exp\left(-\frac{1}{2d'} y\right) \\ &= -\exp\left(-\frac{1}{2d'} y\right) \Big|_{k'}^{\infty} \\ &= \exp\left(-\frac{1}{2d'} k'\right) \end{aligned} \quad (\text{IV-50})$$

Therefore the conditional false-alarm probability becomes, from Eq. (IV-40),

$$\alpha = 1 - \left[1 - \exp\left(-\frac{1}{2d'} k'\right)\right]^{B T} \quad (\text{IV-51})$$

If

$$BT \exp \left(- \frac{1}{2d'} k' \right) \ll 1 ,$$

then the false-alarm probability is approximately

$$\alpha \approx BT \exp \left(- \frac{1}{2d'} k' \right) \quad (\text{IV-52})$$

Whenever one or more of the test quantities q_i exceeds the preset threshold k' , the decision is made that the desired signal is present. Therefore the conditional probability of false dismissal is

$$\beta = P [\text{all } q_i < k' / \text{signal and noise}] , i = 1, 2, \dots, BT$$

(IV-53)

When a signal is present in the received data, the false-dismissal probability, or equivalently the detection probability, depends upon the actual frequency location of the signal.

Upper Bound on Detectability

Two bounds on conditional detection probability will therefore be considered. An upper bound on signal detectability is given by the situation in which a signal is present and its frequency happens to coincide with one of the BT correlator frequencies. The work leading to Eq. (IV-38) showed that when the correlator frequencies are chosen at uniform intervals equal to $\frac{1}{T}$ and when noise only is present, then the quantities $\psi_i, \psi_j, i \neq j$ are again statistically independent, a fact which greatly simplifies the computation of signal detectability.

Since, with signal and noise present, the received signal $v(t)$ is again a gaussian random process, the quantities x_{c1} and x_{s1} in Eqs. (IV-23) and (IV-24) are again gaussian random variables and therefore Eq. (IV-26) still holds as the joint p.d.f. for ψ_1 and ψ_2 , test quantities generated at frequencies f_1 and f_2 respectively. The covariances μ_{13} and μ_{14} are now required for the signal-and-noise case. The covariance μ_{13} is

$$\begin{aligned}\mu_{13} &= \langle x_{c1} x_{c2} \rangle_{S+N} \\ &= \left\langle \int_0^T dt v(t) \cos 2\pi f_1 t \int_0^T ds v(s) \cos 2\pi f_2 s \right\rangle_{S+N} \\ &= \int_0^T dt \int_0^T ds \langle v(t) v(s) \rangle_{S+N} \cos 2\pi f_1 t \cos 2\pi f_2 s\end{aligned}$$

(IV-54)

Since the signal and noise processes are assumed to be independent,

$$\text{and } \langle v(t) \rangle_S = \langle v(t) \rangle_N = 0,$$

$$\mu_{13} = \int_0^T dt \int_0^T ds \left[\langle v(t) v(s) \rangle_S + \langle v(t) v(s) \rangle_N \right] \cos 2\pi f_1 t \cos 2\pi f_2 s$$

(IV-55)

But it can be seen from Eq. (IV-35) that

$$\int_0^T dt \int_0^T ds \langle v(t) v(s) \rangle_N \cos 2\pi f_1 t \cos 2\pi f_2 s \approx 0$$

when

$$f_1 - f_2 = \pm n \frac{1}{T}, \quad n = 1, 2, \dots$$

Therefore

$$\mu_{13} \approx \int_0^T dt \int_0^T ds \langle v(t) v(s) \rangle_S \cos 2\pi f_1 t \cos 2\pi f_2 s \quad (\text{IV-56})$$

The signal has a bandwidth B_S centered at some frequency f_c .

For the moment it will be assumed that f_c may be any frequency within the prescribed processing band. Thus

$$\mu_{13} \approx \int_0^T dt \int_0^T ds \frac{A^2}{2} \text{sinc } B_S(t - s) \cos 2\pi f_c(t - s) \cos 2\pi f_1 t \cos 2\pi f_2 s \quad (\text{IV-57})$$

Under the assumption of short observation time, i.e. $B_S T \ll 1$,

being made here, Eq. (IV-57) may be written approximately as

[See Eq. (IV-4)]

$$\begin{aligned}
u_{13} &\approx \frac{A^2}{2} \int_0^T dt \int_0^T ds \cos 2\pi f_c(t-s) \cos 2\pi f_1 t \cos 2\pi f_2 s \\
&= \frac{A^2}{8} \int_0^T dt \int_0^T ds \left\{ [\cos 2\pi(f_c+f_1)t + \cos 2\pi(f_c-f_1)t] [\cos 2\pi(f_c+f_2)s + \cos 2\pi(f_c-f_2)s] \right. \\
&\quad \left. + [\sin 2\pi(f_c+f_1)t + \sin 2\pi(f_c-f_1)t] [\sin 2\pi(f_c+f_2)s + \sin 2\pi(f_c-f_2)s] \right\} \\
&= \frac{A^2}{8} \left\{ \left[\frac{\sin 2\pi(f_c+f_1)T}{2\pi(f_c+f_1)} + \frac{\sin 2\pi(f_c-f_1)T}{2\pi(f_c-f_1)} \right] \left[\frac{\sin 2\pi(f_c+f_2)T}{2\pi(f_c+f_2)} + \frac{\sin 2\pi(f_c-f_2)T}{2\pi(f_c-f_2)} \right] \right. \\
&\quad \left. + \left[\frac{1-\cos 2\pi(f_c+f_1)T}{2\pi(f_c+f_1)} + \frac{1-\cos 2\pi(f_c-f_1)T}{2\pi(f_c-f_1)} \right] \left[\frac{1-\cos 2\pi(f_c+f_2)T}{2\pi(f_c+f_2)} + \frac{1-\cos 2\pi(f_c-f_2)T}{2\pi(f_c-f_2)} \right] \right\} \\
&\quad \quad \quad (IV-58)
\end{aligned}$$

$$\begin{aligned}
&\approx \frac{A^2}{8} \left[\frac{\sin 2\pi(f_c-f_1)T}{2\pi(f_c-f_1)} \cdot \frac{\sin 2\pi(f_c-f_2)T}{2\pi(f_c-f_2)} + \frac{1-\cos 2\pi(f_c-f_1)T}{2\pi(f_c-f_1)} \cdot \frac{1-\cos 2\pi(f_c-f_2)T}{2\pi(f_c-f_2)} \right] \\
&\quad \quad \quad (IV-59)
\end{aligned}$$

The approximation embodied in Eq. (IV-59) follows from the fact that the first term in each of the four sets of brackets in Eq. (IV-58) may be neglected under the assumption that $2(f_c+f_1) \gg 1$ and $2(f_c+f_2) \gg 1$.

It can be seen that if $f_c - f_1$ and $f_c - f_2$ are different integral multiples of $\frac{1}{T}$, Eq. (IV-59) will yield zero. Therefore if the correlator frequencies are spaced at intervals equal to $\frac{1}{T}$ and if the signal frequency f_c coincides with any one of these correlator frequencies, then the covariance μ_{13} relating x_{c1} at correlator frequency f_1 and x_{c2} at correlator frequency f_2 is equal to zero. Similarly it can be shown that μ_{14} is

$$\begin{aligned}\mu_{14} &= \left\langle x_{c1} x_{s2} \right\rangle_{S+N} \\ &= \frac{A^2}{8} \left[-\frac{\sin 2\pi(f_c - f_1)T}{2\pi(f_c - f_1)} \cdot \frac{1 - \cos 2\pi(f_c - f_2)T}{2\pi(f_c - f_2)} + \frac{1 - \cos 2\pi(f_c - f_1)T}{2\pi(f_c - f_1)} \cdot \frac{\sin 2\pi(f_c - f_2)T}{2\pi(f_c - f_2)} \right] \\ &= \frac{A^2}{8} \frac{\sin 2\pi(f_2 - f_1)T - 2 \sin \pi(f_1 - f_2)T \cos \pi(2f_c - f_1 - f_2)T}{4\pi^2(f_c - f_1)(f_c - f_2)} \quad (\text{IV-60})\end{aligned}$$

It may be seen from Eq. (IV-60) that if the frequencies f_1 and f_2 are separated by a non-zero integral multiple of $\frac{1}{T}$, $\mu_{14} = 0$, regardless of the signal center frequency f_c .

Thus when the signal appears at one of the correlator frequencies,

$$\mu_{13}^2 + \mu_{14}^2 = 0$$

and the quantities ψ_i, ψ_j , $i \neq j$ are again independent, and their joint p.d.f. is given again by Eq. (IV-38). The variance μ_{11} must now be obtained. From Eqs. (IV-23) and (IV-27), μ_{11} is calculated as

$$\begin{aligned}
 \mu_{11} &= \left\langle \int_0^T dt v(t) \cos 2\pi f_1 t \int_0^T ds v(s) \cos 2\pi f_1 s \right\rangle_{S+N} \\
 &= \int_0^T dt \int_0^T ds \left\langle v(t) v(s) \right\rangle_{S+N} \cos 2\pi f_1 t \cos 2\pi f_1 s \\
 &= \int_0^T dt \int_0^T ds \left[\left\langle v(t) v(s) \right\rangle_S + \left\langle v(t) v(s) \right\rangle_N \right] \cos 2\pi f_1 t \cos 2\pi f_1 s
 \end{aligned} \tag{IV-61}$$

The second integral in Eq. (IV-61) is obtained from Eq. (IV-45) as

$$\int_0^T dt \int_0^T ds \left\langle v(t) v(s) \right\rangle_N \cos 2\pi f_1 t \cos 2\pi f_1 s = \frac{N_0}{4} T \tag{IV-62}$$

The first integral in Eq. (IV-61) can be obtained directly from Eq. (IV-59) by letting $f_2 = f_1$, which yields

$$\begin{aligned}
 &\int_0^T dt \int_0^T ds \left\langle v(t) v(s) \right\rangle_S \cos 2\pi f_1 t \cos 2\pi f_1 s \\
 &= \frac{A^2}{8} \left\{ \left[\frac{\sin 2\pi(f_c - f_1)T}{2\pi(f_c - f_1)} \right]^2 + \left[\frac{1 - \cos 2\pi(f_c - f_1)T}{2\pi(f_c - f_1)} \right]^2 \right\} \\
 &= \frac{A^2}{8} T^2 \text{sinc}^2 (f_c - f_1)T
 \end{aligned} \tag{IV-63}$$

Thus, from Eqs. (IV-61), (IV-62) and (IV-63), when the signal is located at the correlation frequency f_1 for which μ_{11} is being calculated, then

$$\mu_{11} = \frac{A^2 T^2}{8} + \frac{N_0}{4} T \tag{IV-64}$$

and when the signal is located at some correlator frequency other than f_1

$$u_{11} = \frac{N_0}{k} T \quad (\text{IV-65})$$

The upper bound on conditional signal detectability can now be calculated. When a signal appears at one correlator frequency, only the test quantity q_1 corresponding to that frequency is affected by the presence of signal. Therefore the conditional false-dismissal probability is

$$\beta = P [\text{one quantity } q_1 < k', \text{ given that a signal is present at } f_1, \text{ and } BT - 1 \text{ quantities } q_j < k' \text{ given that these quantities are affected by noise only}]$$

Using the independence of $\psi_i, \psi_j, i \neq j$ and hence of $q_i, q_j, i \neq j$, one can write

$$\beta = \beta_1 \left(1 - \alpha_1 \right)^{BT - 1} \quad (\text{IV-66})$$

where β_1 is the probability that q_1 falls below the threshold k' given that a signal is present at the corresponding frequency f_1 , and α_1 is the probability that q_1 exceeds the threshold given that no signal appears at f_1 . An expression for α_1 has already been derived and is given in Eq. (IV-50). The probability β_1 will now be found. The p.d.f. for q_1 , given that a signal is present at f_1 , is found from Eqs. (IV-44) and (IV-64) to be

$$f(y/s_1) = \frac{N_0^2}{4 \left(\frac{A^2}{8} T^2 + \frac{N_0}{k} \right) A^2} \exp \left[- \frac{N_0^2}{4 \left(\frac{A^2}{8} T^2 + \frac{N_0}{k} T \right) A^2} y \right], \quad y \geq 0$$

or

$$f(y/s_1) = \frac{1}{2d'(d'+1)} \exp\left[-\frac{1}{2d'(d'+1)} y\right], \quad y \geq 0$$

(IV-67)

where

$$d' = \frac{A^2}{2N_0} T$$

The test quantity q_1 is of course always a positive number, and

β_1 is calculated as

$$\begin{aligned} \beta_1 &= \frac{1}{2d'(d'+1)} \int_0^{k'} dy \exp\left(-\frac{1}{2d'(d'+1)} y\right) \\ &= -\exp\left(-\frac{1}{2d'(d'+1)} y\right) \Big|_0^{k'} \\ &= 1 - \exp\left(-\frac{1}{2d'(d'+1)} k'\right) \end{aligned} \quad (\text{IV-68})$$

Using Eq. (IV-50) one may write β_1 in terms of α_1 :

$$\beta_1 = 1 - \alpha_1^{\frac{1}{d'+1}} \quad (\text{IV-69})$$

With this and with Eq. (IV-66), the upper bound on conditional signal detectability becomes

$$1 - \beta \leq 1 - \left(1 - \alpha_1^{\frac{1}{d'+1}}\right) \left(1 - \alpha_1\right)^{(\text{BT}-1)} \quad (\text{IV-70})$$

This upper bound on $1 - \beta$ can now be calculated for a fixed value of false-alarm probability α by first solving Eq. (IV-40) at each value of normalized integration time BT for the value of α_1

which produces the prescribed value of α . Then Eq. (IV-70) can be used to calculate $1 - \beta$ for various values of R_S , since

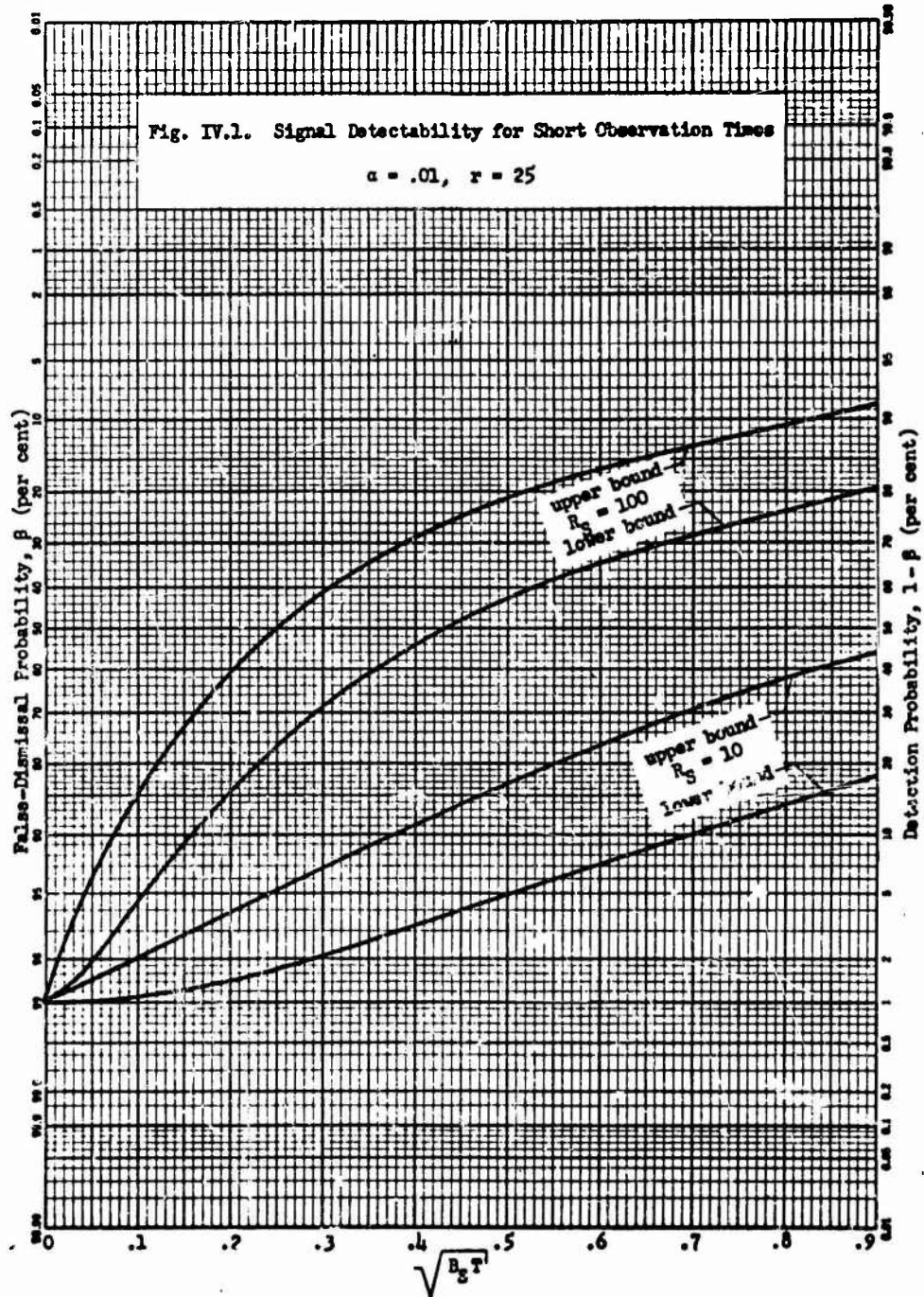
$$d' = R_S B_S T \quad (\text{IV-71})$$

$$= R_S \frac{B T}{r} \quad (\text{IV-72})$$

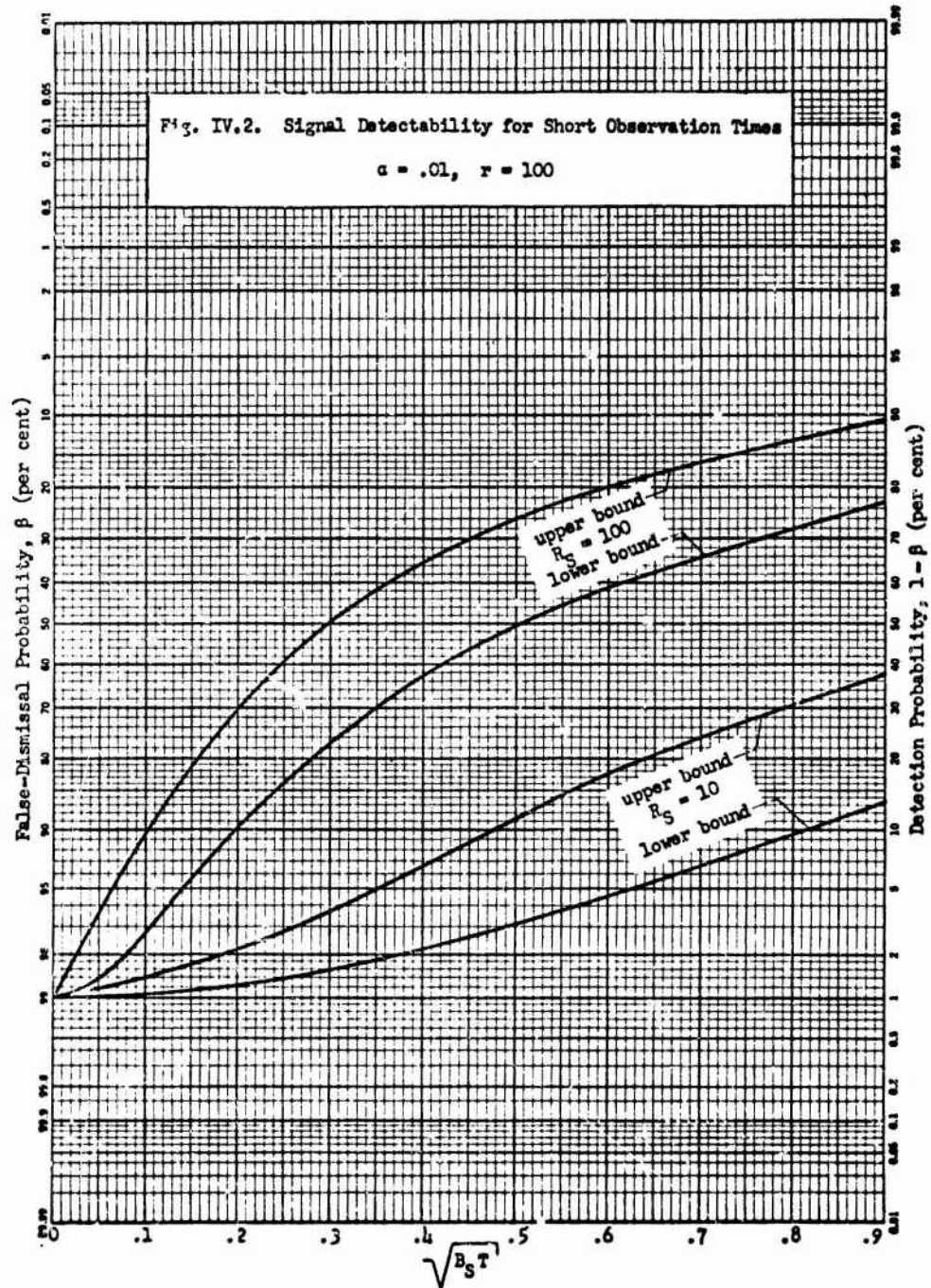
where r is the frequency uncertainty ratio. It should be noted that detectability cannot be stated as a function of the detection index d' only, but that both R_S and BT must be separately specified. In Figs. IV.1 and IV.2 are plotted detectability curves giving conditional detectability $1 - \beta$ or conditional false-dismissal probability β as a function of $\sqrt{B_S T}$ for two fixed values of pre-detection SNR R_S and two values of signal frequency uncertainty r . In all cases the false-alarm probability is fixed at $\alpha = .01$. The curves obtained from Eq. (IV-70) according to the above discussion are labelled "upper bound". The curves are carried out only to $\sqrt{B_S T} = 0.9$, since the analysis thus far in this chapter has been based upon the assumption of short observation times.

Comparison of Fig. IV.1 with Fig. IV.2 shows that the upper bound detectability curves in Fig. IV.2 ($r = 100$) fall below the corresponding curves in Fig. IV.1 ($r = 25$). This means that if points on corresponding curves in the two figures are compared at the same value of $\sqrt{B_S T}$, the probability of detection is somewhat poorer for the higher value of r . This is quite reasonable since the selection of a single value of $\sqrt{B_S T}$ implies that the

K-E
PROBABILITY SCALE 3-23
2-50 DIVISIONS
BRUNNELL & SONS CO. MADE IN U.S.A.



K&E
PROBABILITY SCALE 355-23
7 SO DIVISIONS
SCOFFEL & COHEN CO. NEW YORK, N.Y.



signal bandwidth is being held fixed, and an increase in r from 25 to 100 then corresponds to an increase in the width of the processing band B by a factor 4. Increasing B increases the amount of noise power in the signal being processed, and the detectability is thereby decreased. Of special importance however, is the fact that the signal detectability has decreased only slightly in view of this sizeable increase in noise power. This point will be discussed more fully in the concluding chapter.

An Approximate Lower Bound on Detectability

An approximate lower bound on detectability for short observation times will now be obtained by calculating (approximately) the detectability given that a signal is present and its center frequency lies exactly midway between two neighboring correlator frequencies.

It has not been proved that this situation actually represents a lower bound on detectability. However, in the weak-signal analysis of Section III.4, where signal detectability was calculated for a number of possible signal frequency locations, detectability did exhibit a minimum when the center frequency of the signal appeared midway between the center frequencies of two adjacent filters. It is being assumed that this minimum would be obtained under the same circumstances in the strong-signal case.

The covariances μ_{13} and μ_{14} are again required. The covariance μ_{13} relating the quantity x_{c1} generated at frequency f_1

and the quantity x_{c2} generated at f_2 , where f_1 and f_2 are separated by a non-zero multiple of $\frac{1}{T}$, has already been obtained, given noise plus a signal at the general frequency f_c . This result is given in Eq. (IV-59). Inspection of that equation shows that μ_{13} has a non-zero value except in instances where f_c coincides with one of the correlator frequencies in the processing band. Thus when a signal appears midway between neighboring correlator frequencies, as is being assumed in this derivation of a lower bound on $1 - \beta$, μ_{13} will always be non-zero, and therefore any two quantities $\psi_i, \psi_j, i \neq j$ will in general be correlated random variables. Thus the test quantities $q_i, q_j, i \neq j, i, j = 1, 2, \dots, BT$ in general be correlated, and an exact calculation of $1 - \beta$ in this lower-bound case cannot be carried out on the basis of independent probabilities. The conditional false-dismissal probability is

$$\begin{aligned} \beta &= P \{ \text{all } q_i < k', \text{ given that noise is present together} \\ &\quad \text{with a signal located at a frequency midway between} \\ &\quad \text{any two adjacent correlator frequencies} \}, \\ &\quad i = 1, 2, \dots, BT \\ &= P[q_1 < k'] P[q_2 < k' / q_1 < k'] \cdots P[q_{BT} < k' / q_1 < k', \dots, q_{BT-1} < k'] \end{aligned} \quad (\text{IV-73})$$

Each of the probabilities on the right side of Eq. (IV-73) is of course conditional upon the presence of signal and noise. Calculation of β using the exact expression given in Eq. (IV-73) would be a considerable task, and this will not be done here.

Instead two approximations to that expression will be made. The first approximation consists in ignoring the correlation among quantities q_i except for those generated at the two adjacent correlator frequencies between which the signal appears. That is, if the signal is assumed to appear midway between correlator frequencies f_j and f_{j+1} , only the correlation between q_j and q_{j+1} will be considered. It can be shown that this approximation is reasonable accurate. For example, the correlation coefficient relating q_j and q_{j+2} , or relating q_{j-1} and q_{j+1} , is approximately one tenth as large as that relating q_j and q_{j+1} ; correlation coefficients relating other pairs of test quantities are even smaller. Since the correlation between pairs of test quantities always enters the p.d.f. in Eq. (IV-26) through the sum of squares of u_{13} and u_{14} , non-zero values of these covariances always produce positive correlation. This positive correlation makes the conditional probabilities in Eq. (IV-73) larger than the corresponding unconditional probabilities would be. Therefore, ignoring the correlation among a group of test quantities results in a consistently low approximation to the right side of Eq. (IV-73), or in other words, a lower bound on β as given by that equation. Thus this approximation may be expressed as

$$\beta \geq P[q_1 < k'] P[q_2 < k'] \cdots P[q_j < k'] P[q_{j+1} < k' / q_j < k'] P[q_{j+2} < k'] \\ \cdots P[q_{BT} < k']$$

(IV-74)

Now a second approximation will be obtained in the form of a bound on the right side of Eq. (IV-74), using the inequality

$$P [q_{j+1} < k' / q_j < k'] \leq 1$$

It is readily seen that if this inequality is inserted into Eq. (IV-74), the result is an upper bound on the right side of the equation, namely,

$$\begin{aligned} & P[q_1 < k'] P[q_2 < k'] \cdots P[q_j < k'] P[q_{j+1} < k' / q_j < k'] P[q_{j+2} < k'] \cdots P[q_{BT} < k'] \\ & \leq P[q_1 < k'] P[q_2 < k'] \cdots P[q_j < k'] P[q_{j+2} < k'] \cdots P[q_{BT} < k'] \end{aligned}$$

(IV-75)

which is in conflict with the bound previously derived. Thus the two bounds tend to offset each other, but it cannot be stated with certainty whether the result is a consistent upper or lower bound on β as given by Eq. (IV-73). Since the first approximation, contained in Eq. (IV-74), is very accurate, it is highly probable that the upper bound on β is preserved and is given by the right side of Eq. (IV-75). Since this cannot be stated with certainty, the result will be stated as an approximation to β , that is,

$$\beta \approx P[q_1 < k'] P[q_2 < k'] \cdots P[q_j < k'] P[q_{j+2} < k'] \cdots P[q_{BT} < k']$$

(IV-76)

or

$$\beta \approx \beta_j [1 - \alpha_1]^{BT-2}$$

(IV-77)

where β_j is the probability that q_j falls below its threshold, given that the signal is present midway between the j^{th} and $(j+1)^{\text{th}}$ correlator frequencies. The probability α_i has already been derived and is given by Eq. (IV-50). Since the expression for β given by Eq. (IV-73) itself represents an upper bound on the conditional false-dismissal probability for the optimum detector, Eq. (IV-77) gives an approximation to this upper bound, or equivalently, an approximation to a lower bound on signal detectability. This may be expressed as

$$1 - \beta > \text{apx} \left[1 - \beta_j \left(1 - \alpha_i \right)^{BT-2} \right] \quad (\text{IV-78})$$

In order to calculate β_j in Eq. (IV-78), the p.d.f. for q_j must be obtained under the condition that, together with noise, a signal is present at a frequency midway between the correlator frequencies f_j and f_{j+1} . The general form of the p.d.f. is obtained from Eq. (IV-44) as

$$f(y/s) = \frac{N_o^2}{4\mu_{11}A^2} \exp - \left(\frac{N_o^2}{4\mu_{11}A^2} y \right), \quad y \geq 0 \quad (\text{IV-79})$$

The variance μ_{11} may be obtained from Eqs. (IV-45), (IV-59) and (IV-61). The second integral in Eq. (IV-61) is found in Eq. (IV-45) to be

$$\int_0^T dt \int_0^T ds \left\langle v(t) v(s) \right\rangle_N \cos 2\pi f_1 t \cos 2\pi f_1 s = \frac{N_o}{4} T \quad (\text{IV-80})$$

The first integral in Eq. (IV-61) may, for the case at hand, be obtained from Eq. (IV-59) by letting

$$f_2 = f_1$$

and

$$f_c = f_1 + \frac{1}{2T}$$

which yields

$$\int_0^T dt \int_0^T ds \langle v(t) v(s) \rangle_s \cos 2\pi f_1 t \cos 2\pi f_1 s = \frac{4}{\pi^2} \frac{A^2}{8} T^2 \quad (\text{IV-81})$$

When Eqs. (IV-80) and (IV-81) are substituted into Eq. (IV-61) the result is

$$\mu_{11} = \frac{4}{\pi^2} \frac{A^2}{8} T^2 + \frac{N_0}{4} T \quad (\text{IV-82})$$

The p.d.f. for q_j , given in Eq. (IV-79), now becomes

$$f(y/s) = \frac{N_c^2}{4 \left(\frac{4}{\pi^2} \frac{A^2}{8} T^2 + \frac{N_0}{4} T \right) A^2} \exp \left[- \frac{N_0^2}{4 \left(\frac{4}{\pi^2} \frac{A^2}{8} T^2 + \frac{N_0}{4} T \right) A^2} y \right]$$

$$= \frac{1}{2d' \left(\frac{4}{\pi^2} d' + 1 \right)} \exp \left[- \frac{1}{2d' \left(\frac{4}{\pi^2} d' + 1 \right)} y \right] \quad (\text{IV-83})$$

The probability β_j is

$$\begin{aligned}
 \beta_j &= \frac{1}{2d' \left(\frac{4}{\pi^2} d' + 1 \right)} \int_0^{k'} dy \exp \left[- \frac{1}{2d' \left(\frac{4}{\pi^2} d' + 1 \right)} y \right] \\
 &= - \exp \left[- \frac{1}{2d' \left(\frac{4}{\pi^2} d' + 1 \right)} y \right] \Big|_0^{k'} \\
 &= 1 - \exp \left[- \frac{1}{2d' \left(\frac{4}{\pi^2} d' + 1 \right)} k' \right] \quad (IV-84)
 \end{aligned}$$

Using Eq. (IV-50), one may write α_i in terms of β_i as follows:

$$\beta_i = 1 - \alpha_i^{\left(\frac{1}{\frac{4}{\pi^2} d' + 1} \right)} \quad (IV-85)$$

When Eq. (IV-85) is substituted into Eq. (IV-78), the lower bound on signal detectability becomes

$$1 - \beta > \text{apx} \left\{ 1 - \left[1 - \alpha_i^{\left(\frac{1}{\frac{4}{\pi^2} d' + 1} \right)} \right] (1 - \alpha_i)^{BT-2} \right\} \quad (IV-86)$$

Detectability curves obtained from Eq. (IV-86) are plotted in Figs. IV.1 and IV.2 and are labelled "lower bound". As with the "upper bound" curves discussed earlier, these curves show conditional detection probability $1 - \beta$ or conditional false-dismissal probability β as a function of $\sqrt{B_S T}$ for various values of pre-detection SNR and frequency uncertainty r . The false-alarm probability is held fixed at .01. It is evident from Figs. IV.1 and IV.2 that these upper and lower bounds, derived under the assumption that $B_S T \ll 1$, are reasonably close.

The detectability curves in Figs. IV.1 and IV.2 were obtained for a detector structure employing a bank of correlator pairs whose frequencies are spaced at intervals equal to $\frac{1}{T}$ cps. This spacing of correlator frequencies is the closest spacing for which detectability can be conveniently derived. A closer spacing of correlator frequencies, representing an improved approximation to the optimum detector, would of course result in tighter bounds on signal detectability but would require considerable computation in the evaluation of integrals involving the p.d.f. in Eq. (IV-26) or p.d.f.'s of larger numbers of Chi-squared variables. Such computations have not been deemed justifiable for the purposes of this work and therefore Eq.(IV-70) and Eq. (IV-86) will be taken as bounds on detectability for $B_S T \ll 1$.

Attention will now be given to the problem of detection in the strong-signal case when the observation time of the signal is long with respect to the signal correlation time, i.e., when $B_S T \gg 1$.

IV.3 Detection for Long Observation Times ($B_S T \gg 1$)

When the observation time of the received signal is long with respect to the inverse of the signal bandwidth, i.e., when $B_S T \gg 1$, then in forming the test quantity $L(\underline{y}/f_c)$ for the optimum detector [See Eq. (III-14)], the received signal may be pre-filtered to a band of width B_S centered at the frequency $f = f_c$. Then from the results of sampling analysis discussed in Section III.3, the received signal vector \underline{y} represents a vector of $n = 2B_S T$ independent samples. The test quantity $\log L(\underline{y}/f_c)$ then becomes

$$\log L(\underline{y}/f_c) = -\frac{n}{2} \log \left(\frac{A^2}{2N} + 1 \right) - \frac{1}{2} \left(\frac{1}{\frac{A^2}{2N} + 1} \right) \frac{A^2}{2N^2} \underline{y}' \underline{I} \underline{y} \quad (\text{IV-87})$$

as was given in Eq. (III-23). The noise variance N is the noise power in a narrow band of width B_S , that is

$$N = N_0 B_S \quad (\text{IV-88})$$

It will now be convenient to define as a test quantity

$$\begin{aligned} Q'(z) &= \frac{A^2}{4N^2} \underline{y}' \underline{I} \underline{y} \\ &= \frac{A^2}{4N^2} \sum_{i=1}^n v_i^2 \end{aligned} \quad (\text{IV-89})$$

This test quantity, being a sum of squares of n independent gaussian random variables, has a Chi-squared p.d.f. with n degrees of freedom. In Sections III.3 and III.4 a gaussian approximation

to the Chi-squared distribution was used. The accuracy of such an approximation rests, however, on the assumption of a low pre-detection SNR and is no longer valid when $R_g \gg 1$, as is being assumed in this chapter. For this reason an exact Chi-squared distribution for $Q'(f)$ will be used.

The p.d.f. of a sum of squares of n independent gaussian random variables v_i , each having zero mean and variance denoted by $\text{var}(v)$ is given by[†]

$$f(x) = \frac{1}{\text{var}(v)} k_n \left[\frac{x}{\text{var}(v)} \right], \quad x \geq 0 \quad (\text{IV-90})$$

where $k_n(z)$ is the standardized Chi-squared p.d.f. with n degrees of freedom. Therefore the p.d.f. for $Q'(f)$ becomes

$$f(x) = \frac{4N^2}{A^2 \text{var}(v)} k_n \left[\frac{4N^2}{A^2 \text{var}(v)} x \right], \quad x \geq 0 \quad (\text{IV-91})$$

As in Section III.4 the signal detectability will be estimated by considering the performance of a band-splitting approximation to the optimum detector. When pre-detection filters in a band-splitting detector have overlapping frequency responses, their outputs are correlated, which means that the corresponding test quantities $Q'(f_i)$ are also correlated. Therefore computation of error rates in general involves integrations with respect to

[†] See, for example, Cramer, (I, Chapter 18.)

joint p.d.f.'s for correlated Chi-squared variables. It may be recalled that a similar point arose in Section IV.2 where detectability in the strong-signal case with short observation time was being considered. There the test quantity was found to be a Chi-squared variable with two degrees of freedom, and the joint p.d.f. for two such correlated test quantities was a function involving a modified Bessel function [See Eq. (IV-26)]. It can thus be seen that even in cases where only pair-wise correlation between test quantities need be considered, the calculation of error probabilities would involve considerable labor. For the purposes of this investigation such computations will not be carried out. Rather, a detector structure will be analyzed which employs a band of pre-detection filters whose frequency responses are spaced as closely as possible without overlapping. That is, since

$$B = r B_g$$

the detector will use r rectangular filters, each of bandwidth B_g , covering the total band of signal frequency uncertainty B . The outputs of the filters will then be uncorrelated and the test quantities $Q'(f_i)$ will thus be independent. Upper and lower bounds on optimum signal detectability will be derived using this detector model.

The general expressions for the false-alarm rate and for the conditional detection probability may be obtained from the work done in Section III.4. From Eq. (IV-53) the false-alarm probability is obtained as

$$\alpha = 1 - \prod_{i=1}^r (1 - \alpha_i) \quad (\text{IV-92})$$

where, here,

$$\alpha_i = P \{Q'(f_i) > k' \text{ / noise only} \} , \quad i = 1, 2, \dots, r \quad (\text{IV-93})$$

When a signal is present, its spectrum will in general overlap the frequency responses of two pre-detection filters. Thus the conditional probability of false dismissal is given by Eq. (III-60)

$$\beta = \beta_{1(s)} \beta_{1(1-s)} \left(1 - \alpha_i \right)^{r-2} \quad (\text{IV-94})$$

where

$$\beta_{1(p)} = P \{ Q'(f_i) < k' , \text{ given that the filter band contains a fraction } p \text{ of the total signal power} \}$$

The false-alarm probability will be considered first. When only noise is present, the variance of a sample of the received signal is

$$\text{var}(v) = N \quad (\text{IV-95})$$

When this is substituted into Eq. (IV-91), the p.d.f. for one of the test quantities $Q'(f_i)$ becomes

$$f(x/0) = \frac{4N}{A^2} k_n \left(\frac{4N}{A^2} x \right) , \quad x \geq 0 \quad (\text{IV-96})$$

Using the definition of pre-detection SNR,

$$R_S = \frac{A^2}{2N} \quad (\text{IV-97})$$

the p.d.f. for $Q'(f_1)$ may be rewritten as

$$r(x/0) = \frac{2}{R_S} k_n \left(\frac{2}{R_S} x \right) \quad , \quad x \geq 0 \quad (\text{IV-98})$$

The probability α_1 then becomes

$$\alpha_1 = \frac{2}{R_S} \int_{k'}^{\infty} dx k_n \left(\frac{2}{R_S} x \right)$$

or

$$\alpha_1 = \int_{\frac{2k'}{R_S}}^{\infty} dz k_n(z) \quad (\text{IV-99})$$

This result is in the form of the standardized Chi-squared integral, which is available in tables[†]. Thus the false-alarm probability may be calculated with Eqs. (IV-92) and (IV-99).

When a signal is present, signal power will appear in the pass bands of two adjacent band-splitting filters. If a fraction σ of the signal power $A^2/2$ appears in one pass band, then the variance of a sample of the signal at the output of that filter

[†] See National Bureau of Standards (III, Sec. 26.)

will be

$$\text{var}(v) = \sigma \frac{A^2}{2} + N, \quad 0 \leq \sigma \leq 1 \quad (\text{IV-100})$$

Therefore, from Eqs. (IV-91) and (IV-100) one obtains the following p.d.f.'s for test quantities $Q'(f_1)$ generated for the two bands containing signal power:

$$f(x/\sigma) = \frac{2}{R_S(\sigma R_S + 1)} k_n \left[\frac{2}{R_S(\sigma R_S + 1)} x \right], \quad x > 0 \quad (\text{IV-101})$$

and

$$f(x/1-\sigma) = \frac{2}{R_S[(1-\sigma)R_S + 1]} k_n \left\{ \frac{2}{R_S[(1-\sigma)R_S + 1]} x \right\}, \quad x > 0 \quad (\text{IV-102})$$

The probabilities $\beta_1(\sigma)$ and $\beta_1(1-\sigma)$ are obtained by integrating the above distributions:

$$\beta_1(\sigma) = \frac{2}{R_S(\sigma R_S + 1)} \int_0^{k'} dx \left[k_n \frac{2}{R_S(\sigma R_S + 1)} x \right]$$

or

$$\beta_1(\sigma) = \int_0^{\frac{2k'}{R_S(\sigma R_S + 1)}} dz k_n(z) \quad (\text{IV-103})$$

And similarly

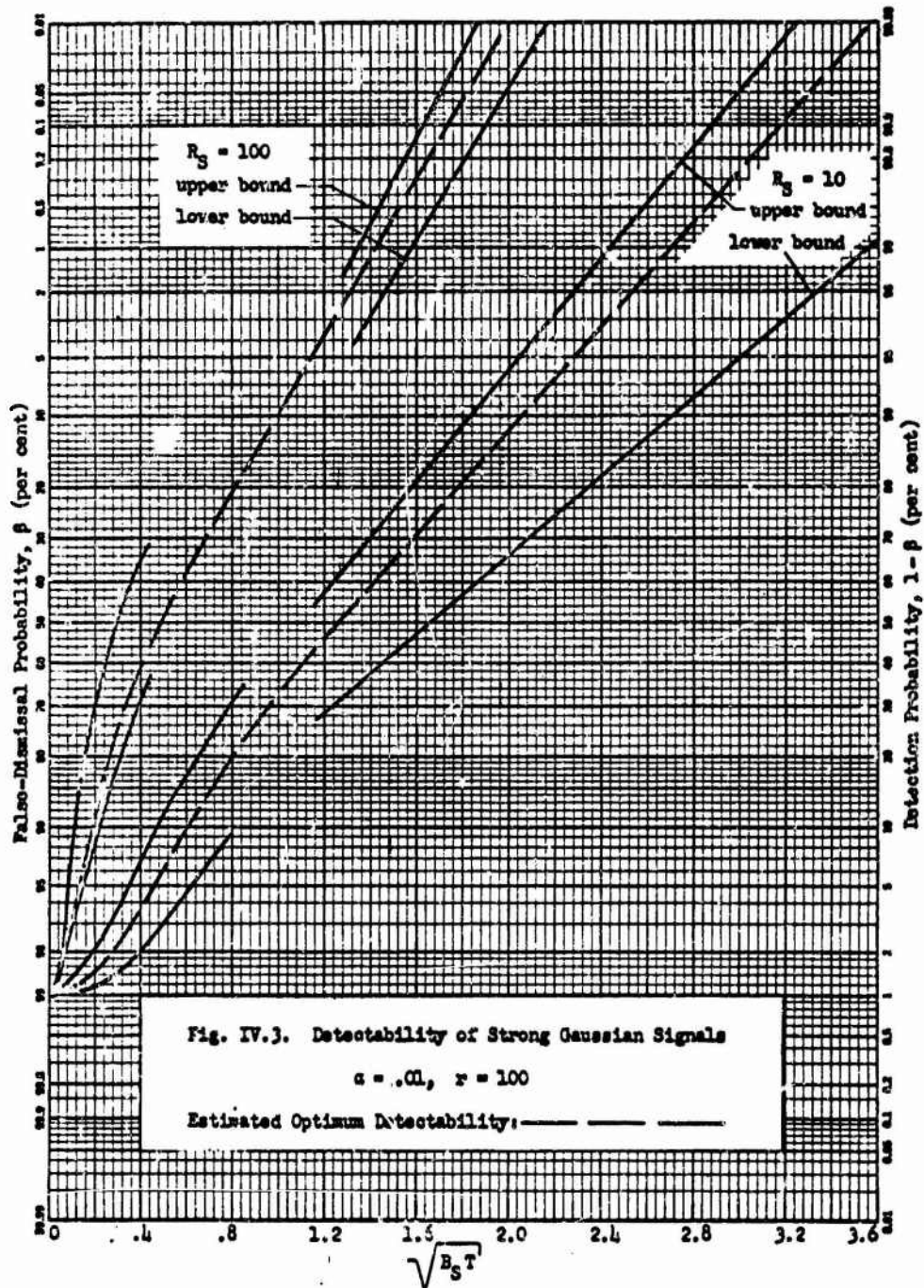
$$\beta_{1(1-\sigma)} = \int_0^{\frac{2k'}{R_S[(1-\sigma)R_S+1]}} dz k_n(z) \quad (\text{IV-104})$$

The conditional false-dismissal probability β or the conditional detectability $1 - \beta$ can now be calculated from Eqs. (IV-94), (IV-99), (IV-103) and (IV-104). The detectability will of course depend upon the actual frequency location of a received signal in the overall band of interest, that is, upon the signal overlap factor σ . In Fig. IV.3 are plotted curves of signal detectability as a function of $\sqrt{B_S T}$ for a fixed false-alarm probability $\alpha = .01$. The frequency uncertainty ratio r is taken to be 100, and the pre-detection SNR R_S takes on values of 10 and 100. The curves labelled "upper bound" and "lower bound" correspond to the following situations: (1) When a signal is present, the highest detectability is achieved when the signal spectrum is exactly aligned with the passband of one of the pre-detection filters. Then $\sigma = 1$ and the detection probability, obtained from Eq. (IV-94), becomes

$$1 - \beta = 1 - \beta_{1(1)} \left(1 - \alpha_1 \right)^{r-1} \quad (\text{IV-105})$$

since

$$\beta_{1(0)} = 1 - \alpha_1 \quad (\text{IV-106})$$



(2) When a signal appears with a center frequency midway between the center frequencies of two adjacent filters, the detectability is the poorest. Then $\sigma = \frac{1}{2}$ and the detection probability becomes

$$1 - \beta = 1 - \beta_{1(1/2)}^2 \left(1 - \alpha_1 \right)^{r-2} \quad (\text{IV-107})$$

These two situations therefore represent upper and lower bounds on detectability for the detector model considered. The inclusion of more band-splitting filters for the same overall processing bandwidth B , representing a closer approximation to the optimum detector, would result in tighter upper and lower bounds on detectability. If the approximation were refined by adding a larger and larger number of filters, the bounds should converge to the optimum signal detectability.

Bounds on signal detectability, derived in Section IV.2 for short observation times [See Eqs. (IV-70) and (IV-86)] are also plotted in Fig. IV.3 for small values of $\sqrt{B_S T}$.

The bounds on signal detectability obtained in the strong-signal case are not as tight as those obtained for the weak-signal case. However, if Figs. III.3 and IV.3 are compared, it may be seen that the upper and lower bound detectability curves of Fig. IV.3 for $B_S T \gg 1$ show trends similar to the maximum and minimum curves of Fig. III.3 for $b = r$. There is no reason to suspect that a further approximation to the optimum detector in the strong-signal case would yield detectability curves much different in character from those shown in Fig. III.3 for $b = 2r$; therefore on the basis

of this comparison one might make a fairly accurate estimate of optimum signal detectability in the strong-signal case.

Such estimates were made and are shown in Fig. IV.3. Using these results obtained in the strong-signal case an example will now be considered which will demonstrate the gain in detectability obtained from the knowledge that the signal power is confined to a band of width B_S somewhere within the band being processed, of width $B = rB_S$.

Example 1

Suppose that the overall frequency band to be processed has a width $B = 500$ cps, and the allowable integration time is $T = 1$ sec. Let the input SNR, R , defined as the ratio of total signal power to total noise power in the overall band B , be -10 db, that is,

$$R = \frac{A^2/E}{N_0 B}$$

$$= 0.1$$

Suppose now that the signal spectrum is known to have a width of 5 cps and that the signal spectrum may lie anywhere within the overall frequency band B . The optimum detector would now employ pre-detection filters each of bandwidth $B_S = r$ cps, and hence

$$r = \frac{B}{B_S} = 100$$

The pre-detection SNR R_S , defined with respect to a band of width B_S , is

$$R_B = \frac{A^2/2}{N_0 B}$$

$$= r R$$

$$= 10$$

Since $R_B = 10 \gg 1$, the detectability curves of Fig. IV.3 are applicable. If the false-alarm rate is to be held fixed at $\alpha = .01$, then with $R_B = 10$ and $\sqrt{R_B T} = 2.24$, the conditional detection probability is estimated to be

$$1 - \beta = 95 \text{ per cent (estimated)}$$

If, however, the signal power were uniformly spread over the entire band of width $B = 500$ cps, then a value of input SNR R greater than 0.1 (-10 db) would be required in order to achieve a detectability of 95 per cent at $\alpha = .01$, assuming that the integration time is still held at $T = 1$ sec. The required SNR in this case is found from Fig. III.5, where the curve labelled $r = 1$ yields $1 - \beta = 95$ per cent when

$$\sqrt{D} = R \sqrt{BT} = 4$$

Therefore the required input SNR is

$$R = \frac{4}{\sqrt{BT}}$$

$$= \frac{4}{\sqrt{500}}$$

$$= .179$$

or

$$10 \log_{10} (.179) = -7.5 \text{ db}$$

Thus the effective gain in input SNR due to knowledge that the signal has a narrow spectrum of unknown center frequency within the band being processed is

$$-7.5 - (-10 \text{ db}) = 2.5 \text{ db}$$

This gain appears to be modest in view of the fact that the pre-detection SNR is apparently increased from $R = .1$ to $R = 10$, an increase of 20 db. Most of the effect of this 20 db increase is lost, however, due to the fact that when $R_g \gg 1$, the variance of the test quantity $Q'(f)$, as well as the average value of $Q'(f)$ increases appreciably with R_g .

A second example will give further insight into this point.

Example 2

Suppose that the processing band again has a width $B = 500$ cps, and $T = 1$ sec. It was found in Example 1 that if the signal power is spread uniformly over the processing band B , then an input SNR $R = .179$ is required to achieve 95 per cent detectability at $\alpha = .01$.

Suppose now that the signal spectrum is known to have a width of 100 cps; the frequency uncertainty ratio is then $r = 5$. The value of pre-detection SNR R_g required to produce $1 - \beta = .95$ at $\alpha = .01$ is now found from Fig. III.5, where the curve labelled $r = 5$ yields $1 - \beta = .95$ at

$$\sqrt{D} = R_g \sqrt{B_g T} = 5.1$$

Therefore the input SNR R_B , defined with respect to B_B , is

$$R_B = \frac{5.1}{\sqrt{B_B T}} = \frac{5.1}{\sqrt{100}} = .51$$

and R , defined with respect to B , is

$$R = \frac{1}{r} R_B = \frac{.51}{5} = .102$$

Thus the effective gain in input SNR due to the knowledge that the signal has a spectrum 5 times narrower than the processing band is

$$10 \log_{10} \left(\frac{.179}{.102} \right) \approx 2.4 \text{ db}$$

It is seen that this is very close to the 2.5 db gain in input SNR demonstrated in Example 1, where the signal spectrum was assumed to be 100 times narrower than the processing band. Hence further increase of the uncertainty ratio r from 5 to 100 (with B assumed fixed) only yields an additional 0.1 db effective gain in input SNR.

Thus it appears that substantial gains in detectability can be achieved by narrowing the signal spectrum within the processing band up to the point where R_B is on the order of unity. Then as the signal spectrum is narrowed further, the corresponding change in detectability becomes very small.

This observation suggests an interesting question with regard to the detectability of stochastic signals in cases of high pre-detection SNR, the question whether concentration of a given amount of signal power into a steadily narrower frequency band produces a

monotone increase in detectability (with a maximum detectability at zero signal bandwidth) or whether maximum detectability occurs at some non-zero bandwidth. This question may be considered quite apart from the problem of signal frequency uncertainty and some remarks will be made to this point in the concluding chapter.

CHAPTER V

CONCLUSION

This investigation has produced two principal results with regard to the detection of signals of unknown frequency. The first result concerns the form of the optimum detector for the detection of such a signal in the presence of additive noise.

When the signal to be detected is a coherent sinusoid with an unknown frequency given by a probability distribution over a discrete set of frequency values, the work of Chapter II showed that the optimum receiver structure for the detection of such a signal is essentially a band-splitting detector. This band-splitting detector becomes exactly optimum as the post-detection SNR is made increasingly large.

The detection of a gaussian stochastic signal with a center frequency given by a discrete probability distribution was discussed at the beginning of Chapter III, where it was shown that for this signal case optimum detection is once again achieved with a band-splitting detector.

When the center frequency of the stochastic signal has a continuous p.d.f. over a prescribed frequency band, the work of Chapter III indicated that the optimum detector becomes a band-sweeping detector. A practical approximation to the band-sweeping detector is a band-splitting detector employing a finite

number of pre-detection filters. The results presented in Chapter III show that very nearly optimum detectability is achieved with a bank of filters equal in number to twice the frequency uncertainty ratio r .

The second principal result which has been obtained is that in the detection of weak signals, detectability is governed primarily by the pre-detection SNR R_g , defined in a band of the width of the signal spectrum, even though the frequency location of the signal may be unknown within a wider processing band. The implications of this result may be discussed from two points of view.

From one point of view the signal spectrum may be regarded as fixed while the processing band B may be wider than the signal spectrum by various amounts, corresponding to various values of the frequency uncertainty ratio r , $r \geq 1$. The uncertainty regarding the exact frequency location of the signal makes necessary the use of a bank of band-splitting filters. A test quantity is generated from the output of each of these filters and a threshold test is made on each of these quantities. As the frequency uncertainty ratio r is increased from unity, the number of required filters also increases. If a constant false alarm probability is to be maintained, the threshold levels must be raised accordingly. This raising of the threshold levels tends to degrade the detectability somewhat, but the results obtained in this investigation show that this degradation is small compared with sizeable increase in noise power which results from

widening of the processing band by a factor r .

From a second point of view, one may regard the overall processing bandwidth as fixed. In this case a unity value for r describes a situation in which the signal power is spread uniformly across the entire processing band B , and an increase of the uncertainty ratio r from unity corresponds to concentration of the signal power into a narrower band somewhere within B .

Since the results of this work show that the detectability in the weak-signal case depends critically upon the pre-detection SNR R_S in the narrow signal band, then when the signal power is contained within a band of width B_S instead of being uniformly spread over the band $B = rB_S$, $r \geq 1$, the pre-detection SNR is increased by the factor r , and increased detectability is accordingly gained. As has been discussed, the frequency uncertainty necessitates the use of a band-splitting detector with a resulting loss in detectability, which partly offsets the effect of increased pre-detection SNR. However a net gain in detectability is still obtained. The weak-signal analysis presented in Chapter III shows that the increase in R_S by a factor r results in an effective gain in pre-detection SNR almost equal to r . In typical cases the loss in effective SNR due to frequency uncertainty is on the order of 2 db.

The results are somewhat different in the strong-signal situation however. It appears that appreciable improvement in detectability through narrowing of the signal spectrum can be realized only up to the point where R_S is on the order of unity.

When R_g is unity or greater, then an increase in R_g not only increases the deflections of the test quantities generated by the band-splitting detector but also increases the variances of these test quantities, and this second effect tends to oppose the first, thus offsetting the increase in R_g . This effect of course also manifests itself when the frequency location of the signal spectrum is known exactly and thus may be considered independently of the frequency uncertainty problem.

This suggests the desirability of a more complete analysis of the optimum detection problem under the assumption of strong pre-detection SNR with the aim of answering such questions as the following: Given that a stochastic signal of fixed total power is to be detected in a background of spectrally flat noise in a fixed length of time, how does the signal detectability (for a fixed false alarm probability) vary as the band width of the signal is varied? Is maximum detectability obtained by concentrating the signal power in an arbitrarily narrow band or is there some non-zero signal bandwidth for which signal detectability is a maximum?

The analysis in Chapter IV can be used to find partial answers to these questions, under restrictions of either very short observation time or very long observation time. One interesting result is that if the signal energy and noise spectral level are fixed, signal detectability can be greater at some non-zero value of signal bandwidth than in the limiting case of zero bandwidth. That this can occur may be argued as follows:

As the signal bandwidth is steadily reduced while the signal power is fixed, the ratio of signal to noise power in the narrow signal band steadily increases, which tends to improve detectability. However if the observation time T is fixed, then the correlation time of the signal becomes steadily longer with respect to T and thus detectability depends less upon the average signal energy and more upon the short-term statistics of the signal energy, e.g., the variance of the signal energy appearing in each observation interval. For example in Section IV.2 the detection of a gaussian signal was considered with the assumption that the observation time was much shorter than the reciprocal of the signal bandwidth. The signal amplitude was seen to be essentially constant during each observation interval and this amplitude was distributed with a Rayleigh density function over the ensemble of all observations. Thus if some amplitude is chosen, it can be said that for a certain percentage of the observations the signal will never rise above that chosen amplitude. Therefore it can be seen that the detectability for this case might be poorer than some case of wider bandwidth (and hence shorter correlation time in comparison with the observation time of the signal) but comparable pre-detection SNR, where detectability is governed more by the average signal energy than by the variance of the signal energy appearing in each observation interval.

It is apparent from this discussion that a more thorough analysis of the optimum detection problem in the strong signal situation is called for. To date no such analysis has been presented in the literature. It is suggested that this might prove to be a fruitful subject for further research.

APPENDIX A

DEFLECTIONS OF TERMS IN THE POWER SERIES FOR $\log i(y)^{\dagger}$

As was discussed in Section I.4, the average LR $i(y)$, given by Eq. (I-7) for detection in gaussian noise, can be expanded in a power series involving terms of all powers in $-\frac{1}{2} \mathbf{z}' \mathbf{K}^{-1} \mathbf{z}$ and $\mathbf{z}' \mathbf{K}^{-1} \mathbf{y}$. The average $\langle \rangle_n$ can then be carried out term by term. If $\log i(y)$ is expanded in a second power series and if terms contributing no deflection are dropped, the result is

$$\begin{aligned} \log i(y) = & -\frac{1}{2} \mathbf{z}' \mathbf{K}^{-1} \mathbf{z} + \frac{1}{2} \langle (\mathbf{z}' \mathbf{K}^{-1} \mathbf{y})^2 \rangle \\ & + \frac{1}{4!} \langle (\mathbf{z}' \mathbf{K}^{-1} \mathbf{y})^4 \rangle - \frac{1}{8} \langle (\mathbf{z}' \mathbf{K}^{-1} \mathbf{y})^2 \rangle^2 \\ & + O(\mathbf{z}^6) \end{aligned} \quad (A-1)$$

The deflection of a term or a set of terms is defined as the change in average value in going from the noise-only situation to the signal-plus-noise situation. The deflection will be denoted by $\Delta E []$. The following deflections are obtained from Eq. (A-1) in general form:

$$\Delta E [O(\mathbf{z}^2)] = \Delta E \left[\frac{1}{2} \langle (\mathbf{z}' \mathbf{K}^{-1} \mathbf{y})^2 \rangle \right] \quad (A-2)$$

$$\Delta E [O(\mathbf{z}^4)] = \Delta E \left[\frac{1}{4!} \langle (\mathbf{z}' \mathbf{K}^{-1} \mathbf{y})^4 \rangle - \frac{1}{8} \langle (\mathbf{z}' \mathbf{K}^{-1} \mathbf{y})^2 \rangle^2 \right] \quad (A-3)$$

These two deflections were evaluated for the three signal cases outlined in Section I.4. In addition the following deflection was

[†] These results are taken from Levesque (1).

evaluated for the sinusoidal signal, case 3):

$$\Delta E \frac{1}{6!} \left[\left\langle (\underline{s}' \underline{K}^{-1} \underline{y})^6 \right\rangle \right] \quad (A-4)$$

This is the most significant term in $\Delta E [O(\underline{s}^6)]$.

The results are summarized in Table A.1, shown on the following page. The symbols used in the table are defined as follows:

B = Width of the band of signal frequency uncertainty,

i.e., the band being processed, in cps.

R = Input or pre-detection SNR, defined in this case

as

$$\frac{\text{Total signal power}}{\text{Total noise power in the frequency band } B}$$

T = Integration time in sec.

r = Frequency uncertainty ratio, defined as

$$\frac{\text{Processing bandwidth } B}{\text{Signal bandwidth } B_s}$$

It was assumed in the analysis that $BT \gg 1$ and, in signal case 2), $BT \gg B_s T \gg 1$.

It is first seen from the table that deflections of terms of order \underline{s}^2 are identical for the three signal cases. Thus a detector constructed on the basis of these lowest-order terms of the series would yield the same performance for the three cases. It can be shown that this term represents a quadratic operation on \underline{y} , i.e., an energy measurement of the signal received in the band B . Thus detection would depend upon the total power in the band and no use would be made of the narrowband nature of the signal in cases 2) and 3).

	1) Broadband gaussian signal	2) Narrowband gaussian signal	3) Sinusoidal signal
$\Delta E [0(\underline{s}^2)]$	$R^2 BT$	$R^2 BT$	$R^2 BT$
$\Delta E [0(\underline{s}^4)]$	$- R^3 BT$	$R^4 \left[\left(\frac{R}{3} - \frac{1}{2} \right) (BT)^2 + \left(\frac{R^2}{2} - \frac{3R}{8} \right) (BT) \right] - R^3 (BT)$	$\frac{16}{4!} R^4 (BT)^3 - R^4 (BT)^2 - R^3 (BT)$
$\Delta E \left[\frac{1}{6!} (\underline{s} \cdot \underline{R}^{-1} \cdot \underline{v})^6 \right]$	(not calculated)	(not calculated)	$\frac{1}{3} R^6 (BT)^5$

Table A.1. Deflections of Terms in a Power Series Expansion of $\log z(\underline{v})$

When deflections of higher-order terms are considered, the three signal cases produce different results. The deflections in column 1) are all seen to grow linearly with the integration time and have as coefficients progressively higher powers of the input SNR, P . Thus if $R \ll 1$ the major contribution to the total deflection of $\log l(\underline{y})$ is from the $O(\underline{s}^2)$ term and higher-order terms in the series can be neglected.

When the signal power is confined to a band much narrower than B , it is seen from column 2) that $\Delta E [O(\underline{s}^4)]$ contains terms which grow as the square of the integration time. Thus for any value of R , however small, the magnitude of $\Delta E [O(\underline{s}^4)]$ can be made equal to or greater than that of $\Delta E [O(\underline{s}^2)]$ by making the integration time sufficiently long. Therefore higher order terms in the power series cannot be neglected simply on the basis of low input SNR. Similar remarks apply to signal case 3). There, $\Delta E [O(\underline{s}^4)]$ involves a term growing as $(BT)^3$ and $\Delta E [O(\underline{s}^6)]$ grows as $(BT)^5$.

APPENDIX B

A SMALL-SIGNAL APPROXIMATION TO THE OPTIMUM DETECTOR
FOR THE CASE OF COHERENT DETECTION

In the optimum detection of a signal with unknown parameters, the detector must calculate the average LR

$$L(\underline{y}) = \left\langle \exp \left[-\frac{1}{2} \underline{s}' \underline{K}^{-1} \underline{s} + \underline{s}' \underline{K}^{-1} \underline{y} \right] \right\rangle \quad (B-1)$$

where $\langle \rangle$ implies $\langle \rangle_S$. If the exponential in Eq. (B-1) is expanded in a power series, the average over signal parameters taken term by term and the function $\log L(\underline{y})$ expanded in a second power series, the result is

$$\log L(\underline{y}) = -\frac{1}{2} \langle \underline{s}' \underline{K}^{-1} \underline{s} \rangle + \langle \underline{s}' \underline{K}^{-1} \underline{y} \rangle + \frac{1}{2} \left[\langle (\underline{s}' \underline{K}^{-1} \underline{y})^2 \rangle - \langle \underline{s}' \underline{K}^{-1} \underline{y} \rangle^2 \right] + O(\underline{s}^3) \quad (B-2)$$

In the weak-signal situation, when the signal to be detected is coherent,[†] the major contribution to $\log L(\underline{y})$ is from the term $\langle \underline{s}' \underline{K}^{-1} \underline{y} \rangle$. As an approximation, the terms of the order \underline{s}^2 can be replaced by their averages taken with noise only present. These averages, together with the term $-\frac{1}{2} \langle \underline{s}' \underline{K}^{-1} \underline{s} \rangle$, are then taken as bias terms in threshold test. The three bias terms are thus

[†] By definition the signal \underline{s} is described as coherent if $\langle \underline{s} \rangle_S \neq 0$.

$$\begin{aligned}
 -\frac{1}{2} \langle \underline{z}' \underline{K}^{-1} \underline{z} \rangle &= \left\langle \sum_i \sum_j z_i z_j K_{ij}^{-1} \right\rangle \\
 &= \sum_i \sum_j \langle z_i z_j \rangle K_{ij}^{-1} \\
 &= \text{tr} \left(\langle \underline{z} \underline{z}' \rangle \underline{K}^{-1} \right) \quad (B-3)
 \end{aligned}$$

$$\begin{aligned}
 -\frac{1}{2} \frac{\langle (\underline{z}' \underline{K}^{-1} \underline{y})^2 \rangle}{N} &= \frac{\langle \underline{y}' \underline{K}^{-1} \underline{z} \underline{z}' \underline{K}^{-1} \underline{y} \rangle}{N} \\
 &= \frac{\underline{y}' \underline{K}^{-1} \langle \underline{z} \underline{z}' \rangle \underline{K}^{-1} \underline{y}}{N} \\
 &= \sum_i \sum_j \frac{y_i y_j}{N} \left(\underline{K}^{-1} \langle \underline{z} \underline{z}' \rangle \underline{K}^{-1} \right)_{ij} \\
 &= \text{tr} \left(\underline{K} \underline{K}^{-1} \langle \underline{z} \underline{z}' \rangle \underline{K}^{-1} \right) \\
 &= \text{tr} \left(\langle \underline{z} \underline{z}' \rangle \underline{K}^{-1} \right) \quad (B-4)
 \end{aligned}$$

$$\begin{aligned}
 -\frac{1}{2} \frac{\langle \underline{z}' \underline{K}^{-1} \underline{y} \rangle^2}{N} &= -\frac{1}{2} \underline{y}' \underline{K}^{-1} \langle \underline{z} \rangle \langle \underline{z}' \rangle \underline{K}^{-1} \underline{y} \\
 &= -\frac{1}{2} \sum_i \sum_j \frac{y_i y_j}{N} \left(\underline{K}^{-1} \langle \underline{z} \rangle \langle \underline{z}' \rangle \underline{K}^{-1} \right)_{ij} \\
 &= -\frac{1}{2} \text{tr} \left(\langle \underline{z} \rangle \langle \underline{z}' \rangle \underline{K}^{-1} \right) \\
 &= -\frac{1}{2} \sum_i \sum_j \langle z_i \rangle \langle z_j \rangle K_{ij}^{-1} \\
 &= -\frac{1}{2} \langle \underline{z}' \rangle \underline{K}^{-1} \langle \underline{z} \rangle \quad (B-5)
 \end{aligned}$$

Therefore,

$$\log i(\underline{y}) \approx \langle \underline{s}' \rangle \underline{K}^{-1} \underline{y} - \frac{1}{2} \langle \underline{s}' \rangle \underline{K}^{-1} \langle \underline{s} \rangle \quad (B-6)$$

If the signal is a sinusoid of known amplitude and phase with an unknown frequency given by a discrete distribution, then

$$\langle \underline{s} \rangle = \sum_{i=1}^m p_i \underline{s}(f_i) \quad (B-7)$$

If the m frequencies are equally probable,

$$\langle \underline{s} \rangle = \frac{1}{m} \sum_{i=1}^m \underline{s}(f_i) = \frac{1}{m} \sum_{i=1}^m \underline{s}_i \quad (B-8)$$

If, in addition, the noise is white with variance N ,

$$\log i(\underline{y}) \approx \frac{1}{mN} \sum_{i=1}^m \underline{s}_i' \underline{y} - \frac{1}{2mN} \sum_{i=1}^m \sum_{j=1}^m \underline{s}_i' \underline{s}_j \quad (B-9)$$

Since \underline{s}_i and \underline{s}_j represent sinusoids of different frequencies,

$$\begin{aligned} \frac{1}{N} \underline{s}_i' \underline{s}_j &\approx 0, & i \neq j \\ &= \frac{1}{N} \sum_{k=1}^n s_i^2(t_k) = d, & i = j \end{aligned} \quad (B-10)$$

Thus,

$$\begin{aligned} \log i(\underline{y}) &= \frac{1}{mN} \sum_{i=1}^m \underline{s}_i' \underline{y} - \frac{d}{2m} \\ &= \frac{1}{m} \sum_{i=1}^m \left(\frac{1}{N} \underline{s}_i' \underline{y} - \frac{d}{2} \right) + \left(1 - \frac{1}{m} \right) \frac{d}{2} \end{aligned} \quad (B-11)$$

From Eqs. (II-12) and (II-13),

$$\log i(\underline{y}) = \frac{1}{m} \sum_{i=1}^m \log L_i + \left(1 - \frac{1}{m}\right) \frac{d}{2} \quad (\text{B-12})$$

Therefore the weak-signal approximation leads to the threshold test

$$\sum_{i=1}^m \log L_i \geq m \log k - (m-1) \frac{d}{2} \quad (\text{B-13})$$

As an example, let $m = 2$. The detector then performs the threshold test

$$\log L_1 + \log L_2 \geq 2 \log k - \frac{d}{2}$$

If $\log L_1$ and $\log L_2$ are considered as coordinates in a two-dimensional decision space, the curve dividing the space into "signal" and "no signal" regions is given by

$$\log L_1 + \log L_2 = 2 \log k - \frac{d}{2} \quad (\text{B-14})$$

This is seen to represent a straight line with slope -1 .

APPENDIX C

ERROR PROBABILITIES FOR A BAND-SPLITTING DETECTOR
WITH INDEPENDENT OUTPUTS

The conditional error probabilities are derived for a band-splitting detection scheme. The following events are defined:

S_0 = Event that noise only is present.

S_1 = Event that signal is present with frequency

$f_1, i = 1, 2, \dots, m.$

E_0 = Event that all m outputs lie below the fixed threshold value.

E_1 = Event that the i^{th} output exceeds its threshold value, $i = 1, 2, \dots, m.$

False Alarm

The conditional false alarm probability is given by

$$\begin{aligned} \alpha &= P [\text{at least one output exceeds its threshold} \\ &\quad \text{value, given that noise only is present}] \\ &= 1 - \prod_{i=1}^m [1 - P(E_i/S_0)] \end{aligned} \quad (C-1)$$

If the m outputs are independent, the probability of an event E_1 is not affected by the presence or absence of signal at any frequency other than f_1 . Thus

$$\text{Thus} \quad P(E_1/S_0) = P(E_1/S_1^*) \quad (C-2)$$

The right-hand side of Eq. (C-2) is seen to be the conditional false alarm probability for the threshold test at the i^{th} frequency, that is

$$P(E_i/S_1^0) = \alpha_i = P \left[\begin{array}{l} \text{the } i^{\text{th}} \text{ output exceeds its} \\ \text{threshold, given that no signal} \\ \text{is present with the frequency } f_i \end{array} \right] \quad (\text{C-3})$$

Thus, from Eqs. (C-1), (C-2), and (C-3),

$$\alpha = 1 - \prod_{i=1}^m (1 - \alpha_i) \quad (\text{C-4})$$

If α_i has the same value for $i = 1, 2, \dots, m$, then

$$\alpha = 1 - (1 - \alpha_i)^m \quad (\text{C-5})$$

False Dismissal

The conditional false dismissal probability is given by

$$\begin{aligned} \beta &= P \left[\begin{array}{l} \text{all } m \text{ outputs lie below the fixed threshold} \\ \text{value, given that the signal is present at any} \\ \text{one of the possible frequencies} \end{array} \right] \\ &= P(E_0/S_1 + S_2 + \dots + S_m) \end{aligned} \quad (\text{C-6})$$

If all m outputs are independent and have the same mean and variance, the probability of the event E_0 in the presence of signal is independent of the signal frequency. Thus

$$P(E_0/S_1 + S_2 + \dots + S_m) = P(E_0/S_i) \quad i = 1, 2, \dots, m \quad (\text{C-7})$$

From Eqs. (C-6) and (C-7) and the definition of E_0 ,

$$\begin{aligned} \beta &= P(E_0/S_1) & i &= 1, 2, \dots, m \\ &= P(E_1^*, E_2^*, \dots, E_m^*/S_1) & i &= 1, 2, \dots, m \end{aligned} \quad (C-8)$$

Since the outputs are independent,

$$\beta = \prod_{j=1}^m P(E_j^*/S_1) \quad i = 1, 2, \dots, m \quad (C-9)$$

For $i = j$,

$$P(E_j^*/S_j) = \beta_j = P[\text{the } j^{\text{th}} \text{ output is below its threshold,} \\ \text{given that a signal is present at the} \\ \text{frequency } f_j]$$

and for $i \neq j$,

$$P(E_j^*/S_i) = P(E_j^*/E_j^*) = 1 - \alpha_j \quad (C-10)$$

The first equality in Eq. (C-10) follows from the fact that the event E_j^* is independent of the presence or absence of signal at any frequency other than f_j . Since β_j is assumed to have the same value for all $j = 1, 2, \dots, m$ and α_j the same value for all $j = 1, 2, \dots, m$, Eq. (C-9) can be rewritten as

$$\beta = \beta_j (1 - \alpha_j)^{m-1}$$

(C-11)

APPENDIX D

CORRELATION COEFFICIENT RELATING Q_1 AND Q_2

The correlation coefficient is defined as

$$\rho = \frac{\text{cov}_N(Q_1, Q_2)}{\text{var}_N(Q_1) \text{var}_N(Q_2)} \quad (\text{D-1})$$

where:

$$Q_1 = \frac{A^2}{4N^2} \mathbf{v}_1' \mathbf{I} \mathbf{v}_1 + \text{bias} \quad (\text{D-2})$$

and

$$Q_2 = \frac{A^2}{4N^2} \mathbf{v}_2' \mathbf{I} \mathbf{v}_2 + \text{bias} \quad (\text{D-3})$$

where \mathbf{v}_j , $j = 1, 2, \dots$ represents a vector of samples of the output of the j^{th} pre-detection filter, an idealized rectangular filter of bandwidth B_S centered at the frequency f_j . For convenience, ρ will be calculated in terms of the following functional forms:

$$\lambda_1 = \int_0^T dt \, v_1^2(t) \quad (\text{D-4})$$

and

$$\lambda_2 = \int_0^T ds \, v_2^2(s) \quad (\text{D-5})$$

Thus Eq. (D-1) may be rewritten in the following equivalent form:

$$\rho = \frac{\text{cov}_N(\lambda_1, \lambda_2)}{\text{var}(\lambda_1) \text{var}(\lambda_2)} \quad (\text{D-6})$$

The numerator in Eq. (D-6) is

$$\begin{aligned} \text{cov}_N(\lambda_1, \lambda_2) &= \left\langle \left[\int_0^T dt v_1^2(t) - \left\langle \int_0^T dt v_1^2(t) \right\rangle_N \right] \left[\int_0^T ds v_2^2(s) - \left\langle \int_0^T ds v_2^2(s) \right\rangle_N \right] \right\rangle_N \\ &= \left\langle \int_0^T dt v_1^2(t) \int_0^T ds v_2^2(s) \right\rangle_N - \left\langle \int_0^T dt v_1^2(t) \right\rangle_N \left\langle \int_0^T ds v_2^2(s) \right\rangle_N \\ &= \int_0^T dt \int_0^T ds \left\langle v_1^2(t) v_2^2(s) \right\rangle_N - \int_0^T dt \left\langle v_1^2(t) \right\rangle_N \int_0^T ds \left\langle v_2^2(s) \right\rangle_N \\ &= \int_0^T dt \int_0^T ds \left[2 \left\langle v_1(t) v_2(s) \right\rangle_N^2 + N^2 \right] - \int_0^T dt N \int_0^T ds N \\ &= 2 \int_0^T dt \int_0^T ds \left\langle v_1(t) v_2(s) \right\rangle_N^2 \quad (\text{D-7}) \end{aligned}$$

The covariance $\left\langle v_1(t) v_2(s) \right\rangle_N$ represents the cross-correlation between the outputs of two pre-detection filters, one centered at f_1 and the other at f_2 . If steady state conditions

(i.e., $B_S T \gg 1$) are assumed, the cross-correlation function relating the outputs, x and y , of two linear filters having as inputs the same random noise process can be written as[†]

$$R_{xy}(\tau) = \int_{-\infty}^{\infty} d\sigma R_N(\sigma) \int_{-\infty}^{\infty} df H_1(j2\pi f) H_2(-j2\pi f) \exp[j2\pi f(-\sigma)] \quad (D-8)$$

where $R_N(\sigma)$ is the a.c.f. of the noise input, and $H_1(j2\pi f)$ and $H_2(j2\pi f)$ are the frequency response functions for the two filters. Here the noise is assumed white, hence

$$R_N(\sigma) = \frac{N_0}{2} \delta(\sigma) \quad (D-9)$$

Thus

$$R_{xy}(\tau) = \frac{N_0}{2} \int_{-\infty}^{\infty} df H_1(j2\pi f) H_2(-j2\pi f) \exp(j2\pi f\tau) \quad (D-10)$$

In the problem at hand, $H_1(j2\pi f)$ and $H_2(j2\pi f)$ are rectangular frequency responses of width B_S centered at f_1 and f_2 respectively. Thus the product of $H_1(j2\pi f)$ and $H_2(j2\pi f)$ indicated in Eq. (D-10) equals zero when $H_1(j2\pi f)$ and $H_2(j2\pi f)$ do not overlap in frequency; and when there is overlap, the product is another rectangular frequency response of bandwidth $B_S - |f_1 - f_2|$ centered at the frequency $(f_1 + f_2)/2$. Equation (D-10) expresses the inverse Fourier transform of this product,

[†] See, for example, Middleton (II, Section 3.4-2).

thus

$$R_{v_1 v_2}(\tau) = \begin{cases} N_0 \left(B_B - |f_1 - f_2| \right) \operatorname{sinc} \left(B_B - |f_1 - f_2| \right) \tau \cos \pi (f_1 + f_2) \tau & \text{if } |f_1 - f_2| < B_B \\ 0 & \text{if } |f_1 - f_2| \geq B_B \end{cases}$$

(D-11)

This cross-correlation function is

$$R_{v_1 v_2}(\tau) = \langle v_1(t) v_2(s) \rangle_N \quad (D-12)$$

where

$$\tau = t - s \quad (D-13)$$

The double integral in Eq. (D-7) may now be written as

$$\operatorname{cov}_N[\lambda_1, \lambda_2] = 2N_0^2 \left(B_B - |f_1 - f_2| \right)^2 \int_0^T dt \int_0^T ds \operatorname{sinc}^2 \left(B_B - |f_1 - f_2| \right) (t-s) \cos^2 \pi (f_1 + f_2)(t-s)$$

$$= N_0^2 \left(B_B - |f_1 - f_2| \right)^2 \int_0^T dt \int_0^T ds \operatorname{sinc}^2 \left(B_B - |f_1 - f_2| \right) (t-s)$$

$$= N_0^2 \int_0^{[B_B - |f_1 - f_2|]T} dx \int_0^{[B_B - |f_1 - f_2|]T} dy \operatorname{sinc}^2(x-y)$$

Therefore

$$\operatorname{cov}_N(\lambda_1, \lambda_2) = N_0^2 [B_B - |f_1 - f_2|]T \quad , \quad |f_1 - f_2| < B_B \quad (D-14)$$

The last approximation leading to Eq. (D-14) requires that

$[B_S - |f_1 - f_2|]T \gg 1$. Similarly,

$$\begin{aligned}
 \text{var}_N(\lambda_1) &= \left\langle \left[\int_0^T dt v_1^2(t) - \left\langle \int_0^T dt v_1^2(t) \right\rangle_N \right] \left[\int_0^T ds v_1^2(s) - \left\langle \int_0^T ds v_1^2(s) \right\rangle_N \right] \right\rangle_N \\
 &= \left\langle \int_0^T dt v_1^2(t) \int_0^T ds v_1^2(s) \right\rangle_N - \left\langle \int_0^T dt v_1^2(t) \right\rangle_N \left\langle \int_0^T ds v_1^2(s) \right\rangle_N \\
 &= \int_0^T dt \int_0^T ds \left\langle v_1^2(t) v_1^2(s) \right\rangle_N - \int_0^T dt \left\langle v_1^2(t) \right\rangle_N \int_0^T ds \left\langle v_1^2(s) \right\rangle_N \\
 &= \int_0^T dt \int_0^T ds \left[2 \left\langle v_1(t) v_1(s) \right\rangle_N^2 + N^2 \right] - \int_0^T dt N \int_0^T ds N \\
 &= 2 \int_0^T dt \int_0^T ds \left\langle v_1(t) v_1(s) \right\rangle_N^2 \\
 &= 2N_0^2 B_S^2 \int_0^T dt \int_0^T ds \text{sinc}^2 B_S(t-s) \cos^2 2f_1(t-s) \\
 &\approx N_0^2 B_S^2 \int_0^T dt \int_0^T ds \text{sinc}^2 B_S(t-s)
 \end{aligned}$$

Therefore

$$\text{var}_N(\lambda_1) = N_o^2 B_B T \quad (D-15)$$

Also

$$\text{var}_N(\lambda_2) = N_o^2 B_B T \quad (D-16)$$

When Eqs. (D-14), (D-15) and (D-16) are substituted into Eq. (D-6), the result is

$$\rho = \frac{B_B - |f_1 - f_2|}{B_B}, \quad |f_1 - f_2| < B_B \quad (D-17)$$

When the frequency responses of the two pre-detection filters overlap by an amount

$$B_B - |f_1 - f_2| = \frac{B_B}{2} \quad (D-18)$$

then

$$\rho = \frac{1}{2} \quad (D-19)$$

APPENDIX E DIAGRAMS FOR THE EXPERIMENTAL DETECTOR

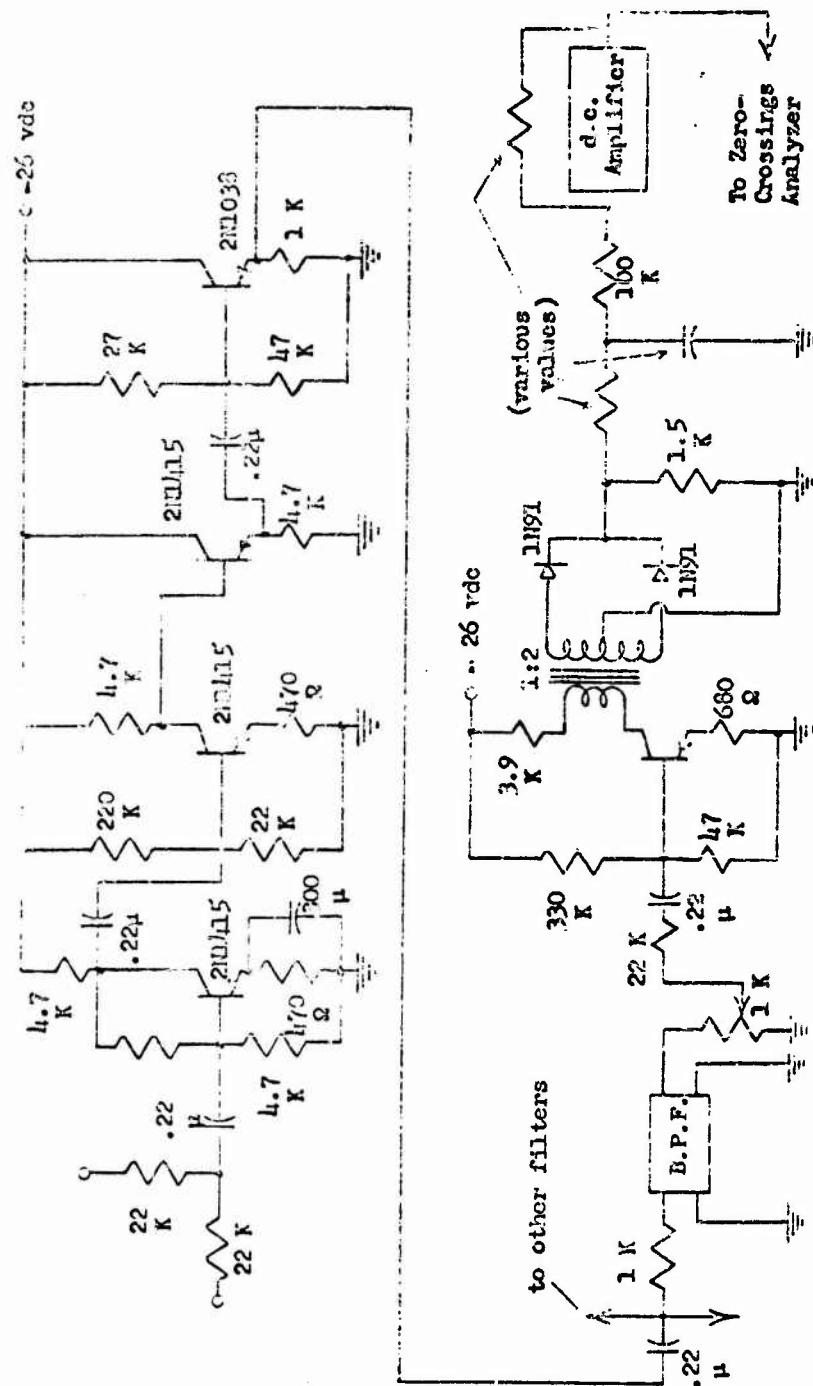


Fig. E.1. One Channel of the Experimental Band-Splitting Detector

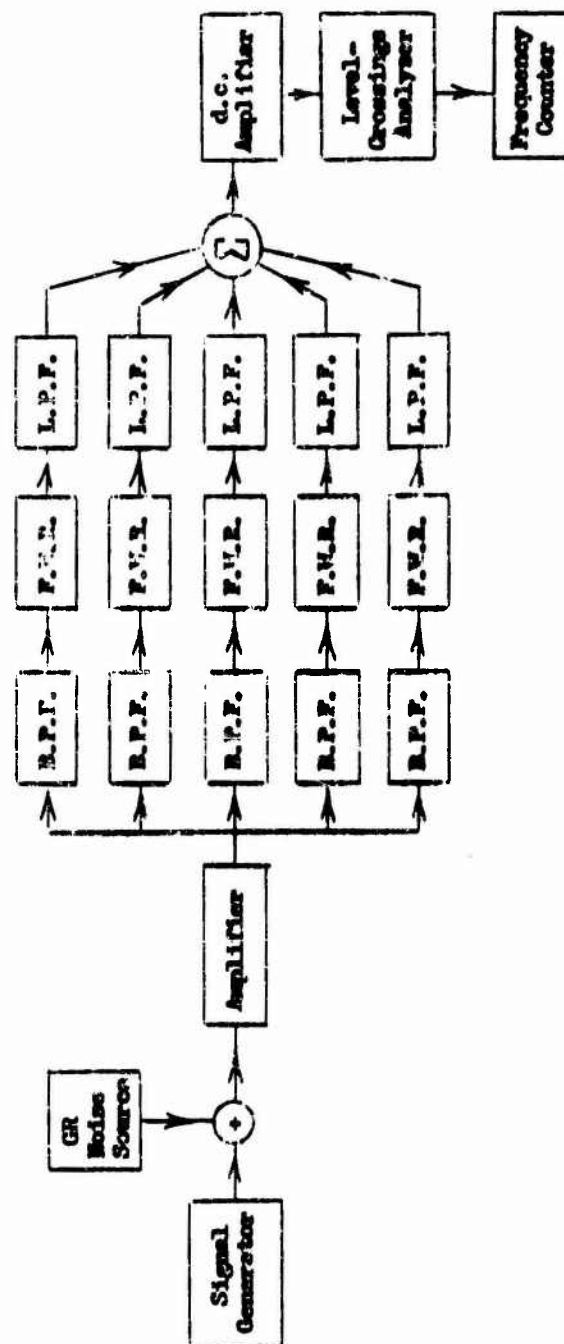


Fig. E.2. Instrumentation of an Experimental Detector
(See-and-Test Configuration Shown)

LIST OF PRINCIPAL SYMBOLS

$\frac{A^2}{2}$	= signal power
a	= a signal amplitude
B	= width of processing band
B_S	= width of signal spectrum
b	= number of filters in a band-splitting detector
D, d, d'	= detection indices
\underline{G}_c	= detector coefficient matrix
f	= signal frequency
f_c	= signal center frequency
\underline{K}	= noise covariance matrix
k, k'	= threshold settings
$L(h, k, \rho)$	= standardized bivariate normal probability integral
$L(\underline{y}/f)$	= likelihood ratio, given the signal frequency
$\bar{l}(\underline{y})$	= average likelihood ratio
N	= noise variance
N_0	= noise spectral level, volt ² /cps
n	= number of time samples
\underline{n}	= noise vector
\underline{P}	= signal covariance matrix
$Q(f), Q'(f), q(f)$	= test quantities generated by band-splitting detectors
R, R_S	= pre-detection signal-to-noise ratios
$R(\tau)$	= an autocorrelation function
r	= frequency uncertainty ratio

- $s(t), \underline{s}$ = signal to be detected
- T = observation time of the received signal
- $v(t), \underline{v}$ = received signal
- $\hat{v}(t), \hat{\underline{v}}$ = Hilbert transforms of $v(t)$ and \underline{v}
- W = cutoff frequency of the noise spectrum
- α, α_1 = conditional false-alarm probabilities
- β, β_1 = conditional false-dismissal probabilities
- μ_{ij} = a covariance
- ρ = correlation coefficient
- σ = that fraction of the signal power appearing in the pass band of a pre-detection filter
- ψ = output of an envelope detector
- $\{A_{ij}\}$ = a matrix of terms A_{ij}
- $\det \underline{A}$ = determinant of the matrix \underline{A}
- $\text{tr } \underline{A}$ = trace of the matrix \underline{A} = sum of the diagonal elements of \underline{A}

Abbreviations

- a.c.f. = autocorrelation function
- LR = likelihood ratio
- p.d.f. = probability density function

REFERENCES

Cramér, Harald:

- I. Mathematical Methods of Statistics, Princeton University Press, Princeton, New Jersey, 1946.

Davenport, Wilbur B., and William L. Root:

- I. An Introduction to the Theory of Random Signals and Noise, McGraw-Hill Book Company, New York, 1958.

Deutsch, Ralph:

- I. Nonlinear Transformations of Random Processes, Prentice-Hall, Inc., Englewood Cliffs, New Jersey, 1962.

Helstrom, Carl W.:

- I. Statistical Theory of Signal Detection, Pergamon Press, New York, 1960.

Lehmann, E. L.:

- I. Testing Statistical Hypotheses, J. Wiley and Sons, New York, 1959.

Levesque, Allen H.:

- I. "Likelihood Ratio Detection for Long Observation Times," Progress Report No. 14, General Dynamics/Electric Boat Research, Yale University, May 1964.
- II. "Optimal Detection of a Coherent Sinusoid With Unknown Frequency," Progress Report No. 15, General Dynamics/Electric Boat Research, Yale University, June 1964.

Middleton, David:

- I. "On the Detection of Stochastic Signals in Additive Normal Noise - Part I," IRE Trans. on Information Theory, IT-3, pp. 86-121, June 1957.
- II. An Introduction to Statistical Communication Theory, McGraw-Hill Book Company, New York, 1960.

National Bureau of Standards:

- I. Tables of Normal Probability Functions, Applied Mathematics Series, No. 23, Washington, 1953.
- II. Tables of the Bivariate Normal Distribution Function and Related Functions, Applied Mathematics Series, No. 50, Washington, 1959.
- III. Handbook of Mathematical Functions, Applied Mathematics Series, No. 55, Washington, 1964.

Neyman, J., and E. S. Pearson:

- I. "On the Problem of the Most Efficient Tests of Statistical Hypotheses", Phil. Trans. Royal Soc. London, A231, pp. 289-337, 1933.

Rice, Steven G.:

- I. "Mathematical Analysis of Random Noise", reprinted in Wax, Nelson, Selected Papers on Noise and Stochastic Processes, Dover, New York, 1954.



SOME SUBOPTIMAL TECHNIQUES FOR DETECTING PASSIVE SONAR TARGETS
IN THE PRESENCE OF INTERFERENCE

by

Peter M. Schultheiss

Progress Report No. 21

General Dynamics/Electric Boat Research

(53-00-10-0231)

(8050-33-55001)

June 1965

DEPARTMENT OF ENGINEERING
AND APPLIED SCIENCE

YALE UNIVERSITY

Summary

This report deals with suboptimal instrumentations that approximate the performance of the likelihood-ratio detector described in Report No. 17. The objective is the detection of a weak target in the presence of interference from a possibly very much stronger target as well as ambient noise. The proposed instrumentations eliminate interference by steering the array on the interference and then subtracting the outputs of various hydrophones pairwise. The signal components of the resultant differences are then aligned by a second set of delay elements whose outputs are added, squared and smoothed in conventional manner. The results of the report indicate in general that it is quite feasible to approach the performance of the likelihood-ratio detector of Report No. 17 with instrumentations of moderate complexity.

The simplest instrumentation investigated uses adjacent hydrophones to null the interference. For arrays of reasonable size and targets separated from the interference by more than a certain minimum angle, the degradation in output signal-to-noise ratio relative to the likelihood-ratio detector is quite small. Specifically, for a 40-element linear array with 2-ft hydrophone spacing and a bandwidth of $2\pi \times 5000$ rad/sec, it amounts to less than 1.5 db in equivalent input signal-to-noise ratio as long as the interference is separated by at least 5° from the (broadside) target. On the other hand, with the same parameter values the average bearing response pattern shows a significantly reduced peak for targets closer than about 20° from the interference. To overcome this difficulty an analysis was carried out on a modified instrumentation that nulls interference by subtracting non-adjacent hydrophone outputs (after alignment with the interference). By this procedure it was possible to obtain only small reductions in target peaks for targets as close as 5° to the interference.

I. Introduction

Report No. 17 discussed the performance of an optimal (likelihood-ratio) detector for the passive detection of a sonar target in the presence of ambient noise and interference from a second target. One result of this study was the conclusion that interference angularly separated from the target by more than some minimal amount can be eliminated completely at the expense of no more than one hydrophone. In other words, it is possible to design a detector whose performance in the presence of interference is no worse than that of a detecting array using one less hydrophone and operating under the same conditions of ambient noise and target signal but in the absence of interference. No attempt was made to determine the complexity of the instrumentation required to realize the optimum detector or to find simple suboptimal schemes that might approximate the performance of the likelihood-ratio detector. The present report deals with two such suboptimal schemes.

The first proposed instrumentation is shown schematically in Fig. 1. A linear array consisting of M equally spaced hydrophones is assumed.

The hydrophone outputs s_1+n_1, \dots, s_M+n_M are delayed to align the interference components and are then subtracted pairwise to eliminate the interference. The resulting differences x_1, x_2, \dots, x_{M-1} are delayed once more in such a manner as to align their signal components. The outputs of the second set of delays are summed, squared and filtered in the conventional manner.

Suppose that the signal bearing is such that the signal delay from hydrophone to hydrophone is t_0 . Then the signal components s_i of the hydrophone outputs are related by the equation

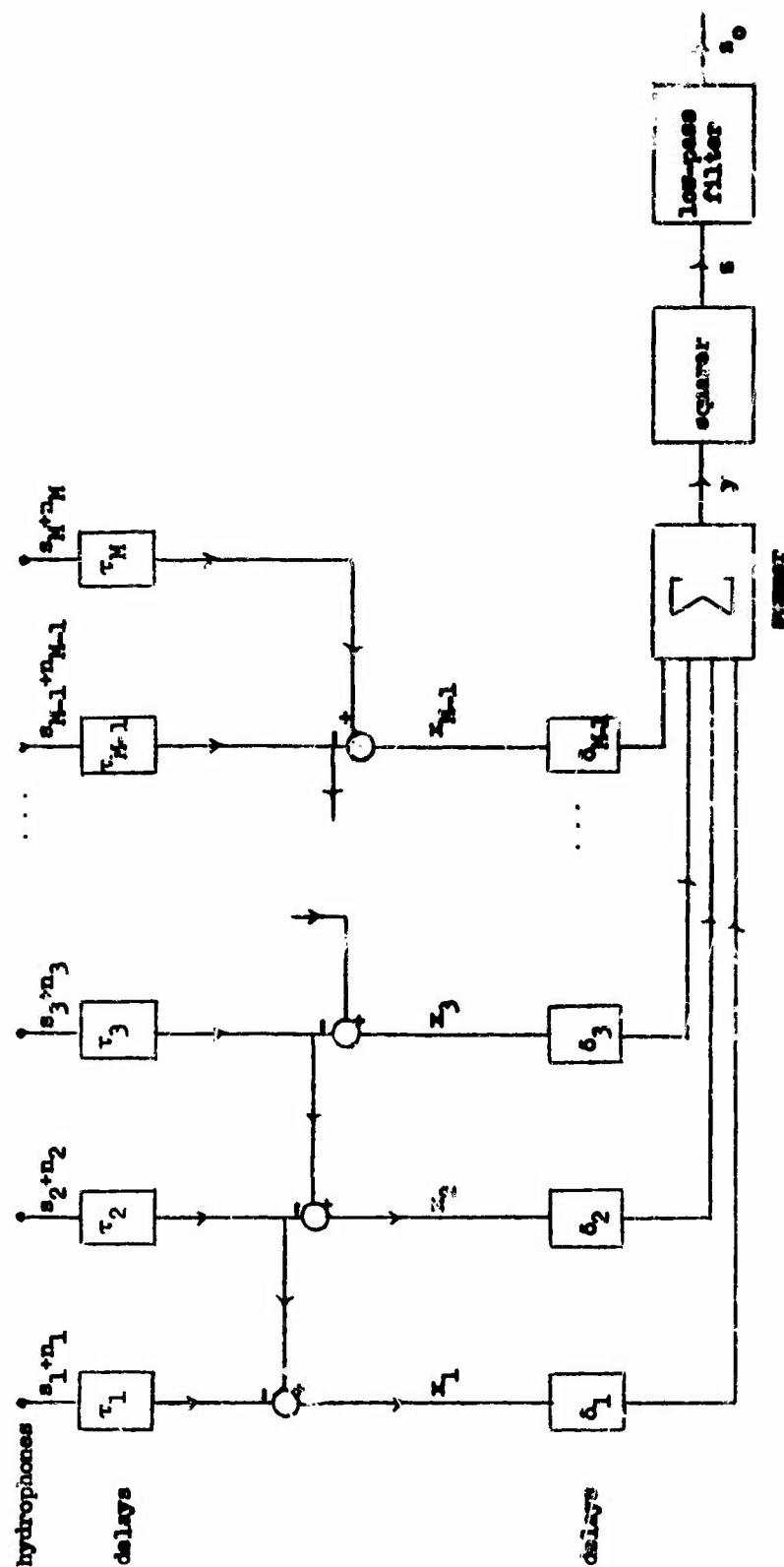


FIGURE 1

$$s_i(t) = s_1[t + (1-i)t_0] \quad , \quad i=1,2,\dots,M \quad (1)^1$$

Suppose, further, that the interference delay from hydrophone to hydrophone is Δ . Then the delays τ_i required for interference elimination are given by

$$\tau_i = (i-1)\Delta \quad , \quad i=1,2,\dots,M \quad (2)^2$$

It follows that the outputs of the subtracting circuits assume the form

$$x_i(t) = s_1[t + i(t_0 - \Delta)] - s_1[t + (i-1)(t_0 - \Delta)] + n_{i+1}[t - i\Delta] - n_1[t - (i-1)\Delta] \quad ,$$

$$i=1,2,\dots,M-1 \quad (3)$$

Here $n_i(t)$ is the ambient noise component of the i^{th} hydrophone output. The parameter $t_0 - \Delta$ is, of course, a measure of the target bearing relative to the interference bearing. Thus if the target bearing is θ_T and the interference bearing θ_I (both measured counterclockwise from the broadside condition),

$$t_0 - \Delta = \frac{d}{c}(\sin \theta_I - \sin \theta_T) \quad (4)$$

where d is the spacing from hydrophone to hydrophone and c is the velocity of sound.

The second set of delays (δ_i) is adjusted so that

$$\delta_i = i(t_0 - \Delta) \quad , \quad i=1,2,\dots,M-1 \quad (5)$$

Then the output $y(t)$ of the summer is given by

¹This implies a target located to the right of the broadside condition if $t_0 > 0$.

²This implies interference located to the right of the broadside condition if $\Delta > 0$.

$$\begin{aligned}
 y(t) &= \sum_{i=1}^{M-1} \left\{ s_1(t) - s_1[t-(t_0-\Delta)] + n_{1+1}(t-t_0) - n_1(t-t_0+\Delta) \right\} \\
 &= (M-1) \left\{ s_1(t) - s_1[t-(t_0-\Delta)] \right\} + \sum_{i=1}^{M-1} \left\{ n_{1+1}(t-t_0) - n_1(t-t_0+\Delta) \right\} \quad (6)^1
 \end{aligned}$$

The output of the squarer now assumes the form

$$\begin{aligned}
 z(t) &= (M-1)^2 \left\{ s_1(t) - s_1[t-(t_0-\Delta)] \right\}^2 \\
 &\quad + 2(M-1) \left\{ s_1(t) - s_1[t-(t_0-\Delta)] \right\} \left\{ \sum_{i=1}^{M-1} [n_{1+1}(t-t_0) - n_1(t-t_0+\Delta)] \right\} \\
 &\quad + \sum_{i=1}^{M-1} \sum_{j=1}^{M-1} [n_{1+1}(t-t_0) - n_1(t-t_0+\Delta)] [n_{j+1}(t-t_0) - n_j(t-t_0+\Delta)] \quad (7)
 \end{aligned}$$

As in previous reports, the performance of the system will be characterized by the figure of merit $\frac{A(\text{DC output})}{D(\text{output})}$, i.e., by the ratio of the difference of the average values of s_0 with and without target divided by the standard deviation of s_0 (the latter computed in the absence of target under the usual small-signal assumption).

¹The difference form of the signal term reflects a loss of signal due to the interference elimination procedure. Note, however, that the noise term also contains combinations such as $n_2(t-t_0) - n_2[t-t_0-(t_0-\Delta)]$, so that the overall sacrifice in signal-to-noise ratio (and hence detectability) is not as great as might appear at first glance.

II. Computation of the Figure of Merit

The numerator of the figure of merit is easily computed. The change in DC output is clearly independent of the noise, and if the DC gain of the low-pass filter is unity (as can be assumed without loss of generality), the average of s_o is the same as the average of s . It follows that

$$\Delta(\text{DC output}) = (M-1)^2 \left[E\{s_1^2(t)\} + E\{s_1^2[t-(t_o-\Delta)]\} - 2E\{s_1(t) s_1[t-(t_o-\Delta)]\} \right] \quad (8)$$

where $E\{\}$ denotes the expectation of the bracketed quantity. If the signal is a stationary random process with average power S and normalized autocorrelation function $\rho_s(\tau)$, then Eq. (8) becomes

$$\Delta(\text{DC output}) = 2(M-1)^2 S [1 - \rho_s(t_o - \Delta)] \quad (9)$$

The variance of s_o is obtained most conveniently by integrating the output power spectrum. The bandwidth of the low-pass filter is undoubtedly very narrow compared with the bandwidth of $s(t)$, so that the spectrum of s can be well approximated for the entire band passed by the low-pass filter by its value $G_s(0)$ at zero frequency. Hence it suffices to calculate $G_s(0)$, which for Gaussian signal and noise is readily derived from the spectrum $G_y(\omega)$ of y . The latter spectrum will therefore be derived first.

From Eq. (6) the autocorrelation $R_y(\tau)$ of y is

$$\begin{aligned} R_y(\tau) &= (M-1)^2 S \left\{ 2\rho_s(\tau) - \rho_s(\tau+t_o-\Delta) - \rho_s[\tau-(t_o-\Delta)] \right\} \\ &\quad + \sum_{i=1}^{M-2} \left[2\rho_n(\tau) - \rho_n(\tau+t_o-\Delta) - \rho_n(\tau-t_o+\Delta) \right] + 2N\rho_n(\tau) \\ &= (M-1)^2 S \left\{ 2\rho_s(\tau) - \rho_s(\tau+t_o-\Delta) - \rho_s[\tau-(t_o-\Delta)] \right\} \\ &\quad + N \left\{ 2(M-1)\rho_n(\tau) - (M-2)[\rho_n(\tau+t_o-\Delta) + \rho_n(\tau-t_o+\Delta)] \right\} \end{aligned} \quad (10)$$

where $M\rho_n(\tau)$ is the autocorrelation of the noise at each hydrophone, and the noise outputs at different hydrophones are assumed to be uncorrelated.¹ Under the usual small-signal assumption $[(M-1)E \ll N]$ the signal term in Eq. (10) will be ignored in further computations.

If the noise component of each hydrophone output is a Gaussian random process, then the entire noise component of Eq. (6) is a Gaussian random process. For this case Rice has derived a simple relation between the power spectrum $G_y(\omega)$ of $y(t)$ and the power spectrum $G_z(\omega)$ of $z(t) = y^2(t)$. In terms of the nomenclature used in this report the desired zero-frequency value of $G_z(\omega)$ is

$$G_z(0) = 2 \int_0^{\infty} G_y^2(\omega) d\omega \quad (11)^2$$

The spectrum is here defined in such a manner that the integral over all positive frequencies yields the total power.

In order to carry the analysis further, it is necessary to assume a specific form for the noise autocorrelation function $\rho_n(\tau)$. One would not expect this choice to be critical as long as it corresponds to a reasonable distribution of noise power over an appropriate frequency band. A convenient idealized version of such a distribution is represented by

$$\rho_n(\tau) = \frac{\sin \omega_0 \tau}{\omega_0 \tau} \quad (12)$$

¹The effect of noise correlation from hydrophone to hydrophone has been studied in several earlier reports (see, e.g., Report No. 3) and is not of central interest to the present investigation.

²S. O. Rice, "The Mathematical Analysis of Random Noise," B.S.T.J., January 1945, Eq. 4.5-5.

which corresponds to the power spectrum

$$G_R(\omega) = \begin{cases} \frac{N}{\omega_0} & |\omega| \leq \omega_0 \\ 0 & |\omega| > \omega_0 \end{cases} \quad (13)^1$$

A somewhat different noise spectrum will be considered later for comparison.

Under the definitions used here, spectra and correlation functions are related by the expression

$$G(\omega) = \frac{1}{\pi} \int_{-\infty}^{\infty} R(\tau) e^{-j\omega\tau} d\tau \quad (14)$$

Applying Eqs. (14) and (12) to Eq. (10) and ignoring the term in 3, one obtains

$$G_Y(\omega) = \frac{2}{\pi} N(M-1) \int_{-\infty}^{\infty} \frac{\sin \omega_0 \tau}{\omega_0 \tau} e^{-j\omega\tau} d\tau \\ - \frac{1}{\pi} N(M-2) \int_{-\infty}^{\infty} \left[\frac{\sin \omega_0 (\tau+t_0-\Delta)}{\omega_0 (\tau+t_0-\Delta)} + \frac{\sin \omega_0 (\tau-t_0+\Delta)}{\omega_0 (\tau-t_0+\Delta)} \right] e^{-j\omega\tau} d\tau \quad (15)$$

Using Eq. (13) and the real translation theorem, one can write down the result of this integration immediately:

$$G_Y(\omega) = \begin{cases} \frac{2N}{\omega_0} [(M-1) - (M-2) \cos \omega(t_0-\Delta)] & \text{for } |\omega| \leq \omega_0 \\ 0 & \text{for } |\omega| > \omega_0 \end{cases} \quad (16)$$

¹More generally, this may be regarded as the effective noise spectrum after the customary prewhitening operation with a band limitation to $0 \leq \omega \leq \omega_0$.

Now from Eq. (11)

$$\begin{aligned}
 G_s(0) &= \frac{6N^2}{\omega_o^2} \int_0^{\omega_o} \left[(M-1) - (M-2) \cos \omega(t_o - \Delta) \right]^2 d\omega \\
 &= \frac{6N^2}{\omega_o} \left\{ (M-1)^2 + \frac{1}{2}(M-2)^2 - 2(M-1)(M-2) \frac{\sin \omega_o(t_o - \Delta)}{\omega_o(t_o - \Delta)} + \frac{1}{2}(M-2)^2 \frac{\sin 2\omega_o(t_o - \Delta)}{2\omega_o(t_o - \Delta)} \right\}
 \end{aligned}
 \quad (17)$$

If the low-pass filter is a finite time integrator averaging $s(t)$ over the past T seconds, then from Report No. 3, Eq. (39), the variance of $z_o(t)$ is

$$\begin{aligned}
 D^2(z_o) &= \frac{\pi}{T} G_s(0) \\
 &= \frac{6\pi}{\omega_o T} N^2 \left\{ (M-1)^2 + \frac{1}{2}(M-2)^2 - 2(M-1)(M-2) \frac{\sin \omega_o(t_o - \Delta)}{\omega_o(t_o - \Delta)} \right. \\
 &\quad \left. + \frac{1}{2}(M-2)^2 \frac{\sin 2\omega_o(t_o - \Delta)}{2\omega_o(t_o - \Delta)} \right\}
 \end{aligned}
 \quad (18)$$

Now from Eqs. (9) and (18)¹

$$\begin{aligned}
 \frac{\Delta(\text{DC output})}{D(\text{output})} &= \frac{1 - \frac{\sin \omega_o(t_o - \Delta)}{\omega_o(t_o - \Delta)}}{\sqrt{1 + \frac{1}{2} \left(\frac{M-2}{M-1} \right)^2 - 2 \left(\frac{M-2}{M-1} \right) \frac{\sin \omega_o(t_o - \Delta)}{\omega_o(t_o - \Delta)} + \frac{1}{2} \left(\frac{M-2}{M-1} \right)^2 \frac{\sin 2\omega_o(t_o - \Delta)}{2\omega_o(t_o - \Delta)}}} \\
 &= (M-1) \sqrt{\frac{\omega_o T}{2\pi}} \frac{S}{N}
 \end{aligned}
 \quad (19)$$

¹ Assuming the form $\rho_s(\tau) = (\sin \omega_o \tau) / \omega_o \tau$ for the normalized signal autocorrelation function.

Figure 2 shows Eq. (19), normalized with respect to $\sqrt{\frac{\omega_0 T}{2\pi}} \frac{S}{N}$, plotted as a function of $\omega_0(t_0 - \Delta)$ for $M=40$. The curve is labelled "nulling detector with prewhitening."¹ Also shown is the corresponding curve for a likelihood-ratio detector, taken from Report No. 17, Fig. 4. For large values of $\omega_0(t_0 - \Delta)$, Eq. (19) reduces to

$$\frac{\Delta(\text{LC output})}{D(\text{output})} \approx (M-1) \sqrt{\frac{\omega_0 T}{2\pi}} \frac{S}{N} \frac{1}{\sqrt{1 + \frac{1}{2} \left(\frac{M-2}{M-1} \right)^2}} \quad (20)^2$$

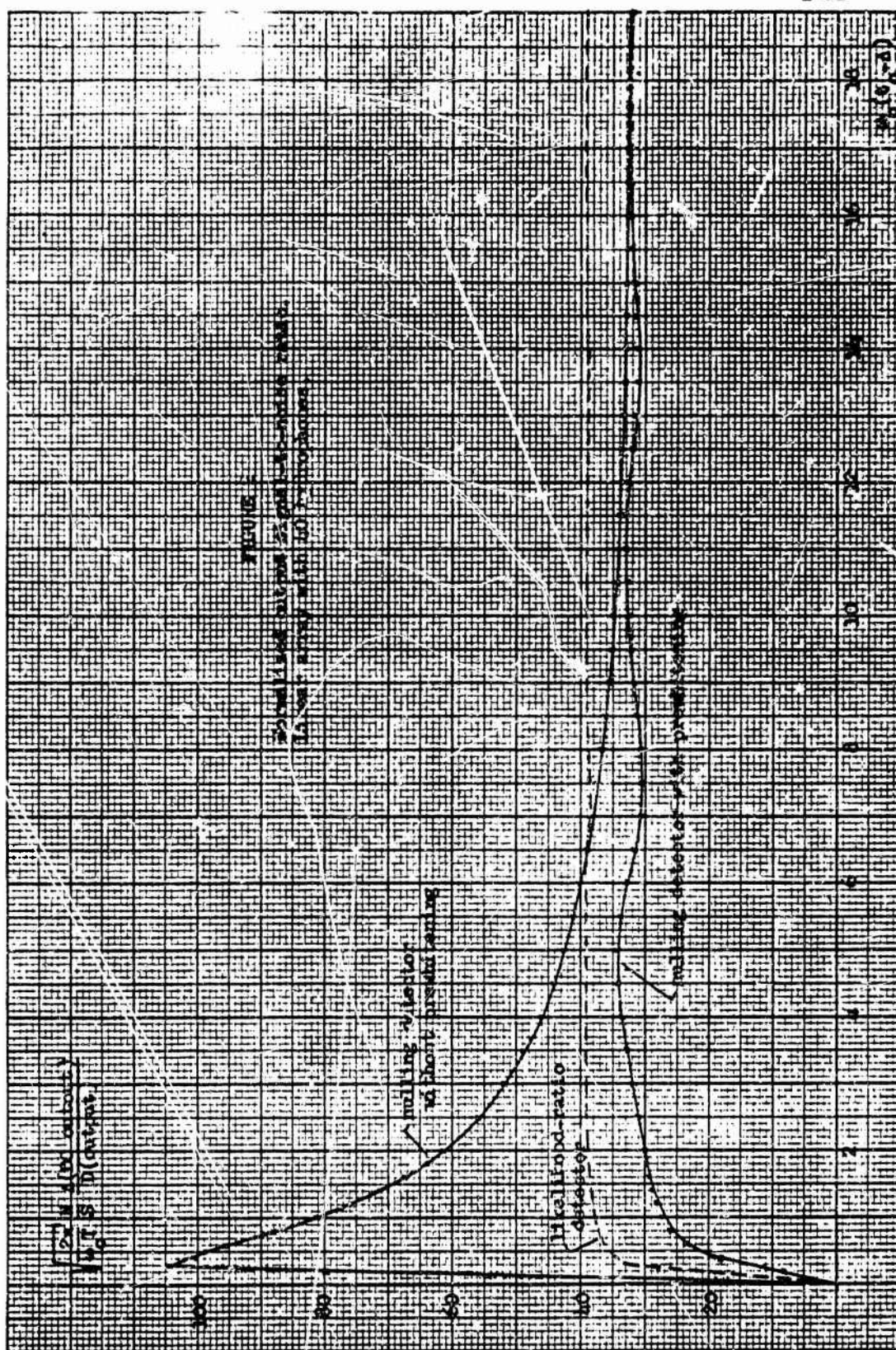
The radical in the denominator of Eq. (20) has a minimum value of unity for $M=2$ and a maximum value of $\sqrt{\frac{3}{2}}$ for $M \rightarrow \infty$. The expression for large M for the likelihood-ratio detector is from Report No. 17 [Eq. (38)]:

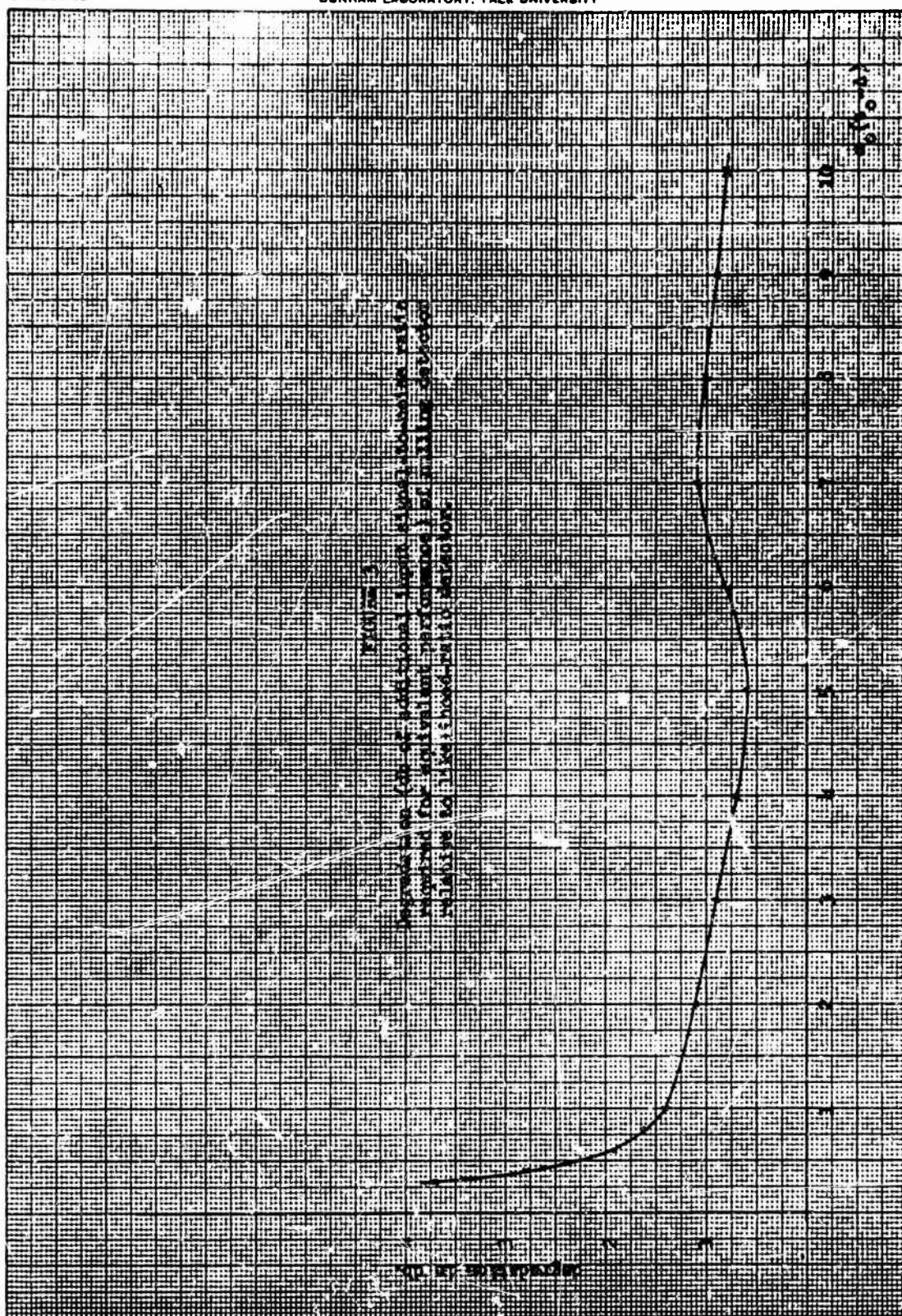
$$\frac{\Delta(\text{DC output})}{D(\text{output})} \approx (M-1) \sqrt{\frac{\omega_0 T}{2\pi}} \frac{S}{N} \quad (21)$$

Hence the degradation of performance of the proposed nulling detector relative to the likelihood-ratio detector is equivalent to only 0.88 db of input signal-to-noise ratio for large M and for target and interference well separated in angle. While the exact amount of degradation obviously depends on the relative bearing of target and interference, Fig. 2 suggests that this dependence is not very strong for relative bearings above a rather small minimum value. Figure 3 clarifies this point by showing the degradation (in terms of equivalent input signal-to-noise ratio) as a function of $(t_0 - \Delta)\omega_0$.

¹The oscillatory behavior for large values of $\omega_0(t_0 - \Delta)$ is the result of the somewhat artificial assumption of sharp cutoff of the signal band at $\omega = \omega_0$.

²This is also the exact expression for values of $\omega_0(t_0 - \Delta)$ equal to integral multiples of π .





The curve shows no drastic deviation from the asymptotic value for $\omega_0(t_0 - \Delta)$ above the order of unity. With $\omega_0 = 2\pi \times 5000$ rad/sec, a hydrophone spacing of 2 feet and the target in broadside condition, $\omega_0(t_0 - \Delta) = 1$ corresponds to an interference bearing of about 5° .

If the hydrophone outputs are not prewhitened, it might be reasonable to assume signal and noise spectra of the form

$$G_s(\omega) = \frac{2\omega_s S}{\pi(\omega^2 + \omega_s^2)} \quad (22)$$

and

$$G_n(\omega) = \frac{2\omega_n N}{\pi(\omega^2 + \omega_n^2)} \quad (23)$$

These correspond to the normalized autocorrelation functions

$$\rho_s(\tau) = \rho_n(\tau) = e^{-\omega_s |\tau|} \quad (24)$$

Following a computational procedure entirely equivalent to that covered by Eqs. (14)-(19), one arrives at the figure of merit

$$\frac{1(\text{DC output})}{D(\text{output})} = (M-1) \sqrt{\frac{\omega_s T}{2}} \frac{S}{N} \times \frac{e^{-\omega_s |t_0 - \Delta|}}{1 - e^{-\omega_s |t_0 - \Delta|}} \sqrt{1 + \frac{1}{2} \left(\frac{M-2}{M-1} \right)^2 - 2 \left(\frac{M-2}{M-1} \right) \left[1 + |t_0 - \Delta| \omega_s \right] e^{-|t_0 - \Delta| \omega_s} + \frac{1}{2} \left(\frac{M-2}{M-1} \right)^2 \left[1 + 2 |t_0 - \Delta| \omega_s \right] e^{-2 |t_0 - \Delta| \omega_s}} \quad (25)$$

Equation (25) is shown plotted on Fig. 2 with the label "mulling detector without prewhitening." For the reasons discussed in Report No. 17 (page 23), the parameter ω_s is chosen as $\omega_s = \omega_0/\pi$. The curve exhibits a strikingly

high peak near $\omega_0 |t_0 - \Delta| = 0.3$, a peak well above the level reached by the corresponding curve for the likelihood-ratio detector. This does not represent a contradiction, because Eq. (25) implies that the processed frequency range is infinite, whereas the likelihood ratio detector [and the instrumentation of Eq. (19)] was limited rather arbitrarily to the band $0 \leq \omega \leq \omega_0$. From a physical point of view, the peak is due to the fact that each noise component (except n_1 and n_N) enters twice into y , once with positive sign and once with negative sign. If the delay between these two contributions is small compared with the correlation time of $p_n(\tau)$, there is effective noise cancellation. There is also signal cancellation, of course, but for a small range of values of $\omega_0 |t_0 - \Delta|$ the noise cancellation effect dominates. One should keep in mind, however, that both signal and noise levels are very small, so that even small amounts of circuit noise entering after the subtracting circuits would drastically degrade performance. One should also keep in mind that with sharp limitation of the processed frequency range (probably required in practice by the dominance of self-noise at higher frequencies) the figure of merit cannot exceed that of the likelihood-ratio detector. It appears unlikely, therefore, that the sharp peak in the unprewhitened curves can be exploited to practical advantage.

III. The Bearing Response Pattern

The figure of merit computed in the previous section measures detection capability with the array steered on target. The results of that section together with the results of Report No. 17 indicate that the postulated instrumentation can eliminate the effect of a single interfering signal at a cost of one hydrophone and about 1 db of effective input signal-to-noise

ratio.¹ A second measure of performance frequently used in practice is the average bearing response pattern, the average value of s_0 as a function of steering angle. If the pattern of the proposed instrumentation is similar to that of a simple M-element linear array operating in the absence of interference, then it certainly appears reasonable to assert that the nulling procedure handles the interference problem effectively. On the other hand, if the average bearing response pattern of the proposed instrumentation shows a less pronounced peak at the target bearing, one should not conclude immediately that the target is therefore less detectable. Equations (19) and (25) indicate, in fact, that for a given observation time the output signal-to-noise ratio (and hence detectability) will be almost as great as that of the linear M-element array operating in the absence of interference. However, what is necessary to achieve detection is to compare the output for each bearing with a threshold preset in accordance with the ambient noise power² and the allowed false-alarm rate. Simple visual observation of the bearing response pattern may not be the most useful detection procedure. The results of Sections III and IV should be read with these considerations in mind.

The array is steered on target by adjusting the delays $\delta_1, \delta_2, \dots, \delta_{M-1}$ in Fig. 1 to the values given by Eq. (5). A general steering angle is obtained by choosing

$$\delta_i = 1(t_1 - \Delta) \quad , \quad i = 1, 2, \dots, M-1 \quad (26)$$

¹Except for interference in very close angular proximity to the target.

²This implies the assumption that the ambient noise power is known. However, the results of Report No. 18 suggest strongly that no serious degradation in performance would result from lack of a priori knowledge of the ambient noise power as long as the number of hydrophones is reasonably large ($M=40$ should be ample). The ambient noise power can then in effect be measured to an adequate degree of accuracy during the observation period.

and permitting t_1 to vary. The delays $\tau_1, \tau_2, \dots, \tau_M$ remain adjusted as specified by Eq. (2) in order to maintain interference elimination. Using Eqs. (3) and (26), one obtains for the output $y(t)$ of the summer

$$y(t) = \sum_{i=1}^{M-1} \left\{ a_1 [t + i(t_0 - t_1)] - a_1 [t + i(t_0 - t_1) - (t_0 - \Delta)] + n_{i+1}(t - it_1) - n_i(t - it_1 + \Delta) \right\} \quad (27)$$

The output $z(t)$ of the squarer is

$$z(t) = \sum_{i=1}^{M-1} \sum_{j=1}^{M-1} \left\{ a_1 [t + i(t_0 - t_1)] - a_1 [t + i(t_0 - t_1) - (t_0 - \Delta)] + n_{i+1}(t - it_1) - n_i(t - it_1 + \Delta) \right\} \times \\ \left\{ a_1 [t + j(t_0 - t_1)] - a_1 [t + j(t_0 - t_1) - (t_0 - \Delta)] + n_{j+1}(t - jt_1) - n_j(t - jt_1 + \Delta) \right\} \quad (28)$$

The average bearing response pattern is the average value of Eq. (28) plotted as a function of t_1 . Using the fact that each noise component is uncorrelated with the signal and with all other noise components, one can easily compute the average (expected) value of Eq. (28):

$$\langle z(t) \rangle = \sum_{i=1}^{M-1} \sum_{j=1}^{M-1} \left\{ 2\rho_s [(i-j)(t_0 - t_1)] - \rho_s [(i-j)(t_0 - t_1) + (t_0 - \Delta)] - \rho_s [(i-j)(t_0 - t_1) - (t_0 - \Delta)] \right. \\ \left. + \sum_{i=1}^{M-1} \sum_{j=1}^{M-1} \left\{ \overline{n_{i+1}(t - it_1) n_{j+1}(t - jt_1)} + \overline{n_i(t - it_1 + \Delta) n_j(t - jt_1 + \Delta)} \right. \right. \\ \left. \left. - \overline{n_{i+1}(t - it_1) n_j(t - jt_1 + \Delta)} - \overline{n_i(t - it_1 + \Delta) n_{j+1}(t - jt_1)} \right\} \right\} \quad (29)$$

where the bar indicates an averaging operation over all random parameters of the functions involved.

The first two noise terms yield non-zero contributions to the average only when $i = j$. The last two terms yield non-zero contributions only when $j = i+1$ and $j = i-1$ respectively. Hence

$$\begin{aligned}
E\{z(t)\} = & 3 \sum_{i=1}^{M-1} \sum_{j=1}^{M-1} \left\{ 2\rho_s[(1-j)(t_0-t_1)] - \rho_s[(1-j)(t_0-t_1) + (t_0-\Delta)] - \rho_s[(1-j)(t_0-t_1) - (t_0-\Delta)] \right\} \\
& + 2N \sum_{i=1}^{M-1} \rho_n(0) - N \sum_{i=1}^{M-2} \rho_n(t_1-\Delta) - N \sum_{i=2}^{M-1} \rho_n(t_1-\Delta)
\end{aligned} \quad (30)$$

Since the indices i and j in the double sum appear only in the combination $i-j$, the expression can be simplified by the change of variable

$$i - j = q \quad (31)$$

Noting further that $\rho_n(0) = 1$ and that $\rho_n(t_1-\Delta)$ is independent of i , one obtains

$$\begin{aligned}
E\{z(t)\} = & 3 \sum_{q=-(M-2)}^{M-2} \left\{ 2\rho_s[q(t_0-t_1)] - \rho_s[q(t_0-t_1) + (t_0-\Delta)] - \rho_s[q(t_0-t_1) - (t_0-\Delta)] \right\} (M-1-|q|) \\
& + 2N [(M-1) - (M-2)\rho_n(t_1-\Delta)] \\
= & 2S \sum_{q=-(M-2)}^{M-2} \left\{ \rho_s[q(t_0-t_1)] - \rho_s[q(t_0-t_1) - (t_0-\Delta)] \right\} (M-1-|q|) \\
& + 2N [(M-1) - (M-2)\rho_n(t_1-\Delta)]
\end{aligned} \quad (32)$$

Using

$$\rho_s(\tau) = \rho_n(\tau) = \frac{\sin \omega_0 \tau}{\omega_0 \tau} \quad (33)^1$$

one obtains from Eq. (32)

$$\begin{aligned}
E\{z(t)\} = & 2S \sum_{q=-(M-2)}^{M-2} \left\{ \frac{\sin \omega_0 q(t_0-t_1)}{\omega_0 q(t_0-t_1)} - \frac{\sin \omega_0 [q(t_0-t_1) - (t_0-\Delta)]}{\omega_0 [q(t_0-t_1) - (t_0-\Delta)]} \right\} (M-1-|q|) \\
& + 2N [(M-1) - (M-2) \frac{\sin \omega_0 (t_1-\Delta)}{\omega_0 (t_1-\Delta)}]
\end{aligned} \quad (34)$$

¹This corresponds to flat signal and noise spectra over $0 \leq \omega \leq \omega_0$ or, more generally, to signal and noise spectra of the same form with prewhitening filters following each hydrophone and a processed frequency range of $0 \leq \omega \leq \omega_0$.

Conversion to bearing angles is accomplished through the relations

$$t_0 = -\frac{d}{c} \sin \theta_T \quad (35)$$

$$\Delta = -\frac{d}{c} \sin \theta_I \quad (36)$$

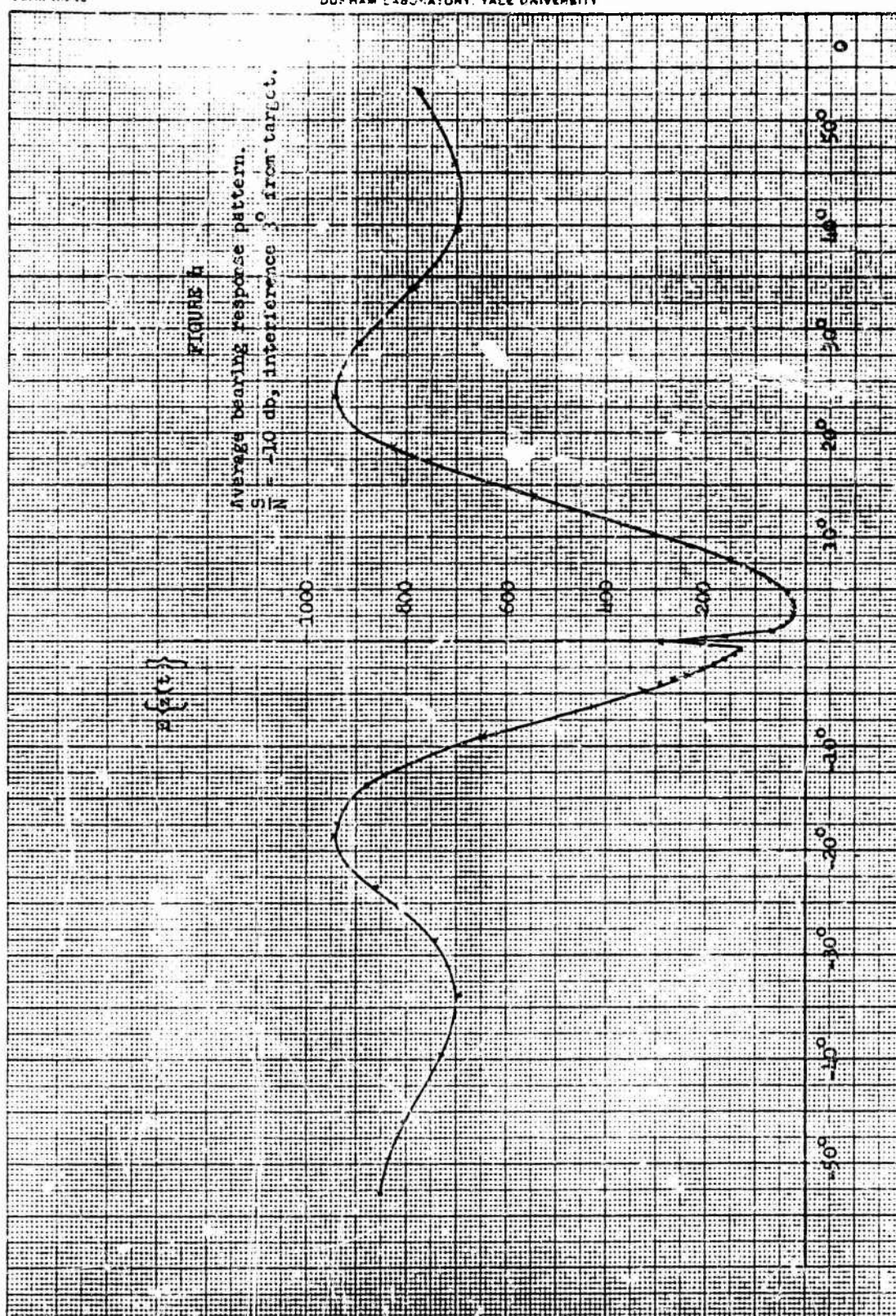
$$t_1 = -\frac{d}{c} \sin \theta \quad (37)$$

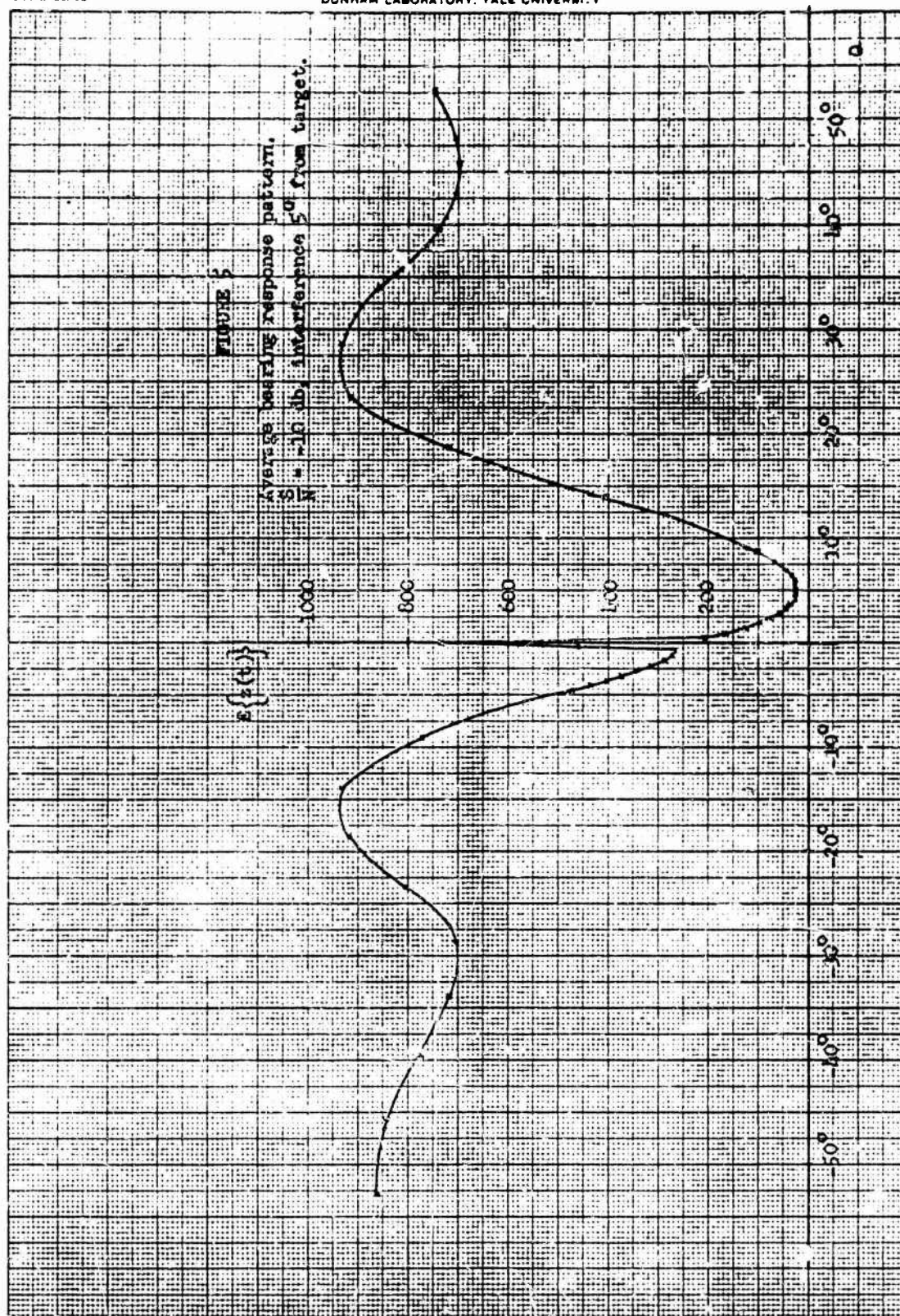
θ_T and θ_I are target and interference bearings relative to the broadside condition, with the convention on signs as discussed on p. 2 (i.e., angles measured counterclockwise from broadside). θ is the looking angle, the independent variable of the average bearing response pattern.

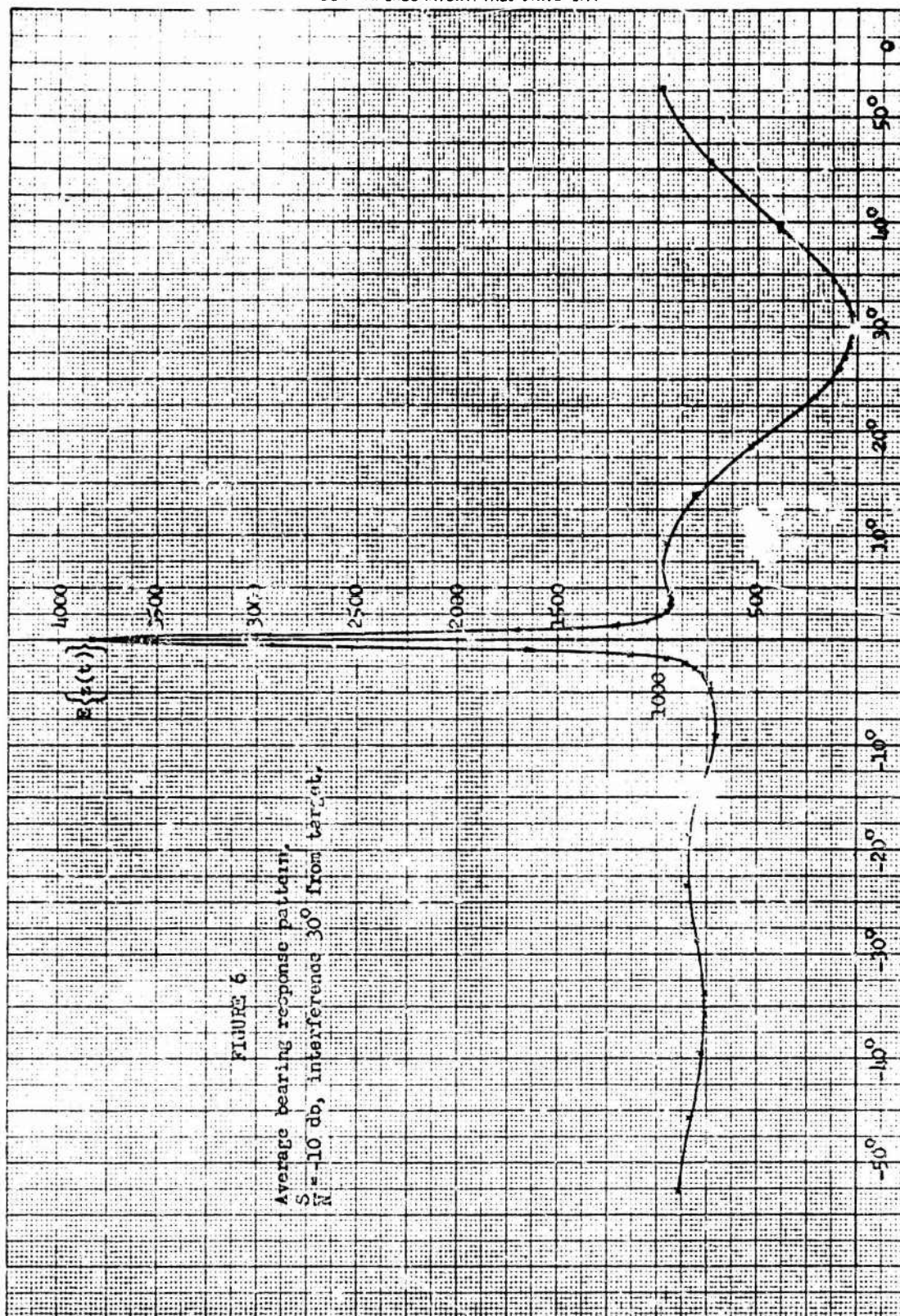
Figures 4-8 show plots of the average bearing response pattern for the following parameters: $M = 40$, $\omega_0 = 2\pi \times 5000$ rad/sec, $d = 2$ ft, $c = 5000$ ft/sec, $\theta_T = 0^\circ$. Figures 4, 5, and 6 give the pattern for interference bearings $\theta_I = 3^\circ, 5^\circ$ and 30° respectively with $\frac{S}{N} = -10$ db.¹ Figures 7, 8, and 9 present the patterns for the same set of values of θ_I but with $\frac{S}{N} = -20$ db.¹ For large angular separations of target and interference (30° or more), the pattern is quite similar to that of a conventional power detector except for the null near the interference bearing.² It should be noted, however, that the dip in the pattern near the interference bearing has a half-width of the order of 20° and that a reduction of the peak (on target) value occurs when the target lies within this range. Figures 7 and 8, in particular, represent situations in which the target would be very difficult to detect from

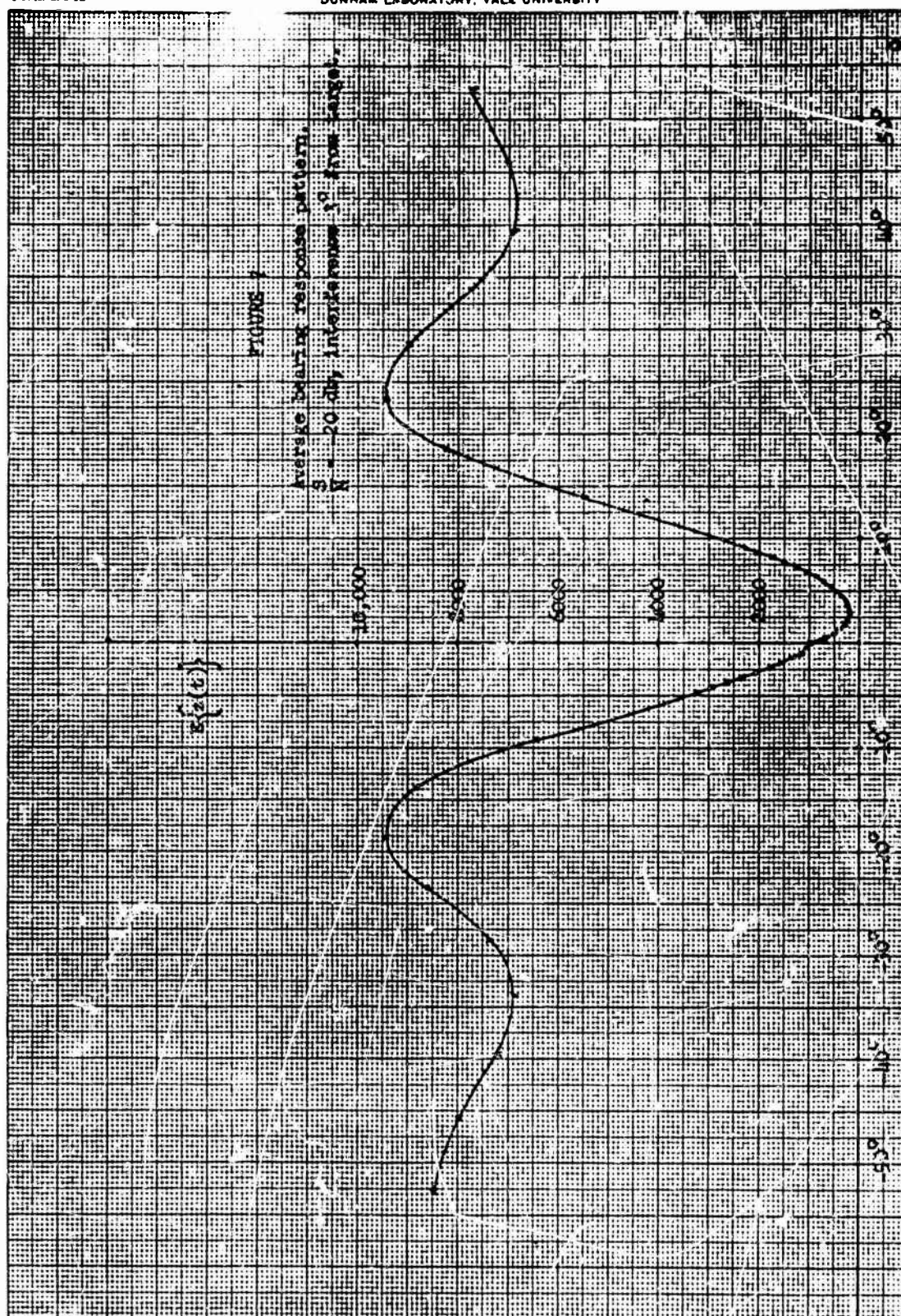
¹For computational convenience S was chosen as unity in all cases.

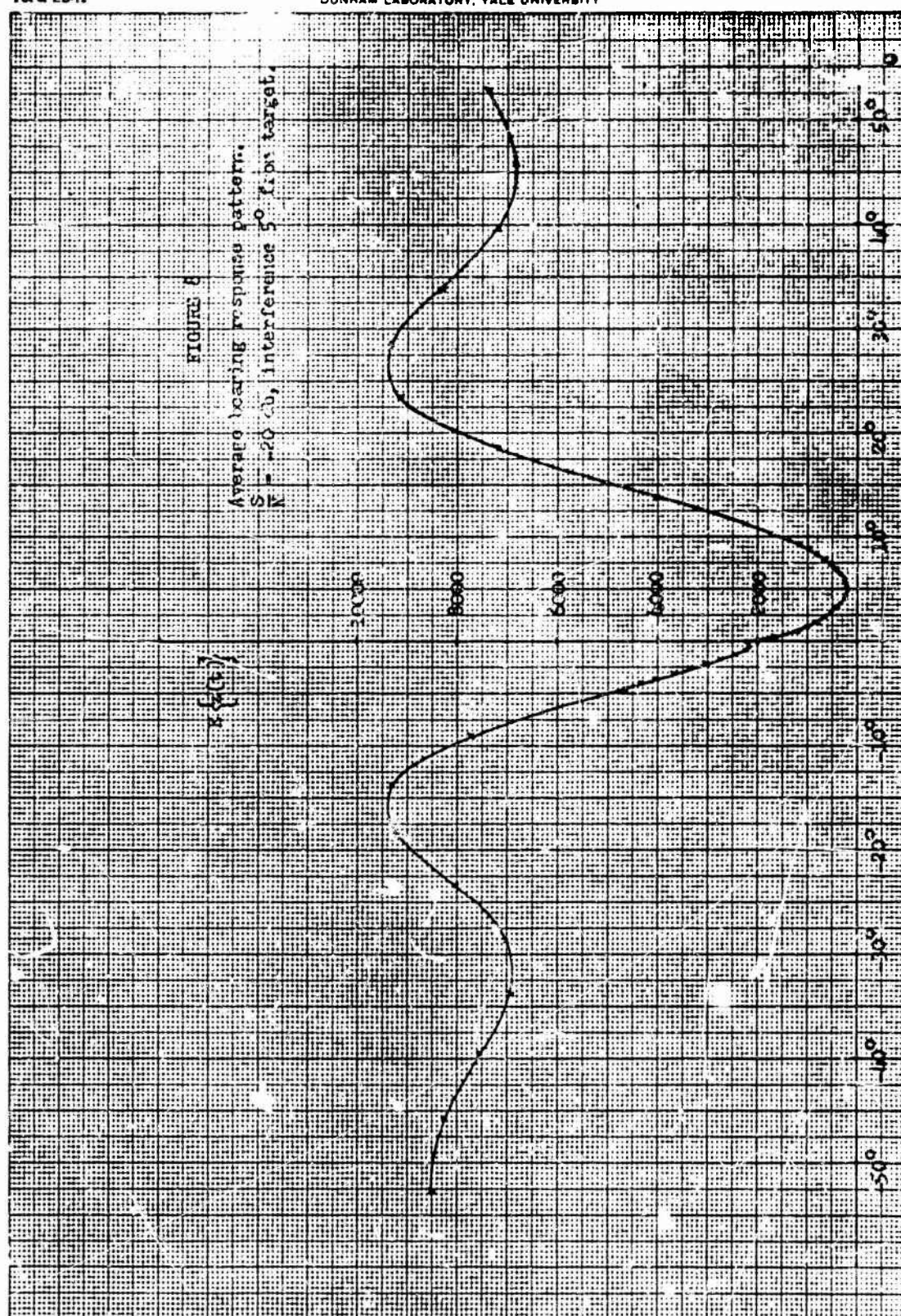
²Provision could presumably be made to compensate for this effect so as to present an essentially flat pattern in the absence of a target.

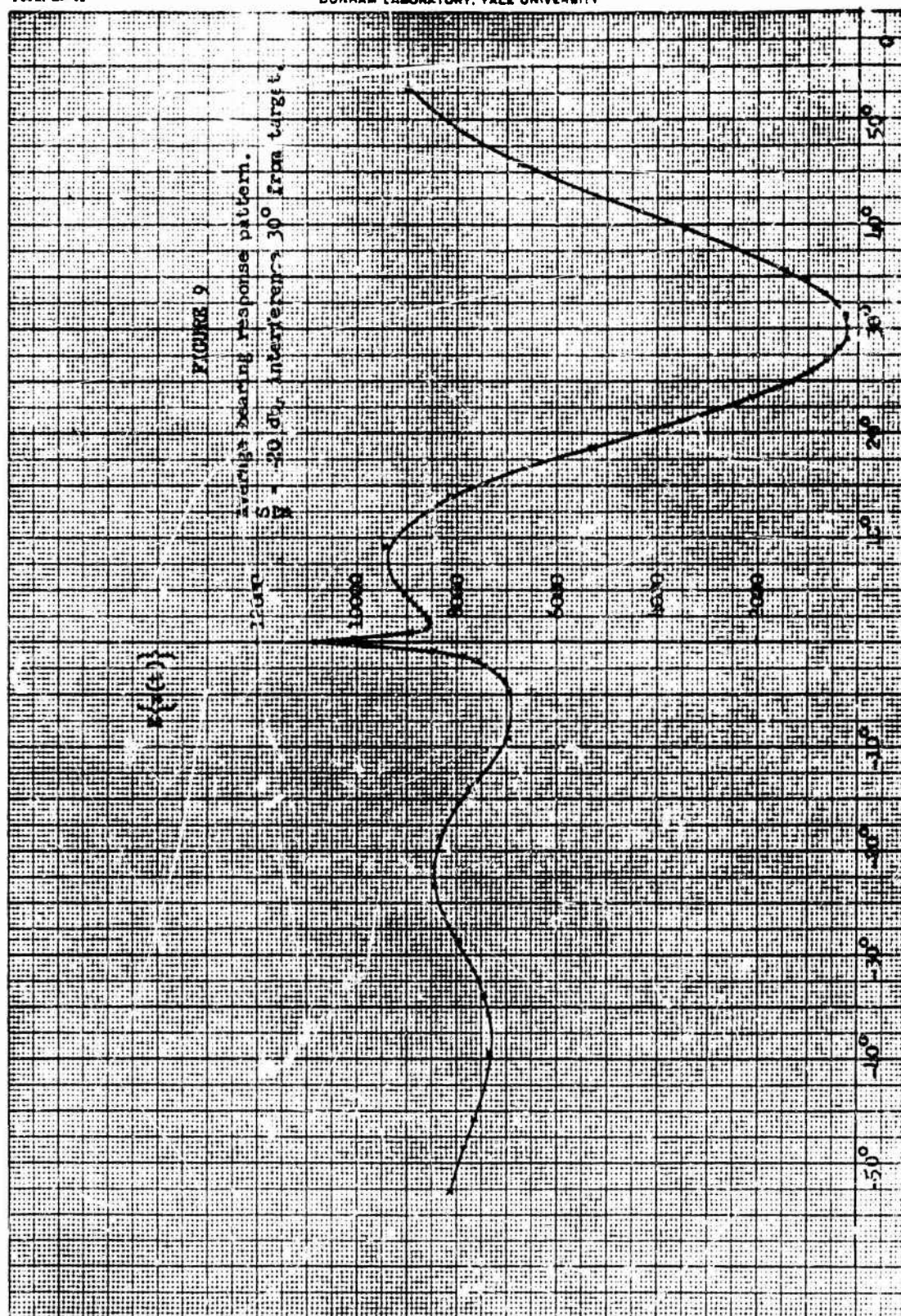












inspection of the bearing response pattern. The reasons for this difficulty are quite clear from Eq. (32). The width of the dip and the magnitude of the on-target response are proportional, respectively, to the deviation of $\rho_n(t_1 - \Delta)$ and $\rho_g(t_1 - \Delta)$ from unity. In other words, the allowable angular proximity of target and interference is not determined by the width of the array pattern as a whole, but by the width of the pattern formed by adjacent hydrophones. This immediately suggests a remedy: Instead of subtracting the delayed outputs of adjacent hydrophones, one can obtain a null on the interference bearing by pairwise subtraction of more remote hydrophones. The resulting instrumentation is analyzed in the following section.

IV. Bearing Response Pattern of a Modified Instrumentation

Let the hydrophones (numbered in order from 1 to M as before) be divided into the following K groups:

$$(1, K+1, 2K+1, \dots, M-K+1), (2, K+2, 2K+2, \dots, M-K+2), \dots, (K, 2K, 3K, \dots, M)$$

For convenience we postulate that $\frac{M}{K}$ is an integer. Each hydrophone clearly appears in one and only one group. Each group consists of a linear array with spacing Kd between hydrophones and interference nulling is achieved for each group as in Figure 1. The signal components of all outputs are then brought in phase by proper delays and added. Figure 10 shows the resultant instrumentation for $K=3$.

In order to achieve interference elimination, one sets the delays τ_i as in Eq. (2):

$$\tau_i = (i-1)\Delta, \quad i=1, 2, \dots, M \quad (38)$$

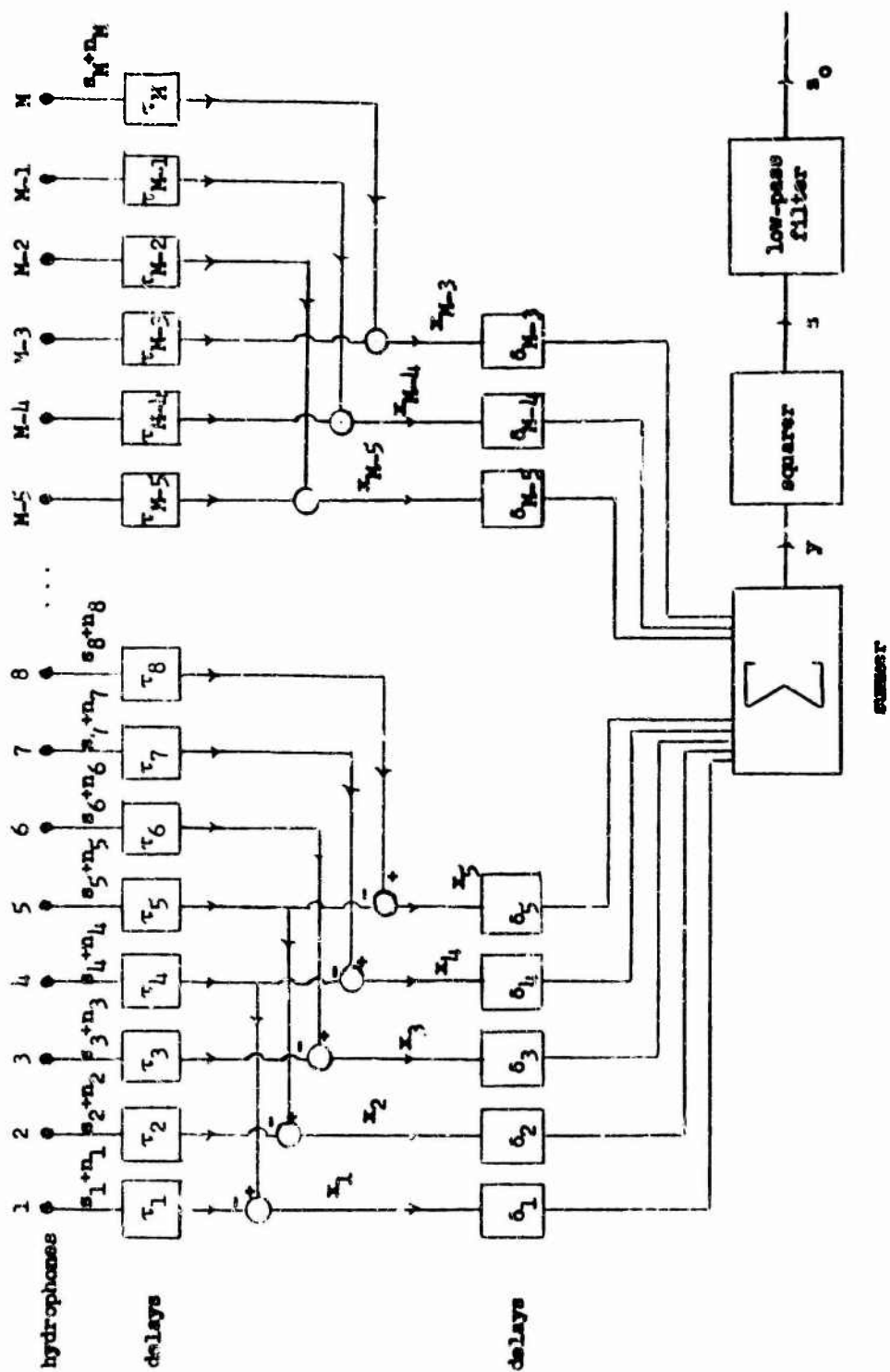


FIGURE 10

This yields the K groups of interference-free signals

$$(x_1, x_{K+1}, x_{2K+1}, \dots, x_{M-K+1}), (x_2, x_{K+2}, x_{2K+2}, \dots, x_{M-K+2}), \dots, (x_K, x_{2K}, x_{3K}, \dots, x_M)$$

The x_i 's are given by

$$x_i(t) = s_1[t + (1-K)(t_0 - \Delta)] \dots s_1[t + (1-K)(t_0 - \Delta)] + n_{1+K}[t - (1-K)\Delta] - n_1[t - (1-K)\Delta],$$

$i = 1, 2, \dots, M-K$
(39)

The delays δ_i are adjusted as follows:

$$\delta_i = (1-K)(t_1 - \Delta), \quad i = 1, 2, \dots, M-K \quad (40)$$

Then the output of the summer is

$$y(t) = \sum_{i=1}^{M-K} \left\{ s_1[t + (1-K)(t_0 - t_1)] \dots s_1[t + (1-K)(t_0 - t_1) - K(t_0 - \Delta)] \right. \\ \left. + n_{1+K}[t - (1-K)t_1] - n_1[t - (1-K)t_1 + K\Delta] \right\} \quad (41)^1$$

Hence the output of the squarer is

$$z(t) = \sum_{i=1}^{M-K} \sum_{j=1}^{M-K} \left\{ s_1[t + (1-K)(t_0 - t_1)] - s_1[t + (1-K)(t_0 - t_1) - K(t_0 - \Delta)] \right. \\ \left. + n_{1+K}[t - (1-K)t_1] - n_1[t - (1-K)t_1 + K\Delta] \right\} \times \\ \left\{ s_1[t + (j-1+K)(t_0 - t_1)] - s_1[t + (j-1+K)(t_0 - t_1) - K(t_0 - \Delta)] + n_{j+K}[t - (j-1+K)t_1] \right. \\ \left. - n_j[t - (j-1+K)t_1 + K\Delta] \right\} \quad (42)$$

¹With $K=1$ this expression clearly reduces to Eq. (27).

The average bearing response is therefore

$$\begin{aligned}
 E\{z(t)\} = & 3 \sum_{i=1}^{M-K} \sum_{j=1}^{M-K} \left\{ 2\rho_s [(1-j)(t_0 - t_1)] - \rho_s [(1-j)(t_0 - t_1) + K(t_0 - \Delta)] - \rho_s [(1-j)(t_0 - t_1) - K(t_0 - \Delta)] \right\} \\
 & + \sum_{i=1}^{M-K} \sum_{j=1}^{M-K} \frac{\bar{n}_{i+K}[t - (1+K)t_1] \bar{n}_{j+K}[t - (1+K)t_1]}{+ \bar{n}_i[t - (1+K)t_1 + K\Delta] \bar{n}_j[t - (1+K)t_1 + K\Delta]} \\
 & - \frac{\bar{n}_{i+K}[t - (1+K)t_1] \bar{n}_j[t - (1+K)t_1 + K\Delta]}{+ \bar{n}_i[t - (1+K)t_1 + K\Delta] \bar{n}_{j+K}[t - (1+K)t_1]} \\
 & - \frac{\bar{n}_i[t - (1+K)t_1 + K\Delta] \bar{n}_{j+K}[t - (1+K)t_1]}{+ \bar{n}_{i+K}[t - (1+K)t_1] \bar{n}_j[t - (1+K)t_1]} \quad (43)
 \end{aligned}$$

where the bar indicates an averaging operation over all random parameters.

The first two noise terms yield non-zero contributions when $i = j$, the third when $i+K = j$ and the fourth when $i = j+K$. Hence

$$\begin{aligned}
 E\{z(t)\} = & 3 \sum_{i=1}^{M-K} \sum_{j=1}^{M-K} \left\{ 2\rho_s [(1-j)(t_0 - t_1)] - \rho_s [(1-j)(t_0 - t_1) + K(t_0 - \Delta)] - \rho_s [(1-j)(t_0 - t_1) - K(t_0 - \Delta)] \right\} \\
 & + 2N \left\{ (M-K) - (M-2K) \rho_n [K(t_1 - \Delta)] \right\}
 \end{aligned}$$

Finally, using the change of variable

$$1-j = q \quad (44)$$

one obtains

$$\begin{aligned}
 E\{z(t)\} = & 23 \sum_{q=-(M-K-1)}^{M-K-1} \left\{ \rho_s [q(t_0 - t_1)] - \rho_s [q(t_0 - t_1) + K(t_0 - \Delta)] - \rho_s [q(t_0 - t_1) - K(t_0 - \Delta)] \right\} (M-K-|q|) \\
 & + 2N \left\{ (M-K) - (M-2K) \rho_n [K(t_1 - \Delta)] \right\} \quad (45)
 \end{aligned}$$

Equation (45) clearly reduces to Eq. (32) when $K=1$.¹ The on-target response is now proportional to the deviation from unity of $\rho_e[K(t_0-\delta)]$ so that the interference can be K times closer in angle to the target before the same degradation in performance occurs as in the original instrumentation. At the same time the width of the null near the interference bearing is $\frac{1}{K}$ times as large in the modified instrumentation. On the deficit side, one should point out that the sum in Eq. (45) has only $2(M-K-1)+1$ terms as opposed to the $2(M-2)+1$ terms of Eq. (32). This is, of course, simply a reflection of the fact that the summer in the modified instrumentation has only $M-K$ inputs as compared to $M-1$ in the instrumentation of Fig. 1. One could presumably improve the situation by forming additional summer inputs through subtraction of the outputs of other hydrophone pairs with indices separated by at least K . However, as long as K is small compared to M , the entire effect is not serious in any case and a more elaborate analysis would have little practical significance.

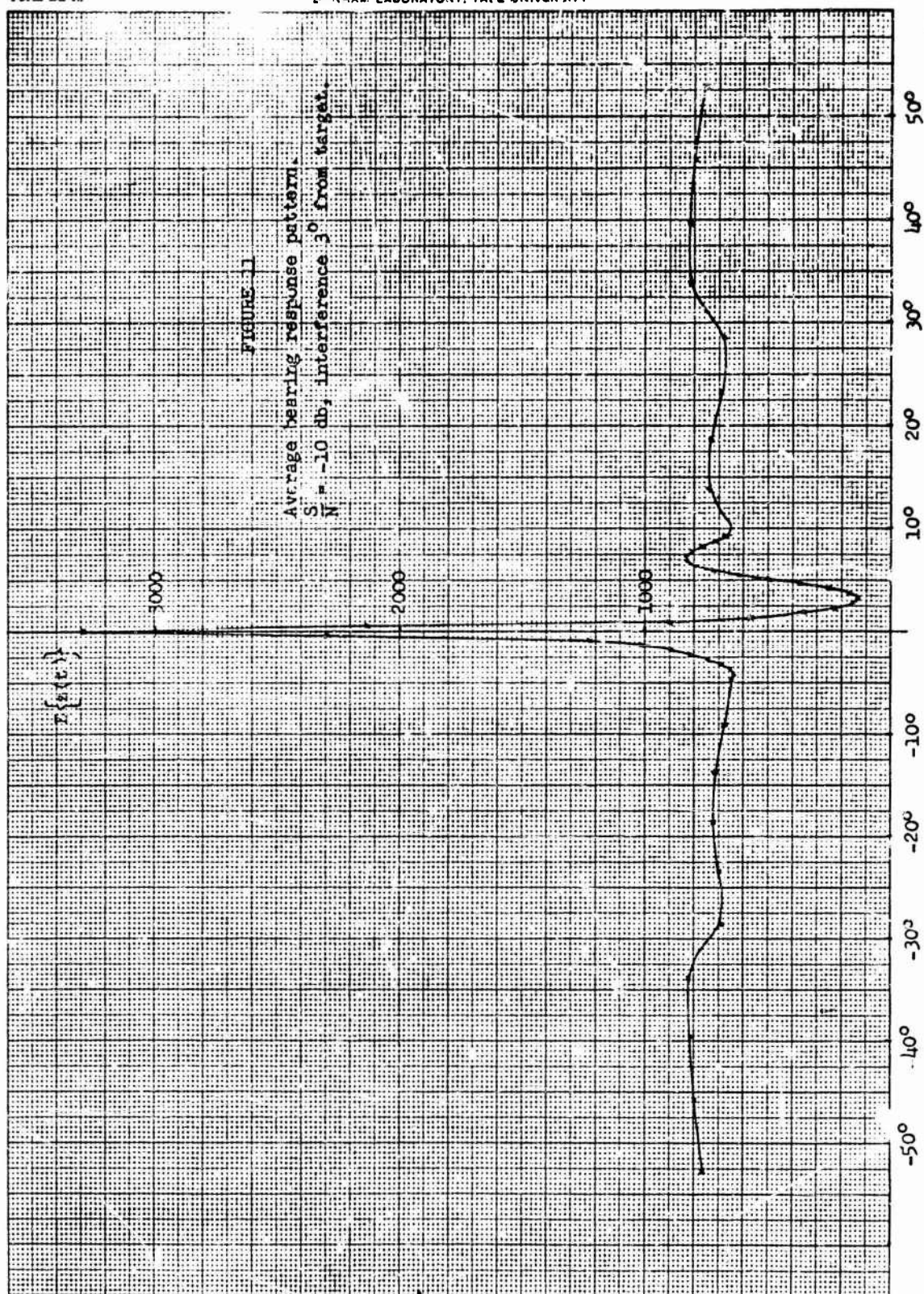
Figures 11 and 12 give the average bearing response pattern of the modified instrumentation with $K=5$ for the parameter values used in Figs. 4 and 7 respectively. The target peak is now clearly visible and of a height not greatly different from that obtained in Figs. 6 and 9 (remote interference).

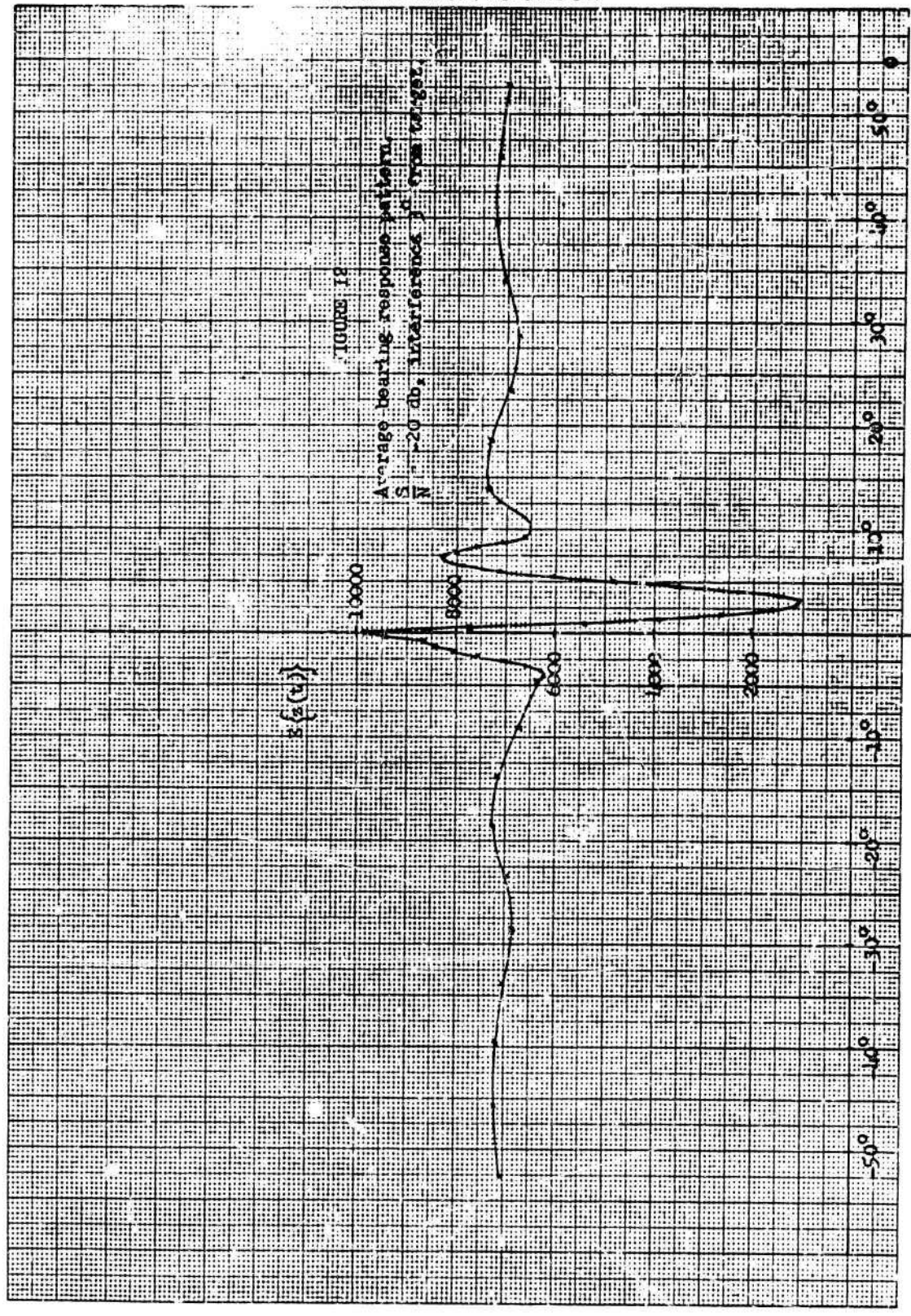
V. Concluding Remarks

The results of this report indicate that detection of targets in the presence of interference can be achieved with instrumentations of only

¹For comparison, the average bearing response pattern of a conventional power detector operating in the absence of interference is

$$E\{u(t)\} = S \sum_{q=-(M-1)}^{M-1} \rho_e[q(t_0-t_1)] (M-|q|) + MN$$





moderate complexity without serious loss in performance relative to the optimum (likelihood-ratio) technique. From a practical point of view, the need for an additional set of adjustable delay elements is the most serious objection to the proposed instrumentation. This practical difficulty could be lessened considerably by the use of digital techniques. It therefore becomes important to investigate the effect of sampling and quantizing on the performance of the detector. The most convenient procedure would be to hard-clip the output of each hydrophone and perform all further processing on the resultant binary data. The effect of such a technique on detector performance is currently under investigation.

A further extension of some interest would be the development of procedures for eliminating two or more interfering signals. No specific work in this direction has been undertaken to date, but it appears clear from Fig. 1 that the nulling procedure could be iterated by delaying the signals $\{x_i\}$ by amounts appropriate to achieve alignment of the second interference components, subtracting pairwise once more and then aligning the signal components with a third set of delay elements.



PASSIVE DETECTION OF A WEAK SONAR TARGET
FROM HARD-LIMITED INPUT DATA

by

Morton Kanefsky

Progress Report No. 22

General Dynamics/Electric Boat Company

(53-00-10-0231)
(8050-33-55001)

June 1965

DEPARTMENT OF ENGINEERING
AND APPLIED SCIENCE

YALE UNIVERSITY

Summary

This report deals with the passive detection of a sonar target in the presence of a gaussian noise background whose power is unknown or non-stationary. A standard procedure in this environment is to reduce the data by sampling and then hard limiting. When the receiving array consists of two hydrophones, this procedure leads to the polarity coincidence correlator (PCC), which has been analyzed in some detail in the literature. In this report a general class of polarity coincidence array detectors (PCA), which are logical extensions of the two-channel PCC, are discussed. The following results are obtained:

- 1) The optimum PCA detector represents an implementation of the locally optimum array detector based on hard-limited independent samples from gaussian inputs. This implementation is essentially that employed in the DIMUS system.
- 2) Some suboptimum devices which are only slightly less efficient, but which may be more easily implemented, are demonstrated.
- 3) When the input data is a sequence of independent samples from a stationary gaussian process, the optimum PCA detector introduces a loss of 1.96 db in the input signal relative to the locally optimum detector based on unclipped stationary gaussian inputs. For the least efficient detector considered, this loss is 3.30 db. As long as the input samples are independent, however, the PCA detectors are nonparametric and their efficiencies greatly improve when the stationary and/or gaussian assumptions are violated.
- 4) When the input samples are dependent, it is necessary to assume gaussian inputs in order to analyze the PCA detectors; however, these devices are still unaffected by a nonstationary noise level.

- 5) The loss due to clipping is considerably reduced as the sample dependence (i.e., sampling rate) increases. For example, when the input power spectrum is determined by a single-pole, low-pass pre-filter and the detector is operated essentially continuously, the loss due to clipping is reduced to 0.63 db for the optimum PCA detector and not much more for the suboptimum devices.
- 6) The spectral shapes of the inputs must be known fairly accurately if it is desirable to set the threshold with some degree of accuracy and at the same time to sample fast enough to recover some of this loss due to clipping.

I. Introduction

In underwater sound detection (SONAR) one typically decides whether or not a random signal is present to an array of receivers (hydrophones) which contain noise processes that are independent but statistically identical [1, 2, 3, 4, 5]. As the noise power is often nonstationary, the input data is sometimes reduced by sampling and then hard limiting [1, 2, 3, 4]. A detector which operates on the polarity coincidence of two channels is called a polarity coincidence correlator (PCC) [1, 6]. This device has interesting nonparametric properties when the inputs are a sequence of independent samples. The false-alarm probability can be set for any sequence of samples whose amplitude densities have zero median [6]. For certain nongaussian noise processes, particularly of the impulse type, the PCC can be more efficient than the optimum two-channel detector based on stationary gaussian inputs [6, 7]. Furthermore, the PCC is exceedingly simple to implement. In sonar practice, however, it is desirable to consider an array of receivers that may be quite large. Polarity coincidence techniques can be extended to the array case, but suggested procedures [1] are very inefficient for large arrays. Efficient hard limiting procedures have been utilized (i.e., the DIMUS system [4]), but they are not regarded as logical extensions of the PCC.

In this paper a general class of polarity coincidence array detectors (PCA), which are logical extensions of the two-channel PCC, are discussed. The implementations considered include the locally optimum* detector based on stationary gaussian inputs [10], as well as some suboptimum devices that may be more easily implemented and are still quite efficient.

*A locally optimum detector is one that is optimum in the Neyman-Pearson sense [8] in the limit as the input signal-to-noise ratio in each channel approaches zero [9].

II. Terminology

Under the hypothesis H (noise with zero median and signal absent), approximately half the channels will have the same sign. Under the alternative K (signal present), the number of channels with the same sign as the signal will increase. Let $\delta(t)$ be the difference between the number of channels having the most prevalent sign at time t and half the number of channels. Hence

$$\delta(t) = \left| \frac{1}{2} \sum_{j=1}^M \operatorname{sgn}(x_j(t)) \right|, \quad (1)$$

where $x_j(t)$ are the M inputs, and $\operatorname{sgn}(\xi) = \begin{cases} 1 & ; \xi > 0 \\ -1 & ; \xi < 0 \end{cases}$. The PCA detectors

sample the inputs and then perform some memoryless monotonic operation on δ_1 [$\delta_1 = \delta(t + i\tau)$ where τ is the sampling interval]. Thus the PCA test statistics are of the form

$$S_{\text{pca}} = \sum_{i=1}^N g(\delta_1), \quad (2)$$

where N is the total sample size and $g(\cdot)$ is some arbitrary monotonic function. This test statistic is then compared with a threshold c and the detector decides that the signal is present if $S_{\text{pca}} > c$. See Figure 1 for a schematic diagram of these detectors. With little loss in generality the function $g(\cdot)$ can be normalized so that $g(\delta) = \delta$ when $\delta = 0$ or 1 . With this normalization the PCA detectors reduce to the PCC detector when there are two inputs.

For large N , S_{pca} is approximately normally distributed and hence c can be set equal to

$$c = E_H\{S_{\text{pca}}\} + \Phi^{-1}(1-\alpha) \sqrt{\operatorname{Var}_H\{S_{\text{pca}}\}}, \quad (3)$$

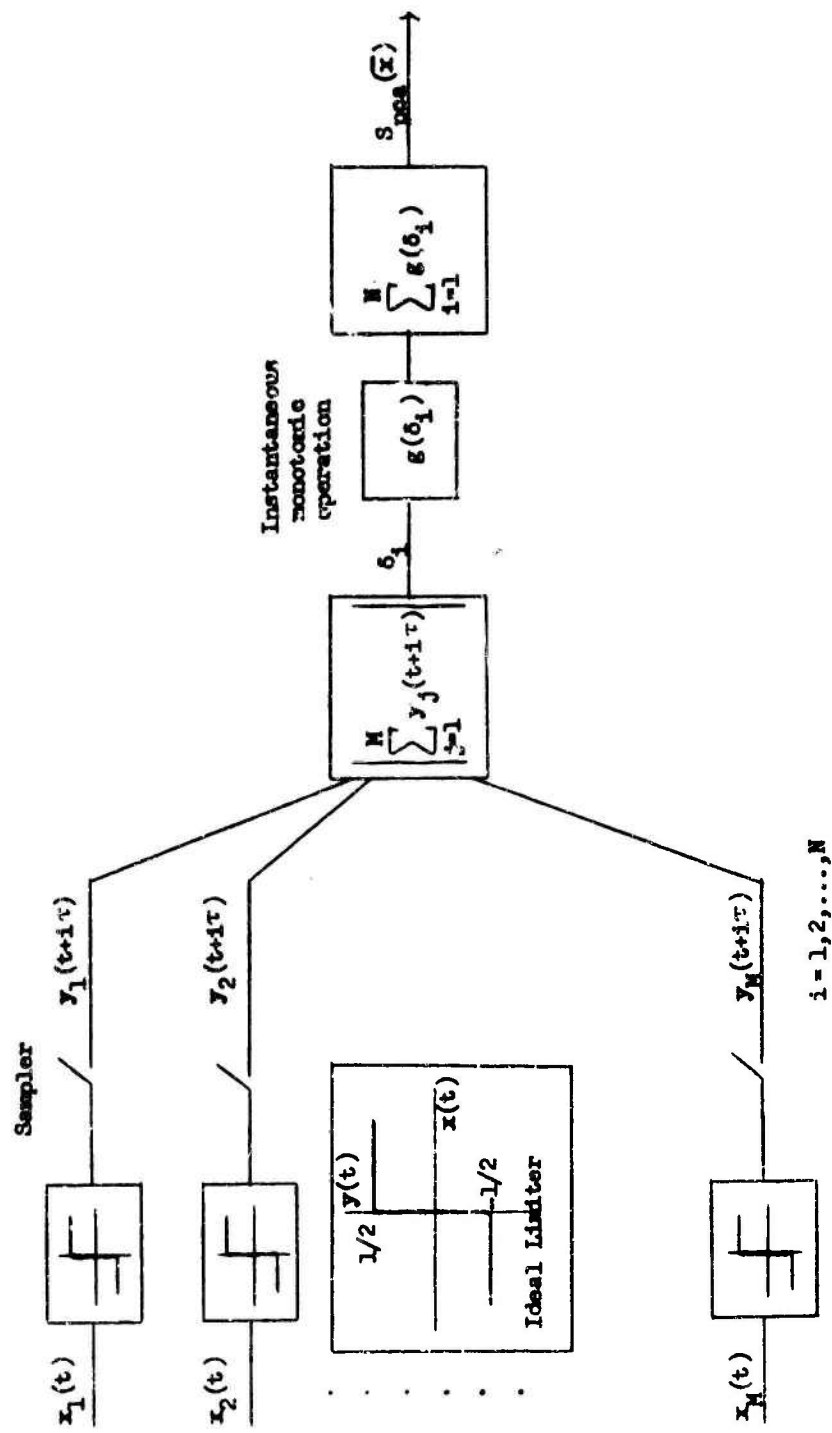


FIGURE 1 Schematic for Polarity Coincidence Array Detectors

where \bar{Q} is the normalized gaussian cumulative distribution function, α the false-alarm probability, $E_H\{\}$ the expected value with respect to the hypothesis, and $\text{Var}_H\{\}$ the variance under the hypothesis. Thus

$$\alpha = \text{Prob}(S_{\text{pca}} > c / H) .$$

The output signal-to-noise ratio of a detector D is defined as

$$\text{SNR}_D = \frac{E_K\{S_D\} - E_H\{S_D\}}{[\text{Var}_K\{S_D\}]^{1/2}} . \quad (4)$$

For many practical applications the input signal-to-noise power ratio σ_s^2/σ_n^2 in each channel is small ($M \sigma_s^2/\sigma_n^2 \ll 1$). This is of course the justification for considering locally optimum detectors. Hence we will compare detectors by calculating the limit of SNR_D as $\sigma_s^2/\sigma_n^2 \rightarrow 0$. Thus

$$\text{SNR}_D \stackrel{e}{=} \lim_{\sigma_s^2/\sigma_n^2 \rightarrow 0} \frac{E_K\{S_D\} - E_H\{S_D\}}{[\text{Var}_H\{S_D\}]^{1/2}} . \quad (5)$$

Under the assumptions that the cumulative distribution function of the noise can be expanded in a Taylor series near the origin and that the signal is amplitude limited with zero mean, it is shown in Appendix I that

$$\lim_{\sigma_s^2/\sigma_n^2 \rightarrow 0} [E_K\{S_D\} - E_H\{S_D\}] = 8N\sigma_n^2 f^2(0) \frac{\sigma_s^2}{\sigma_n^2} \frac{2}{2^M} \sum_{r=\frac{M}{2}+1}^M \left(\frac{M}{r}\right) \left[\left(r - \frac{M}{2}\right)^2 - \frac{M}{4}\right] g(r - \frac{M}{2}) \quad (6)$$

$$= 8N\sigma_n^2 f^2(0) \frac{\sigma_s^2}{\sigma_n^2} \left[E_H\{\delta^2 g(\delta)\} - \frac{M}{4} E_H\{g(\delta)\} \right] , \quad (7)$$

where $f(0)$ is the value of the noise amplitude density at the origin and

$$z = \begin{cases} 0 & , M \text{ even} \\ 1/2 & , M \text{ odd} \end{cases} . \quad \text{The relationship between Eqs. (6) and (7) follows}$$

from the fact that $\delta_1 = (r - \frac{M}{2})$ with probability $\frac{2}{2^M} \binom{M}{r}$ under the hypothesis, where r is the number of channels having the most prevalent sign. Hence $E_H\{f(\delta_1)\}$ is given by

$$\sum_{r=\frac{M}{2}+1}^M \frac{2}{2^M} \binom{M}{r} f(r - \frac{M}{2}) . \quad \text{Thus for independent samples}$$

$$\text{SNR}_D = 8\sqrt{N} \sigma_n^2 f^2(0) \frac{\sigma_n^2}{\sigma_n^2} \frac{\left[E_H\{\delta_1^2 g(\delta)\} - \frac{M}{4} E_H\{g(\delta)\} \right]}{\left[E_H\{g^2(\delta)\} - E_H^2\{g(\delta)\} \right]^{1/2}} . \quad (8)$$

We will now consider particular implementations of the PCA, all of which reduce to the PCC for $M=2$.

III. Polarity Coincidence Array Detectors

Consider the detector $D_{\text{pca.1}}$ which calculates the test statistic

$$S_{\text{pca.1}} = \sum_{i=1}^N \delta_1^2 . \quad (9)$$

Since $g(\delta_1) = \delta_1^2$, $E_H\{\delta_1^2\} = \frac{M}{4}$, and $E_H\{\delta_1^4\} = 3\frac{M^2}{16} - \frac{2M}{16}$ [see Appendix III], it follows that

$$E_H\{S_{\text{pca.1}}\} = N \frac{M}{4} ; \quad \text{Var}_H\{S_{\text{pca.1}}\} = \frac{N}{8} M(M-1) , \quad (10)$$

and from Eq. (8),

$$\text{SNR}_{\text{pca.1}} = \sqrt{N} \sqrt{8} \sigma_n^2 f^2(0) \frac{\sigma_n^2}{\sigma_n^2} \sqrt{M(M-1)} . \quad (11)$$

But this is exactly the output signal-to-noise ratio determined for the locally optimum detector for independent clipped gaussian samples [10]. Therefore $D_{pca.1}$ is the optimum PCA detector and the others will be compared to it. Note that, when $M=2$, Eq. (11) holds for all the PCA detectors to be considered.

Let us next analyze the suboptimum PCA, $D_{pca.2}$, which calculates the following test statistic:

$$S_{pca.2} = \sum_{i=1}^N \delta_i \quad (12)$$

It is observed in Appendix II that sums of the type $\sum_{r=-\frac{M}{2}}^{\frac{M}{2}} \left| \frac{r}{r} \right| \frac{2}{2^M} f(r - \frac{M}{2})$ approach $2 \int_{-\frac{2e-1}{\sqrt{M}}}^{\infty} \frac{1}{\sqrt{2\pi}} e^{-\frac{1}{2}y^2} f\left(\frac{\sqrt{M}}{2}y\right) dy$ for large M ($M > 10$). The later

integrals are easily evaluated. Therefore Eq. (8) can be evaluated for large M using the fact that $g(\delta) = \delta$, resulting in

$$SNR_{pca.2} \xrightarrow{M \rightarrow \infty} \sqrt{N} \sqrt{8} \sigma_n^2 f^2(0) \frac{\sigma_s^2}{\sigma_n^2} \frac{M}{\sqrt{N-2}}, \quad (13)$$

where the limit is rapidly approached, particularly for M odd.

Thus $D_{pca.2} = D_{pca.1}$ for $M=2$, and for large arrays $D_{pca.2}$ introduces a loss of 0.29 db in the input signal power over and above the loss inherent in hard limiting. It follows that the squaring of δ_i does not improve the detectability significantly. Note, however, that δ_i is defined as the absolute value of some quantity and squaring may not be more difficult to implement than the absolute value operation.

Finally we wish to consider the suboptimum PCA that introduces an intermediate threshold. Thus

$$S_{\text{pca},3} = \sum_{i=1}^N u(\delta_i - \bar{\delta}) , \quad (14)$$

where $u(\xi) = \begin{cases} 1, & \xi > 0 \\ 0, & \xi \leq 0 \end{cases}$, and $\bar{\delta}$ is some constant. This intermediate

threshold reduces the test statistic to a sum of 0's and 1's and may possibly be more easily implemented. In fact, $D_{\text{pca},3}$ is probably the most natural extension of the two-channel PCC detector.* $S_{\text{pca},3}$ is binomially distributed under the hypothesis with probability of success p_0 given by

$$p_0 = \text{Prob}_H(\delta_1 > \bar{\delta}) = \frac{2}{2^M} \sum_{r=\lceil \frac{M}{2} + \bar{\delta} \rceil}^M \binom{M}{r} , \quad (15)$$

where $\lceil x \rceil$ is the smallest integer greater than x . The false-alarm probability α can be set exactly for any N if the threshold c is the smallest integer such that

$$\sum_{r=c}^N \binom{N}{r} p_0^r (1-p_0)^{N-r} \leq \alpha . \quad (16)$$

We wish to choose that $\bar{\delta}$ which maximizes the output signal-to-noise ratio. Since $\text{Var}_H[S_{\text{pca},3}] = N p_0 (1-p_0)$, the output signal-to-noise ratio is seen from Eqs. (5), (6) and (14) to be

$$\text{SNR}_{\text{pca},3} = \sqrt{N} \frac{\sigma_s^2 r^2(0)}{\sqrt{p_0(1-p_0)}} \frac{1}{2} \sum_{r=\lceil \frac{M}{2} + \bar{\delta} \rceil}^M \binom{M}{r} \left[\left(r - \frac{M}{2} \right)^2 - \frac{M}{4} \right] . \quad (17)$$

*Paran and Hills consider this implementation where they set $\bar{\delta} = \frac{M}{2} - 1$. Thus the output is 1 only if all the channels have the same sign.

As $\sqrt{p_0(1-p_0)}$ is a relatively slowly varying function, we pick $r' = \left\lceil \frac{M}{2} + \delta \right\rceil$ to be the smallest integer that satisfies

$$\left(r' - \frac{M}{2}\right)^2 - \frac{M}{4} > 0 \quad (18)$$

It follows that

$$r_{\text{opt}} = \frac{\sqrt{M}}{2} \quad (19)$$

From Appendix II it is seen that

$$p_0 = \frac{2}{2^M} \sum_{r=\left\lceil \frac{M}{2} + \frac{\sqrt{M}}{2} \right\rceil}^M \binom{M}{r} \xrightarrow{M \rightarrow \infty} 2[1 - \phi(1)] \approx 0.3174 \quad (20)$$

and

$$\frac{2}{2^M} \sum_{r=\left\lceil \frac{M}{2} + \frac{\sqrt{M}}{2} \right\rceil}^M \binom{M}{r} \left[\left(r - \frac{M}{2}\right)^2 - \frac{M}{4} \right] \xrightarrow{M \rightarrow \infty} \frac{M}{\sqrt{8\pi}} e^{-1/2} \approx 0.1210 M \quad (21)$$

Hence it follows that

$$\overline{\text{SNR}}_{\text{pca.3}} \xrightarrow{M \rightarrow \infty} \sqrt{N} \sqrt{8} \sigma_n^2 r^2(0) \frac{\sigma_s^2}{\sigma_n^2} \frac{M}{1.360} \quad (22)$$

Thus $D_{\text{pca.3}} = D_{\text{pca.1}}$ for $M=2$, and for large arrays $D_{\text{pca.3}}$ introduces a loss of 1.34 db in the input signal power over and above the loss inherent in hard limiting. Table 1 gives p_0 , $\text{SNR}_{\text{pca.3}}/\text{SNR}_{\text{pca.1}}$, and the intermediate threshold $\left\lceil \frac{M}{2} + \frac{\sqrt{M}}{2} \right\rceil$ for different values of M . Observe the random fluctuations caused by the discreteness of the intermediate threshold.

M	2	3	4	5	6	7	8	14	20	26	32	38	44	50	→
$\left[\frac{M}{2} + \frac{\sqrt{M}}{2} \right]$	2	3	4	4	5	5	6	9	13	16	19	23	26	29	→
P ₀	.500	.250	.125	.375	.219	.453	.289	.424	.263	.327	.377	.256	.291	.322	→ .317
$\text{SNR}_{\text{pca.3}} / \text{SNR}_{\text{pca.1}}$	1	1	.926	.817	.878	.719	.820	.700	.794	.749	.712	.784	.762	.744	→ .735

Table 1
Performance Data for D_{pca.3}

IV. Optimum Detection of Unclipped Gaussian Samples

The array detector that approaches a monotonic function of the likelihood ratio in the limit as the input signal-to-noise ratio approaches zero, when the samples have gaussian amplitude densities with unknown but stationary variance, calculates the following test statistic [11]:*

$$S_{\text{opt}} = \sum_{i=1}^N \left[\sum_{j=1}^M \sum_{\ell=1}^M x_j(t+i\tau) x_{\ell}(t+i\tau) \right] \quad (23)$$

The output signal-to-noise ratio of this locally optimum detector D_{opt} for arbitrary stationary inputs with zero mean is given by

$$\overline{\text{SNR}}_{\text{opt}} = \sqrt{\frac{N}{2}} \frac{\sigma_s^2}{\sigma_n^2} \sqrt{M(M-1)} \quad (24)$$

If we define J_{D_1/D_2} as $\overline{\text{SNR}}_{D_1}/\overline{\text{SNR}}_{D_2}$, then

$$J_{\text{pca.1/opt}} = 4\sigma_n^2 f^2(0) \quad (25)$$

It also follows that

$$J_{\text{pca.3/opt}} = 4\sigma_n^2 f^2(0) J_{\text{pca.3/pca.1}} \quad (26)$$

It is therefore observed that for gaussian inputs $\left[\sigma_n f(0) = \frac{1}{\sqrt{2\pi}} \right]$,

$J_{\text{pca.1/opt}} = \frac{2}{\pi}$ and thus the process of hard limiting introduces an inherent loss in input signal power of 1.96 db. Note that these losses are all based on the assumption of independent samples.

*To fix the false-alarm probability, the test statistic S_{opt} must be compared with a suitable estimate of the noise power [11]. In practice, however, S_{opt} as given in Eq. (23) is displayed as a function of possible target direction and the output is compared with the off-target output by inspection.

Let us now compare the PCA detectors with D_{opt} when the stationary gaussian assumption is violated. For input probability densities that are peaked at the origin (impulse noise), the PCA detectors may become more efficient relative to D_{opt} . For example, consider input noise processes

that have the double exponential density
$$f(x) = \frac{1}{\sqrt{2}\sigma_n^2} e^{-\sqrt{2}\left|\frac{x}{\sigma_n}\right|}.$$

For these inputs $J_{pca,1/opt} = 2$ and therefore D_{opt} introduces a loss of 3.01 db in the input signal power relative to $D_{pca,1}$. Thus the PCA detectors can improve greatly relative to D_{opt} when the gaussian assumption is violated.

The analysis of the PCA detectors depends only on the sample median, and hence the PCA is invariant with respect to any nonstationarity in the noise level [3]. This is not true of the optimum detector based on stationary gaussian inputs. If the noise level varies sinusoidally about some mean, then $\text{Var}_H\{S_{opt}\}$ increases by an amount which approaches $\left(1 + \frac{k^2}{2}\right)$ asymptotically, where k is the modulation index. Thus SNR_{opt} decreases by the square root of this amount, and the false-alarm rate increases from its assumed value if the threshold was set on the assumption of stationarity. Hence $J_{pca/opt}$ is increased by as much as 1.225 for 100 per cent modulation (or a 0.88 db gain in signal power for the PCA detectors). The increase in false-alarm rate is also significant for these large modulations.

V. Operation of PCA Detectors with Dependent Samples

The nonparametric properties of the PCA array detectors follow from the assumption that independent samples are available. For realisable narrowband signals there is no sampling rate for which the independent

sample assumption is valid, although a reasonable approximation may be obtained with sufficiently slow sampling. This procedure, however, can be very inefficient given a finite decision time, and it may therefore be desirable to sample as fast as possible. The false-alarm rate of the PCA detectors can be fixed with dependent samples (and therefore continuously) only if the shape of the noise spectrum and the distribution of zero crossings are known [12,13]. However, there are still definite advantages, other than simplicity of implementation, in using these detectors instead of some optimum device.

Let us assume that the shape of the noise spectrum is essentially determined by pre-filters that are based on knowledge of the signal spectrum. If any instantaneous nonstationarity in the noise level is slow enough relative to the inverse of the bandwidth of the pre-filter, then the other spectral properties of the noise are essentially stationary. Hence the PCA detectors, while no longer nonparametric in the strict sense, are still unaffected by any sufficiently slow nonstationary noise level. For a sinusoidally varying noise level that is sufficiently slow but nevertheless fast relative to the inverse of the decision time (not at all unreasonable), $J_{pca/opt}$ is still increased by the factor $\left[1 + \frac{k^2}{2}\right]^{1/2}$.

It will now be shown that, under the assumption that the zero crossings

are the same as those from a gaussian process, $J_{pca/opt}$ increases as the samples become more dependent. This improvement is a function of the sampling rate and the spectral shape of the noise. It will be seen that for sufficiently fast sampling, or continuous operation, much of the cost of clipping is recovered.

When the input samples are dependent, the only change in the output signal-to-noise ratios of the detectors considered is the result of an increase in the variance of the test statistics. For any test statistic of the form $S = \sum_{i=1}^N h(\bar{x}_i)$, where $\bar{x}_i = x_j(t+i\tau)$, $j=1, \dots, M$, and h is any memoryless operation, the variance for independent samples is given by $\text{Var}\{S\} = N \text{Var}\{h[\bar{x}(t)]\}$. When the samples are dependent, it is easily shown (See Appendix III) that

$$\text{Var}_H\{S\} = N \text{Var}_H\{h[\bar{x}(t)]\} \left[1 + 2 \sum_{k=1}^N \left(1 - \frac{k}{N}\right) R(k\tau) \right], \quad (27)$$

where

$$R(k\tau) = \frac{E_H\{h[\bar{x}(t)] h[\bar{x}(t+k\tau)]\} - E_H^2\{h[\bar{x}(t)]\}}{\text{Var}_H\{h[\bar{x}(t)]\}}. \quad (28)$$

It follows that the output signal-to-noise expressions of Eqs. (6) or (8) hold for dependent samples if N is replaced by

$$N_{eq} \triangleq \frac{T}{\tau + 2\tau \sum_{k=1}^N \left(1 - \frac{k}{N}\right) R(k\tau)} \xrightarrow{\tau \rightarrow 0} \frac{T}{2 \int_0^T \left(1 - \frac{\xi}{T}\right) R(\xi) d\xi}, \quad (29)$$

where T is the decision time. The function $R(k\tau)$ depends on the detector considered and on the spectral shape [or normalized correlation function $\rho_n(\tau)$] of the noise inputs.

The following results are given in Appendix III. For arbitrary stationary inputs, R_{opt} is given by

$$R_{opt}(k\tau) = \rho_n^2(k\tau). \quad (30)$$

When the zero crossings are those of a gaussian process, $R_{pca.1}$ is given by

$$R_{pca.1}(k\tau) = \left(\frac{2}{\pi} \sin^{-1} [\rho_n(k\tau)] \right)^2 . \quad (31)$$

In the limit as M approaches infinity, $R_{pca.3}$ is given by

$$R_{pca.3}(k\tau) \xrightarrow{M \rightarrow \infty} \frac{1}{p_0(1-p_0)} \int_{-1}^1 g(\tilde{\rho}, y) \frac{1}{\sqrt{2\pi}} e^{-\frac{1}{2}y^2} dy - \frac{(1-p_0)}{p_0} , \quad (32)$$

where

$$g(\tilde{\rho}, y) = \int_{\frac{-1-\tilde{\rho}y}{\sqrt{1-\tilde{\rho}^2}}}^{\frac{1-\tilde{\rho}y}{\sqrt{1-\tilde{\rho}^2}}} \frac{1}{\sqrt{2\pi}} e^{-\frac{1}{2}\xi^2} d\xi ,$$

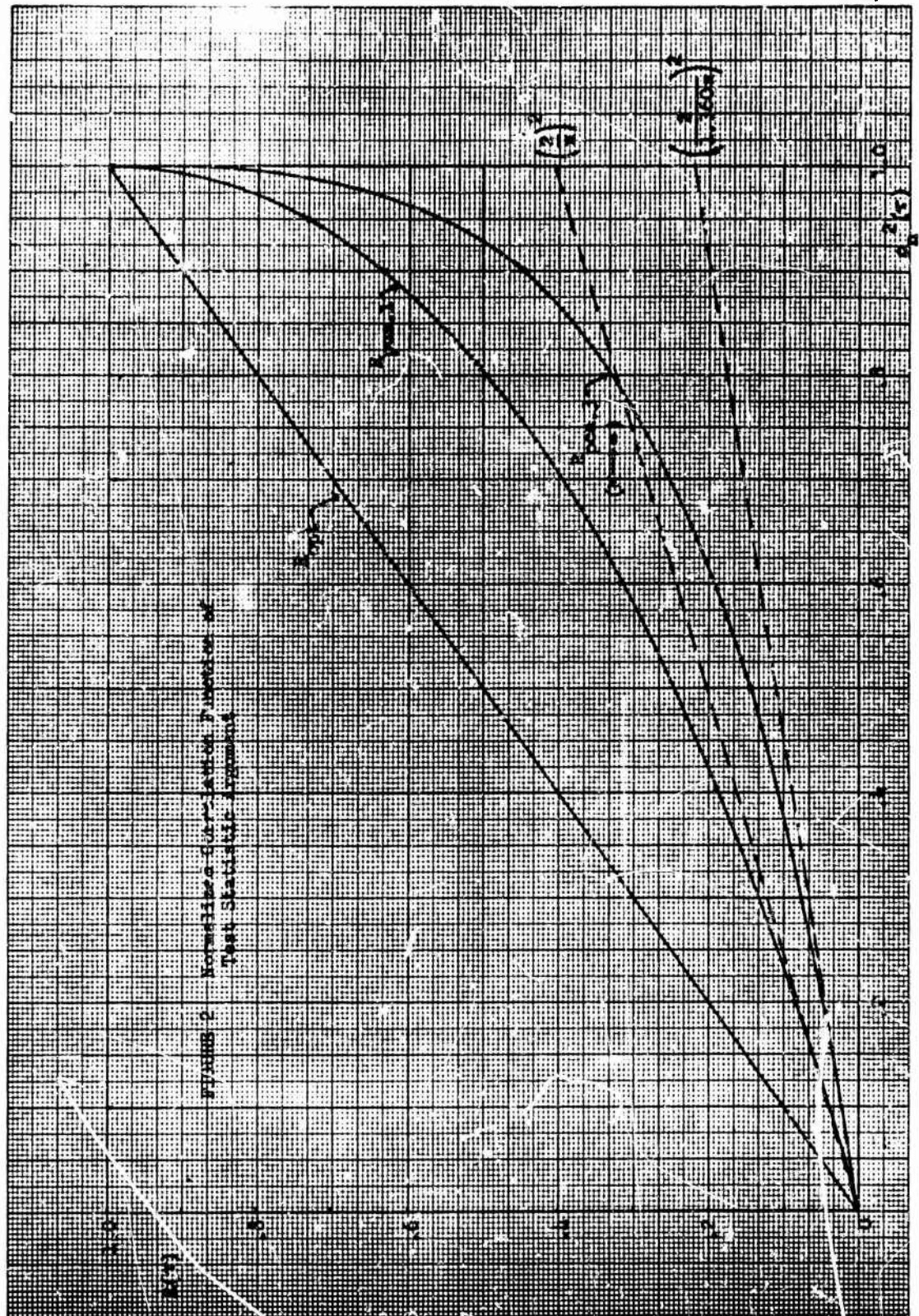
and

$$\tilde{\rho} = \frac{2}{\pi} \sin^{-1} [\rho_n(k\tau)] .$$

These functions are plotted versus $\rho_n^2(\tau)$ in Figure 2.

Since $R_{pca} < R_{opt}$ for $\rho(k\tau) \neq 0$, it follows that, for a given decision time, the equivalent number of uncorrelated samples $[N_{eq}]$ for the PCA detectors is larger than that of D_{opt} . Therefore, when the input samples are dependent, $J_{pca/opt}$ is larger than when they are independent. Observe from Figure 2 that $R_{pca.1} > \left(\frac{2}{\pi}\right)^2 \rho^2$ and

$R_{pca.3}(M \rightarrow \infty) > \left(\frac{2}{\pi} \frac{1}{1.360}\right)^2 \rho^2$. Thus it can be determined from Eq. (29) that even in the limit as $\tau \rightarrow 0$, $J_{pca/opt} < 1$. This is as it should be, since we are assuming essentially gaussian inputs. Nevertheless, much of the loss due to clipping should be recovered in the limit as $\tau \rightarrow 0$.



If we define I as the ratio of J_{pca}/opt with dependent samples to that with independent samples, then from Eqs. (8) and (29) one obtains

$$I^2 = \frac{1 + 2 \sum_{k=1}^N \left(1 - \frac{k}{N}\right) \rho_n^2(k\tau)}{1 + 2 \sum_{k=1}^N \left(1 - \frac{k}{N}\right) R_{pca}(k\tau)} \quad (33)$$

Under the assumption that the decision time is much larger than the width of $\rho_n(t)$, this expression can be accurately approximated by

$$I^2 \approx \frac{1 + 2 \sum_{k=1}^{\infty} \rho_n^2(k\tau)}{1 + 2 \sum_{k=1}^{\infty} R_{pca}(k\tau)} \quad (34)$$

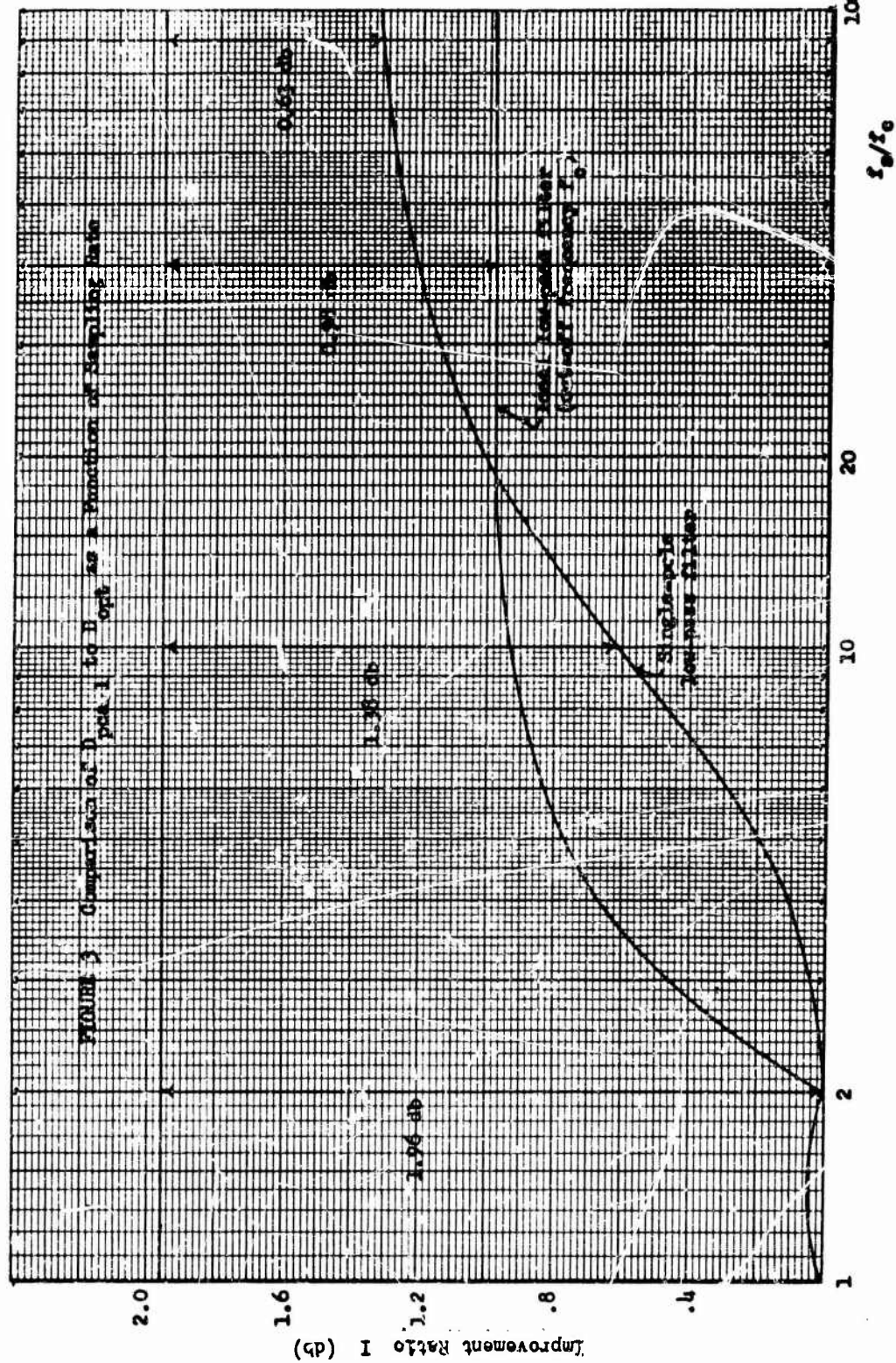
This improvement in the PCA detectors relative to D_{opt} depends of course on the spectral shape.

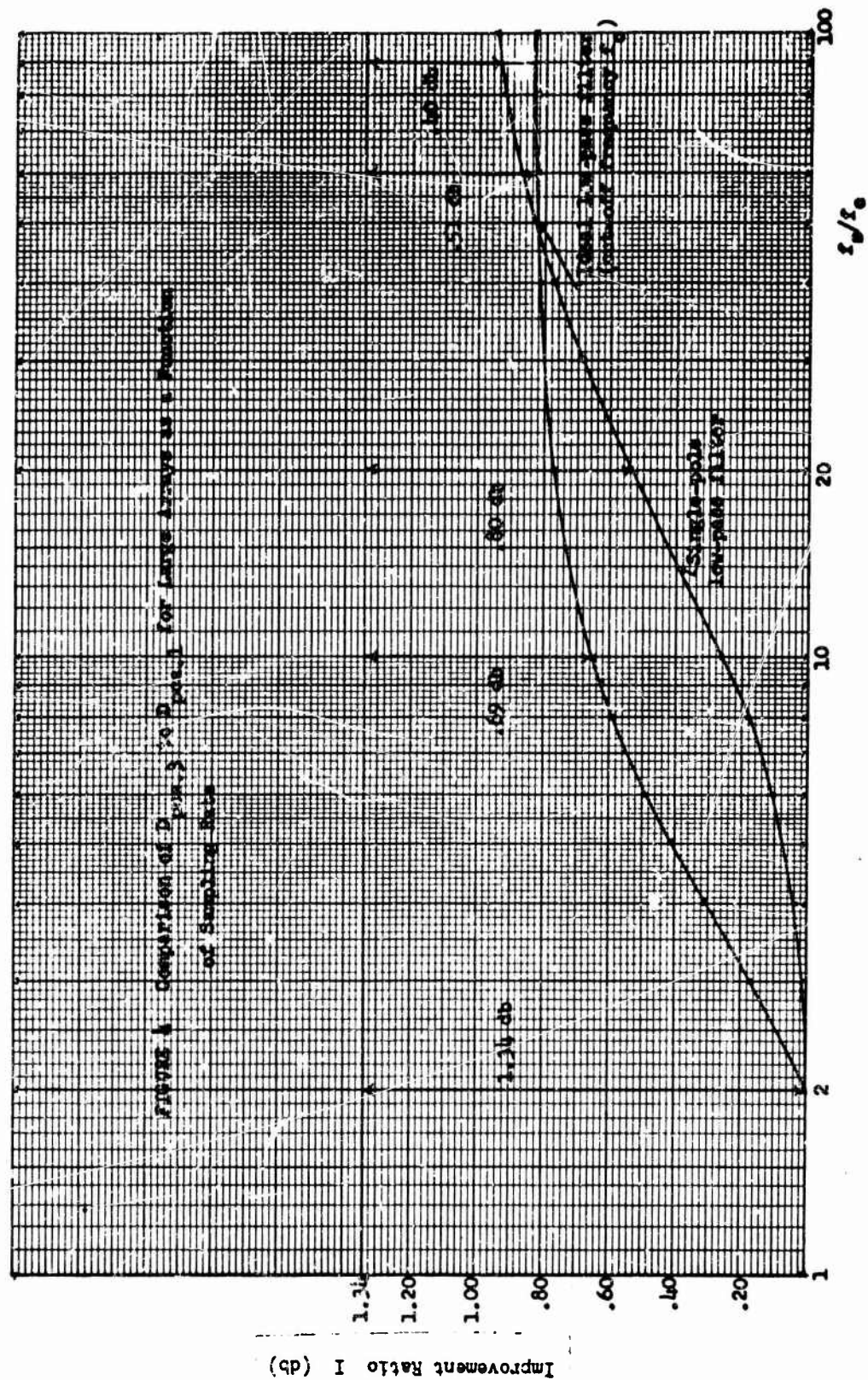
In underwater sound detection one is normally looking for acoustic signals, and hence the pre-filters are often low-pass filters. Let us consider the single pole low-pass filter that falls off at a rate of 6 db/octave $\left(\rho_n(k\tau) = e^{-\omega_c k\tau} \right)$, and the ideal low-pass filter $\left(\rho_n(k\tau) = \frac{\sin \omega_c k\tau}{\omega_c k\tau} \right)$, where $\frac{\omega_c}{2\pi}$ is the cut-off frequency or the bandwidth.

Given a particular sampling rate f_s , I can be evaluated for either case.

The improvement of $D_{pca,1}$ relative to D_{opt} versus the sampling rate is given in Figure 3, and the improvement of $D_{pca,3}(M \rightarrow \infty)$ relative to $D_{pca,1}$ is given in Figure 4.

Observe first that for a sufficiently fast sampling rate, or continuous operation, much of the loss due to clipping (as well as the loss due to an





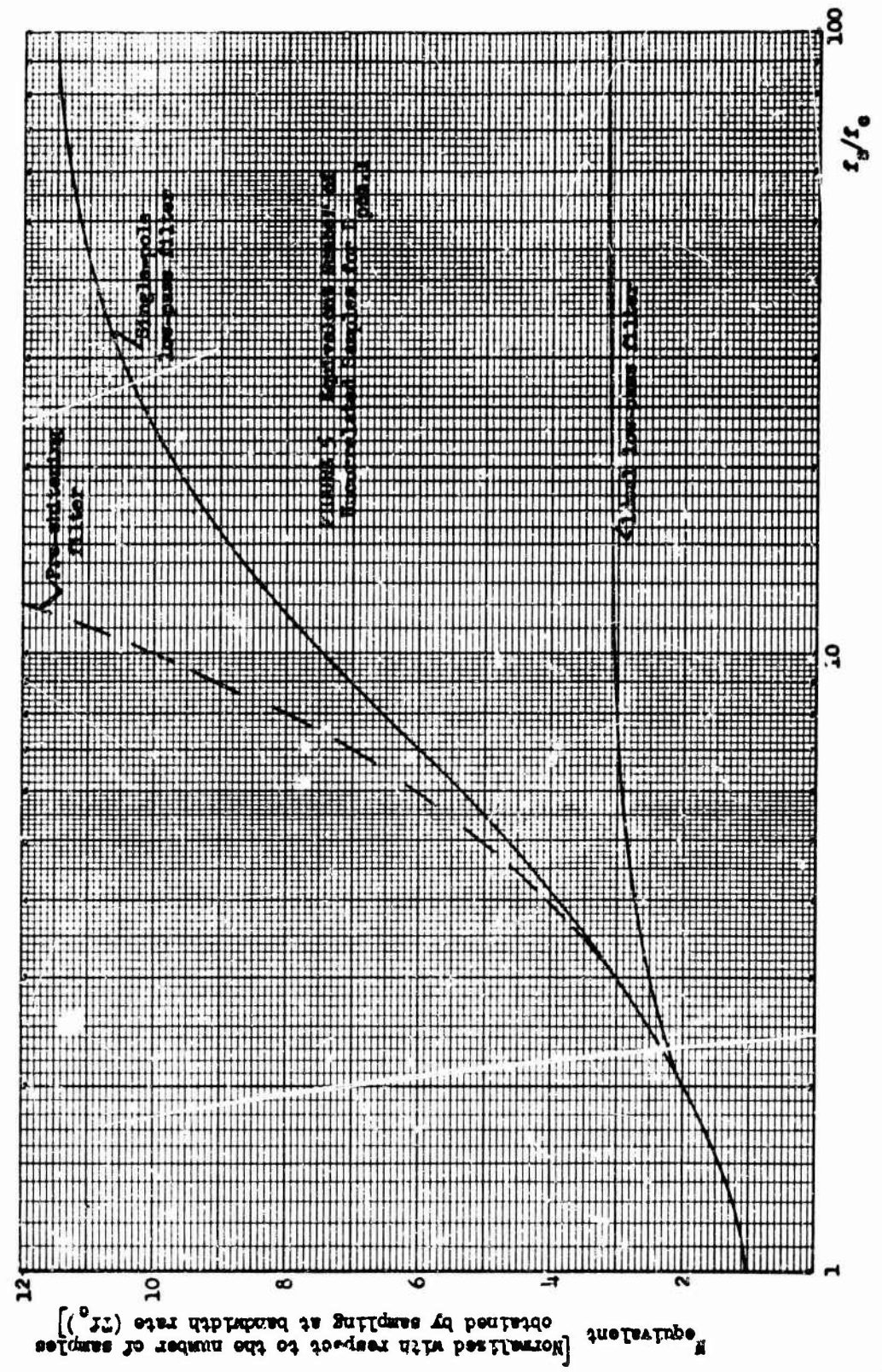
intermediate threshold) is recovered. Thus for essentially gaussian inputs and continuous operation, $D_{pca.1}$ introduces a loss in the signal power as low as 0.63 db for the single pole pre-filter. The loss depends somewhat on the filter shape. In addition, some of the remaining loss can be recovered if the noise level is non-stationary.

It should be pointed out, however, that when using D_{opt} there is little point in sampling faster than $2f_c$ for the ideal filter (Nyquist rate) or $6f_c$ for the single pole filter. For these sampling rates the loss due to clipping is almost that amount calculated for independent samples. Thus one would have to sample at a rate faster than typical to recover some of the loss due to clipping.

One way of looking at this phenomenon is that the process of clipping spreads the spectrum of the input processes. In order to receive all the available information, one has to sample faster than the Nyquist rate of the unclipped inputs. Thus the 2-db loss due to clipping is due in part to this spreading of the spectrum and only in part to an actual loss in information. Practically speaking, the loss due to the change in bandwidth is recovered only when the devices are operated essentially continuously. Figure 5 is a plot of the equivalent number of uncorrelated samples for a fixed decision time versus the sampling rate for $D_{pca.1}$. The results indicate that, when operated continuously, it is necessary to know the spectral shape accurately in order to set the threshold properly. If the spectral shape is not known and it is desirable to set the threshold with some degree of accuracy, then one cannot sample significantly faster than $2f_c$.

NO. 21.192. 30 DIVISIONS PER INCH (120 DIVISIONS) BY TWO 4 1/2-INCH CYCLES RATIO BULING.

CORRE MOORE COMP. INC. BOSTON, MASSACHUSETTS.
MADE IN U.S.A.



VI. Conclusions

Polarity coincidence array detectors have been analyzed and compared with the optimum parametric device based on stationary gaussian inputs. While devices based on clipped data are inherently less efficient than the optimum detector, their nonparametric properties can make them more efficient when the stationary gaussian assumption is violated. In addition, when the PCA detectors are operated as a parametric device with dependent samples, the loss due to clipping can be greatly reduced with sufficiently fast sampling. Even under these conditions, the PCA detectors are unaffected by certain types of nonstationarities in the noise level. The advantages for either mode of operation coupled with the obvious ease of implementation could make the PCA array detectors useful devices for underwater sound detection. There are, however, some additional problems that have not been considered in this report that have bearing on the usefulness of hard limiting.

It is important to analyze the performance of the PCA detectors when the input signal-to-noise ratio is large. The loss due to clipping might be radically different in this environment. It is conceivable that allowing freedom to set the intermediate threshold of the suboptimum device $D_{pca,3}$ can be used to advantage in these circumstances. Another problem is the effect that hard limiting has on the bearing response pattern. If this array pattern is altered, the ability to detect a target in the presence of strong interfering targets would be greatly affected. This of course brings up still another problem, namely how one optimally uses the clipped data in the presence of one or more interference targets.

Appendix I. Output Signal-to-Noise Ratio

The PCA test statistics have the form

$$S_{\text{pca}} = \sum_{i=1}^N g(\delta_i) ,$$

where

$$\delta_i = \left| \frac{1}{2} \sum_{j=1}^M \text{sgn } x_j(t+i\tau) \right| .$$

When r channels have the most prevalent sign, $\delta_i = r - \frac{M}{2}$. If $p(r)$ is the probability that r channels have the same sign, then

$$E\{S_{\text{pca}}\} = N \sum_{r=\lceil \frac{M}{2} \rceil}^M g(r - \frac{M}{2}) p(r) ,$$

where $\lceil x \rceil$ is the smallest integer greater than or equal to x . Under the hypothesis, the m inputs are independent and have zero median, and hence

$$p_H(r) = 2 \binom{M}{r} \left(\frac{1}{2} \right)^M . \text{ Thus}$$

$$E_H\{S_{\text{pca}}\} = N \sum_{r=\lceil \frac{M}{2} \rceil}^M \frac{2}{2^M} \binom{M}{r} g(r - \frac{M}{2}) .$$

Under the alternative, there is an additive signal common to the m channels, hence

$$p_K(r) = \binom{M}{r} \left[\int_{-\infty}^{\infty} \left\{ [1 - F(-u)]^r [F(-u)]^{M-r} + [F(-u)]^r [1 - F(-u)]^{M-r} \right\} f_s(u) du \right] ,$$

where $F(\)$ is the cumulative distribution function of the noise and $f_s(\)$ is the amplitude density of the signal. It will now be assumed that $F(\)$ can be expanded in a Taylor series about the origin over a finite range, thus

$$F(-u) = F(0) - uf(0) + \frac{u^2}{2}f''(0) - \frac{u^3}{3}f'''(0) + o[u^3] .$$

Substituting this expression into the previous equation and expanding leads to the result, where $F(0) = \frac{1}{2}$,

$$p_K(r) = \left(\frac{M}{r}\right) \frac{2}{2^M} \left\{ 1 + 2 \left[(2r-M)^2 - M \right] f^2(0) \int_{-\infty}^{\infty} u^2 f_s(u) du + o \left[\int_{-\infty}^{\infty} u^3 f_s(u) du \right] \right\} ,$$

where convergence is assumed. If the signal is amplitude limited, then for some sufficiently small input signal-to-noise ratio (σ_s^2/σ_n^2) convergence is guaranteed and

$$p_K(r) = p_H(r) + 2\sigma_n^2 f^2(0) \frac{\sigma_s^2}{\sigma_n^2} \frac{2}{2^M} \left(\frac{M}{r}\right) \left[(2r-M)^2 - M \right] + o \left[\frac{\sigma_s^3}{\sigma_n^3} \right] .$$

This result follows from the fact that

$$f^n(0) \int_{-A\sigma_s}^{A\sigma_s} u^n f_s(u) du < f^n(0) (A\sigma_s)^n = \left(f(0)\sigma_n \right)^n \left(\frac{\sigma_s}{\sigma_n} \right)^n A^n ,$$

and hence $\frac{\sigma_s}{\sigma_n} < \frac{1}{A}$ is a sufficient condition. Therefore

$$E_K \left\{ S_{pca} \right\} - E_H \left\{ S_{pca} \right\} \xrightarrow[\frac{\sigma_s}{\sigma_n} \rightarrow 0]{} 2\sigma_n^2 f^2(0) \frac{\sigma_s^2}{\sigma_n^2} \frac{2}{2^M} \sum_{r=\lfloor \frac{M}{2} \rfloor}^M \left(\frac{M}{r}\right) \left[\left(r - \frac{M}{2}\right)^2 - \frac{M}{4} \right] g\left(r - \frac{M}{2}\right) .$$

Recognizing that $p_H(r) = \frac{2}{2^M} \left(\frac{M}{r}\right)$, one can rewrite the last equation in the following form.

$$E_H\{S_{pca}\} - E_H\{S_{pca}\} \xrightarrow[\frac{\sigma_s^2}{\sigma_n^2} \rightarrow 0]{} 8M\sigma_n^2 r^2(0) \frac{\sigma_s^2}{\sigma_n^2} \left[E_H\{\delta^2 s(\delta)\} - \frac{M}{L} E_H\{s(\delta)\} \right] .$$

This result can be used to calculate the limiting form of the output signal-to-noise ratio from Eq. (5) in the text.

Appendix II. Limiting Results for Certain Sums

We are concerned with evaluating, for large values of M , sums of the type

$$\sum_{r=L}^M p_H(r) f(r - \frac{M}{2}) ,$$

where $p_H(r) = \frac{1}{2^M} \binom{M}{r}$. The term $p_H(r)$ corresponds to the binomial distribution with probability of "success" equal to 0.5 and is therefore closely approximated by the normal distribution with mean $\frac{M}{2}$ and variance $\frac{M}{4}$. Thus the sums can be approximated by [14]:

$$\int_{L-\frac{1}{2}}^{\infty} \frac{1}{\sqrt{2\pi} \frac{\sqrt{M}}{2}} \exp\left\{-\frac{1}{2} \frac{(r - \frac{M}{2})^2}{\frac{M}{4}}\right\} f(r - \frac{M}{2}) dr .$$

Changing variables by setting $(r - \frac{M}{2})/\sqrt{\frac{M}{4}} = y$, one obtains

$$\int_{\frac{2L-M-1}{\sqrt{M}}}^{\infty} \frac{1}{\sqrt{2\pi}} e^{-\frac{1}{2}y^2} \left| \frac{\sqrt{M}}{2} y \right| dy .$$

In Eq. (15) the term p_0 was defined as

$$p_0 = 2 \sum_{r=\left[\frac{M}{2}+\frac{\sqrt{M}}{2}\right]}^M \frac{1}{2^{\frac{r}{2}}} \left(\frac{M}{r}\right) .$$

It follows that for large M ,

$$p_0 \approx 2 \int_{1'}^{\infty} \frac{1}{\sqrt{2\pi}} e^{-\frac{1}{2}y^2} dy = 2[1 - \Phi(1')] ,$$

where $1'$ is equal to $\left(2\left[\frac{M}{2}+\frac{\sqrt{M}}{2}\right]-M-1\right)/\sqrt{M}$ which equals $\left(1+\frac{\epsilon}{\sqrt{M}}\right)$, where $-1 < \epsilon < 1$. In the limit as $M \rightarrow \infty$,

$$p_0 \xrightarrow{M \rightarrow \infty} 2[1 - \Phi(1)] = 0.3174 .$$

In Eq. (17) we were concerned with the term

$$p' \approx 2 \sum_{r=\left[\frac{M}{2}+\frac{\sqrt{M}}{2}\right]}^M \frac{1}{2^{\frac{r}{2}}} \left(\frac{M}{r}\right) \left[\left(\frac{r}{2}\right)^2 - \frac{M}{4}\right] .$$

It follows that for large M

$$p' \approx 2 \frac{M}{4} \int_{1'}^{\infty} \frac{1}{\sqrt{2\pi}} e^{-\frac{1}{2}y^2} (y^2 - 1) dy .$$

Integrating by parts, it is easily shown that

$$p' \approx \frac{M}{\sqrt{8\pi}} (1') e^{-\frac{1}{2}(1')^2}$$

Hence

$$p' \xrightarrow{M \rightarrow \infty} \frac{M}{\sqrt{8\pi}} e^{-\frac{1}{2}} = 0.1210 M .$$

Appendix III. Test Statistic Variance for Dependent Samples

Consider an arbitrary test statistic of the form

$$S = \sum_{i=1}^N h[\bar{x}(t+i\tau)] ,$$

where $h(\cdot)$ may be any memoryless operation on the vector $\bar{x}(t+i\tau)$ whose elements are samples (with uniform sampling interval τ) of specific independent representations of the same stochastic process $\{x(t)\}$. The variance of S is given by

$$\begin{aligned} \text{Var}(S) &= E\{S^2\} - E^2\{S\} \\ &= E\left\{\sum_{i=1}^N \sum_{j=1}^N \left[h[\bar{x}(t+i\tau)] h[\bar{x}(t+j\tau)] - E\{h[\bar{x}(t)]\} \right]\right\} \\ &= \sum_{i=1}^N \left[E\{h^2[\bar{x}(t+i\tau)]\} - E^2\{h[\bar{x}(t)]\} \right] \\ &\quad + \sum_{i \neq j}^N \sum_{j=1}^N \left[E\{h[\bar{x}(t+i\tau)] h[\bar{x}(t+j\tau)]\} - E^2\{h[\bar{x}(t)]\} \right] \\ &= N \text{Var}\{h[\bar{x}(t)]\} + \sum_{i \neq j}^N \sum_{j=1}^N \left[E\{h[\bar{x}(t+i\tau)] h[\bar{x}(t+j\tau)]\} - E^2\{h[\bar{x}(t)]\} \right] , \end{aligned}$$

where the second term is zero if the samples are independent, assuming $\{\bar{x}(t)\}$ is stationary, and since there are $2(N-k)$ terms where $|j-i|=k$, one obtains

$$\text{Var}(S) = N \text{Var}\{h[\bar{x}(t)]\} \left[1 + 2 \sum_{k=1}^N \left(1 - \frac{k}{N}\right) R(k\tau) \right] ,$$

where

$$R(k\tau) \triangleq \frac{E\{h[\bar{x}(t)] h[\bar{x}(t+k\tau)]\} - E^2\{h[\bar{x}(t)]\}}{\text{Var}\{h[\bar{x}(t)]\}}.$$

The function $R(k\tau)$ depends not only on the function $h(\cdot)$, but also on the normalized correlation function of $\{\bar{x}(t)\}$ denoted by $\rho(\tau)$.

Let us now consider the test statistic S_{opt} defined by Eq. (23).

For this detector $h[\bar{x}(t)] = \sum_{i=1}^M \sum_{j=1}^M x_i(t) x_j(t)$, where $x_j(t+i\tau)$,

$j=1, \dots, M$, are the M components of the vector $\bar{x}(t+i\tau)$ and where it is assumed that $E\{x_j(t)\} = 0$ for all j . It follows that

$$E\{h[\bar{x}(t)]\} = \sum_{i=1}^M \sum_{j=1}^M E\{x_i(t) x_j(t)\} = 0,$$

and

$$\begin{aligned} \text{Var}\{h[\bar{x}(t)]\} &= E\{h^2[\bar{x}(t)]\} = \sum_{i=1}^M \sum_{j=1}^M \sum_{r=1}^M \sum_{s=1}^M E\{x_i(t) x_j(t) x_r(t) x_s(t)\} \\ &= 2 \sum_{i=1}^M \sum_{j=1}^M E\{x_i^2(t) x_j^2(t)\} = 2(M^2 - M) \text{Var}^2\{x(t)\}, \end{aligned}$$

and

$$\begin{aligned} E\{h[\bar{x}(t)] h[\bar{x}(t+k\tau)]\} &= \sum_{i=1}^M \sum_{j=1}^M \sum_{r=1}^M \sum_{s=1}^M E\{x_i(t) x_j(t) x_r(t+k\tau) x_s(t+k\tau)\} \\ &= 2 \sum_{i=1}^M \sum_{j=1}^M E\{x_i(t) x_i(t+k\tau) x_j(t) x_j(t+k\tau)\} \\ &= 2(M^2 - M) \text{Var}^2[x(t)] \rho^2(k\tau). \end{aligned}$$

Hence by the definition of $R(k\tau)$, it is seen that

$$R_{\text{opt}}(k\tau) = \rho^2(k\tau) .$$

Next let us consider the detector $D_{\text{pos},1}$ in which $h[\bar{x}(t)] = \delta^2[\bar{x}(t)]$

where $\delta[\bar{x}(t)] = \left| \frac{1}{2} \sum_{i=1}^M \text{sgn}[x_i(t)] \right|$. For this test statistic

$$\begin{aligned} E\{h[\bar{x}(t)]\} &= \frac{1}{4} \sum_{i=1}^M \sum_{j=1}^M E\{\text{sgn}[x_i(t)] \text{sgn}[x_j(t)]\} \\ &= \frac{1}{4} \sum_{i=1}^M E\{\text{sgn}^2[x_i(t)]\} = \frac{M}{4} , \end{aligned}$$

and

$$\begin{aligned} \text{Var}\{h[\bar{x}(t)]\} &= \frac{1}{16} \sum_i \sum_j \sum_r \sum_s E\{\text{sgn}[x_i(t)] \text{sgn}[x_j(t)] \text{sgn}[x_r(t)] \text{sgn}[x_s(t)]\} - \frac{M^2}{16} \\ &= \frac{1}{16} \sum_{i=1}^M E\{\text{sgn}^4[x_i(t)]\} - \frac{3}{16} \sum_{i \neq j} E\{\text{sgn}^2[x_i(t)] \text{sgn}^2[x_j(t)]\} - \frac{M^2}{16} \\ &= \frac{M}{16} + \frac{3}{16}(M^2 - M) - \frac{M^2}{16} = \frac{1}{8} M(M-1) , \end{aligned}$$

and

$$\begin{aligned} E\{h[\bar{x}(t)] h[\bar{x}(t+k\tau)]\} &= \frac{1}{16} \sum_i \sum_j \sum_r \sum_s E\{\text{sgn}[x_i(t)] \text{sgn}[x_j(t)] \text{sgn}[x_r(t+k\tau)] \text{sgn}[x_s(t+k\tau)]\} \\ &= \frac{1}{16} \sum_i \sum_j E\{\text{sgn}^2[x_i(t)] \text{sgn}^2[x_j(t+k\tau)]\} \\ &\quad + \frac{2}{16} \sum_{i \neq j} E\{\text{sgn}[x_i(t)] \text{sgn}[x_i(t+k\tau)] \text{sgn}[x_j(t)] \text{sgn}[x_j(t+k\tau)]\} \\ &= \frac{M^2}{16} + \frac{1}{8}(M^2 - M) E\{\text{sgn}[x(t)] \text{sgn}[x(t+k\tau)]\} \\ &= \frac{M^2}{16} + \frac{1}{8} M(M-1) \left(\frac{2}{\pi} \sin^{-1}[\rho(k\tau)] \right)^2 . \end{aligned}$$

The result just given for the correlation function of a hard-limited process was shown by Van Vleck [15] and is based on the assumption that the distribution of zero crossings of $[x(t)]$ is the same as that of a gaussian process with zero mean. From the definition of $R(k\tau)$, it is seen that

$$R_{\text{pca},1}(k\tau) = \left(\frac{2}{\pi} \sin^{-1} [\rho(k\tau)] \right)^2.$$

Finally we wish to consider the detector $D_{\text{pca},3}$ in which $h[\bar{x}(t)] = s\left\{\bar{x}(t) - \frac{\sqrt{M}}{2}\right\}$. For this statistic

$$\begin{aligned} E\{h[\bar{x}(t)]\} &= \text{Prob}\left[s\left\{\bar{x}(t) - \frac{\sqrt{M}}{2}\right\} > \frac{\sqrt{M}}{2}\right] \\ &= \frac{2}{2^M} \sum_{r=\left\lceil \frac{M}{2} + \frac{\sqrt{M}}{2} \right\rceil}^M \binom{M}{r} = p_0, \end{aligned}$$

and

$$\text{Var}\{h[\bar{x}(t)]\} = p_0(1 - p_0),$$

and

$$E\{h[\bar{x}(t)]h[\bar{x}(t+k\tau)]\} = \text{Prob}\left[s\left\{\bar{x}(t+k\tau) - \frac{\sqrt{M}}{2}\right\} > \frac{\sqrt{M}}{2}, s\left\{\bar{x}(t) - \frac{\sqrt{M}}{2}\right\} > \frac{\sqrt{M}}{2}\right].$$

This last probability can be evaluated conveniently for large M if we define $s\left\{\bar{x}(t+k\tau) - \frac{\sqrt{M}}{2}\right\} \triangleq \xi_k \frac{\sqrt{M}}{2}$. Then ξ_k is a random variable with zero mean and unit variance that is asymptotically normally distributed as M increases beyond bound. Furthermore $E\left\{\xi_k \xi_0\right\} = \frac{2}{\pi} \sin^{-1} [\rho(k\tau)] \triangleq \tilde{\rho}$. It follows that

$$R_{\text{pos.3}}(k\tau) = \frac{1}{p_0(1-p_0)} \left[\int_{-1}^1 \int_{-1}^1 W_2(\xi_k, \xi_0) d\xi_k d\xi_0 + \int_{-1}^1 \int_{-1}^1 W_2(\xi_k, \xi_0) d\xi_k d\xi_0 \right. \\ \left. + \int_{-1}^1 \int_{-1}^1 W_2(\xi_k, \xi_0) d\xi_k d\xi_0 + \int_{-1}^1 \int_{-1}^1 W_2(\xi_k, \xi_0) d\xi_k d\xi_0 \right] - \frac{p_0}{1-p_0} ,$$

or by symmetry

$$R_{\text{pos.3}}(k\tau) = \frac{1}{p_0(1-p_0)} \int_{-1}^1 W_2(\xi_k, \xi_0) d\xi_k d\xi_0 - \frac{(1-p_0)}{p_0} ,$$

where

$$W_2(\xi_k, \xi_0) \xrightarrow{u \rightarrow \infty} \frac{1}{2\pi\sqrt{1-\rho^2}} \exp \left[-\frac{1}{2(1-\rho^2)} (\xi_k^2 - 2\rho\xi_k\xi_0 + \xi_0^2) \right] .$$

By completing the square and changing variables, one obtains

$$R_{\text{pos.3}}(k\tau) \xrightarrow{u \rightarrow \infty} \frac{1}{p_0(1-p_0)} \int_{-1}^1 \frac{1}{\sqrt{2\pi}} e^{-\frac{1}{2}x^2} \int_{\frac{-1-\rho x}{\sqrt{1-\rho^2}}}^{\frac{1-\rho x}{\sqrt{1-\rho^2}}} \frac{1}{\sqrt{2\pi}} e^{-\frac{1}{2}y^2} dy dx - \frac{(1-p_0)}{p_0} ,$$

where

$$(1-p_0) \xrightarrow{u \rightarrow \infty} \int_{-1}^1 \frac{1}{\sqrt{2\pi}} e^{-\frac{1}{2}x^2} dx .$$

These normalized covariance functions are plotted in Figure 2.

References

1. Faran, J. J., and R. Hills, "The Application of Correlation Techniques to Acoustic Receiving Systems," Acoustic Research Lab., Tech. Memo. No. 26, Harvard University; 1952.
2. Anderson, V. C., "Arrays for the Investigation of Ambient Noise in the Ocean," J. Acoust. Soc. Am., vol. 30, p. 470; 1958.
3. Thomas, J. B., and T. R. Williams, "On the Detection of Signals in Non-Stationary Noise by Product Arrays," J. Acoust. Soc. Am., vol. 31, p. 453; 1959.
4. Rudnick, P., "Small Signal Detection in the Dimer Array," J. Acoust. Soc. Am., vol. 32, p. 867; 1960.
5. Bryn, F., "Optimal Signal Processing by Three-Dimensional Arrays Operating on Gaussian Signals and Noise," J. Acoust. Soc. Am., vol. 34, p. 289; 1962.
6. Wolff, S. S., J. B. Thomas and T. R. Williams, "The Polarity Coincidence Correlator: A Nonparametric Device," IRE Trans. on Information Theory, vol. IT-8, n. 5; 1962.
7. Kanefsky, M., "On Sign Tests and Adaptive Techniques for Nonparametric Detection," Ph.D. Dissertation, Princeton University, May 1964.
8. Lehmann, E. L., Testing Statistical Hypotheses, John Wiley and Sons, Inc., New York, p. 60; 1959.
9. Lehmann [8], p. 329.
10. Schultheiss, P. M., and F. B. Tuteur, "Optimum and Suboptimum Detection of Directional Gaussian Signals in an Isotropic Gaussian Noise Field, Part II: Degradation of Detectability Due to Clipping," IEEE Trans. on Military Electronics, July 1965.
11. Tuteur, F. B., "Optimum Detection of a Stochastic Signal in a Gaussian Noise of Unknown Strength," Correspondence to the Proceedings of the IEEE; 1965.
12. Kanefsky, M., and J. B. Thomas, "Polarity Coincidence Correlation Using Dependent Samples," Proceedings of the National Electronics Conference, vol. 20, p. 714; 1964.
13. Ekre, H., "Polarity Coincidence Correlation Detection of a Weak Noise Source," IEEE Trans. on Information Theory, pp. 18-23, January 1963.
14. Feller, W., An Introduction to Probability Theory and Its Applications, John Wiley and Sons, Inc., New York, p. 172; 1957.
15. Van Vleck, J. H., "The Spectrum of Clipped Noise," Radio Research Lab., Harvard University, Report No. 51; 1943.

<p>GENERAL DYNAMICS, ELECTRIC BOAT DIVISION Technical Report U417-65-033 Processing of Data from Sonar Systems, Volume III Yale University August 23, 1965; 372 Pages</p> <p>This report is concerned with problems in passive sonar detection which arise when signal or noise properties deviate significantly from the simplest possible model (a target acting as a point source of broadband Gaussian signal in a background of isotropic Gaussian noise). Problems investigated were concerned with improvements in detectability obtained from a knowledge of the special features of signal or noise and with degradation in detector performance as a result of an inadequate knowledge of signal or noise statistics or a deliberate exclusion of some available information so as to simplify the instrumentation.</p>		<p>GENERAL DYNAMICS, ELECTRIC BOAT DIVISION Technical Report U417-65-033 Processing of Data from Sonar Systems, Volume III Yale University August 23, 1965; 372 Pages</p> <p>This report is concerned with problems in passive sonar detection which arise when signal or noise properties deviate significantly from the simplest possible model (a target acting as a point source of broadband Gaussian signal in a background of isotropic Gaussian noise). Problems investigated were concerned with improvements in detectability obtained from a knowledge of the special features of signal or noise and with degradation in detector performance as a result of an inadequate knowledge of signal or noise statistics or a deliberate exclusion of some available information so as to simplify the instrumentation.</p>	
<p>GENERAL DYNAMICS, ELECTRIC BOAT DIVISION Technical Report U417-65-033 Processing of Data from Sonar Systems, Volume III Yale University August 23, 1965; 372 Pages</p> <p>This report is concerned with problems in passive sonar detection which arise when signal or noise properties deviate significantly from the simplest possible model (a target acting as a point source of broadband Gaussian signal in a background of isotropic Gaussian noise). Problems investigated were concerned with improvements in detectability obtained from a knowledge of the special features of signal or noise and with degradation in detector performance as a result of an inadequate knowledge of signal or noise statistics or a deliberate exclusion of some available information so as to simplify the instrumentation.</p>		<p>GENERAL DYNAMICS, ELECTRIC BOAT DIVISION Technical Report U417-65-033 Processing of Data from Sonar Systems, Volume III Yale University August 23, 1965; 372 Pages</p> <p>This report is concerned with problems in passive sonar detection which arise when signal or noise properties deviate significantly from the simplest possible model (a target acting as a point source of broadband Gaussian signal in a background of isotropic Gaussian noise). Problems investigated were concerned with improvements in detectability obtained from a knowledge of the special features of signal or noise and with degradation in detector performance as a result of an inadequate knowledge of signal or noise statistics or a deliberate exclusion of some available information so as to simplify the instrumentation.</p>	

Unclassified

Security Classification

DOCUMENT CONTROL DATA - R&D		
(Security classification of title, body of abstract and indexing annotation must be entered when the overall report is classified)		
1. ORIGINATING ACTIVITY (Corporate author) General Dynamics Corporation, Electric Boat Division, Groton, Connecticut		2a. REPORT SECURITY CLASSIFICATION Unclassified
		2b. GROUP
3. REPORT TITLE PROCESSING OF DATA FROM SONAR SYSTEMS VOLUME III		
4. DESCRIPTIVE NOTES (Type of report and inclusive dates)		
5. AUTHOR(S) (Last name, first name, initial) Kanefsky, Morton; Levesque, Allen H.; Schultheiss, Peter, M.; Tuteur, Franz B.		
6. REPORT DATE July 1964 to July 1, 1965	7a. TOTAL NO. OF PAGES 372	7b. NO. OF REFS
8a. CONTRACT OR GRANT NO. NONr 2512(00)	9a. ORIGINATOR'S REPORT NUMBER(S) U417-65-033	
8b. PROJECT NO.	9b. OTHER REPORT NO(S) (Any other numbers that may be assigned this report)	
c		
d		
10. AVAILABILITY/LIMITATION NOTICES Qualified requestors may obtain copies of this report from DDC.		
11. SUPPLEMENTARY NOTES	12. SPONSORING MILITARY ACTIVITY Office of Naval Research Department of the Navy Washington 25, D.C.	
13. ABSTRACT This report is concerned with problems in passive sonar detection which arise when signal or noise properties deviate significantly from the simplest possible model (a target acting as a point source of broadband Gaussian signal in a background of isotropic Gaussian noise). Problems investigated were concerned with improvements in detectability obtained from a knowledge of the special features of signal or noise and with degradation in detector performance as a result of an inadequate knowledge of signal or noise statistics or a deliberate exclusion of some available information so as to simplify the instrumentation.		

DD FORM 1473
1 JAN 64

Unclassified

Security Classification

Unclassified

Security Classification

14. KEY WORDS	LINK A		LINK B		LINK C	
	ROLE	WT	ROLE	WT	ROLE	WT

INSTRUCTIONS

1. **ORIGINATING ACTIVITY.** Enter the name and address of the contractor, subcontractor, grantee, Department of Defense activity or other organization (corporate author) issuing the report.

2a. **REPORT SECURITY CLASSIFICATION:** Enter the overall security classification of the report. Indicate whether "Restricted Data" is included. Marking is to be in accordance with appropriate security regulations.

2b. **GROUP:** Automatic downgrading is specified in DoD Directive 5200.10 and Armed Forces Industrial Manual. Enter the group number. Also, when applicable, show that optional markings have been used for Group 3 and Group 4 as authorized.

3. **REPORT TITLE:** Enter the complete report title in all capital letters. Titles in all cases should be unclassified. If a meaningful title cannot be selected without classification, show title classification in all capitals in parentheses immediately following the title.

4. **DESCRIPTIVE NOTES:** If appropriate, enter the type of report, e.g., interim, progress, summary, annual, or final. Give the inclusive dates when a specific reporting period is covered.

5. **AUTHOR(S):** Enter the name(s) of author(s) as shown on or in the report. Enter last name, first name, middle initial. If military, show rank and branch of service. The name of the principal author is an absolute minimum requirement.

6. **REPORT DATE:** Enter the date of the report as day, month, year, or month, year. If more than one date appears on the report, use date of publication.

7a. **TOTAL NUMBER OF PAGES:** The total page count should follow normal pagination procedures, i.e., enter the number of pages containing information.

7b. **NUMBER OF REFERENCES:** Enter the total number of references cited in the report.

8a. **CONTRACT OR GRANT NUMBER:** If appropriate, enter the applicable number of the contract or grant under which the report was written.

8b, 8c, & 8d. **PROJECT NUMBER:** Enter the appropriate military department identification, such as project number, subproject number, system numbers, task number, etc.

9a. **ORIGINATOR'S REPORT NUMBER(S):** Enter the official report number by which the document will be identified and controlled by the originating activity. This number must be unique to this report.

9b. **OTHER REPORT NUMBER(S):** If the report has been assigned any other report numbers (either by the originator or by the sponsor), also enter this number(s).

10. **AVAILABILITY/LIMITATION NOTICES:** Enter any limitations on further dissemination of the report, other than those imposed by security classification, using standard statements such as:

- (1) "Qualified requesters may obtain copies of this report from DDC."
- (2) "Foreign announcement and dissemination of this report by DDC is not authorized."
- (3) "U. S. Government agencies may obtain copies of this report directly from DDC. Other qualified DDC users shall request through _____."
- (4) "U. S. military agencies may obtain copies of this report directly from DDC. Other qualified users shall request through _____."
- (5) "All distribution of this report is controlled. Qualified DDC users shall request through _____."

If the report has been furnished to the Office of Technical Services, Department of Commerce, for sale to the public, indicate this fact and enter the price, if known.

11. **SUPPLEMENTARY NOTES:** Use for additional explanatory notes.

12. **SPONSORING MILITARY ACTIVITY:** Enter the name of the departmental project office or laboratory sponsoring (paying for) the research and development. Include address.

13. **ABSTRACT:** Enter an abstract giving a brief and factual summary of the document indicative of the report, even though it may also appear elsewhere in the body of the technical report. If additional space is required, a continuation sheet shall be attached.

It is highly desirable that the abstract of classified reports be unclassified. Each paragraph of the abstract shall and with an indication of the military security classification of the information in the paragraph, represented as (TS), (S), (C), or (U).

There is no limitation on the length of the abstract. However, the suggested length is from 150 to 225 words.

14. **KEY WORDS:** Key words are technically meaningful terms or short phrases that characterize a report and may be used as index entries for cataloging the report. Key words must be selected so that no security classification is required. Identifiers, such as equipment model designation, trade name, military project code name, geographic location, may be used as key words but will be followed by an indication of technical context. The assignment of links, roles, and weights is optional.

Unclassified

Security Classification